Department Biologie I
Bereich Genetik
Ludwig-Maximilians-Universität München

Developmental adaptations of energy and lipid metabolism in *Trypanosoma brucei* insect forms.

Stefan Allmann

Dissertation der Fakultät für Biologie,
Ludwig-Maximilians-Universität München
Eingereicht am 18.09.2014

Erster Gutachter : **Prof. Dr. Michael Boshart**
Biozentrum der Ludwig-Maximilians-Universität München
Bereich Genetik

Zweiter Gutachter: **Prof. Dr. Peter Geigenberger**
Biozentrum der Ludwig-Maximilians-Universität München
Bereich Pflanzenwissenschaften

Datum der Abgabe: 18.09.2014

Datum der mündlichen Prüfung: 24.10.2014

Eidesstattliche Erklärung

Ich versichere hiermit an Eides statt, dass die vorgelegte Dissertation von mir selbstständig und ohne unerlaubte Hilfe angefertigt wurde. Des Weiteren erkläre ich, dass ich nicht anderweitig ohne Erfolg versucht habe eine Dissertation einzureichen oder mich der Doktorprüfung zu unterziehen. Die folgende Dissertation liegt weder ganz, noch in wesentlichen Teilen einer anderen Prüfungskommission vor.

München, 18.09.2014

Statutory declaration

I declare that I have authored this thesis independently, that I have not used other than the declared sources/resources. As well I declare, that I have not submitted a dissertation without success and not passed the oral exam. The present dissertation (neither the entire dissertation nor parts) has not been presented to another examination board.

Munich, 18.09.2014

Eidesstattliche Erklärung III

Statutory declaration III

Abbreviations V

Publications and Manuscripts Originating from this Thesis VII

Contribution to Publications and Manuscripts Presented in this Thesis VIII

Summary IX

Zusammenfassung X

1. Introduction 11
1.1 *Trypanosoma brucei* in a nutshell 11
1.2 The parasite's life cycle 12
1.3 Intermediate and energy metabolism 14
1.4 NADPH balance 17
1.5 Lipid droplets as energy storage 20

2. Cytosolic NADPH Homeostasis in Glucose-starved Procyclic *Trypanosoma brucei* Relies on Malic Enzyme and the Pentose Phosphate Pathway Fed by Gluconeogenic Flux 22

3. Metabolic Control of Insect Stage Differentiation 23
3.1 Carbon Source Regulated Glycosomal NADPH Production is Essential for the Developmental Cycle of *Trypanosoma brucei* in the insect 24
3.2 The Role of Aconitase During Differentiation 42

4. Fatty Acid Storage in *T. brucei* Procyclic Cells 44

5. Acetate Metabolism 62
5.1 Acetate produced in the mitochondrion is the essential precursor for lipid biosynthesis in procyclic trypanosomes 63
5.2 Functional analysis of a CL candidate gene 64

6. Concluding Discussion 67
6.1 Gluconeogenic flux – costs and benefits for metabolic homeostasis 67
6.2 Lipid storage and its role in *T. brucei* 69
6.3 Acetate metabolism and the enigma of the CL candidate gene 70
6.4 Insect stage differentiation and its multitude of regulators 72

References 76

Supplemental Material – Chapter 2 83

Supplemental Material – Chapter 3.1 84

Supplemental Material – Chapter 4 91

Supplemental Material – Chapter 5.2 101

Acknowledgements 105

Curriculum Vitae 107

Abbreviations

6PGDH	6-phosphogluconate dehydrogenase
AAT	animal african trypanosomiasis
ACH	acetyl-CoA hydrolase
ACL	ATP-dependent citrate lyase
ACO	aconitase
ACS	acetyl-CoA synthetase
ASCT	acetate:succinate CoA transferase
ATP	adenosine triphosphate
BSF	bloodstream form
CL	citrate lyase
CoA	coenzyme A
CS	citrate synthase
DHAP	dihydroxyacetone phosphate
EMF	epimastigote form
FCS	fetal calf serum
FRD	fumarate reductase
G3PDH	glycerol-3-phosphate dehydrogenase
G6PDH	glucose-6-phosphate dehydrogenase
G6P	glucose-6-phosphate
GAPDH	glyceraldehyde-3-phosphate dehydrogenase
GlcNAc	N-acetyl-glucosamine
Gly3P	glycerol-3-phosphate
GPI	glycosylphosphatidylinositol
HAT	human african trypanosomiasis
HK	hexokinase
ICL	isocitrate lyase
IDH	isocitrate dehydrogenase
LD	lipid droplet
LS	long slender
ME	malic enzyme
MDH	malate dehydrogenase
MF	metacyclic form
MLS	malate synthase
NADH/NAD^+	nicotinamide adenine dinucleotide (reduced/oxidized)
NADPH/$NADP^+$	nicotinamide adenine dinucleotide phosphate (reduced/oxidized)
OAA	oxaloacetic acid
PCF	procyclic form
PDH	pyruvate dehydrogenase
PEP	phosphoenolpyruvate
PEPCK	phosphoenolpyruvate carboxykinase
PFK	phosphofructokinase
PFR	paraflagellar rod
PGK	phosphoglycerate kinase
PPP	pentose phosphate pathway
RBP6	RNA-binding protein 6
ROS	reactive oxygen species
RT	room temperature
SCoAS	succinyl-CoA synthetase
SHAM	salicylhydroxamic acid
SIF	stumpy induction factor
SOD	superoxide dismutase
SS	short stumpy

TAG	triacylglycerol
TCA	tricarboxylic acid cycle (aka Krebs/citrate cycle)
TR	trypanothione reductase
VSG	variant surface glycoprotein
WHO	world health organization
WT	wild type

Publications and Manuscripts Originating from this Thesis

Chapter 2

Allmann, S., Morand, P., Ebikeme, C., Gales, L., Biran, M., Hubert, J., Brennand, A., Mazet, M., Franconi, J. M., Michels, P. A., Portais, J. C., Boshart, M. & Bringaud, F. (2013) Cytosolic NADPH homeostasis in glucose-starved procyclic Trypanosoma brucei relies on malic enzyme and the pentose phosphate pathway fed by gluconeogenic flux. ***J. Biological Chemistry***. 288(25); 18494-505.

Chapter 3.1

S. Allmann, N. Ziebart, J.-W. Dupuy, M. Bonneu, F. Bringaud, J. Van Den Abbeele and M. Boshart. (2014) Carbon Source Regulated Glycosomal NADPH Production is Essential for the Developmental Cycle of *Trypanosoma brucei* in the insect. **Manuscript**.

Chapter 4

S. Allmann, M. Mazet, N. Ziebart, G. Bouyssou, L. Fouillen, J.-W. Dupuy, M. Bonneu, P. Moreau, F. Bringaud and M. Boshart. (2014). Triacylglycerol Storage in Lipid Droplets in Procyclic *Trypanosoma brucei*. **Manuscript submitted to *PLOS ONE***.

Chapter 5.1

Riviere, L., Moreau, P., Allmann, S., Hahn, M., Biran, M., Plazolles, N., Franconi, J. M., Boshart, M. & Bringaud, F. (2009) Acetate produced in the mitochondrion is the essential precursor for lipid biosynthesis in procyclic trypanosomes. ***PNAS*.** 106(31); 12694-9.

Contribution to Publications and Manuscripts Presented in this Thesis

Chapter 2

S.A., M. Boshart, and F.B. designed research; **S.A.**, P.M., C.E., L.G. and M. Biran performed research; A.B., M.M., J.H., P.A.M., and J.-M.F. contributed new reagents/analytic tools; **S.A.**, L.G., J.-C.P, M. Boshart, and F.B. analyzed data; and **S.A.**, M. Boshart, and F.B. wrote the paper.

Chapter 3.1

S.A., F.B., J.V.D.A., and M. Boshart designed research; **S.A.**, N.Z., J.V.D.A. and J.-W.D. performed research; **S.A.**, N.Z., M. Bonneu, F.B., J.V.D.A. and M. Boshart analyzed data; and **S.A.**, F.B., J.V.D.A., and M. Boshart wrote the paper.

Chapter 4

S.A., M.M., P.M., F.B. and M. Boshart designed research; **S.A.**, M.M., N.Z., G.B., L.F. and J.-W.D. performed research; **S.A.**, N.Z., M. Bonneu P.M., F.B. and M. Boshart analyzed data; and **S.A.**, P.M., F.B. and M. Boshart wrote the paper.

Chapter 5.1

L.R., P.M., M. Boshart, and F.B. designed research; L.R., P.M., **S.A.**, M.H., M. Biran, N.P., and F.B. performed research; J.-M.F. contributed new reagents/analytic tools; L.R., P.M., **S.A.**, M.H.,M. Biran, M. Boshart, and F.B. analyzed data; and L.R., P.M., M. Boshart, and F.B. wrote the paper.

I hereby confirm the above statements

Stefan Allmann Prof. Dr. Michael Boshart

Summary

Adaptations to varying host environments are an essential part of most parasitic life cycles. A flexible and unconventional metabolic network can be part of these adaptations. The scope of this work was to elucidate details of the metabolic flexibility and capability of *T. brucei*'s procyclic form. *T. brucei* has to cope with oxidative stress in the insect and the mammalian host. Due to the lack of catalases the parasite requires NADPH in order to detoxify reactive oxygen species (ROS), thus the focus was set on NADPH production. In most eukaryotes the oxidative pentose phosphate pathway (PPP) is the main contributor to the cytoplasmic NADPH pool. In *T. brucei* the PPP is localized to the cytoplasm and the glycosomes. A major problem for the parasite is the PPP's dependency on glucose 6-phosphate (G6P), concerning the lack of glucose in the insect host.

Thus we wanted to elucidate the putative redundancy of NADPH production in the context of carbon source fluctuations. In the parasite's genome two potential NADPH sources are found for the cytoplasm, the mitochondrion and the glycosomes. We investigated the PPP and the cytosolic malic enzyme (MEc) concerning their contribution to cytoplasmic oxidative stress defense. We found complete redundancy in terms of NADPH production. Each of the two pathways was sufficient to maintain ROS detoxification. Surprisingly, flux through the PPP was maintained also in absence of glucose. We showed that this flux is fueled by gluconeogenesis fed by proline.

A similar situation is found within the glycosomes, where the PPP and the glycosomal isocitrate dehydrogenase (IDHg) are potential NADPH producers. So far the role of NADPH within the parasite's glycosomes was not determined. Hence we investigated potential NADPH consuming pathways for their activity and glycosomal localization. Amongst these putative glycosomal NADPH consumers we investigated β-oxidation activity of the parasite. We characterized the dynamics of lipid droplet (LD) formation and decay and investigated the only candidate gene for β-oxidation activity found in the genome. In conclusion our data make glycosomal β-oxidation unlikely. In the mitochondrion, the lethality of mitochondrial malic enzyme (MEm) downregulation makes a redundancy with the mitochondrial isocitrate dehydrogenase (IDHm) debatable. Investigation of the role of the IDHm is ongoing.

We discovered a role of the IDHg during stage development, leading to a more detailed analysis of the differentiation process and the role of NADPH and carbon sources therein. We showed that a ΔIDHg null mutant was unable to colonize the salivary glands of the insect host. We furthermore used this and other null mutants to validate a newly discovered in culture differentiating system, where the ΔIDHg null mutant showed a clear block in stage development. A similar effect was observed when glucose or glycerol was present in the culture medium. An aconitase null mutant (ΔACO) showed an earlier block than the ΔIDHg in differentiation. The reasons for this are under investigation. We postulate a pathway for glycosomal NADPH production and the ether-linked lipid biosynthesis as putative NADPH consumer, which is currently under investigation.

Zusammenfassung

Die Anpassung an wechselnde Wirtsumgebungen ist ein wichtiger Bestandteil der meisten parasitischen Lebenszyklen. Oft ist ein flexibler oder unkonventioneller Stoffwechsel Teil dieser Anpassung. Ziel dieser Arbeit war es Details der metabolischen Flexibilität und Kapazität der procyclischen Form von *T. brucei* aufzuklären. Der Parasit *T. brucei* wird sowohl im Insektenwirt als auch im Säugerwirt mit oxidativem Stress konfrontiert. Das Fehlen von Katalasen erfordert NADPH zur Entgiftung reaktiver Sauerstoffspezies. Aus diesem Grund wurde die NADPH Produktion von *T. brucei* in den Mittelpunkt gestellt. In den meisten Eukaryoten ist der Pentose Phosphatweg (PPP) die Hauptquelle für cytoplasmatisches NADPH. In *T. brucei* ist der Pentose Phosphatweg sowohl im Zytoplasma als auch den Glykosomen zu finden. Bedenkt man das Fehlen von Glucose im Insektenwirt ist die Glucose 6-Phosphat (G6P) Abhängigkeit des Pentose Phosphatwegs ein Problem für den Parasiten.

Aus diesem Grund haben wir eine mögliche Redundanz der NADPH Produktion im Bezug auf sich ändernde Kohlenstoffquellen untersucht. Das Genom von *T. brucei* weist jeweils zwei potentielle NADPH-Quellen für das Zytoplasma, das Mitochondrium und auch die Glykosomen auf. Wir haben den PPP und das zytoplasmatische Malatenzym (MEc) im Bezug auf ihren Beitrag zur oxidativen Stressabwehr im Zytoplasma analysiert. Sie waren komplett redundant in Sachen NADPH Produktion. Jeder der beiden Wege war ausreichend um gleiche Mengen reaktiver Sauerstoffspezies im Zytoplasma abzubauen. Die parallele Aktivität beider Wege führte zu keiner höheren oxidativen Stress Resistenz. Überraschenderweise produzierte der PPP auch NADPH in Abwesenheit von Glucose. Wir konnten zeigen, dass dieser Flux durch Glukoneogenese, ausgehend von Prolin, gespeist wird.

Eine ähnliche Situation findet sich in den Glykosomen, mit dem PPP und einer Isocitrat-dehydrogenase (IDHg) als möglichen NADPH Produzenten. Bisher war die Rolle von glykosomalem NADPH unklar. Daher haben wir potentielle NADPH konsumierende Stoffwechselwege auf ihre Aktivität und glykosomale Lokalisation untersucht. Unter anderem wurde der Parasit auf β-Oxidation Aktivität analysiert. Sowohl das einzige Kandidatengen für β-Oxidation, als auch die Dynamik des Lipidtröpfchen Auf- und Abbaus wurden untersucht. Unsere Ergebnisse machen glykosomale β-Oxidation unwahrscheinlich. Im Mitochondrium macht die Essentialität des Malatenzyms (MEm) eine Redundanz mit der Isocitratdehydrogenase (IDHm) fraglich. Momentan ist die IDHm Bestandteil weiterführender Experimente.

Wir konnten eine essentielle Funktion für die IDHg in der Stadien Differenzierung zeigen. Dies führte zu einer detaillierteren Analyse des Differenzierungsprozesses und dem Einfluss von NADPH und Kohlenstoffquellen auf diesen. Eine ΔIDHg Mutante war nicht in der Lage die Speicheldrüsen der Fliege zu besiedeln. Diese und weitere Deletionsmutanten wurden daraufhin in einem neuen Kultur Differenzierungssystem untersucht. Die ΔIDHg Mutante zeigte den gleichen Phänotypen wie zuvor in den Fliegenexperimenten. Ein ähnlicher Effekt auf die Differenzierung wurde durch die Zugabe von Glucose oder Glycerol verursacht, welche wir als metabolische Regulatoren der Differenzierung identifiziert haben. Die Deletionsmutante der Aconitase (ACO) zeigte einen noch stärkeren Phänotypen. Die Gründe hierfür sind noch nicht identifiziert. Zusammenfassend postulieren wir einen Stoffwechselweg zur Bereitstellung glykosomalen NADPHs, um die Biosynthese von Etherlipiden zu gewährleisten. Dies ist Ziel weiterer Experimente.

1. Introduction

1.1 *Trypanosoma brucei* in a nutshell

Trypanosoma brucei is a unicellular, eukaryotic protozoan parasite belonging to the class of Kinetoplastida. The eponymous structure for this class is the highly organized and densely packed mitochondrial DNA, the kinetoplast. This structure resides within the single elongated mitochondrion close to the basal body of the flagellum (Robinson and Gull, 1991). Other species belonging to this class are *Leishmania*, *Crithidia, Leptomonas* and *T. cruzi*, which is the causative agent of the chagas disease in South America. The geographic distribution of *T. brucei* is governed by the occurrence of its insect host, the Tsetse fly from the *Glossina spp.* and hence limited to sub-Saharan Africa as indicated in Fig.1. Thus the Tsetse fly limits the distribution of *T. brucei*, although it can reside in a wide spectrum of mammals including wild and domestic animals. There are three subspecies of *T. brucei* of which two are pathogenic to humans: *T. b. gambiense* and *T. b. rhodesiense* cause Human African Trypanosomiasis (HAT) whereas *T. b. brucei* causes Nagana in other mammals. The non-pathogenicity of *T. b. brucei* is attributed to the lytic effect of a human lipoprotein (Vanhamme et al., 2003).

Research in *T. brucei* lies beyond the obvious medical interest as many aspects of this parasite make it an ideal model organism. In contrast to other eukaryotic parasitic model organisms, *T. brucei* is relatively easy to culture *in vitro* (Brun and Schonenberger, 1979; Hirumi and Hirumi, 1989) and quite amenable to genetic manipulations, enabling the use of reverse genetic methods and thus the construction of knockout and knockdown mutants (Bringaud et al., 2000; Carruthers et al., 1993; Li and Gottesdiener, 1996; McCulloch et al., 2004; Ngo et al., 1998; ten Asbroek et al., 1990). The availability of the genome sequence (Berriman et al., 2005) has strongly facilitated research on *T. brucei*. Next to the methodological advantages, working with *T. brucei* brings along a lower risk for the researcher, as a non-pathogenic subspecies exists.

As mentioned above, several widespread pathogens belong to the same class and knowledge gained in *T. brucei* research can partially be transferred to other parasites and facilitate research on these. This includes for example *T. cruzi*, the cause of Chagas disease in South America, with about 7-8 million people being infected (WHO, March 2014) or human pathogenic *Leishmania spp.*, occurring in southern Europe, Africa, the Middle East, Asia and Central/South America with more than a million cases (WHO, January 2014). *T. brucei* has a big medical and economical impact in the affected areas, and is one of several so called neglected tropical diseases (WHO). Animal African Trypanosomiasis (AAT), caused by *T. b. brucei* and *T. congolense*, inflicts agricultural and domestic production drastically. About 60 million people live in the Tsetse belt at the risk of being infected with *T. brucei* (Fig.1) and acquiring Human African Trypanosomiasis (HAT), also known as sleeping sickness.

In addition to a better molecular understanding of *T. brucei*'s cell biology research on this parasite has also contributed to the elucidation of conserved biological processes. This is best illustrated by our current knowledge of glycosylphosphatidylinositol (GPI) anchors. GPI anchors are present in a variety of organisms, but were first described in *T. brucei* owing to their high abundance on the membrane surface anchoring the variable surface glycoproteins (VSG) of the bloodstream form (BSF) (Ferguson et al., 1999). VSG is the most abundant protein of the cell and plays a key role in one of the most intriguing immune response evasion mechanisms known as antigenic variation. This is probably the most famous mechanism discovered in *T. brucei* (Pays et al., 1981), reviewed in (Horn and McCulloch, 2010), and also existing in viruses, bacteria and other protozoa.

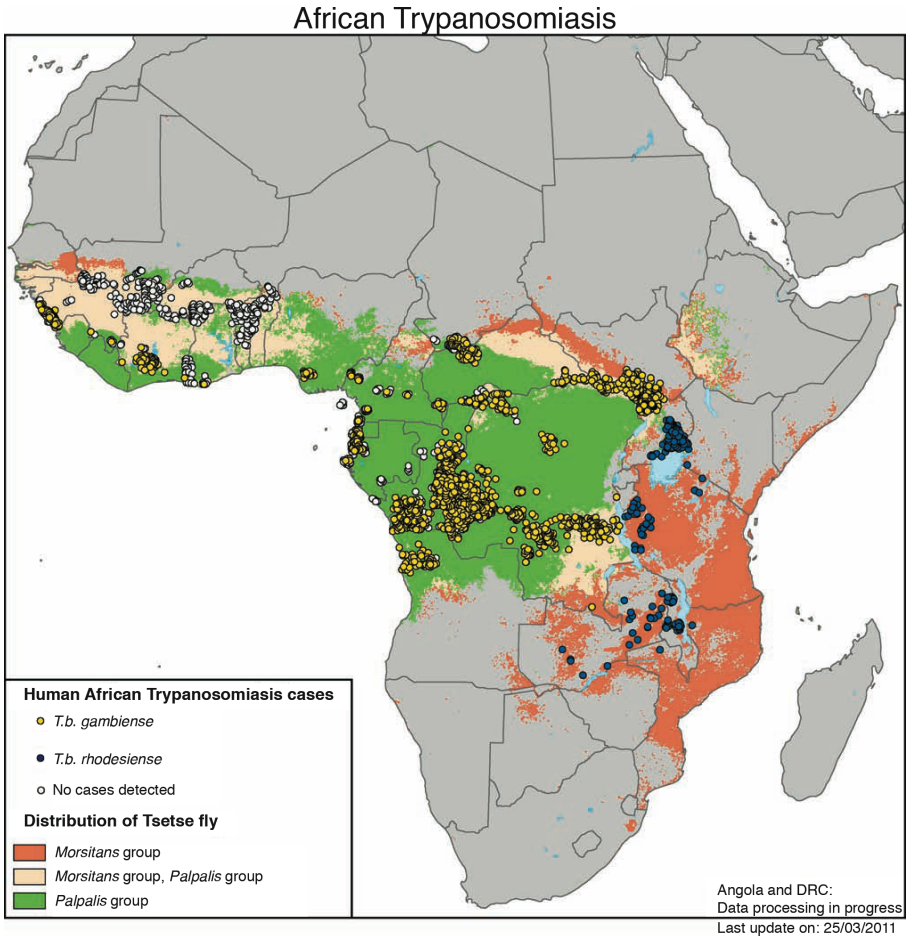

Fig.1: Geographic distribution of *T. brucei* caused Trypanosomiases and their insect vectors. (modified from: Atlas of Human Infectious Diseases; Wiley-Blackwell, 2012).

The treatment of HAT in the early stage, while the parasite still resides in the bloodstream, is easier than the late stage, when the parasite crosses the blood-brain barrier and resides in the central nervous system. Nevertheless available drugs are outdated, they often have extreme side effects, including death of the patient. In addition the prolonged application of the few available drugs leads to increased occurrence of resistances. Research on potential new drug targets and compounds suitable for treatment is one possibility. Another one is investigating the developmental insect stages and understanding the complex processes the parasite undergoes within the insect host. Elucidating the parasite-host interactions and identifying molecular triggers influencing the differentiation process, might reveal a possible Achilles heel, which can be targeted in the insect, and thus prevent transmission onto mammalian hosts.

1.2 The parasite's life cycle

T. brucei exhibits a complex life cycle involving several developmental stages (Fig.2) (Vickerman, 1985). The parasite's size, morphology, metabolism, surface proteins and more characterize these stages. Showing such a high diversity throughout the life cycle indicates the strong need for adaptation to the different hosts, but also to the different tissues within the hosts. Comparing the diversity between mammalian and insect host the high number of insect stages points out the complexity of the maturation within the Tsetse fly. The bloodstream form in the mammalian host has two distinct stages: the proliferating long slender (LS) and the cell cycle arrested short stumpy (SS). The latter already acquired features for survival in the Tsetse midgut.

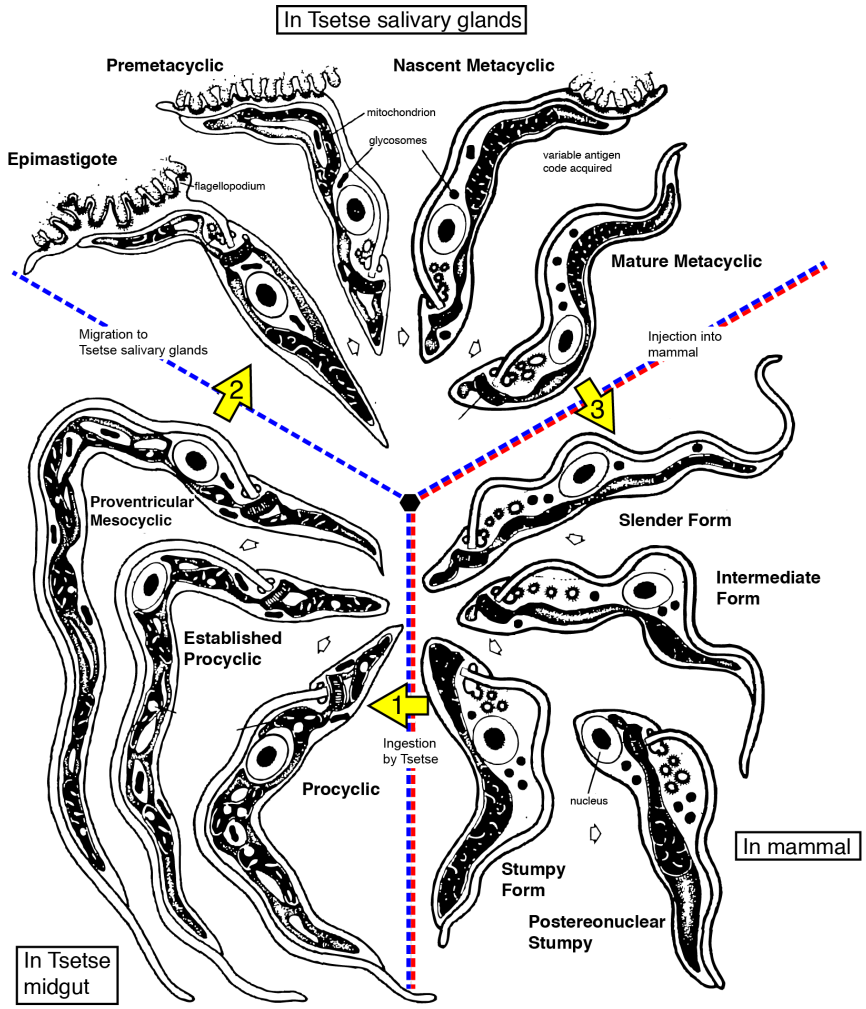

Fig.1: Life cycle of *Trypanosoma brucei*. (modified from Vickerman, 1985). Yellow arrows indicate transitions between hosts (1,3) or between tissues (2). The different stages are displayed in relative sizes. Changes in morphology and intracellular organization are visible.

The larger set of developmental stages within the insect displays the necessity for the parasite to migrate through several tissues before colonizing the salivary gland. This migration process is full of challenges, which have to be faced by adaptation. To date not many biochemical and molecular studies have been performed on the different insect stages, as so far only the procyclic stage could be cultured *in vitro*. In contrast to this the differentiation from BSF into the procyclic form (PCF) can be achieved under culture conditions. The differentiation process from the long slender to the procyclic form can be induced by the synergy of different triggers. First the formation of stumpy forms has to be induced, which happens similar to *quorum sensing* found in many microbes. In fact the first transformation from the LS BSF to the SS BSF is induced by a small molecular weight compound (<500 Da) named the Stumpy Induction Factor (SIF), which so far could not be identified (Reuner et al., 1997; Vassella et al., 1997). When stumpy formation took place, the differentiation into the PCF can be induced by addition of citrate or *cis*-aconitate, which can be facilitated by subjecting the parasites to lower temperatures (≤ 27°C) i.e. cold shock treatment (Engstler and Boshart, 2004). Meanwhile new components of this signaling pathway have been identified (Dean et al., 2009; Szoor et al., 2013; Szoor et al., 2010; Szoor et al., 2006), but still several more have to be elucidated in order to fully understand this complex process.

On the other hand the developmental maturation of the various stages within the Tsetse fly has so far not been characterized to the details of the BSF, as until recently the differentiation process could not be reproduced *in vitro*. The number of cells that can be isolated from Tsetse flies is low, thus limiting subsequent analytical methods. Experiments can be performed within Tsetse

fly populations looking for phenotypes and characteristics of mutant cell lines, but those experiments are tedious and often complicated to conduct and interpret. Recently it has been shown that the differentiation process can be initiated by the overexpression of a specific RNA binding protein (RBP6) *in vitro* (Kolev et al., 2012). Here Kolev and co-workers showed that RBP6 overexpression initiates the differentiation process from procyclic midgut forms to mature metacyclic forms usually present in the salivary glands of the Tsetse fly. For the first time other developmental fly stages than the PCF have been generated *in vitro* which will result in a more comprehensive understanding of this process within the next years.

1.3 Intermediate and energy metabolism

It is not unusual amongst parasitic organisms to exhibit metabolic pathways deviating from the classical textbook knowledge. They often show a very specific and streamlined energy metabolism in environments with stable carbon sources or a very high flexibility if the parasite has to adapt to diverse environments due to a change of host for example.

The metabolic capacities of BSF and PCF have been considered to be very different, but recent studies show that the metabolic complexity of BSF has been underestimated (Mazet et al., 2013). Nevertheless the BSF depends on glucose as main carbon source and rapidly dies in absence of glucose *in vitro*. In contrast the PCF can grow without glucose and utilize a number of alternative carbon sources. Surprisingly PCFs *in vitro* prefer glucose over proline, although it is not present or only at very low concentrations within the insect host, whereas proline is abundant in high amounts. Removing glucose from the medium increases the L-proline consumption of PCF cells by a factor of six (Lamour et al., 2005). Several independent observations indicate that it is the amount of glycolytic flux that influences proline consumption (unpublished data from the Bringaud lab, Bordeaux and this lab). Other carbon sources that are used for specific pathways are threonine or glutamate/glutamine (Cross et al., 1975; Linstead et al., 1977).

Taking a closer look at glucose utilization, the first seven steps of glycolysis (Fig.3; steps 1-7) are compartmentalized in a peroxisome-like organelle named the glycosome (Opperdoes and Borst, 1977). The fact that there is no negative feedback inhibition of the glycolytic enzymes phosphofructokinase (PFK) and hexokinase (HK) (Cronin and Tipton, 1985, 1987; Nwagwu and Opperdoes, 1982) necessitates their compartmentalization to prevent a lethal accumulation of intermediate metabolites and depletion of ATP (Haanstra et al., 2008), which would be a consequence of this turbo design of glycolysis (Teusink et al., 1998). The net ATP gain of glycolysis within the glycosomes is zero, which adds to the high glycolytic flux since there is no inhibition caused by an imbalance of the ADP/ATP ratio. The main control of the glycolytic flux is exerted by the hexose transporter and thus by the abundance of glucose (Bakker et al., 1997, 1999). The constant excess of glucose and this unique glycolytic design allows the BSF to excrete pyruvate instead of channeling it into the TCA cycle. Its additional oxidation and thus gain of ATP and NADH is hence not necessary. Recent data however revealed that mitochondrial acetate production is also essential in BSFs (Mazet et al., 2013). In this work the essentiality of pyruvate or threonine for acetate and subsequent *de novo* lipid synthesis has been shown for BSFs.

In order to reoxidize NADH, reduced during glycolysis within the glycosomes, the PCF has the option of the glycosomal succinate branch (Fig.3, steps 11-14), which is absent in the BSF. Therefore it has to make use of another pathway involving the Gly3P/DHAP shuttle (Fig.3, steps 17, 18). Here the mitochondrial FAD-dependent glycerol-3-phosphate dehydrogenase (G3PDH) is essential for the parasite (Skodova et al., 2013). The BSF has to use the Gly3P/DHAP shuttle in the glycosomal membrane, coupled to the respiratory chain by G3PDH to reoxidize NADH. When utilizing glucose as a carbon source, the PCF does not solely excrete pyruvate, but also produces acetyl-CoA via the pyruvate dehydrogenase (PDH) complex within the mitochondrion. This acetyl-

CoA is used to produce ATP via substrate level phosphorylation (Millerioux et al., 2013; Millerioux et al., 2012; Van Hellemond et al., 1998) and acetate to feed *de novo* lipid synthesis (Riviere et al., 2009).

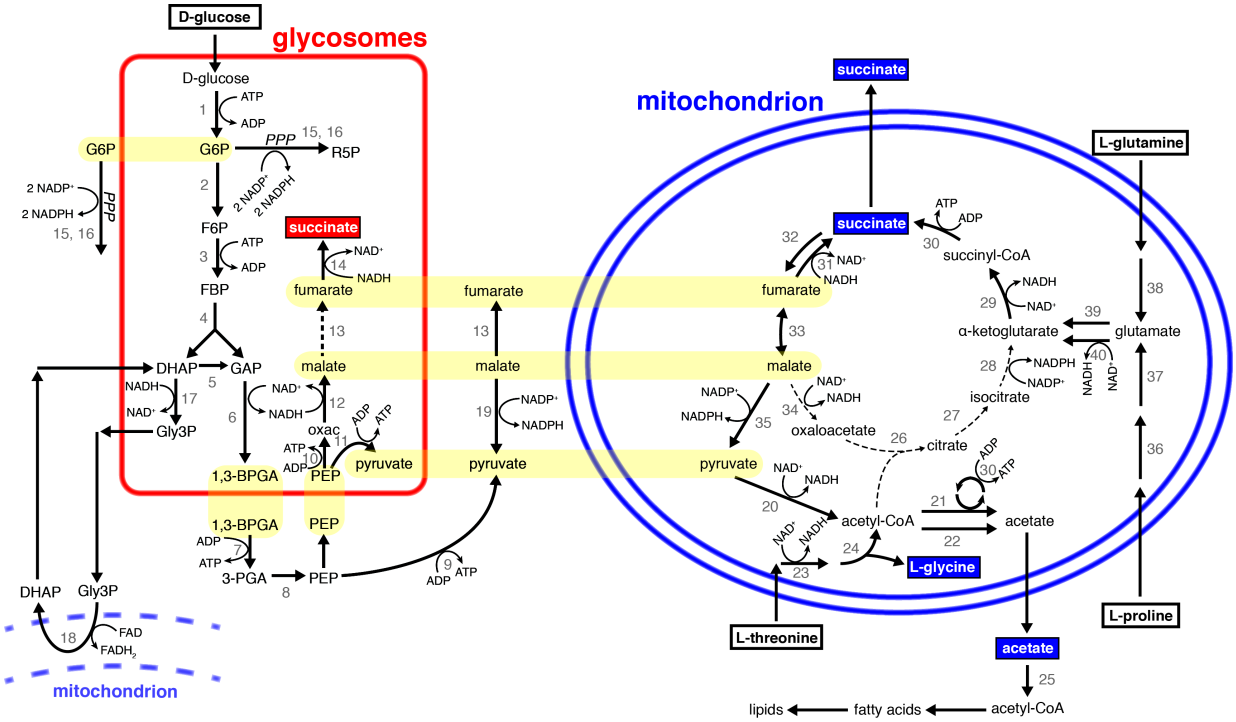

Fig.3: Schematic depiction of the intermediate energy metabolism in *T. brucei* PCFs. Dashed arrows represent reactions without experimental evidence. Yellow background symbolizes pools of metabolites shared between compartments. Black frames indicate carbon sources utilized by PCF. Filled rectangles indicate excreted end-products. Abbreviations: 1,3-BPGA: 1,3-bisphosphoglycerate; 3-PGA: 3-phosphoglycerate; DHAP: dihydroxyacetone phosphate; FBP: fructose 1,6-bisphosphate; F6P: fructose 6-phosphate; GAP: glyceraldehyde 3-phosphate; Gly3P: glyceraldehyde 3-phosphate; G6P: glucose 6-phosphate; oxac: oxaloacetate; PEP: phosphoenolpyruvate; PPP: pentose phosphate pathway; R5P: ribulose 5-phosphate; Enzymes are: 1, hexokinase; 2, glucose-6-phosphate isomerase; 3, phosphofructokinase; 4, aldolase; 5, triose-phosphate isomerase; 6, glyceraldehyde-3-phosphate dehydrogenase; 7, cytosolic phosphoglycerate kinase; 8a, phosphoglycerate mutase; 8b, enolase; 9, pyruvate kinase; 10, phosphoenolpyruvate carboxykinase; 11, pyruvate phosphate dikinase; 12, glycosomal malate dehydrogenase; 13, cytosolic (and glycosomal) fumarase; 14, glycosomal fumarate reductase; 15, glucose 6-phosphate dehydrogenase; 16, 6-phosphogluconate dehydrogenase; 17, glycerol-3-phosphate dehydrogenase; 18, mitochondrial FAD-dependent glycerol-3-phosphate dehydrogenase; 19, cytosolic malic enzyme; 20, pyruvate dehydrogenase complex; 21 acetate:succinate CoA-transferase; 22, Acetyl-CoA thioesterase; 23, threonine dehydrogenase; 24, acetyl-CoA:glycine C-acetyltransferase; 25, acetyl-CoA synthetase; 26, citrate synthase; 27, aconitase; 28, mitochondrial isocitrate dehydrogenase; 29, α-ketoglutarate dehydrogenase complex; 30, succinyl-CoA synthetase; 31, mitochondrial fumarate reductase; 32, succinate dehydrogenase; 33 mitochondrial fumarase; 34, mitochondrial malate dehydrogenase; 35 mitochondrial malic enzyme; 36, proline dehydrogenase; 37, pyrroline-5 carboxylate dehydrogenase; 38, glutamine deaminase; 39, glutamate aminotransferase; 40, glutamate dehydrogenase;

When proline is utilized, it enters the TCA cycle as α-ketoglutarate and is further oxidized to succinate in the mitochondrion, which is excreted (van Weelden et al., 2003; van Weelden et al., 2005). In the absence of glucose proline is oxidized to malate, which is subsequently utilized in the mitochondrion, the cytosol or the glycosomes (Coustou et al., 2008). In the absence of glucose and therefore a lack of substrate phosphorylation, the succinate dehydrogenase (Fig.3, step 32) as link to the oxidative phosphorylation becomes essential (Coustou et al., 2008). Despite the fact that the PCF utilizes glucose up to acetyl-CoA derived from it, they do not feed the TCA cycle from glucose. This has been shown by monitoring the incorporation of radiolabeled glucose, which did not lead to the production of radiolabeled CO_2 (van Weelden et al., 2003). The possibility of glucose-derived citrate or isocitrate cannot be excluded from these data as the first decarboxylation takes place during the conversion of isocitrate into α-ketoglutarate.

The TCA cycle genes are not only present in the *T. brucei* genome (Berriman et al., 2005) but several enzymatic activities and/or proteins have been detected (Durieux et al., 1991; Vertommen et al., 2008). These findings pose the question why all TCA cycle genes are present and most of

them also expressed, but not essential in PCFs. An answer to this might be their role in later developmental stages and this will be addressed in the future with the new *in vitro* differentiation system mentioned above.

Excreting acetate or succinate as partially oxidized end products is a common adaptation of a wide spectrum of parasites such as amoeba, helminthes and diplomonads to their anaerobic environments (Bringaud et al., 2010). Trypanosomatids also utilize this strategy despite the absence of anaerobic environments during their life cycle. The insect stages are exposed to a hypoxic environment throughout, whereas the bloodstream forms have no lack of oxygen supply at all (Bringaud et al., 2010). Some details of the acetate metabolism in PCF trypanosomes have already been mentioned above. It is known that the compartmentalization of glycolysis and the glycosomal succinate fermentation lessen the importance of the oxidative phosphorylation and its ATP production (Besteiro et al., 2002; Coustou et al., 2003; Ebikeme et al., 2010). Due to the high glycolytic flux, substrate phosphorylation is sufficient to cope with the energy needs of the cell. The pyruvate derived from glucose hence enters the mitochondrion and is converted into acetyl-CoA by the PDH complex. The acetyl-CoA is then utilized by the joint reactions of an acetate:succinate-CoA transferase (ASCT) and the succinyl-CoA synthetase (SCoAS), yielding a molecule of ATP and acetate from each acetyl-CoA (Millerioux et al., 2012; Riviere et al., 2004). Part of the acetate is excreted and part of it is utilized by the parasite for anabolic processes such as *de novo* lipid synthesis as mentioned earlier.

The most common mechanism delivering acetyl-CoA equivalents from the mitochondrion into the cytoplasm for *de novo* lipid synthesis is a mitochondrial citrate/malate transporter. Here citrate can be cleaved into oxaloacetic acid (OAA) and acetyl-CoA by a cytosolic citrate lyase (CL) feeding the *de novo* lipid synthesis. In *T. brucei* no mitochondrial citrate/malate shuttle has been identified to date. However, two unconventional tricarboxylic acid transporters with low sequence similarities have been predicted (Colasante et al., 2009), but biochemical evidence of their role is still missing. In chapter 5.1 we show that *de novo* lipid synthesis is dependent on acetate produced in the mitochondrion. It is exported into the cytosol and utilized by an acetyl-CoA synthetase (ACS) to supply acetyl-CoA (Riviere et al., 2009).

Glucose is however not the only source of acetyl-CoA. L-threonine is consumed at a very high rate in standard culture conditions and also contributes to acetate production (Cross et al., 1975; Linstead et al., 1977). Its contribution to acetate production and the subsequent incorporation into fatty acids and sterols is 2.5-fold higher than that of glucose (Millerioux et al., 2013). It has been shown that there is a second acetate-producing enzyme in addition to the ASCT. In contrast to ASCT the acetyl-CoA hydrolase (ACH) acetate production is uncoupled from ATP synthesis (Millerioux et al., 2012).

How acetate is transported through the membrane is still not known. Both carrier mediated and passive diffusion processes have been suggested, as observed in other organisms. In *E. coli* for example the acetate permeates through the membrane (Gimenez et al., 2003) and in *S. cerevisiae* acetate transfer is performed by transporters (Cassio et al., 1987). Another discussed, yet only putative function of the acetate export/diffusion out of the mitochondrion could be a contribution to the mitochondrial membrane potential. If the acetate is not transported in its anionic form but is protonated it is lipophilic and could permeate through membranes by diffusion (Kihara and Macnab, 1981). As a weak acid it would release its proton, contributing to the electrochemical proton gradient of the mitochondrial membrane (Michels et al., 1979; ten Brink and Konings, 1986). The mechanism of acetate export is yet to be investigated in more detail, so far no mitochondrial monocarboxylate transporter has been identified (Colasante et al., 2009).

1.4 NADPH balance

NADPH is another important reducing equivalent, in a addition to the aforementioned NADH (chapter 1.3), and plays a crucial role in a number of cellular processes such as: sterol synthesis, fatty acid synthesis, β-oxidation of unsaturated fatty acids or the detoxification of reactive oxygen species (ROS). In most eukaryotes, homeostasis of the NAD^+/NADH and $NADP^+$/NADPH balances is linked by transhydrogenases (EC 1.6.1.1). These enzymes can compensate an imbalance by transferring electrons from one system to the other. This level of flexibility is absent in *T. brucei* as no transhydrogenases have been identified in its genome (Berriman et al., 2005).

This is surprising for a parasitic organism that has to face oxidative stress throughout the different life cycle stages. BSFs have to face oxidative bursts from the innate immune system of mammals while PCFs are confronted with ROS residing in the proventriculus on their way from the midgut to the salivary glands (Hao et al., 2003). The ability to cope with ROS is therefore essential for survival of *T. brucei*. In *T. brucei* superoxide dismutases degrade primary ROS such as $O_2^{\bullet-}$ or $^{\bullet}OH$ into H_2O_2 (Dufernez et al., 2006; Wilkinson et al., 2006), which is then detoxified by catalases or the glutathione system in other eukaryotes. *T. brucei* possesses an equivalent of the latter known as the trypanothione system but catalases are absent (Berriman et al., 2005). The trypanothione system is similar to the glutathione system except that the trypanothione named molecule results from the condensation of two glutathione and one spermidine molecules (Fairlamb et al., 1985). The cascade responsible for the detoxification of ROS involves in addition to trypanothione a number of dithiol redox proteins (Krauth-Siegel and Comini, 2008) depicted in Fig.4. This cascade is responsible for the detoxification of H_2O_2 and for the production of deoxyribonucleotides. As a result, interfering with it is lethal for *T. brucei* (Arrick et al., 1981; Comini et al., 2007; Huynh et al., 2003; Krieger et al., 2000).

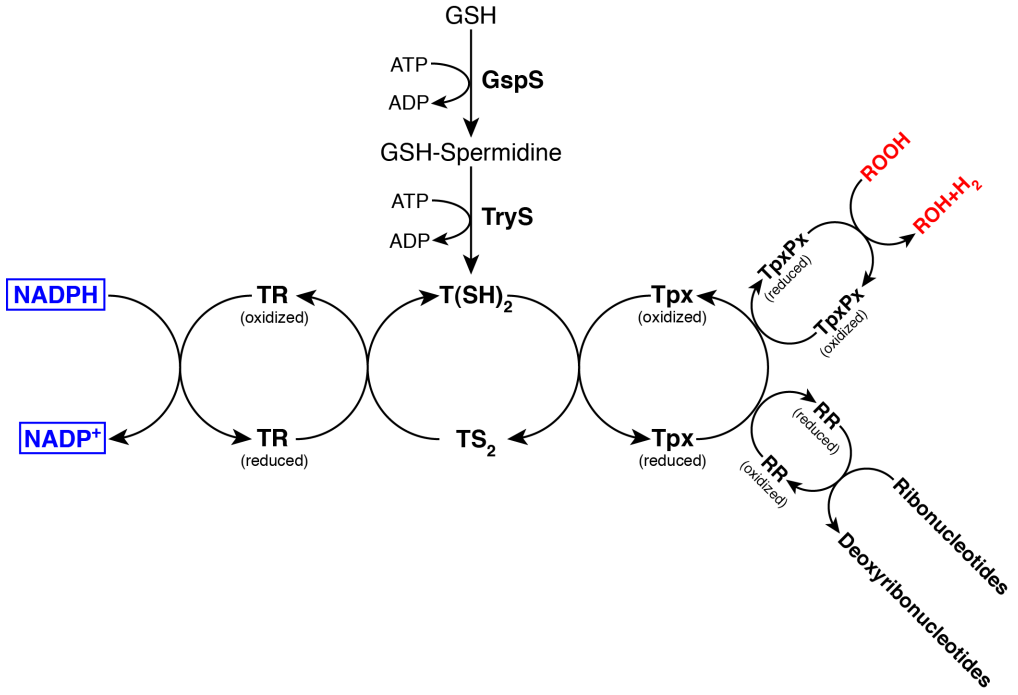

Fig.2: The trypanothione cascade of *T. brucei*. (modified from Krauth-Siegel and Comini, 2008) Abbreviations: GSH: glutathione; GspS: glutathione-spermidine synthase; TryS: trypanothione synthase; TR: trypanothione reductase; $T(SH)_2$: trypanothione (reduced); TS_2: trypanothione (oxidized); Tpx: tryparedoxin; TpxPx: tryparedoxin peroxidase RR: ribonucleotide reductase; ROOH: peroxides;

Considering the dependency of this cascade on the availability of NADPH implies that its depletion has the same effect as interfering with the cascade itself. Taking a look at the possible NADPH producing pathways, we find two alternatives for each subcellular compartment. In the glycosomes,

two steps of the pentose phosphate pathway (PPP) produce NADPH: the glucose-6-phosphate dehydrogenase (G6PDH) and the 6-phosphogluconate dehydrogenase (6PGDH). In addition there is a glycosomal isocitrate dehydrogenase (IDHg) (Colasante et al., 2006) as putative NADPH source.

Within the mitochondrion, a $NADP^+$-dependent IDHm and the mitochondrial malic enzyme (MEm) reside as NADPH sources. Both the PPP and malic enzyme (MEc) are also localized in the cytosol, hence producing cytosolic NADPH (Duffieux et al., 2000; Heise and Opperdoes, 1999). Changing hosts and the subsequent switch between available carbon sources could cause a detrimental effect on the NADPH balance. The PPP is dependent on the glucose-derived glucose-6-phosphate (G6P) meaning that the newly differentiated PCF, residing in the fly midgut, is faced with a sudden absence of glucose and hence a lack of NADPH production. This could be the time when the MEc becomes necessary as a backup system for NADPH production as it can be fed with malate produced from proline, present in the fly hemolymph. The NADPH is required for the regeneration of oxidized trypanothione by trypanothione reductase (TR) in the cytosol. The reduced trypanothione is then transported to the other subcellular compartments (Krauth-Siegel and Comini, 2008; Smith et al., 1991).

The roles of the cytosolic NADPH producing pathways were therefore investigated in detail in chapter 2. The same problem arises for the glycosomal NADPH production in the absence of glucose to feed the PPP. Here the glycosomal isocitrate dehydrogenase (IDHg) could serve as backup system. There are a number of potential NADPH dependent pathways residing in the glycosomes. Thus a closer look at the possible NADPH consuming pathways has to be taken, in order to understand the relevance of a potential backup system. One putative glycosomal NADPH consumer is the β-oxidation of unsaturated fatty acids. In plants and eukaryotic microorganisms like yeast, β-oxidation takes place in the peroxisomes (van den Bosch et al., 1992). In mammalian cells, the β-oxidation pathway is also present in the mitochondria. In the yeast *S. cerevisiae* a peroxisomal IDH has exactly this function. In the absence of other carbon sources (other than unsaturated fatty acids) a null mutant of the *IDP3* gene, a peroxisomal IDH, displays a growth arrest (Henke et al., 1998). In detail, after the activation of the fatty acid by forming a thioester with Co-enzyme A (CoA), four subsequent reactions are necessary to shorten the acyl chain and produce one molecule of acetyl-CoA (Mannaerts and Van Veldhoven, 1993)(Fig.5).

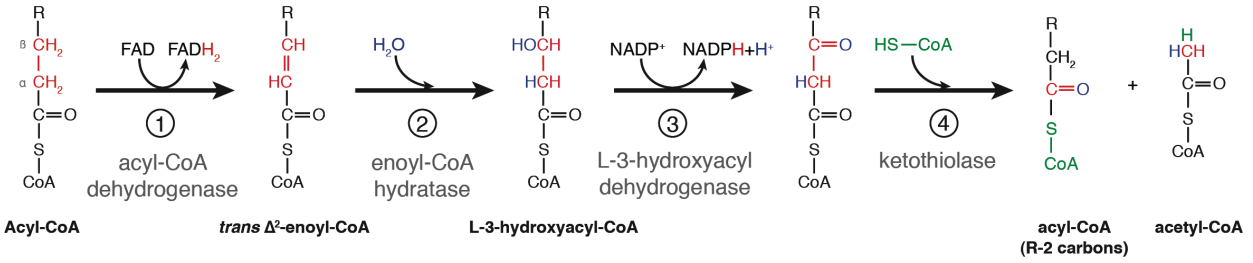

Fig.3: Schematic representation of the β-oxidation steps. red: indicates initial carbon and hydrogen atoms of the fatty acid; blue: indicates added oxygen and hydrogen atoms; green: indicates activation of the fatty acid by CoA. In most eukaryotes step 3 is NAD^+-dependent, but in *T brucei* the detected activity was $NADP^+$-dependent (Wiemer et al., 1996).

Two enzymatic activities involved in β-oxidation have been found to be present in the glycosomes of *T. brucei* (Wiemer et al., 1996) suggesting the presence of glycosomal β-oxidation. The β-oxidation of saturated fatty acids is however of minor interest in correlation with NADPH since no reducing equivalents are required here. In contrast the β-oxidation of unsaturated fatty acids requires reducing equivalents for one of two additional enzymatic steps. The double bond requires an isomerase and a reductase reaction (Fig.6, steps 2,5,6) of which the reductase requires NADPH, which could be delivered by the IDHg in the absence of glucose.

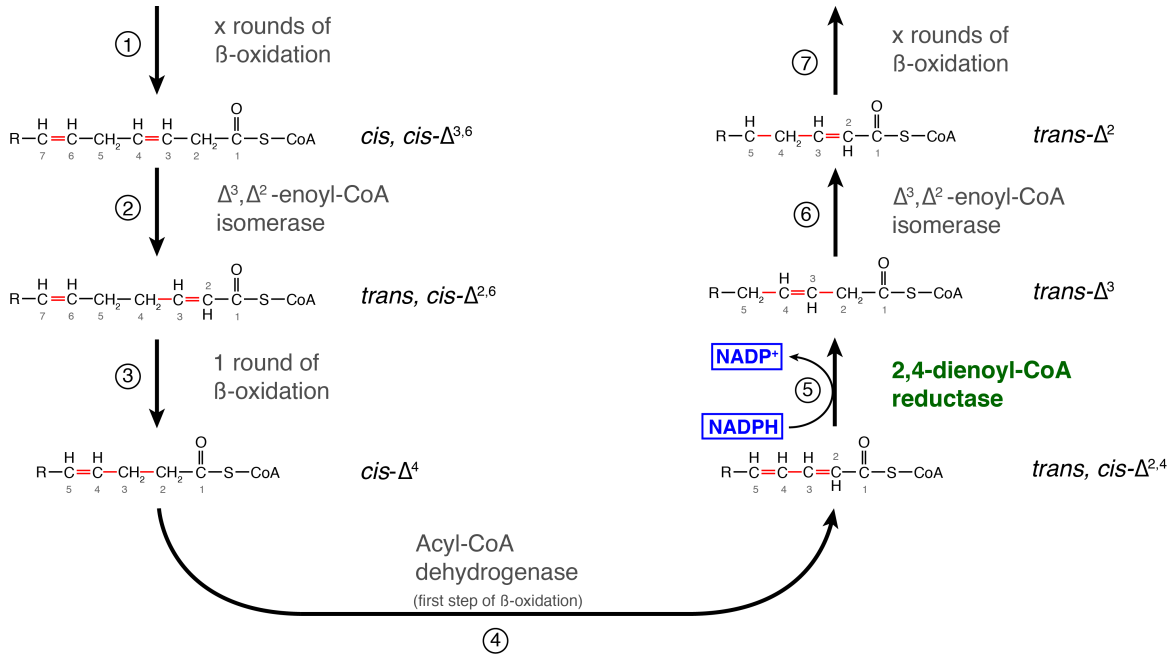

Fig.4: Schematic representation of the β oxidation of unsaturated fatty acids. Only steps required due to unsaturated double bonds are depicted. Next to the molecules the number, position and kind of double bonds are indicated by cis, trans, a number and Δ. The carbon atoms are numbered, whereat 1 corresponds to the alpha and 2 to the beta carbon atom.

Recent data indicate an important role for CoA-activated fatty acids within the glycosomes in the absence of glucose (Igoillo-Esteve et al., 2011). Hence their involvement in β-oxidation is likely. It has been shown that a member of a glycosomal ABC-transporter family is involved in the import of oleoyl-CoA into glycosomes. Downregulation of this transporter (GAT1) had no effect on cell growth in presence, but was lethal in absence of glucose (Igoillo-Esteve et al., 2011). The possible lack of carbon sources during maturation in the fly could necessitate the use of stored lipids as an energy source and thus the requirement of NADPH for utilization of unsaturated fatty acids.

Another potential NADPH consuming pathway is the synthesis of ether-linked lipids. The initial steps of this anabolic pathway are usually located within the peroxisomes in mammals, namely the dihydroxyacetone phosphate (DHAP) pathway (Hajra and Bishop, 1982) (Fig.7). The initial steps have also been identified in *T. brucei*, where the activities of the DHAP-acyltransferase (Fig.7, step 1) and the 1-Alkyl-DHAP synthase (Fig.7, step 2) have been found to be present within the glycosomes (Opperdoes, 1984; Zomer et al., 1999; Zomer et al., 1995). The presence of those activities is of course no proof of an active ether-linked lipid synthesis in *T. brucei*. However *T. brucei*'s lipidome contains ether-linked lipids and some mutants show decreased abundance of them (Patnaik et al., 1993; Voncken et al., 2003). The possible advantage of having ether-linked phospholipids in the plasma membrane is their higher chemical stability compared to ester-bonds. This could be advantageous when facing oxidative environments or organs with extreme pH values where ester-bonds would be more prone to hydrolysis (Aussenac et al., 2005). Studies on archaeal membranes have shown that their high content of ether-linked lipids creates higher bilayer stability and a decreased permeability (Dannenmuller et al., 2000; Shinoda et al., 2004). Thus the lipid composition can be important for the migration within the insect host since the parasite is subjected to lower temperatures and elevated stresses, including ROS and high pH values. In fact PCFs contain a significantly higher fraction of ether-linked lipids than BSFs (Patnaik et al., 1993). It should be noted that the proventriculus was shown to have a pH of 10.6 (Liniger et al., 2003), which indeed can favor cells with a higher ether-linked lipid content in the membrane, being more resistant to basic hydrolysis.

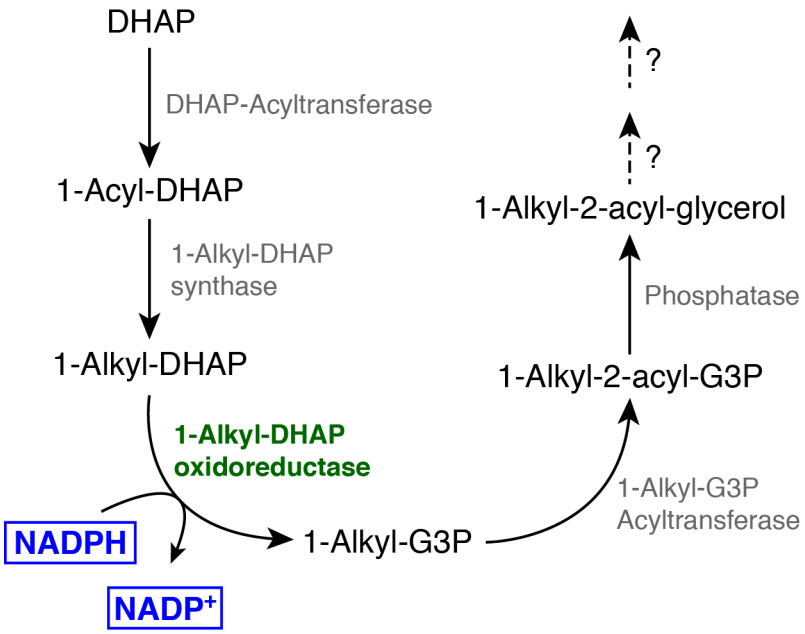

Fig.5: Schematic representation of the DHAP pathway. The first two steps have been identified and localized to the glycosomes. The oxidoreductase step is discussed (Michels et al., 2006)

1.5 Lipid droplets as energy storage

The conversion of fatty acids and sterols into neutral lipids followed by their storage as a source of energy is a process conserved from prokaryotes to eukaryotes (Murphy, 2012). The structure of these storage organelles is comprised of a phospholipid monolayer surrounding predominantly triacylglycerols and cholesteryl esters. The monolayer contains additional associated proteins, which are involved in the dynamic biogenesis of the organelle, reviewed in (Martin and Parton, 2006). *In vitro* accumulation of lipid droplets (LD) has been observed in *T. brucei* but only upon treatment with a serine palmitoyltransferase inhibitor (Flaspohler et al., 2010; Fridberg et al., 2008), causing a severe cytokinesis phenotype as side effect.

In vivo a change in number and size of LDs could be observed when analyzing trypanosomes isolated from Tsetse flies (Steiger, 1973). In this work an ultrastructural analysis of the changes in subcellular structures during development in the Tsetse fly has been undertaken. Amongst others it could be observed that a larger type of LDs occurs during development of established midgut forms compared to BSFs. The quite abundant LDs decreased in parasites isolated from the proventriculus and disappeared in the following stages.

This indicates a role for these storage organelles during the migration in the fly host. The use of stored lipids could help to overcome starvation during migration of the parasite through the insect, especially in regions of limited carbon sources. This becomes more interesting when considering recent data, where it has been shown that motility is essential for *T. brucei* to establish an infection. Mutant parasites with a clear motility phenotype were not able to develop to the epimastigote form (Rotureau et al., 2013).

In mammals the process of LD formation or degradation is highly regulated and dynamic. The catabolism of LD is regulated by a signaling cascade involving G-protein coupled receptors (GPCR), adenylate cyclases and protein kinase A which phosphorylates proteins like lipases or perilipins (Brasaemle et al., 2000; Brasaemle et al., 2009). The degradation of LD in *T. brucei* is very likely to be completely different. First there are no GPCRs (Berriman et al., 2005) and second the PKA-like kinase in *T. brucei* is not cAMP activated (unpublished data, Boshart lab). This complicates

the analysis of LD kinetics, since no known LD degradation pathway can be targeted by chemical inhibition or reverse genetics. This topic will be discussed in detail in chapter 4.

2. Cytosolic NADPH Homeostasis in Glucose-starved Procyclic *Trypanosoma brucei* Relies on Malic Enzyme and the Pentose Phosphate Pathway Fed by Gluconeogenic Flux

NADPH is an essential co-factor for a multitude of biosynthetic pathways. Within these, one pathway has a more accentuated role for the parasite *T. brucei*, compared to other organisms. This is the trypanothione system, the parasite's equivalent to the mammalian glutathione system, which relies on NADPH for regeneration. The parasite solely depends on NADPH in order to detoxify ROS, as it lacks a catalase and so far no transhydrogenases have been identified. According to the genome data, *T. brucei* possesses two putative NADPH producing pathways in each subcellular compartment, including the cytoplasm, the glycosomes and the mitochondrion. This redundancy could be the result of a necessary adaptation to available carbon sources, when shuttling between hosts. As ROS are encountered in both hosts and the PPP is depending on the availability of G6P, we hypothesize that the MEc serves as backup system in glucose-depleted environments to cope for a PPP with no or low activity due to a lack of substrate. This situation applies for the insect stages migrating towards the salivary glands. Hence we tested the importance of the two pathways in the cytoplasm for ROS detoxification depending on nutrient availability.

The Journal of biological chemistry, Allmann, S., Morand, P., Ebikeme, C., Gales, L., Biran, M., Hubert, J., Brennand, A., Mazet, M., Franconi, J. M., Michels, P. A., Portais, J. C., Boshart, M. & Bringaud, F. (2013) Cytosolic NADPH homeostasis in glucose-starved procyclic Trypanosoma brucei relies on malic enzyme and the pentose phosphate pathway fed by gluconeogenic flux.

doi: 10.1074/jbc.M113.462978.

3. Metabolic Control of Insect Stage Differentiation

In the previous chapter we demonstrated the redundancy of cytoplasmic NADPH producing pathways and carbon source dependent flux redistribution. The glycosomal NADPH production might be regulated in the same way. Similar to the cytosolic situation, one of the two pathways is the PPP, depending on G6P. The other putative NADPH producer is a glycosomal isocitrate dehydrogenase (IDHg). First experiments did not reveal any obvious phenotypes in culture. But in the light of a recent publication, which demonstrated in culture differentiation of insect stages for the first time (Kolev et al., 2012), we investigated this mutant for its differentiation capability and the effect of available carbon sources on the differentiation process itself. We show that the presence or absence of specific carbon sources has a strong impact on the stage differentiation, as well as null mutants in a postulated pathway delivering glycosomal NADPH. This pathway involves the mitochondrial enzymes citrate synthase (CS), aconitase (ACO), IDHm and the glycosomal enzyme IDHg. The null mutants of ACO and IDHg display a strong phenotype in the culture differentiation, whereas the ΔCS and ΔIDHm null mutant reveal no or a minor block in differentiation.

3.1 Carbon Source Regulated Glycosomal NADPH Production is Essential for the Developmental Cycle of *Trypanosoma brucei* in the insect

Stefan Allmann[1], Nicole Ziebart[1], Jean-William Dupuy[2], Marc Bonneu[2], Frederic Bringaud[3], Jan Van Den Abbeele[4] and Michael Boshart[1]*

[1]*Fakultät für Biologie, Genetik, Ludwig-Maximilians-Universität München, Biozentrum, Grosshadernerstrasse 2-4, D-82152 Martinsried, Germany*

[2]*Centre de Génomique Fonctionnelle, Plateforme Protéome, Université de Bordeaux, 146 rue Léo Saignat, 33076 Bordeaux, France*

[3]*Centre de Résonance Magnétique des Systèmes Biologiques (RMSB), UMR5536, Université de Bordeaux, CNRS, 146 rue Léo Saignat, 33076 Bordeaux, France*

[4]*Institute of Tropical Medicine Antwerp (ITM), Dept. Biomedical Sciences, Nationalestraat 155, B-2000 Antwerp, Belgium*

Manuscript

*To whom correspondence should be addressed:
Dr. Michael Boshart
Tel.: 49-89-2180-74600;
Fax: 49-89-2180-74629;
E-mail: boshart@lmu.de

Highlights

- Glucose and glycerol regulate differentiation of *T. brucei* insect stages
- Glucose regulates protein expression of citrate metabolism enzymes
- The glycosomal isocitrate dehydrogenase is essential for salivary gland colonization in the fly
- The glycosomal isocitrate dehydrogenase is essential for insect stage differentiation in culture

Summary

Migration and maturation within the insect host are challenging processes for *T. brucei*. They require the recognition of external signals. We took advantage of a new in culture differentiating system and identified glucose and glycerol as metabolic cues, regulating the differentiation process of the insect stages. In addition we demonstrated the regulation of protein expression and activity by glucose. We furthermore identified a glycosomal isocitrate dehydrogenase to be essential for differentiation in culture and in the insect host suggesting an important role of glycosomal NADPH production. This study shed some light upon the complex metabolic adaptations and cross-talk taking place during insect stage differentiation of *T. brucei*. Our data suggest a new metabolic pathway essential for differentiation. Furthermore we demonstrate that the in culture differentiation system is suitable to analyze putative phenotypes instead of performing fly experiments.

Introduction

Trypanosoma brucei, the causative agent of Human African Trypanosomiasis, exhibits a complex life cycle. The parasite uses Tsetse flies of the *Glossina spp*. as vector between mammalian hosts. Understanding the parasite-host interactions in more detail is essential for disease control.

So far knowledge about the intermediate stages occurring within the different tissues of the Tsetse alimentary tract is limited. This is owed to the fact that only one out of a number of insect stages could be cultured so far (Brun and Schonenberger, 1979). In addition the amount and quality of parasite material that can be gained from fly infections is insufficient for a variety of analytical methods. Nevertheless some regulatory mechanisms of importance for the stage development have been identified until today. It has been shown that innate as well as microbiome-regulated immune responses influence the infection and maturation (Hu and Aksoy, 2006; Weiss et al., 2013). The parasite also displayed enhanced maturation in nutritionally stressed flies due to decreased expression of specific immune genes (Akoda et al., 2009a; Akoda et al., 2009b). It is known that different tissues, like the proventriculus, constitute specific challenges for the parasite (Hao et al., 2003), indicating the necessity of adaptations triggered by external signals perceived by the parasite. The finding of a MAP kinase kinase (MKK1) being essential for salivary gland colonization but dispensible in both BSF and PCF *in vitro* (Morand et al., 2012) strongly supports this.

The stage development results in adaptations in metabolism as well as in morphology. A high morphological diversity within the insect stages can be observed (Van Den Abbeele et al., 1999; Vickerman, 1985). The differential surface protein expression of EP and GPEET on PCF cells indicated the cellular metabolism to be involved in marker expression during early stage differentiation as transducer. (Vassella et al., 2000; Vassella et al., 2004). Metabolic cues as triggers for differentiation are not unlikely. It can be seen in a number of organisms like *S. cerevisiae* (Broach, 2012; Cullen and Sprague, 2012) or *C. albicans* (Cullen and Sprague, 2000).Here, changing nutritional environments are linked to cellular differentiation.

In *T.* brucei the cross-talk between metabolic pathways utilizing different carbon sources has already been demonstrated with the examples of glucose repressing proline metabolism (Coustou et al., 2008; Lamour et al., 2005), or ablation of glycosomal NADH oxidation promoting proline metabolism (Ebikeme et al., 2010).

Metabolic regulation can go far beyond mere feedback inhibition within a pathway. In mammalian cancer cells metabolism has been shown to regulate cellular differentiation involving the intermediate metabolite 2-hydroxyglutarate (Dang et al., 2009; Martinez-Calvillo et al., 2010; Rohle et al., 2013; Sasaki et al., 2012). Furthermore other metabolites than 2-hydroxyglutarate also act as signal molecules. Succinate and fumarate were found to interfere with epigenetic and transcriptional regulation (Cai and Tu, 2012; Ito et al., 2010; Mills and O'Neill, 2014; Moran-Crusio et al., 2011; Quivoron et al., 2011). Succinate can also be found as posttranslational modification influencing a number of metabolic pathways like glycolysis and the TCA cycle (Park et al., 2013; Zhang et al., 2011).

Facing diverse environments and displaying a high variety of developmental stages we expect *T. brucei* also to inherit such a cross-talk between metabolism and differentiation. This can now be investigated due to a work from Kolev and coworkers (Kolev et al., 2012), enabling insect stage differentiation in culture by ectopic expression of the RNA-binding protein RBP6. We take advantage of this and analyze the influence of carbon source availability on the differentiation process.

Experimental procedures

Trypanosomes and Cell Cultures - The procyclic form of *T. brucei* EATRO1125 and AnTat 1.1 1313 was cultured at 27°C in SDM79 medium containing 10% (v/v) heat-inactivated fetal calf serum and 35 μg/mL hemin (Brun and Schonenberger, 1979). The SDM79 used for glucose-depleted growth was modified by omitting glucose and the addition of 50 mM N-Acetylglucosamine (GlcNAc), which is a non metabolized glucose analogue inhibiting glucose import (Allmann et al., 2013; Azema et al., 2004). For some experiments an additional SDM79 modification was the addition of 20 mM glycerol.

Execution of the fly infection experiments - Male *Glossina morsitans morsitans* flies from the colony at the Institute of Tropical Medicine (Antwerp, Belgium) were used in the trypanosome infection experiments. Experimental flies were maintained at 26±0.5°C and 65-75% relative humidity. Within 24-48 hours after their emergence, young flies were fed their first blood meal through *in vitro* membrane feeding on a mixture of saline-washed red blood cells (derived from commercially available defibrinated horse blood – E&O Laboratories) with procyclic trypanosomes in SDM79 medium (without antibiotics) at a final concentration of 5 x 10^6 parasites/ml. Fully engorged flies were selected and subsequently maintained for 28 days by feeding 3 times/week on a naïve rabbit. Then, midgut and salivary glands of the flies were dissected and microscopically examined (phase-contrast, 400x) for the presence of trypanosomes in the respective tissues. Animal ethics approval for the tsetse fly feeding on live animals was obtained from the Animal Ethical Committee of the Institute of Tropical Medicine, Antwerp (Belgium) (Ethical clearance n° PAR014-MC-K-Tryp).

Knockout of the IDHg gene - Replacement of the glycosomal isocitrate dehydrogenase (IDHg: Tb927.11.900) by the hygromycin (HYG) and neomycin (NEO) resistance markers via homologous recombination was performed with DNA fragments containing a resistance marker gene flanked by the IDHg UTR sequences. The IDHg knockout was generated in the AnTat 1.1 1313 parental cell line, which constitutively expresses the tetracycline repressor. The first and second IDHg alleles were replaced by hygromycin- and neomycin-resistance genes respectively. Transfected cells were selected in SDM79 medium containing 20% FCS, hygromycin B (25 μg/mL), neomycin (10 μg/mL), and phleomycin (2.5 μg/mL). The selected cell line (TetR-BLE ΔIDHg::HYG/ΔIDHg::NEO) is called ΔIDHg.

Knockout of the IDHm gene - Replacement of the mitochondrial isocitrate dehydrogenase (IDHm: Tb927.8.3690) by the hygromycin (HYG) and neomycin (NEO) resistance markers via homologous recombination was performed with DNA fragments containing a resistance marker

gene flanked by the IDHm UTR sequences. The IDHm knockout was generated in the AnTat 1.1 1313 parental cell line, which constitutively expresses the tetracycline repressor. The first and second IDHm alleles were replaced by hygromycin- and neomycin-resistant genes, respectively. Transfected cells were selected in SDM79 medium containing 20% FCS, hygromycin B (25 µg/mL), neomycin (10 µg/mL), and phleomycin (2.5 µg/mL). The selected cell line (TetR-BLE ΔIDHm::HYG/ΔIDHm::NEO) is called ΔIDHm.

Knockout of the CS gene – Replacement of the citrate synthase gene (CS: Tb927.10.13430) by the hygromycin (HYG) and neomycin (NEO) resistance markers via homologous recombination was performed with DNA fragments containing a resistance marker gene flanked by the CS UTR sequences. The CS knockout was generated in the AnTat 1.1 1313 parental cell line, which constitutively expresses the tetracycline repressor. The first and second CS alleles were replaced by hygromycin- and neomycin-resistant genes, respectively. Transfected cells were selected in SDM79 medium containing 20% FCS, hygromycin B (25 µg/mL), neomycin (10 µg/mL), and phleomycin (2.5 µg/mL). The selected cell line (TetR-BLE ΔCS::HYG/ΔCS::NEO) is called ΔCS.

Genetic rescue of the ΔIDHg knockout – Genetic rescues were created in the ΔIDHg C9 clone. The IDHg open reading frame was amplified by PCR and cloned into the pTSARib(PUR) backbone (Xong et al., 1998), as well as into the pHD309(PUR/HYG) backbone (Cross lab). Cloning into pTSARib was performed by HindIII/BamHI. For the pHD309(PUR/HYG) backbone the IDHg ORF was first cloned into pHD615 (Biebinger et al., 1997), where it was amplified with the adjacent PARP and VSG UTRs adding SmaI and SphI sites. This fragment was cloned into pHD309 using the SmaI and SphI site to replace the hygromycin resistance cassette.

Knockout of the IDHg gene for RBP6 differentiation – For the RBP6 *in vitro* differentiation experiments the knockout of IDHg has been created in the EATRO1125 procyclic form cell line (EATRO1125.T7T), constitutively expressing the T7 RNA polymerase gene and the tetracycline repressor under the control of a T7 RNA polymerase promoter for tetracycline-inducible expression (Bringaud et al., 2000), aiming for a high expression of RBP6. For gene replacement the constructs mentioned before were used with exchanged resistance markers. Here blasticidin (BLA) and puromycin (PUR) were used. The RBP6 gene was amplified by PCR and cloned into pLew100v5b1d via HindIII/BamHI.

Knockout of the CS gene for RBP6 differentiation – For the RBP6 *in vitro* differentiation experiments the knockout of CS has been created in the EATRO1125 procyclic form cell line (EATRO1125.T7T), constitutively expressing the T7 RNA polymerase gene and the tetracycline repressor under the control of a T7 RNA polymerase promoter for tetracycline-inducible expression (Bringaud, 2000), aiming for a high expression of RBP6. For gene replacement the constructs mentioned before were used with exchanged resistance markers. Here blasticidin (BLA) and puromycin (PUR) were used. The RBP6 gene was amplified by PCR and cloned into pLew100v5b1d via HindIII/BamHI.

Knockout of the IDHm gene for RBP6 differentiation – For the RBP6 *in vitro* differentiation experiments the knockout of IDHm has been created in the EATRO1125 procyclic form cell line (EATRO1125.T7T), constitutively expressing the T7 RNA polymerase gene and the tetracycline repressor under the control of a T7 RNA polymerase promoter for tetracycline-inducible expression (Bringaud, 2000), aiming for a high expression of RBP6. For gene replacement the constructs mentioned before were used with exchanged resistance markers. Here blasticidin (BLA) and puromycin (PUR) were used. The RBP6 gene was amplified by PCR and cloned into pLew100v5b1d via HindIII/BamHI.

Trypanosome transfection – The EATRO1125 procyclic form cell line (EATRO1125.T7T), constitutively expressing the T7 RNA polymerase gene and the tetracycline repressor under the control of a T7 RNA polymerase promoter for tetracycline-inducible expression (Bringaud et al., 2000), was the recipient of transfections as well as the AnTat 1.1 1313 cell line constitutively

expressing the tetracycline repressor (Alibu et al., 2005). Transfection and selection in SDM79 medium containing combinations of hygromycin B (25 μg/mL), neomycin (10 μg/mL), blasticidin (10 μg/mL), phleomycin (5 μg/mL for EATRO; 2.5 μg/ml for AnTat) and puromycin (1 μg/mL) followed previous reports (Riviere et al., 2004).

Enzymatic IDH assays – Cells were sonicated and centrifuged at 14.000 g for 10 min. The protein content of the supernatants was analyzed by a Bradford assay and 300-500 μg of total protein were used for a single measurement. The assays were performed according to (Overath et al., 1986), with the modification of an increased isocitrate concentration of 5 mM. The background activity was measured before adding the substrate (isocitrate) and has been subtracted from the total activity. For each biological replicate three technical replicates were measured and averaged.

Enzymatic CS assays – Cells were sonicated and centrifuged at 14.000 g for 10 min. Supernatant equivalent to $2x10^6$ cells was used for a single measurement. The reaction of the CS produces a coenzyme A, which has a free thiol group, in contrast to acetyl-CoA. This free thiol group reacts with 5,5'-dithiobis-(2-nitrobenzoic acid) (Ellman's reagent, or DTNB) by cleaving the disulfide bond and generating a NTB^{2-}dianion, which can be measured photometrically at a wavelength of 412 nm (Eidels and Preiss, 1970). The background activity was measured before adding the substrate (oxaloacetate)) and has been subtracted from the total activity. For each biological replicate three technical replicates were measured and averaged. Reaction carried out in: 50 mM Tris/HCl, 2 mM EDTA, pH 8.0; 0.1 mM oxaloacetate; 0.15 mM acetyl-CoA and 0.1 mM DTNB.

Microscopic analysis – The expression of RBP6 was induced by addition of tetracycline and samples were taken for 10 days. For each time point the developmental stage of >100 cells was determined according to size, morphology and relative positioning of nucleus and kinetoplast. About $1x10^7$ cells were concentrated in a volume of 10-20 μl and pipetted on one side of a microscope slide. The cells were distributed on the slide by pulling another slide in a 30° angle along the first slide, creating a smear of cells. These were dried at room temperature for at least 20 minutes and then fixed in MeOH at -20°C overnight or up to several days. Prior to DAPI staining the cells were rehydrated in PBS for 20 minutes. Then DNA staining was performed using 1 μg/ml 4,6-diamidino-2-phenylindole (DAPI). Incubation with DAPI was done for 5 min at RT. Two washing steps with PBS and one final washing step with dH_2O and subsequent embedding in Vectashield antifade medium before sealing were done.

Western blot analyses – Total protein extracts of the procyclic form of *T. brucei* ($2x10^6$ cells) were separated by SDS-PAGE (10%) and blotted on Immobilon-FL membrane (Millipore) (Harlow and Lane, 1988). Immunodetection was performed as described (Harlow and Lane, 1988; Sambrook et al., 1989) using as primary antibodies the monoclonal paraflagellar rod (PFR) mouse anti-serum L13D6 (1:2000) (Kohl et al., 1999), the monoclonal Ty1-tag mouse anti-serum BB2 (1:2000) (Bastin et al., 1996), the monoclonal heat shock protein 60 (HSP60) mouse anti-serum (1:10.000) (Bringaud et al., 1995), the polyclonal *αTb*PGKB rabbit anti-serum (1:5000) (P. Michels, Brussels), the polyclonal *αTb*PPDK rabbit anti-serum (1:2000) (Bringaud et al., 1995), the polyclonal *αTb*ASCT rabbit anti-serum (1:2000) (Riviere et al., 2004), the polyclonal *αTb*CS rabbit anti-serum (1:2000), the polyclonal *αTb*IDHg rabbit anti-serum (1:5000), and the polyclonal *αTb*IDHm rabbit anti-serum (1:2000). Infrared fluorescence detection was performed with an Odyssee scanner (LI-COR). The polyclonal rabbit anti-sera were detected by the goat anti-rabbit antibody IRDye680LT (1:25.000) (LI-COR). The mouse anti-sera were detected with the goat anti-mouse IRDye800 (1:10.000) (LI-COR). Affinity purification of the *αTb*CS serum did not improve the results. The unspecific bands were still observed.

Digitonin titration – AnTat 1.1 1313 cells were washed in PBS buffer and resuspended at $6.5x10^8$ cells (3.3 mg of protein)/ml in STE buffer supplemented with 150 mM NaCl and the CompleteTM Mini EDTA-free protease inhibitor mixture (Roche AppliedScience). Cell aliquots were

incubated for 4 min at 25 °C within increasing concentrations of digitonin, before being centrifuged at 14,000 g for 2 min, as described before (Marche et al., 2000).

Antibody raising – The antibodies from Pineda Antikörperservice (αCS, αIDHg, αIDHm) were raised against recombinant full length *T.* brucei protein expressed in *E. coli,* according to the standard protocol, but with differences in the immunization length. After the primary immunization (i.d., FCA), six boosts (s.c., FIA) followed until day 90. From day 90 on boosts followed every 14 days until the final bleed. Blood samples were taken at day 40, day 75, day 90 and beyond this every 30 days. Abbreviations: i.d., intradermal; s.c., subcutaneous; FCA, Freund's complete adjuvant; FIA, Freund's incomplete adjuvant. Immunization periods: αCS: animal 1, final bleed: 180th day; αIDHg: animal 2, final bleed: 145th day; αIDHm: animal 2, final bleed: 180th day.

Sample preparation for proteomic analysis - Samples were loaded on a 10% acrylamide SDS-PAGE gel. Migration was stopped when samples had just entered the resolving gel, proteins were visualized by Colloidal Blue staining, and the unresolved region of the gel cut into 1 mm x 1 mm gel pieces. Gel pieces were destained in 25 mM ammonium bicarbonate (NH_4HCO_3), 50% Acetonitrile (ACN) and shrunk in ACN for 10 min. After ACN removal, gel pieces were dried at room temperature. Proteins were first reduced in 10 mM dithiothreitol, 100 mM NH_4HCO_3 for 30 min at 56°C then alkylated in 100 mM iodoacetamide, 100 mM NH_4HCO_3 for 30 min at room temperature and shrunken in ACN for 10 min. After ACN removal, gel pieces were rehydrated with 100 mM NH_4HCO_3 for 10 min at room temperature. Before protein digestion, gel pieces were shrunken in ACN for 10 min and dried at room temperature. Proteins were digested by incubating each gel slice with 10 ng/µL of trypsin (T6567, Sigma-Aldrich) in 40 mM NH_4HCO_3, 10% ACN, rehydrated at 4°C for 10 min, and finally incubated overnight at 37°C. The resulting peptides were extracted from the gel by three steps: a first incubation in 40 mM NH_4HCO_3, 10% ACN for 15 min at room temperature and two incubations in 47.5 % ACN, 5% formic acid for 15 min at room temperature. The three collected extractions were pooled with the initial digestion supernatant, dried in a SpeedVac, and resuspended with 25 µL of 0.1% formic acid before nanoLC-MS/MS analysis.

NanoLC-MS/MS analysis - Online nanoLC-MS/MS analyses were performed using an Ultimate 3000 system (Dionex, Amsterdam, The Netherlands) coupled to a nanospray LTQ Orbitrap XL mass spectrometer (Thermo Fisher Scientific, Bremen, Germany). Ten microliters of each peptide extract were loaded on a 300 µm ID x 5 mm PepMap C_{18} precolumn (LC Packings, Dionex, USA) at a flow rate of 20 µL/min. After 5 min desalting, peptides were online separated on a 75 µm ID x 15 cm C_{18}PepMap™ column (LC packings, Dionex, USA) with a 2-40% linear gradient of solvent B (0.1% formic acid in 80% ACN) during 108 min. The separation flow rate was set at 200 nL/min. The mass spectrometer operated in positive ion mode at a 1.8 kV needle voltage and a 42 V capillary voltage. Data were acquired in a data-dependent mode alternating an FTMS scan survey over the range m/z 300-1700 with the resolution set to a value of 60 000 at m/z 400 and six ion trap MS/MS scans with Collision Induced Dissociation (CID) as activation mode. MS/MS spectra were acquired using a 3 m/z unit ion isolation window and normalized collision energy of 35. Mono-charged ions and unassigned charge-state ions were rejected from fragmentation. Dynamic exclusion duration was set to 30 sec.

Database search and results processing - Mascot and Sequest algorithms through Proteome Discoverer 1.4 Software (Thermo Fisher Scientific Inc.) were used for protein identification in batch mode by searching the Trypanosoma brucei TREU927 database (TritrypDB release 6.0, 90307 entries) at http://tritrypdb.org/. Two missed enzyme cleavages were allowed. Mass tolerances in MS and MS/MS were set to 10 ppm and 0.6 Da. Oxidation of methionine, acetylation of lysine and deamidation of asparagine and glutamine were searched as variable modifications. Carbamidomethylation on cysteine was searched as fixed modification. Peptide validation was performed using Percolator algorithm (Käll et al., 2007) and only "high confidence" peptides were retained corresponding to a 1% false positive rate at peptide level.

Label-Free Quantitative Data Analysis - Raw LC-MS/MS data were imported in Progenesis LC-MS 4.1 (Nonlinear Dynamics Ltd, Newcastle, U.K) for feature detection, alignment, and quantification. All sample features were aligned according to retention times by manually inserting up to two hundred landmarks followed by automatic alignment to maximally overlay all the two-dimensional (m/z and retention time) feature maps. Singly charged ions and ions with higher charge states than six were excluded from analysis. All remaining features were used to calculate a normalization factor for each sample that corrects for experimental variation. Peptide identifications (with $p < 0.01$, see above) were imported into Progenesis. For quantification, all unique peptides of an identified protein were included and the total cumulative abundance was calculated by summing the abundances of all peptides allocated to the respective protein. No minimal thresholds were set for the method of peak picking or selection of data to use for quantification. For each biological replicate, the mean normalized intensities and standard deviation were calculated and ratio was deducted. Noticeably, only non-conflicting features and unique peptides were considered for calculation at protein level. Quantitative data were considered for proteins quantified by a minimum of 2 peptides. As an indication of the confidence of that protein's presence, the sum of the peptide scores (confidence score) is calculated for each protein from the search algorithm. This score includes unique peptides as well as switched off peptides, the later decreasing the confidence score.

Results

T. brucei's stage development within the Tsetse fly is a complex process. The numerous stages display great morphological differences (Vickerman, 1985), and next to these also metabolic adaptations are crucial for the parasite. We are interested in these metabolic adaptations the parasite is undergoing. Our aim is the identification of metabolic signals perceived by the parasite and involved in the differentiation process.

Metabolic Cues Regulate T. brucei Insect Stage Differentiation

We used a culture differentiation system (Kolev et al., 2012) to differentiate procyclic (PCF) into metacyclic form (MF) parasites. We modified this by the utilization of glucose-depleted SDM79. The lack of glucose resembles a more physiological environment, as glucose is low or absent in the insect host. The kinetics of the differentiation was significantly faster under these conditions (Fig.1A) than reported before. After 4 days MF cells contributed about 30% of the total population. Representative pictures of the observed developmental stages are shown in Fig.1D. The cell morphology was assessed by DIC and the relative positioning of the nucleus and the kinetoplast by DAPI staining.

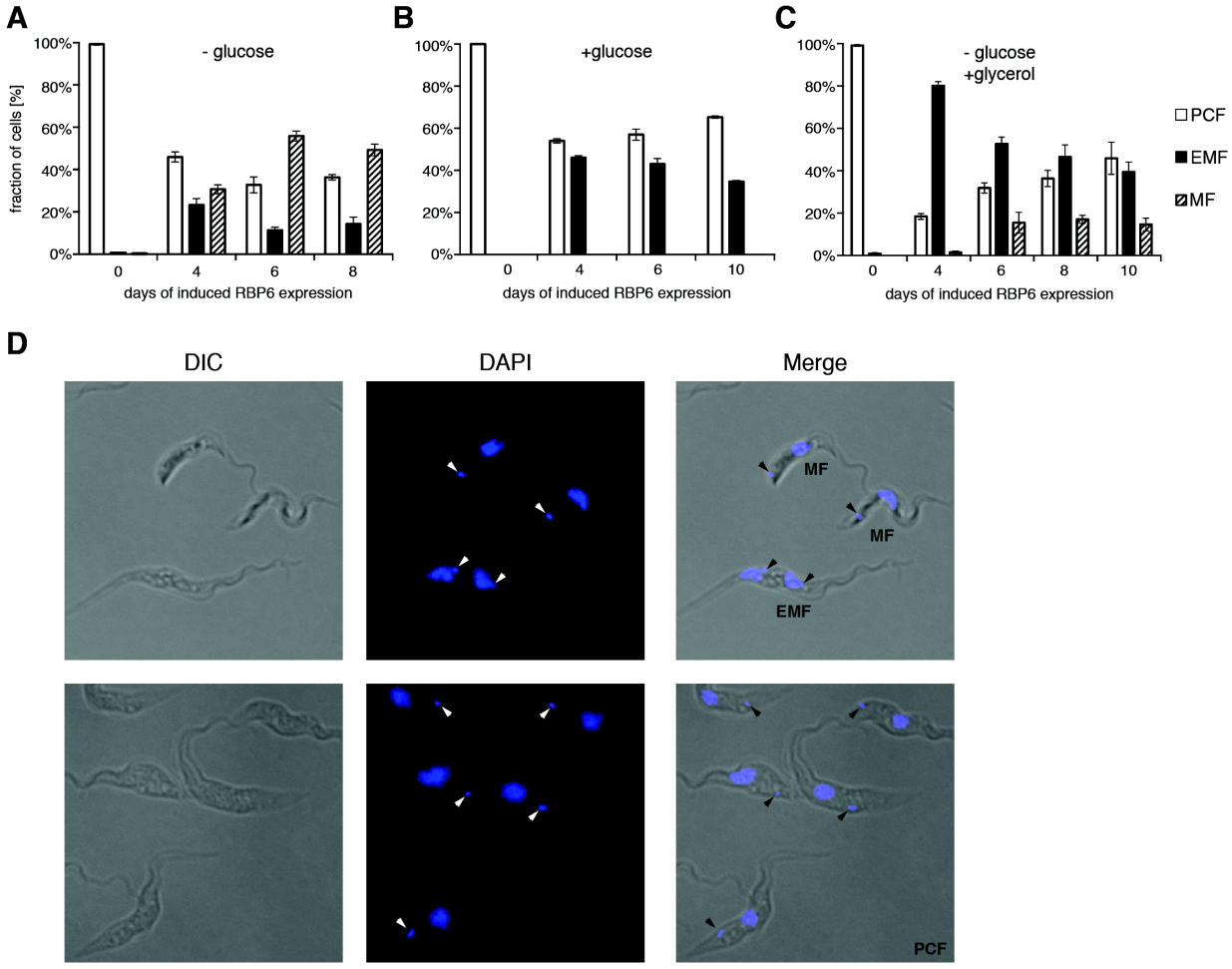

Fig.1: RBP6-induced differentiation in different nutritional environments. Differentiation of EATRO1125 cells in (A) glucose-depleted SDM79, (B) glucose-containing SDM79 and (C) glucose-depleted SDM79 including 20 mM glycerol. Error bars represent the SEM of (n=3) independent experiments. (D) Representative pictures of the different observed developmental stages are shown. DNA has been stained with DAPI. Arrowheads indicate the localization of the kinetoplast. MF: metacyclic form, EMF: epimastigote form, PCF: procyclic form.

The Cunningham's medium used by Kolev and coworkers contains more glucose compared to our SDM79 glucose-depleted medium. To demonstrate that glucose is the metabolic cue regulating the differentiation kinetics we added glucose to SDM79 glucose-depleted medium, and observed differentiation after 10 days to epimastigote forms (EMF) but no MF cells (Fig.1B). Here glucose

prevents the formation of MF cells, proving our hypothesis. The less efficient differentiation in SDM79 containing glucose, compared to differentiation in Cunningham's may be due to the higher concentration of glucose in SDM79.

RBP6 expression levels were checked by western blotting and shown to be similar or even lower in absence of glucose (Fig.S1D). This excludes higher RBP6 expression levels as the reason for a more efficient differentiation in the glucose-depleted medium, as the amount of RBP6 expression is directly linked to the percentage of MF formation (Kolev et al., 2012). Differentiation caused a decrease in population doubling time (Fig.S1A-C), in agreement with the non-proliferating state of long EMF and the MF cells (Van Den Abbeele et al., 1999).

T. brucei can also utilize glycerol as carbon source (Ryley, 1962). In addition it has been shown that glycerol affects early differentiation marker expression in PCF forms (Vassella et al., 2000). We therefore tested the effect of glycerol upon differentiation in the RBP6 system. Glycerol exhibited a similar effect as glucose, with a reduced number of MF cells and an initial accumulation of EMF cells (Fig.1C).

Glucose withdrawal induces TCA cycle genes expression

Looking for proteins regulated by glucose, we performed a quantitative proteomics experiment. The results on 64 enzymes involved in 9 metabolic pathways are depicted. Withdrawal of glucose resulted in a strong upregulation of only 3 enzymes (Fig.2). Strikingly two of them are part of the TCA cycle. The citrate synthase (CS) shows a more than 10-fold and the aconitase (ACO) a 3-fold upregulation. Another, more than 3-fold, upregulated enzyme was one of two isocitrate dehydrogenase (IDH) isoforms, that carries a PTS1 glycosomal targeting signal.

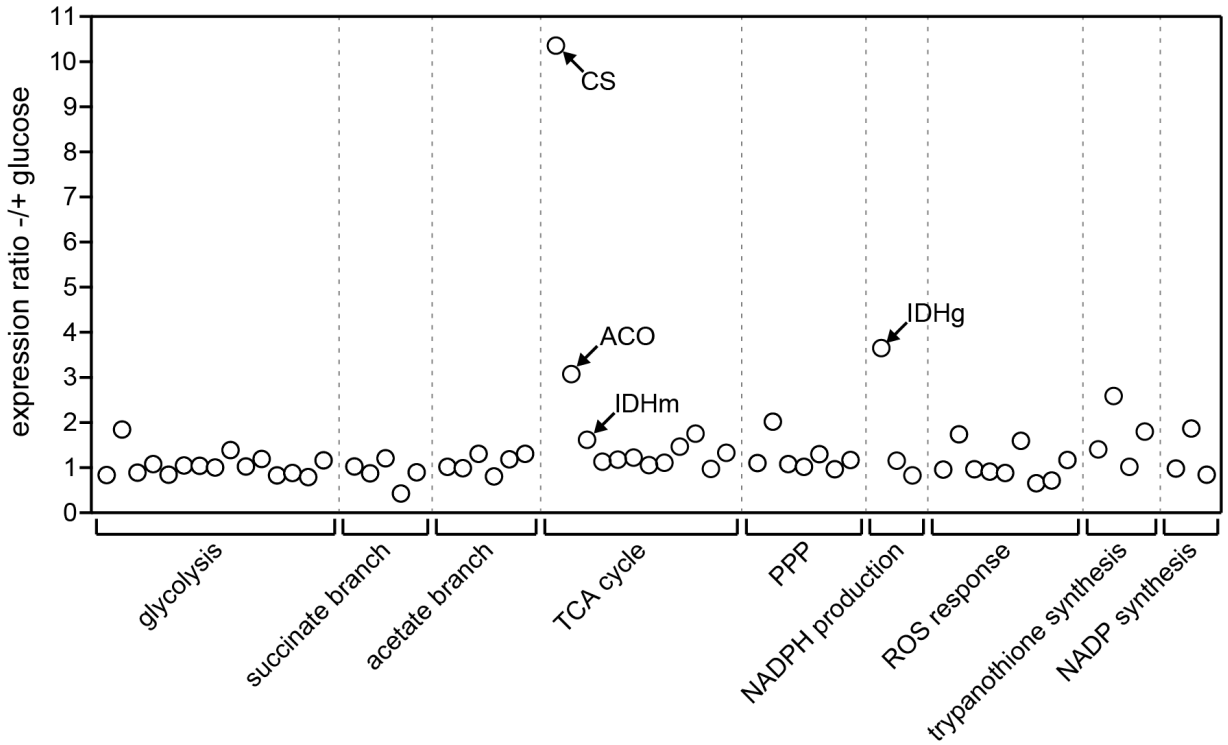

Fig.2: Glucose-regulated enzymes identified by quantitative proteomics. Proteins are clustered into metabolic pathways. The expression ratio between glucose-depleted and glucose-rich condition is depicted on the y-axis. Proteins of interest are labelled by arrows. Raw data are depicted in Fig.S2. EATRO1125 cells were used.

To validate the proteomics results we performed western blot analyses for the proteins of interest. This gave quantitatively very similar results with an upregulation of the CS, ACO and glycosomal IDH (IDHg) and no regulation of mitochondrial IDH (IDHm) (Fig.3). Probing cell extracts with the

CS antiserum resulted in several bands, thus we verified the CS upregulation by additionally probing a ΔCS null mutant (Fig.S3B).

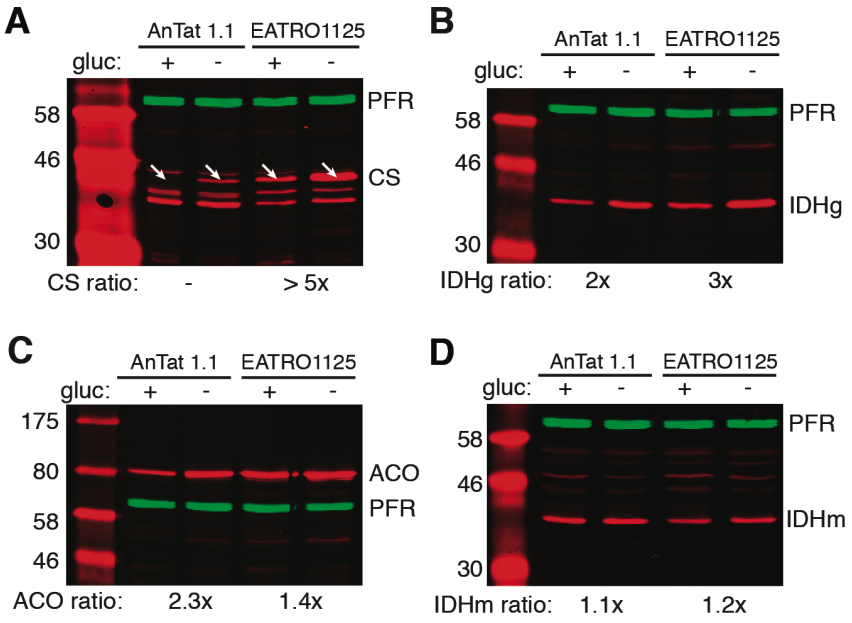

Fig.3: Detection of glucose-regulated proteins by western blotting. Western blotting was performed for two cell lines, AnTat 1.1 and EATRO1125. PFR served as loading control. The following proteins were analyzed: (A) the citrate synthase (CS), (B) the glycosomal isocitrate dehydrogenase (IDHg), (C) the aconitase (ACO) and (D) the mitochondrial isocitrate dehydrogenase (IDHm). White arrowheads indicate the position of the CS protein band. PFR: paraflagellar rod; Probing cell extracts with the CS antiserum resulted in several bands, thus we verified the CS upregulation by additionally probing a ΔCS null mutant (Fig.S3B). Fold induction is indicated below lanes as calculated from fluorescent values normalized to PFR.

The specificities of the two IDH antisera for the respective isoforms were verified by probing on lysates of WT and null mutants (Fig.S3A). The low expression or absence of CS, in the AnTat cell line may explain why in a previous mitochondrial proteomics approach this protein was not detected (Vertommen et al., 2008). In addition, so far only two publications showed CS activity in PCF cells (Durieux et al., 1991; Haanstra et al., 2011). The results indicate a high variation of expression levels between parasite strains. We determined the annotated enzymatic activity of the *Tb*CS gene by inducible overexpression of CS and enzyme assays (Fig.S3E).

The presence of two IDH isoforms and their inferred differential subcellular localizations from predicted targeting signals and previous proteomics data (Colasante et al., 2006; Guther et al., 2014; Vertommen et al., 2008) led us to investigate their localizations. We performed a digitonin titration, where gradually increasing amounts of digitonin release proteins into the supernatant according to their subcellular localization. At low concentrations cytoplasmic, then glycosomal and later mitochondrial proteins are released. We show that the two IDH isoforms release in the same pattern as the used glycosomal (PPDK) and mitochondrial (HSP60, ASCT) markers respectively (Fig.4), demonstrating their subcellular localizations.

To evaluate the contribution of each IDH isoform to the total IDH activity in presence as well as absence of glucose we performed IDH enzyme assays (Fig.5). The major cellular IDH activity was previously shown to be $NADP^+$-dependent and no activity could be observed with NAD^+ (Overath et al., 1986). We used cell lysates of wildtype cells and null mutants of each IDH isoform. The activity was increased in cells from glucose-depleted medium. Deletion of the IDHg isoform caused no significant change in total IDH activity. This demonstrates an increase of IDHm activity in the absence of glucose. Deletion of the IDHm isoform resulted in absence of IDH activity in the presence of glucose, whereas the absence of glucose IDHg-specific activity was measured. This suggests a specific role of the IDHg in an environment lacking glucose, such as the insect host.

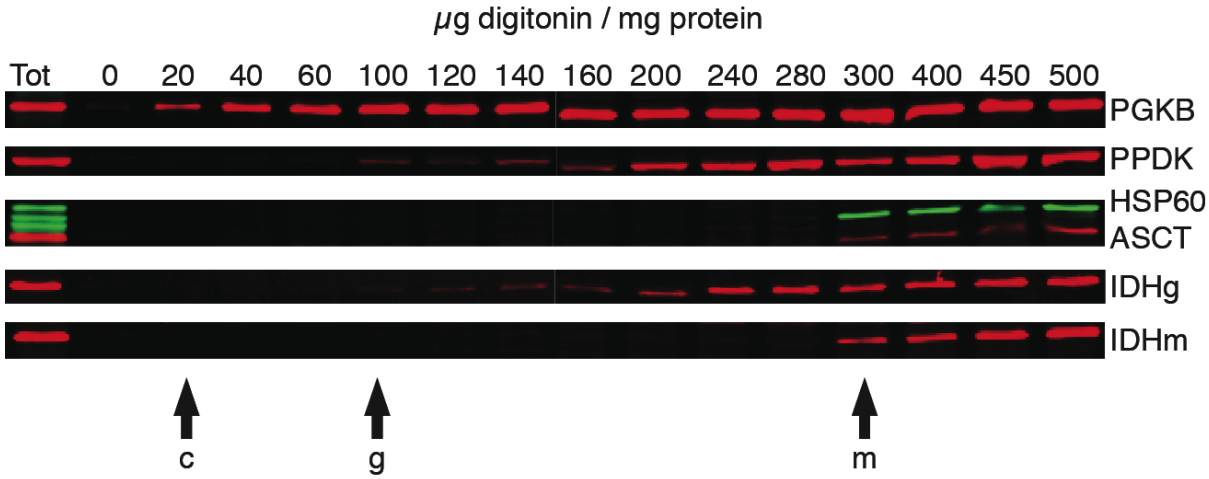

Fig.4: Subcellular localization of IDH isoforms. AnTat PCF cells were permeabilized by increasing concentrations of digitonin. The soluble fractions were blotted and probed with antisera. PGKB, PPDK and HSP60 and ASCT were used as cytosolic, glycosomal and mitochondrial markers respectively. c: release of cytosolic proteins, g: release of glycosomal proteins, m: release of mitochondrial proteins.

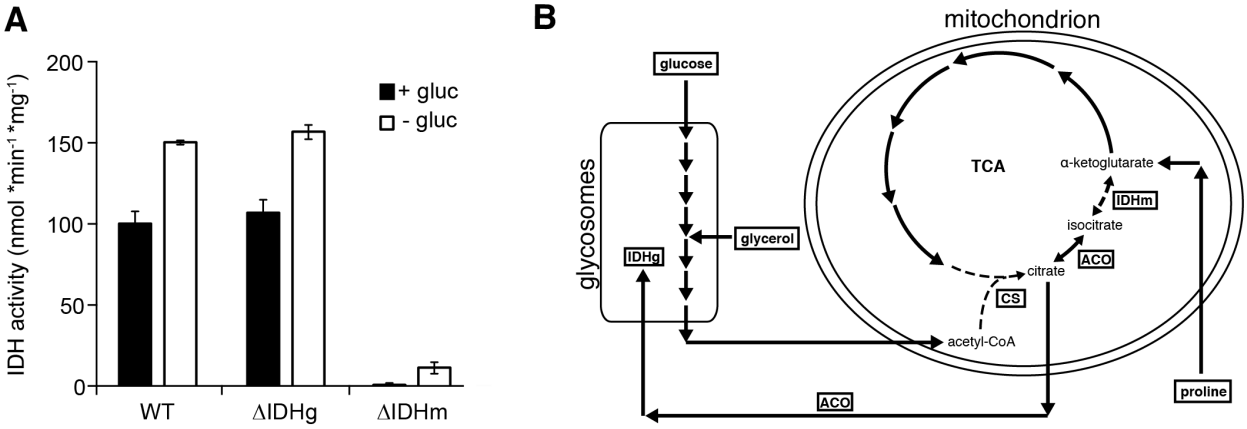

Fig.5: Glucose-regulation of IDH enzymatic activities. (A) AnTat cell extracts of WT, ΔIDHg and ΔIDHm grown in SDM79 with (black columns) or without (white columns) glucose were used for $NADP^+$-dependent IDH enzyme assays. Error bars represent the SEM of (n=3) independent replicates. (B)Schematic representation of localization and fluxes of the enzymes of interest. ACO: aconitase, CS: citrate synthase, IDH: isocitrate dehydrogenase (g: glycosomal, m: mitochondrial, TCA: tricarboxylic acid (cycle).

Taking together all data, one hypothesis could be, that the absence of glucose induces the TCA cycle activity and that the metabolic flux might influence the differentiation process. Considering the upregulation of the CS, the ACO and the IDHg we postulate an alternative pathway involving these three enzymes, producing NADPH in the glycosomes. This is also supported by the dual localization of ACO (Saas et al., 2000). The pathway would be independent from the NADPH production by the PPP and thus independent from glucose, becoming essential during migration in the insect host.

The IDHg is essential in later developmental stages

Due to the glucose-regulated expression of CS, ACO and IDHg, we investigated the null mutants for growth phenotypes in medium lacking glucose (Fig.6). The mutants were controlled by integration PCR (Fig.S3-5). No significant growth phenotypes were observed, neither in presence nor in absence of glucose for the null mutants. The ΔIDHm null mutant showed a minor growth phenotype in both conditions compared to the WT (Fig.6D).

We showed that the regulation of protein expression is induced by a lack of glucose, but the functions are not essential in procyclic cells in culture. They could be essential in later

developmental stages. Thus we fed procyclic *T. brucei* cells to the insect host *Glossina spp.* and compared the infection efficiency of the different cell lines.

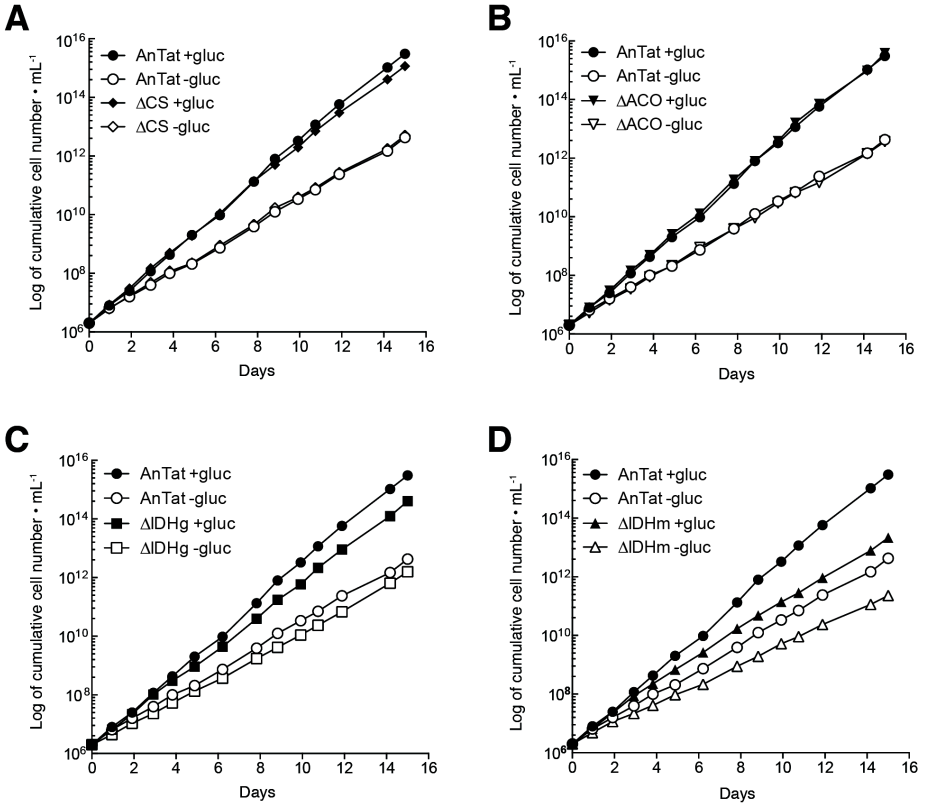

Fig.6: *In vitro* growth of the null mutants. AnTat PCF null mutants were grown in SDM79 with and without glucose and growth was compared to the WT. Growth for the following null mutants was investigated: ΔCS (A), ΔACO (B), ΔIDHg (C) and ΔIDHm (D).

We fed WT, ΔIDHg and two independent genetic rescue lines of the ΔIDHg null mutant and checked their ability to colonize the midgut and the salivary glands (Fig.7). There are no significant differences between WT and ΔIDHg cells in their ability to colonize the midgut in any of the three independent experiments. Comparing the salivary gland infection after 30 days, it is obvious that the ΔIDHg null mutant is significantly impaired. This is the first observation of a metabolic enzyme being essential for salivary gland colonization.

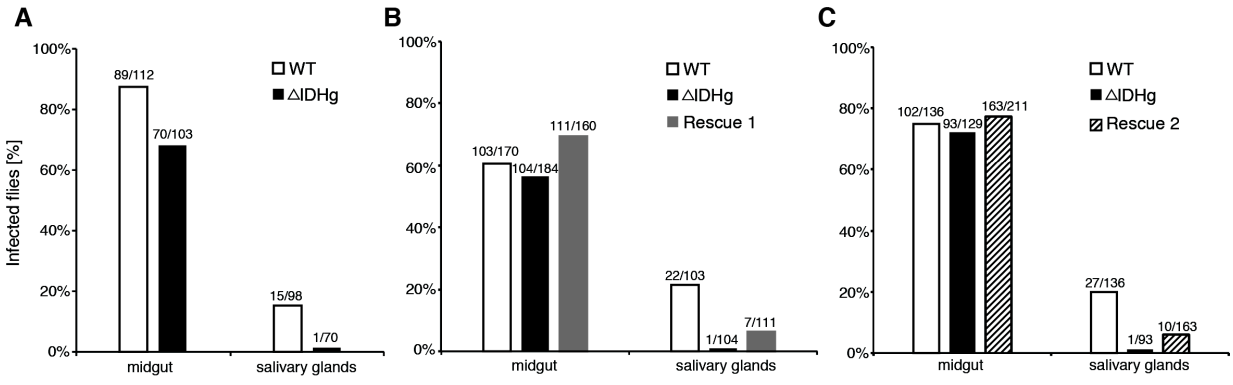

Fig.7: Essential role of IDHg during development within Tsetse flies. Tsetse flies have been fed with AnTat procyclic trypanosomes. 30 days post-infection midguts and salivary glands have been checked for trypanosome colonization. Each panel represents an independent experiment with several months in between and thus different fly populations as well as different lots of horse blood were used. Only salivary glands of flies that showed midgut colonization were checked for colonization. Independent genetic rescue cell lines were used in B and C. Number of flies for each cell line and experiment: A: WT(N=112), ΔIDHg(N=103); B: WT(N=170), ΔIDHg(N=184), Rescue 1(N=160); C: WT(N=136), ΔIDHg(N=129), Rescue 2(N=211).

The two genetic rescues show differences in IDHg expression (Fig.S7), but similar salivary gland infection efficiencies. Prolonged passaging and additional genetic manipulation of the rescues can explain the lower colonization efficiency compared to the WT. Our experience showed that these factors influence salivary gland infection efficiencies.

Fly infection experiments are time-consuming and the amount of parasites that can be harvested is small, thus limiting subsequent analytical methods. We decided to investigate the differentiation behavior in culture upon RBP6 expression in the null mutants. We introduced the inducible RBP6 vector into the null mutants, ΔCS, ΔIDHm and the ΔIDHg, as these enzymes are the first and the last steps of our postulated pathways for glycosomal NADPH production. For technical reasons the RBP6 expression had to be done in another strain containing a T7 polymerase, to reach sufficient protein levels. These null mutants had to be created in this strain and were controlled by western blotting (Fig.S4C,5C,6C). RBP6 was induced in these null mutants in SDM79 lacking glucose and the same analysis by microscopy and western blotting as for previous experiments was performed.

For the ΔIDHg null mutant, we saw a clear block in differentiation in the epimastigote stage. There were no metacyclic forms visible in any of the experiments performed (Fig.8B). Surprisingly no differentiation phenotype was observed for the ΔCS null mutant (Fig.8C). An intermediate differentiation phenotype was observed for the ΔIDHm mutant (Fig.8D). RBP6 expression was inducible to quantitatively similar levels in all cell lines(Fig.S1D-G).

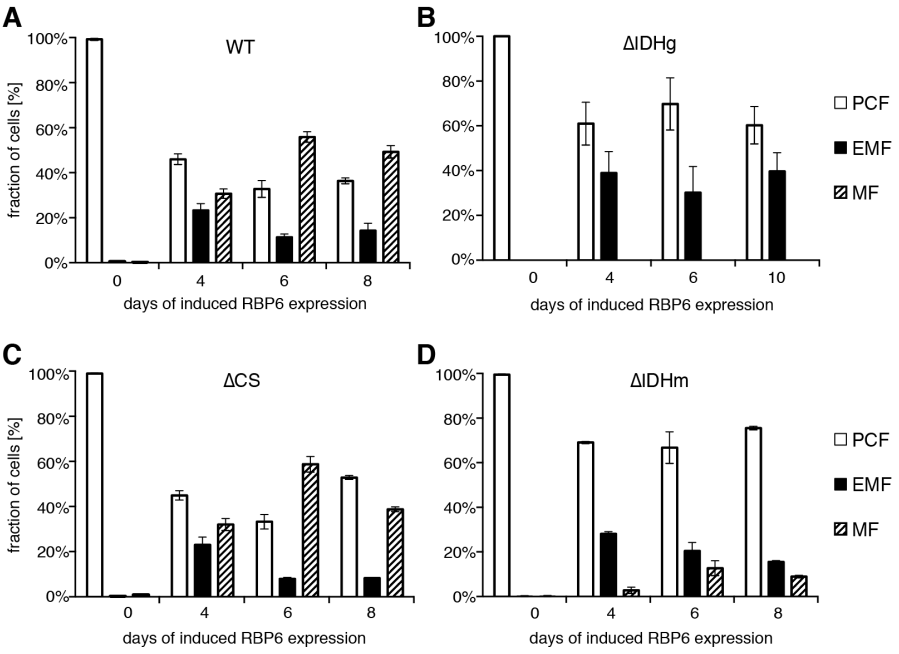

Fig.8: RBP6-induced differentiation of ΔIDHg, ΔCS and ΔIDHm cells. RBP6 was inducible expressed in the EATRO WT (A), ΔIDHg (B), ΔCS (C), and ΔIDHm (D) null mutants. All experiments were performed in glucose-depleted SDM79. For each time point the developmental stage of >100 cells was determined. The WT data (A) are the same as shown in Fig.1, but depicted here again for easier comparison. Error bars represent the SEM of (n=3)independent replicates.

The culture differentiation of ΔIDHg resulted in a comparable phenotype as observed in our fly infection experiments. This proves the phenotype to be a result of a blocked developmental differentiation and excludes a pure metabolic phenotype due to starvation in the insect host. We showed that there is no or a minor phenotype for the ΔCS and ΔIDHm null mutants respectively. This suggests a redundancy of those two enzymes in terms of citrate/isocitrate production, with a probably higher contribution of the IDHm. This requires the IDHm to perform reductive carboxylation of α-ketoglutarate, which is thermodynamically possible. The in culture differentiation enables subsequent analyses, which are currently ongoing to elucidate the molecular function of glycosomal NADPH.

Discussion

We identified glucose and glycerol as metabolic cues regulating the differentiation of *T. brucei* insect stages. We discovered that glucose-regulated protein expression of metabolic enzymes is involved in this process. Amongst the regulated enzymes we found the IDHg and demonstrated the essential role of the IDHg for salivary gland colonization during fly infection experiments. A differentiation phenotype of the ΔIDHg null mutant was also observed in a culture differentiation system. This is proof that this recent culture differentiation system is suitable to identify candidates essential for fly infection. In our case the phenotype in culture proofs that the phenotype observed in the fly experiments is not due to some metabolic depletion. As this would not be observed in rich culture conditions.

Effects of nutrient availability on the redistribution of metabolic fluxes have been observed before. The presence of glucose represses proline consumption (Coustou et al., 2008; Lamour et al., 2005). This indicates the parasite's ability of recognizing its nutritional environment. We identified two metabolic cues and their impact on the differentiation process from procyclic to metacyclic parasites. We clearly showed that glucose and glycerol affect the efficiency of RBP6-induced differentiation of *T. brucei* fly stages. This indicates a mechanism regulating the differentiation process by recognizing the nutrient availability. This may ensure the right timing of stage development within the insect host, necessary due to the diversity of the different insect tissues, faced during migration towards the salivary glands.

The proteomics as well as the western blot data showed the CS, ACO and IDHg as glucose-regulated proteins. Another regulation could be on the posttranslational level, by stability or modifications. Indeed the upregulation of the IDHg activity is higher than the upregulation of the protein level. Putative posttranslational regulators are part of future investigations. The upregulated proteins suggest an increased TCA cycle activity. Considering that the upregulated IDH isoform displays glycosomal localization we suggest another pathway being upregulated. We suggest that CS, ACO and IDHg are an alternative pathway for the parasite to produced glycosomal NADPH via the IDHg. This might be necessary due to less pentose phosphate pathway produced NADPH in the absence of glucose.

Concerning the biochemical role of the IDHg, there are a few pathways requiring NADPH with a putative glycosomal localization. In the yeast *S. cerevisiae* it has been shown that a peroxisomal IDH is essential for the β-oxidation of unsaturated fatty acids (Henke et al., 1998). A former publication demonstrated two enzymatic activities with a putative function in β-oxidation and their glycosomal localization in procyclic forms (Wiemer et al., 1996). We continued the investigations on β-oxidation, but our data make β-oxidation unlikely in *T. brucei* (manuscript submitted).

A crucial pathway utilizing NADPH is the trypanothione system, essential for detoxification of reactive oxygen species (ROS) (Krieger et al., 2000), which can be of importance when passing the proventriculus (Hao et al., 2003). But the enzyme consuming NADPH is the trypanothione reductase (TR), which is located within the cytosol (Smith et al., 1991). Previous proteomic approaches did not detect the TR within the glycosomes (Colasante et al., 2006), but others detected the TR in the glycosomes (Guther et al., 2014). We showed that cytosolic NADPH production is crucial for detoxification of external derived ROS (Allmann et al., 2013), questioning the importance of glycosomal NADPH for this purpose. Nevertheless we analyzed a ΔIDHg null mutant and compared its oxidative stress susceptibility in the presence of DHEA, a glucose 6-phosphate dehydrogenase inhibitor (Cordeiro et al., 2009), compared to wildtype cells and observed no phenotype (data not shown). Altogether we conclude that the IDHg is not important for external oxidative stress defense.)

Another putative essential use of NADPH in the glycosome could be the synthesis of ether-linked lipids via the dihydroxyacetone phosphate pathway (Michels et al., 2006; Opperdoes, 1984).

Ether-linked lipids can act as stabilizers for the membrane bilayer during physical or chemical stress periods as observed before (Aussenac et al., 2005; Shinoda et al., 2004). It has been shown that ether-linked lipids are more resistant to basic/acidic hydrolysis, which can happen at high or low pH values of the environment, like the proventriculus of the Tsetse fly, which has a pH of 10.6 (Liniger et al., 2003).

Based on the afore mentioned pathway, we investigated the role of the IDHg. The deletion of the IDHg resulted in non-colonized salivary glands in three independent fly infection experiments. The deletion had no effect under normal growth conditions, but blocked the differentiation into metacyclic cells upon RBP6 expression in culture. With these experiments the essential role of the IDHg is clearly demonstrated, but the pathway feeding the IDHg is still unclear.

A citrate synthase (CS) is required to provide citrate, which can be converted by an aconitase (ACO) into isocitrate to feed the IDHg. Thus we created a ΔCS null mutant, but did not observe a differentiation phenotype similar to the ΔIDHg in the culture differentiation. This indicates an alternative citrate or isocitrate source independent from the CS. One possibility is the mitochondrial IDH. For *T. cruzi* it has been shown that *in vitro* the IDH isoforms can also utilize α-ketoglutarate as substrate, but with a very low K_m compared to isocitrate as substrate (Leroux et al., 2011). There is also evidence for a reversed IDH activity in rat liver cells (Des Rosiers et al., 1994). Two pathways for isocitrate production would increase the parasite's metabolic flexibility. This hypothesis is also supported by the observation that the mitochondrial malic enzyme (MEm) is essential in procyclics (Allmann et al., 2013) suggesting that it is the major mitochondrial NADPH source and that the IDHm may consume NADPH in the mitochondrion.

A redundant role for isocitrate formation of the CS or the IDHm would explain the absence of differentiation phenotypes of the respective null mutants. Testing a double knockout mutant of ΔCS and ΔIDHm for differentiation would give formal prove for this hypothesis. This mutant could not be created in our hands. Several transfections have been performed and a number of independent pools were tested, but no double knockout could be verified. This indicates that the double KO is lethal for other reasons in PCF, independent of differentiation.

None of the created null mutants displayed a growth phenotype in culture, but the IDHg clearly is essential for stage development. This phenotype is stage specific, indicating that some metabolic pathways are specifically required in fly stages post PCF.

We suggest that the presence/absence of specific carbon sources and thereby the resulting metabolic fluxes act as regulators of the developmental differentiation of *T. brucei*. The presence of glucose and glycerol has been previously shown to affect early marker expression within the PCF (Vassella et al., 2000; Vassella et al., 2004), whereas we showed their influence on later differentiation processes involving EMF and MF parasites. We speculate that this is a safety mechanism, blocking further differentiation as the parasite still resides within the midgut, requiring the protective surface coat of procyclins. The signal might be conveyed by the glycolytic flux fueled by glucose and glycerol. The glycerol could be derived by digestion of red blood cell membranes and glucose is abundant in millimolar concentrations in mammalian blood.

The effect of glycerol on early differentiation marker expression has been demonstrated (Vassella et al., 2000). Attempts to elucidate the metabolic background showed that the underlying reason is not the changes in ATP abundance. Neither deletion of aconitase, nor RNAi against α-ketoglutarate dehydrogenase or succinate synthetase had an impact on the EP/GPEET switch as well as the inhibition of oxidative phosphorylation by KCN (Vassella et al., 2004). In Contrast, inhibition of the AOX via SHAM lead to a GPEET to EP switch (Vassella et al., 2004).

We show that the presence or absence of specific nutrients has an influence on *T. brucei's* differentiation process of fly stages. In addition we not only showed this with *in vivo* experiments involving fly infections, but have complementary data from the new culture differentiation system.

References

Akoda, K., Van den Bossche, P., Lyaruu, E.A., De Deken, R., Marcotty, T., Coosemans, M., and Van den Abbeele, J. (2009a). Maturation of a Trypanosoma brucei infection to the infectious metacyclic stage is enhanced in nutritionally stressed tsetse flies. Journal of medical entomology *46*, 1446-1449.

Akoda, K., Van den Bossche, P., Marcotty, T., Kubi, C., Coosemans, M., De Deken, R., and Van den Abbeele, J. (2009b). Nutritional stress affects the tsetse fly's immune gene expression. Medical and veterinary entomology *23*, 195-201.

Alibu, V.P., Storm, L., Haile, S., Clayton, C., and Horn, D. (2005). A doubly inducible system for RNA interference and rapid RNAi plasmid construction in Trypanosoma brucei. Molecular and biochemical parasitology *139*, 75-82.

Aussenac, F., Lavigne, B., and Dufourc, E.J. (2005). Toward bicelle stability with ether-linked phospholipids: temperature, composition, and hydration diagrams by 2H and 31P solid-state NMR. Langmuir *21*, 7129-7135.

Bastin, P., Bagherzadeh, Z., Matthews, K.R., and Gull, K. (1996). A novel epitope tag system to study protein targeting and organelle biogenesis in Trypanosoma brucei. Molecular and biochemical parasitology *77*, 235-239.

Biebinger, S., Wirtz, L.E., Lorenz, P., and Clayton, C. (1997). Vectors for inducible expression of toxic gene products in bloodstream and procyclic Trypanosoma brucei. Molecular and biochemical parasitology *85*, 99-112.

Bringaud, F., Peyruchaud, S., Baltz, D., Giroud, C., Simpson, L., and Baltz, T. (1995). Molecular characterization of the mitochondrial heat shock protein 60 gene from Trypanosoma brucei. Molecular and biochemical parasitology *74*, 119-123.

Bringaud, F., Robinson, D.R., Barradeau, S., Biteau, N., Baltz, D., and Baltz, T. (2000). Characterization and disruption of a new Trypanosoma brucei repetitive flagellum protein, using double-stranded RNA inhibition. Molecular and biochemical parasitology *111*, 283-297.

Broach, J.R. (2012). Nutritional control of growth and development in yeast. Genetics *192*, 73-105.

Brun, R., and Schonenberger (1979). Cultivation and in vitro cloning or procyclic culture forms of Trypanosoma brucei in a semi-defined medium. Short communication. Acta Trop *36*, 289-292.

Cai, L., and Tu, B.P. (2012). Driving the cell cycle through metabolism. Annual review of cell and developmental biology *28*, 59-87.

Colasante, C., Ellis, M., Ruppert, T., and Voncken, F. (2006). Comparative proteomics of glycosomes from bloodstream form and procyclic culture form Trypanosoma brucei brucei. Proteomics *6*, 3275-3293.

Cordeiro, A.T., Thiemann, O.H., and Michels, P.A. (2009). Inhibition of Trypanosoma brucei glucose-6-phosphate dehydrogenase by human steroids and their effects on the viability of cultured parasites. Bioorganic & medicinal chemistry *17*, 2483-2489.

Coustou, V., Biran, M., Breton, M., Guegan, F., Riviere, L., Plazolles, N., Nolan, D., Barrett, M.P., Franconi, J.M., and Bringaud, F. (2008). Glucose-induced remodeling of intermediary and energy metabolism in procyclic Trypanosoma brucei. The Journal of biological chemistry *283*, 16342-16354.

Cullen, P.J., and Sprague, G.F., Jr. (2000). Glucose depletion causes haploid invasive growth in yeast. Proceedings of the National Academy of Sciences of the United States of America *97*, 13619-13624.

Cullen, P.J., and Sprague, G.F., Jr. (2012). The regulation of filamentous growth in yeast. Genetics *190*, 23-49.

Dang, L., White, D.W., Gross, S., Bennett, B.D., Bittinger, M.A., Driggers, E.M., Fantin, V.R., Jang, H.G., Jin, S., Keenan, M.C., *et al.* (2009). Cancer-associated IDH1 mutations produce 2-hydroxyglutarate. Nature *462*, 739-744.

Des Rosiers, C., Fernandez, C.A., David, F., and Brunengraber, H. (1994). Reversibility of the mitochondrial isocitrate dehydrogenase reaction in the perfused rat liver. Evidence from isotopomer analysis of citric acid cycle intermediates. The Journal of biological chemistry *269*, 27179-27182.

Durieux, P.O., Schutz, P., Brun, R., and Kohler, P. (1991). Alterations in Krebs cycle enzyme activities and carbohydrate catabolism in two strains of Trypanosoma brucei during in vitro differentiation of their bloodstream to procyclic stages. Molecular and biochemical parasitology *45*, 19-27.

Ebikeme, C., Hubert, J., Biran, M., Gouspillou, G., Morand, P., Plazolles, N., Guegan, F., Diolez, P., Franconi, J.M., Portais, J.C., *et al.* (2010). Ablation of succinate production from glucose metabolism in the procyclic trypanosomes induces metabolic switches to the glycerol 3-phosphate/dihydroxyacetone phosphate shuttle and to proline metabolism. The Journal of biological chemistry *285*, 32312-32324.

Eidels, L., and Preiss, J. (1970). Citrate synthase. A regulatory enzyme from Rhodopseudomonas capsulata. The Journal of biological chemistry *245*, 2937-2945.

Guther, M.L., Urbaniak, M.D., Tavendale, A., Prescott, A., and Ferguson, M.A. (2014). High-Confidence Glycosome Proteome for Procyclic Form Trypanosoma brucei by Epitope-Tag Organelle Enrichment and SILAC Proteomics. Journal of proteome research *13*, 2796-2806.

Haanstra, J.R., Kerkhoven, E.J., van Tuijl, A., Blits, M., Wurst, M., van Nuland, R., Albert, M.A., Michels, P.A., Bouwman, J., Clayton, C., *et al.* (2011). A domino effect in drug action: from metabolic assault towards parasite differentiation. Molecular microbiology *79*, 94-108.

Hao, Z., Kasumba, I., and Aksoy, S. (2003). Proventriculus (cardia) plays a crucial role in immunity in tsetse fly (Diptera: Glossinidiae). Insect Biochem Mol Biol *33*, 1155-1164.

Harlow, E., and Lane, D., eds. (1988). Antibodies : a laboratory manual (Cold Spring Harbor Laboratory Press).

Henke, B., Girzalsky, W., Berteaux-Lecellier, V., and Erdmann, R. (1998). IDP3 encodes a peroxisomal NADP-dependent isocitrate dehydrogenase required for the beta-oxidation of unsaturated fatty acids. The Journal of biological chemistry *273*, 3702-3711.

Hu, C., and Aksoy, S. (2006). Innate immune responses regulate trypanosome parasite infection of the tsetse fly Glossina morsitans morsitans. Molecular microbiology *60*, 1194-1204.

Ito, S., D'Alessio, A.C., Taranova, O.V., Hong, K., Sowers, L.C., and Zhang, Y. (2010). Role of Tet proteins in 5mC to 5hmC conversion, ES-cell self-renewal and inner cell mass specification. Nature *466*, 1129-1133.

Kohl, L., Sherwin, T., and Gull, K. (1999). Assembly of the paraflagellar rod and the flagellum attachment zone complex during the Trypanosoma brucei cell cycle. J Eukaryot Microbiol *46*, 105-109.

Kolev, N.G., Ramey-Butler, K., Cross, G.A., Ullu, E., and Tschudi, C. (2012). Developmental progression to infectivity in Trypanosoma brucei triggered by an RNA-binding protein. Science *338*, 1352-1353.

Krieger, S., Schwarz, W., Ariyanayagam, M.R., Fairlamb, A.H., Krauth-Siegel, R.L., and Clayton, C. (2000). Trypanosomes lacking trypanothione reductase are avirulent and show increased sensitivity to oxidative stress. Molecular microbiology *35*, 542-552.

Lamour, N., Riviere, L., Coustou, V., Coombs, G.H., Barrett, M.P., and Bringaud, F. (2005). Proline metabolism in procyclic Trypanosoma brucei is down-regulated in the presence of glucose. The Journal of biological chemistry *280*, 11902-11910.

Leroux, A.E., Maugeri, D.A., Cazzulo, J.J., and Nowicki, C. (2011). Functional characterization of NADP-dependent isocitrate dehydrogenase isozymes from Trypanosoma cruzi. Molecular and biochemical parasitology *177*, 61-64.

Liniger, M., Acosta-Serrano, A., Van Den Abbeele, J., Kunz Renggli, C., Brun, R., Englund, P.T., and Roditi, I. (2003). Cleavage of trypanosome surface glycoproteins by alkaline trypsin-like enzyme(s) in the midgut of Glossina morsitans. International journal for parasitology *33*, 1319-1328.

Marche, S., Michels, P.A., and Opperdoes, F.R. (2000). Comparative study of Leishmania mexicana and Trypanosoma brucei NAD-dependent glycerol-3-phosphate dehydrogenase. Molecular and biochemical parasitology *106*, 83-91.

Martinez-Calvillo, S., Vizuet-de-Rueda, J.C., Florencio-Martinez, L.E., Manning-Cela, R.G., and Figueroa-Angulo, E.E. (2010). Gene expression in trypanosomatid parasites. J Biomed Biotechnol *2010*, 525241.

Michels, P.A., Bringaud, F., Herman, M., and Hannaert, V. (2006). Metabolic functions of glycosomes in trypanosomatids. Biochimica et biophysica acta *1763*, 1463-1477.

Mills, E., and O'Neill, L.A. (2014). Succinate: a metabolic signal in inflammation. Trends in cell biology *24*, 313-320.

Moran-Crusio, K., Reavie, L., Shih, A., Abdel-Wahab, O., Ndiaye-Lobry, D., Lobry, C., Figueroa, M.E., Vasanthakumar, A., Patel, J., Zhao, X.*, et al.* (2011). Tet2 loss leads to increased hematopoietic stem cell self-renewal and myeloid transformation. Cancer cell *20*, 11-24.

Morand, S., Renggli, C.K., Roditi, I., and Vassella, E. (2012). MAP kinase kinase 1 (MKK1) is essential for transmission of Trypanosoma brucei by Glossina morsitans. Molecular and biochemical parasitology *186*, 73-76.

Opperdoes, F.R. (1984). Localization of the initial steps in alkoxyphospholipid biosynthesis in glycosomes (microbodies) of Trypanosoma brucei. FEBS Lett *169*, 35-39.

Overath, P., Czichos, J., and Haas, C. (1986). The effect of citrate/cis-aconitate on oxidative metabolism during transformation of Trypanosoma brucei. European journal of biochemistry / FEBS *160*, 175-182.

Park, J., Chen, Y., Tishkoff, D.X., Peng, C., Tan, M., Dai, L., Xie, Z., Zhang, Y., Zwaans, B.M., Skinner, M.E.*, et al.* (2013). SIRT5-mediated lysine desuccinylation impacts diverse metabolic pathways. Molecular cell *50*, 919-930.

Quivoron, C., Couronne, L., Della Valle, V., Lopez, C.K., Plo, I., Wagner-Ballon, O., Do Cruzeiro, M., Delhommeau, F., Arnulf, B., Stern, M.H.*, et al.* (2011). TET2 inactivation results in pleiotropic hematopoietic abnormalities in mouse and is a recurrent event during human lymphomagenesis. Cancer cell *20*, 25-38.

Riviere, L., van Weelden, S.W., Glass, P., Vegh, P., Coustou, V., Biran, M., van Hellemond, J.J., Bringaud, F., Tielens, A.G., and Boshart, M. (2004). Acetyl:succinate CoA-transferase in procyclic Trypanosoma brucei. Gene identification and role in carbohydrate metabolism. The Journal of biological chemistry *279*, 45337-45346.

Rohle, D., Popovici-Muller, J., Palaskas, N., Turcan, S., Grommes, C., Campos, C., Tsoi, J., Clark, O., Oldrini, B., Komisopoulou, E.*, et al.* (2013). An inhibitor of mutant IDH1 delays growth and promotes differentiation of glioma cells. Science *340*, 626-630.

Ryley, J.F. (1962). Studies on the metabolism of the protozoa. 9. Comparative metabolism of blood-stream and culture forms of Trypanosoma rhodesiense. The Biochemical journal *85*, 211-223.

Saas, J., Ziegelbauer, K., von Haeseler, A., Fast, B., and Boshart, M. (2000). A developmentally regulated aconitase related to iron-regulatory protein-1 is localized in the cytoplasm and in the mitochondrion of Trypanosoma brucei. The Journal of biological chemistry *275*, 2745-2755.

Sambrook, J., Fritsch, E.F., and Maniatis, T., eds. (1989). Molecular cloning : a laboratory manual., 2 edn (New York: Cold Spring Harbor Laboratory Press).

Sasaki, M., Knobbe, C.B., Munger, J.C., Lind, E.F., Brenner, D., Brustle, A., Harris, I.S., Holmes, R., Wakeham, A., Haight, J.*, et al.* (2012). IDH1(R132H) mutation increases murine haematopoietic progenitors and alters epigenetics. Nature *488*, 656-659.

Shinoda, K., Shinoda, W., Baba, T., and Mikami, M. (2004). Comparative molecular dynamics study of ether- and ester-linked phospholipid bilayers. J Chem Phys *121*, 9648-9654.

Smith, K., Opperdoes, F.R., and Fairlamb, A.H. (1991). Subcellular distribution of trypanothione reductase in bloodstream and procyclic forms of Trypanosoma brucei. Molecular and biochemical parasitology *48*, 109-112.

Van Den Abbeele, J., Claes, Y., van Bockstaele, D., Le Ray, D., and Coosemans, M. (1999). Trypanosoma brucei spp. development in the tsetse fly: characterization of the post-mesocyclic stages in the foregut and proboscis. Parasitology *118 (Pt 5)*, 469-478.

Vassella, E., Den Abbeele, J.V., Butikofer, P., Renggli, C.K., Furger, A., Brun, R., and Roditi, I. (2000). A major surface glycoprotein of trypanosoma brucei is expressed transiently during development and can be regulated post-transcriptionally by glycerol or hypoxia. Genes & development *14*, 615-626.

Vassella, E., Probst, M., Schneider, A., Studer, E., Renggli, C.K., and Roditi, I. (2004). Expression of a major surface protein of Trypanosoma brucei insect forms is controlled by the activity of mitochondrial enzymes. Molecular biology of the cell *15*, 3986-3993.

Vertommen, D., Van Roy, J., Szikora, J.P., Rider, M.H., Michels, P.A., and Opperdoes, F.R. (2008). Differential expression of glycosomal and mitochondrial proteins in the two major life-cycle stages of Trypanosoma brucei. Molecular and biochemical parasitology *158*, 189-201.

Vickerman, K. (1985). Developmental cycles and biology of pathogenic trypanosomes. Br Med Bull *41*, 105-114.
Weiss, B.L., Wang, J., Maltz, M.A., Wu, Y., and Aksoy, S. (2013). Trypanosome infection establishment in the tsetse fly gut is influenced by microbiome-regulated host immune barriers. PLoS pathogens *9*, e1003318.
Wiemer, E.A., L, I.J., van Roy, J., Wanders, R.J., and Opperdoes, F.R. (1996). Identification of 2-enoyl coenzyme A hydratase and NADP(+)-dependent 3-hydroxyacyl-CoA dehydrogenase activity in glycosomes of procyclic Trypanosoma brucei. Molecular and biochemical parasitology *82*, 107-111.
Xong, H.V., Vanhamme, L., Chamekh, M., Chimfwembe, C.E., Van Den Abbeele, J., Pays, A., Van Meirvenne, N., Hamers, R., De Baetselier, P., and Pays, E. (1998). A VSG expression site-associated gene confers resistance to human serum in Trypanosoma rhodesiense. Cell *95*, 839-846.
Zhang, Z., Tan, M., Xie, Z., Dai, L., Chen, Y., and Zhao, Y. (2011). Identification of lysine succinylation as a new post-translational modification. Nature chemical biology *7*, 58-63.

Acknowledgements

We are grateful to Larissa Ivanova (Munich) for competent technical support. We want to thank Nikolay Kolev for providing the RBP6 antibody and the very useful advice concerning the RBP6-induced differentiation.

Work in Munich was supported by the University of Munich and grants DFG 1100/6-2 and BELSPO PAI 6/15 to MB. Work in Antwerp was supported by the Interuniversity Attraction Poles Programme of the Belgian Science Policy. Work in Bordeaux was supported by the Agence Nationale de la Recherche (ANR) through grants ACETOTRYP of the ANR-BLANC-2010 call to FB and PM; FB is also supported by the Centre National de la Recherche Scientifique (CNRS), the Université of Bordeaux, the Laboratoire d'Excellence (LabEx) ParaFrap ANR-11-LABX-0024 and the ParaMet PhD programme of Marie Curie Initial Training Network (FP7). MB and FB have been supported by a research cooperation grant of the Franco-Bavarian university cooperation center (BFHZ/CCUFB).

3.2 The Role of Aconitase During Differentiation

In addition to CS, IDHg and IDHm we find aconitase (ACO) involved in this NADPH producing pathway. We performed *in vitro* as well as *in vivo* experiments assessing its role during differentiation. Fly infection experiments with the ΔACO null mutant and genetic rescue lines have been performed (B. Fast, this lab; in collaboration with D. Berry, Glasgow). Here a comparable phenotype was observed as for the ΔIDHg null mutant in our experiments. In contrast to this the RBP6-induced differentiation in culture gave different results. The ΔACO null mutant showed a stronger differentiation phenotype as the ΔIDHg null mutant. There was a clear block at the stage of procyclic cells, with very few epimastigote forms observed (Fig.8).

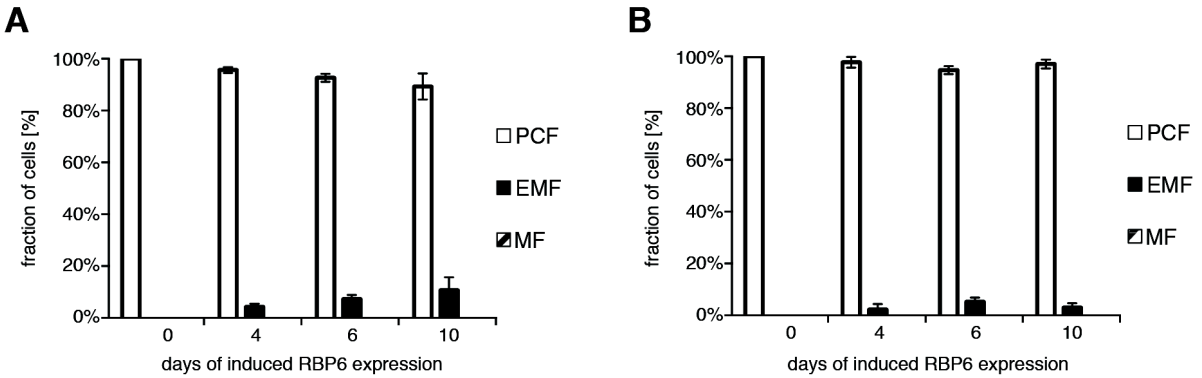

Fig.8: RBP6-induced differentiation is blocked in the ΔACO null mutant. The differentiation process was induced in (A) SDM79 and (B) glucose-depleted SDM79. The expression of RBP6 was induced by addition of tetracycline and samples for microscopy and western blotting were taken for 10 days. For each time point the developmental stage of >100 cells was determined according to size, morphology and relative positioning of nucleus and kinetoplast. Error bars represent the SEM of (n=3) independent experiments.

The growth during these experiments reflects this observation (Fig.9A,B). The wildtype cells in glucose-depleted medium display a strong growth delay with subsequent stagnation of the population size. This is based on the fact, that metacyclic cells are cell cycle arrested and thus a non-proliferative form. The asymmetrical division of epimastigote forms is supposed to result in a non-proliferative form (long epimastigote) and a proliferative form (short epimastigote) (Van Den Abbeele et al., 1999), which will mature into metacyclics later on. In sum this means that successful differentiation into later insect stages has an impact on the observed growth rate, whereas a block in differentiation does not. It has been shown that the formation of metacyclic forms is directly linked to the amount of RBP6 protein expressed to a certain degree (Kolev et al., 2012). Therefore we checked if lower RBP6 expression levels are the reason for the observed phenotype (Fig.9C, D). Indeed we saw a lower RBP6 expression in the ΔACO mutant than in WT cells. Knowing that no clonal population was selected after transfection of the RBP6 construct, this was rather unlikely to be a clonal adaptation.

To unravel this observation, new transfections of the ΔACO null mutant with the RBP6 expression construct have been performed (N. Ziebart, this lab). Four new cell lines have been analyzed for their RBP6 expression upon tetracycline induction, all of them showing the reduced RBP6 expression levels as the previous cell line. This indicates an impact of ACO upon RBP6 expression. The impact upon RBP6 expression levels could be exerted by the accumulation or lack of certain metabolic intermediates and will be part of future investigations.

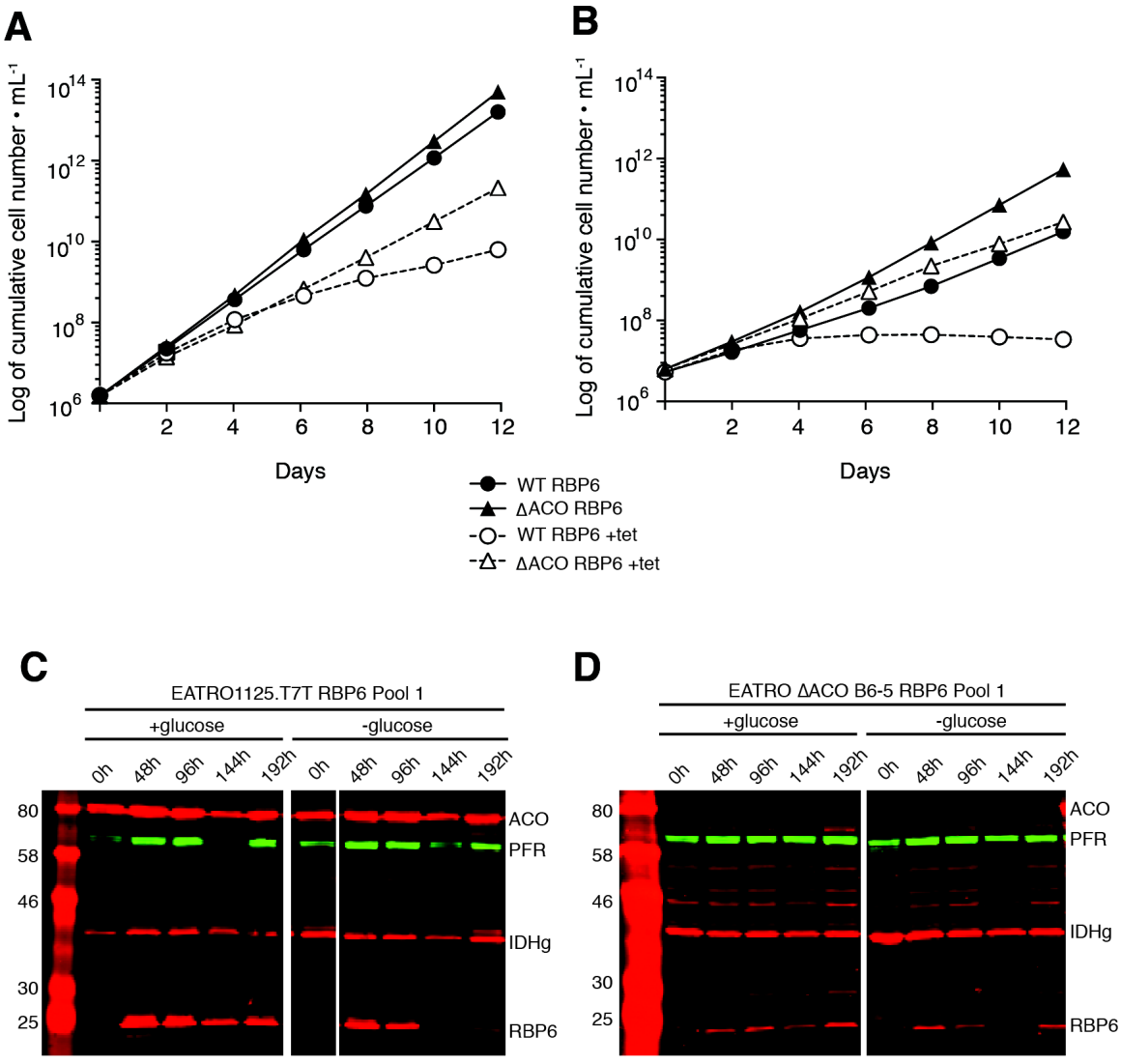

Fig.9: Growth and RBP6 expression during differentiation of the ΔACO mutant. Growth was monitored in (A) normal SDM79 as well as (B) glucose-depleted SDM79. The expression of RBP6 was induced by addition of tetracycline . Filled markers represent the non-induced cell lines and open markers the induced cell lines. The expression levels of RBP6 were controlled by western blotting for the (C) WT and the (D) ΔACO null mutant. PFR was used as loading control. ACO; aconitase, IDHg: glycosomal isocitrate dehydrogenase, PFR: paraflagellar rod, RBP6: RNA-binding protein 6.

4. Fatty Acid Storage in *T. brucei* Procyclic Cells

Chapter 3 clearly shows that glycosomal NADPH production via IDHg is essential for differentiation in culture as well as in the fly. This raised the question which NADPH consuming pathway is fueled by the IDHg. There are three possibilities, which are mentioned in more detail in the introduction chapter 1.4. This chapter focuses on a putative glycosomal β-oxidation, as described for *S. cerevisiae*, where a peroxisomal IDH is essential for the β-oxidation of poly-unsaturated fatty acids (Henke et al., 1998). We established a method for *T. brucei* to form lipid droplets (LDs) under physiological conditions and optimized several analytical methods to follow the fate of these LDs. Using these tools we investigated a candidate gene for β-oxidation activity, which has been observed in *T. brucei* before (Wiemer et al., 1996).

Triacylglycerol Storage in Lipid Droplets in Procyclic *Trypanosoma brucei*

S. Allmann[1], M. Mazet[2], N. Ziebart[1], G. Bouyssou[3], L. Fouillen[3], J.-W. Dupuy[4], M. Bonneu[4], P. Moreau[3], F. Bringaud[2] and M. Boshart[1]*

[1]*Fakultät für Biologie, Genetik, Ludwig-Maximilians-Universität München, Biozentrum, Grosshadernerstrasse 2-4, D-82152 Martinsried, Germany*

[2]*Centre de Résonance Magnétique des Systèmes Biologiques (RMSB), UMR5536, Université de Bordeaux, CNRS, 146 rue Léo Saignat, 33076 Bordeaux, France*

[3]*Laboratoire de Biogenèse Membranaire, UMR 5200, Université de Bordeaux/CNRS, Bât A3, INRA Bordeaux-Aquitaine, 71 Av. E. Bourlaux, 33140 Villenave d'Ornon, France*

[4]*Centre de Génomique Fonctionnelle, Plateforme Protéome, Université de Bordeaux, 146 rue Léo Saignat, 33076 Bordeaux, France*

Manuscript

*To whom correspondence should be addressed:
Dr. Michael Boshart
Tel.: 49-89-2180-74600;
Fax: 49-89-2180-74629;
E-mail: boshart@lmu.de

Abstract:
Carbon storage is likely to enable adaptation of trypanosomes to nutritional challenges or bottlenecks during their stage development and migration in the tsetse. Lipid droplets are candidates for this function. This report shows that feeding of *T. brucei* with oleate results in a 4-5 fold increase in the number of lipid droplets, as quantified by confocal fluorescence microscopy and by flow cytometry of BODIPY 493/503-stained cells. The triacylglycerol (TAG) content also increased 4-5 fold, and labeled oleate is incorporated into TAG. Fatty acid carbon can thus be stored as TAG in lipid droplets under physiological growth conditions in procyclic *T. brucei*. Glycosomal β-oxidation has been suggested in *T. brucei* as a possible catabolic pathway. A single candidate gene, *TFEa1* with coding capacity for a subunit of the trifunctional enzyme complex was identified. A targeted gene deletion was used to probe the pathway. *TFEa1* is expressed in procyclic *T. brucei* and present in glycosomes, yet it does not encode the previously reported 3-hydroxyacyl-CoA dehydrogenase activity. Also a glycosomal assignment of this activity cannot be confirmed. Homozygous *Δtfeα1/Δtfeα1* null mutant cells show a normal growth rate and an unchanged glycosomal proteome in procyclic *T. brucei*. The decay kinetics of accumulated lipid droplets upon oleate withdrawal can be fully accounted for by the dilution effect of cell division. Hence, there is no evidence for catabolism of stored TAG and no evidence for the presence of an active glycosomal b-oxidation pathway in procyclic *T. brucei*, even under strictly glucose-free conditions. The possibility remains that TAG catabolism is developmentally activated in post-procyclic stages in the tsetse.

Introduction

Lipid droplets (LD) are dynamic organelles and conserved throughout prokaryotic and eukaryotic organisms [1]. The dynamic nature and interactions with other subcellular compartments are poorly understood [2]. They are heterogeneous particles bounded by a phospholipid monolayer also containing glycolipids and sterols. The core inside this monolayer contains triacylglycerols (TAG), diacylglycerols (DAG) and sterol esters. The composition varies between organisms and also cell types. The size of the particles ranges between 50 nm and 200 μm, the latter found in adipocytes. The monolayer contains specific proteins that are involved in biogenesis of the LD and mobilization of the stored lipids. LDs form or accumulate in response to starvation and various other stresses. In addition to carbon storage, a role in intracellular lipid trafficking or membrane biogenesis [3-6] was found in yeast as well as in mammalian cells. In *D. melanogaster* embryos intracellular repositioning has been reported during development [7]. In trypanosomes, the biogenesis of LDs seems to be regulated by specific a protein kinase [8], yet their function in metabolism of the organisms is unknown.

Carbon storage requires a pathway to catabolize the stored TAG. β-oxidation converts fatty acids (FA) into acetyl-CoA building blocks. This starts with the release of FA from TAG by a lipase followed by its activation in the cytosol by a long-chain fatty acyl-CoA synthetase (EC 6.2.1.3), giving rise to a fatty acyl-CoA ester. This ester then diffuses (<10 carbons) or is transported into the mitochondrion. Four subsequent steps produce acyl-CoA(n-2) and acetyl-CoA. The acetyl-CoA is oxidized to carbon dioxide, resulting in ATP production in the electron transport chain. In mammalian cells long chain fatty acids (n>22 carbons) are processed first within the peroxisomes, and the shortened acyl-CoA molecules moved to the mitochondrion. The *T. brucei* peroxisome-like organelles harbour glycolysis and thus are called glycosomes. Two enzymatic activities, enoyl-CoA hydratase (EC4.2.1.17) and 3-hydroxyacyl-CoA dehydrogenase (1.1.1.35), that are part of the trifuctional enzyme complex (TFE) of β-oxidation, have been identified and apparently localized to this organelle [9]. This suggested the parasites capability of FA degradation.

Storage and later utilization of FAs in starvation periods helps cells or organisms to survive changing environments and nutritional bottlenecks. This applies to parasitic organisms like *Trypanosoma brucei* during their life cycle in different host and vector environments. The causative

agent of African Trypanosomiasis has a digenetic life cycle in a mammalian host and tsetse flies of the *Glossina spp.* as vector. While residing in the mammalian bloodstream the nutritional environment is homeostatic. In contrast, during the complex development in the insect vector [10] that involves migration through different organs, the parasite is challenged by changing carbon sources, oxidative stress [11] or different pH values [12]. This is particularly important during migrating from the midgut towards the salivary gland. Crossing the parasite-crowded proventriculus area of the foregut to reach the esophagus requires high parasite motility [13], depending on energy. Therefore, *T. brucei* may need energy stores for development within the insect host. This hypothesis is supported by electron microscopical detection of large LDs within the stumpy bloodstream and procyclic forms, while LD size was considerably reduced in parasites isolated from the proventriculus, and few or no LDs were detected in parasites isolated from the salivary glands [14]. This suggests a physiological role of LDs during developmental progression. We hypothesized that LDs were formed in the proliferating midgut stages and lipid stores were utilized during the migration through the proventriculus towards the salivary glands. In agreement with this view, it has been shown that the procyclic forms take up fatty acids at a much faster rate than BSF [15].

Here we show uptake of fatty acids and their storage in LDs under physiological conditions, and followed the decay of LDs. The putative β-oxidation pathway was reinvestigated by reverse genetic tools.

Experimental procedures

Trypanosome Culture and Transfections - The procyclic form of T. brucei AnTat 1.1 and EATRO1125 was cultured at 27°C in SDM79 medium containing 10% (v/v) heat-inactivated fetal calf serum and 35 μg/mL hemin [16]. The SDM79 used for glucose-depleted conditions was either prepared with normal FCS resulting in about 0.5 mM residual glucose (SDM79-Glu) or additionally preconditioned to fully consume glucose (SDM79GluFree). The SDM79GluFree medium was prepared by growing WT procyclic trypanosomes ($5x10^6$ cells/ml) in glucose-free SDM79 supplemented with 20% FCS, during 3 days to late log phase ($2x10^7$ cells/ml), then the spent medium was filtered and completed with one volume of fresh glucose- and FCS-free SDM79. In both media the addition of 50 mM N-acetylglucosamine (GlcNAc) was added to inhibit residual glucose import [17-19]. Oleate feeding was performed with 400 μM oleate complexed with BSA. The SDM79 medium containing oleate was prepared as described in [20]. The EATRO1125 procyclic form cell line constitutively expressing the T7 RNA polymerase gene and the tetracycline repressor under the control of a T7 RNA polymerase promoter for tetracycline-inducible expression (EATRO1125.T7T) [20], was the recipient of all transfections. Transfection and selection in SDM79 medium containing combinations of hygromycin B (25 μg/mL), neomycin (10 μg/mL), blasticidin (10 μg/mL), phleomycin (5 μg/mL) and puromycin (1 μg/mL) is described in [22].

Fluorescence Microscopy - This protocol was carried out as described previously [23] with minor modifications. $1x10^7$ procyclic forms were fixed in 2% formaldehyde at 4°C, then washed three times with PBS for 5 min at 4°C. The fixed cells were attached to silanized coverslips by sedimentation and permeabilized with 0.2% NP-40 in PBS for 10 min at room temperature for BODIPY 493/503 (Molecular Probes®). For nile red staining permeabilization was not necessary. Staining of lipid droplets was done with 1 μg/ml nile red or 5 μg/ml BODIPY for 30 min at RT. Cells were mounted in antifade solution (Vectashield) and analyzed by confocal laser scanning microscopy (CLSM) with a Leica SP5 CLSM microscope. Microscope settings were: 405 nm diode laser at 20%, Argon laser at 20% power and sequential scanning settings for PMT1: 420-473 nm, for PMT3: 498-564 nm. Stacks have been acquired with 0.5 μm step size and a total thickness of 5-8 μm.

Flow Cytometry - We adapted BODIPY 493/503 staining for T. brucei which is widely used in the mammalian field [20] and has also been used for another kinetoplastid [24]. This dye gives the advantage of a higher specificity for nonpolar lipids and is compatible with multicolor imaging. It enables the analysis by flow cytometry, as there is only one emission spectrum and not two overlapping spectra as for nile red, where the binding to polar or nonpolar lipids creates a chromatic shift [20]. $1x10^7$-$2x10^7$ procyclic cells were harvested and washed once in cold PBS (10 min, 900 g, 4°C). The cells were resuspended in 500 µl PBS and were fixed by addition of 500 µl 4% paraformaldehyde in PBS at 4°C for 2 h or over night. After PFA treatment all following centrifugations were carried out at 500 g, 4°C for 10 min. Cells were washed twice with PBS/2 mM EDTA. Permeabilization was done with 0.2% NP-40 in PBS for 15 min at RT. Cells were then washed once with 1 ml PBS/2 mM EDTA. Pellets have been resuspended in 400 µl PBS/2mM EDTA containing 5 µg/ml BODIPY493/503 and incubated for 30 min at RT in the dark. Cells were pelleted and resuspended in 1ml PBS/2mM EDTA and analyzed with a BD FACS Calibur flow cytometer (488 nm Laser).

Labeling with [1-^{14}C]-oleate and lipid analysis - [1-^{14}C]-oleate feeding was performed as follows: 10^8 cells in the late exponential phase were incubated for 30 min, 1h, 2h and 8h in 5 mL of SDM79 medium as indicated above and containing 6 µM [1-^{14}C]-oleate (58.2 mCi/mmol, Perkin-Elmer SAS, Courtaboeuf, France) and 400 µM unlabeled oleate complexed with BSA. The SDM79 medium containing oleate was prepared as described in [20]. Subsequently, lipids were extracted by chloroform:methanol (2:1, v/v) for 30 min at room temperature, and then washed three times with 0.9% NaCl. The solvent was evaporated and lipids were dissolved in an appropriate volume of chloroform/methanol (1:1, v/v). To determine the labeling of total phospholipids and neutral lipids, the lipid extracts were loaded onto HPTLC plates (60F254, Merck) with a CAMAG Linomat IV and developed in hexane/ethylether/acetic acid (90:15:2, v/v). Total phospholipids (start), diacylglycerols (DAG, R_F 0.08), free fatty acids (FFA, R_F 0.29), triacylglycerols (TAG, R_F 0.50) and esters (R_F 0.90) were separated. Lipids were identified by co-migration with known standards and lipid radioactivity was determined with a Storm 860 (GE Healthcare) phosphorimager.

TAG quantification by HPTLC - Lipid extracts were prepared as indicated above. To determine the amount of TAG, the lipid extracts were loaded onto HPTLC plates developed in hexane/ethylether/acetic acid (90:15:2, v/v) as indicated above. TAG amounts were quantified by densitometry using a CAMAG TLC scanner 3 as described in [25].

TAG species identification by ESI/MS/MS - Prior to the MS analysis, the lipid extracts were resuspended with a mixture of chloroform/methanol 1/1 (v/v) containing 0.2 % formic acid+0.028 % NH_3. Shotgun analysis was performed on a QTrap 5500 (ABSciex). Analyses were performed with neutral loss scans in positive mode. Nitrogen was used as curtain gas (set to 15), gas1 (set to 20) and gas2 (set to 0). Needle voltage was at +5,500 V without needle heating; the declustering potential was set at +40 V. The collision gas was also nitrogen and collision energy was adjusted to +40 eV. Samples were analyzed in duplicate. Triacylglycerols were identified and quantified using the Lipidview (ABSciex). Lipid species were quantified by normalizing the intensities of their peaks to the intensity of the peaks of the internal standard (TAG17:0/17:0/17:0) spiked into the sample.

NADP-dependent 3-hydroxyacyl-CoA dehydrogenase activity in cell extracts and glycosome enriched fractions - Cells were washed in PBS and lysed by sonication (5 sec at 4°C) in phosphate buffer (100 mM, pH 6.2). A subcellular fraction enriched in glycosomes was prepared by differential centrifugation of WT procyclic cells and of *Δtfeα1/Δtfeα1* cells. Trypanosomes were harvested by centrifugation for 10 min at 1000 g and the cell pellet was subjected to grinding with silicon carbide (325 mesh) in the presence of homogenization buffer (250 mM sucrose, 25 mM Tris-HCl pH:7.4, 1 mM EDTA) supplemented with a cocktail of protease inhibitors. The disruption of parasites was followed by phase contrast microscopy and continued until at least 95% of the cells were broken. After dilution of the resulting mixture with homogenization buffer the silicon carbide was removed

by centrifugation at 4500 g for 5 min. The homogenate obtained was then centrifuged at 17,000 g for 10 min to sediment glycosomes. The pellet was resuspended in phosphate buffer (100 mM, pH 6.2) and lysed by sonication (5 sec at 4°C). The 3-hydroxyacyl-CoA dehydrogenase activity and the GPDH activity were measured as described before [26,27].

Phylogenetic reconstruction - Sequences belonging to the TFEα2 group, including the mitochondrial Human sequence (P40939), were collected from a recent analysis [28]. Representative prokaryotic and eukaryotic sequences belonging to the TFEα1 group, were obtained by BLAST runs against the nr database with the peroxisomal mouse (BAB23628.1) and the Pseudomonas stutzeri (WP 017245866.1) sequences as query. The multiple sequence alignments of the TFEα1 and TFEα2 sequences, including the trypanosomal and leishmanial orthologous sequences found in TriTrypDB (http://tritrypdb.org/tritrypdb/) were done with the web-based CLUSTALW2 program, and the guide tree obtained was used to construct a dendrogram using the TreeView program.

Knockout of the TFE candidate gene - Replacement of the putative enoyl-CoA hydratase / enoyl-CoA isomerase / 3-hydroxyacyl-CoA dehydrogenase (TFE, Tb927.2.4130) by the puromycin (PAC) and blasticidin (BSD) resistance markers via homologous recombination was performed with DNA fragments containing a resistance marker gene flanked by the *TFEα1* UTR sequences. The *TFEα1* knock out was generated in the EATRO1125.T7T parental cell line, which constitutively expresses the T7 RNA polymerase gene and the tetracycline repressor under the control of a T7 RNA polymerase promoter for tetracycline inducible expression (TetR-HYG T7RNAPOL-NEO) [21]. Transfection and selection of drug-resistant clones were performed as previously reported [29]. The first and second *TFEα1* alleles were replaced by *PAC* and *BSD*, respectively. Transfected cells were selected in SDM79 medium containing hygromycin B (25 μg/mL), neomycin (10 μg/mL), puromycin (1 μg/mL) and blasticidin (10 μg/mL). The selected cell line (TetR HYG T7RNAPOL NEO *Δtfeα1::PAC/Δtfeα1::BSD*) is abbreviated as *Δtfeα1/Δtfeα1.*

Southern blot analysis - 6 μg of genomic DNA from the wild-type and *Δtfeα1/Δtfeα1* cell lines, extracted as previously described [30], were digested with the KpnI restriction enzyme, separated by electrophoresis in a 0.8% agarose gel and transferred onto a nylon membrane (Hybond N^+, Roche Molecular Biochemicals). The membrane was hybridized with digoxigenin-labeled DNA probes synthesized with a PCR DIG probe synthesis kit (Roche Molecular Biochemicals) as recommended by the supplier. The *TFEα1* and *FRD* probes were generated by PCR amplification, using the primer pairs 5'-ATGCGTCGCTTGGAAACCATATC-3' / 5'-GAGCCGCTGCTGCTGTAGTCCCG-3' and 5'-GTGTAACGTCGTTGCTCAGTGAGA-3' / 5'-GCGAAATTAAATGGGCCCCGC GACG-3', respectively. Probe-target hybrids were visualized by a chemiluminescent assay with the DIG luminescent detection kit (Roche Molecular Biochemicals), according to the manufacturer's instructions. Blots were exposed to ImageQuant LAS4010 (GE Healthcare Life Sciences) for approximately 20 min.

Sample preparation for proteomic analysis - Samples were loaded on a 10% acrylamide SDS-PAGE gel. Migration was stopped when samples had just entered the resolving gel, proteins were visualized by Colloidal Blue staining, and the unresolved region of the gel cut into 1 mm x 1 mm gel pieces. Gel pieces were destained in 25 mM ammonium bicarbonate (NH_4HCO_3), 50% Acetonitrile (ACN) and shrunk in ACN for 10 min. After ACN removal, gel pieces were dried at room temperature. Proteins were first reduced in 10 mM dithiothreitol, 100 mM NH_4HCO_3 for 30 min at 56°C then alkylated in 100 mM iodoacetamide, 100 mM NH_4HCO_3 for 30 min at room temperature and shrunken in ACN for 10 min. After ACN removal, gel pieces were rehydrated with 100 mM NH_4HCO_3 for 10 min at room temperature. Before protein digestion, gel pieces were shrunken in ACN for 10 min and dried at room temperature. Proteins were digested by incubating each gel slice with 10 ng/μL of trypsin (T6567, Sigma-Aldrich) in 40 mM NH_4HCO_3, 10% ACN, rehydrated at 4°C for 10 min, and finally incubated overnight at 37°C. The resulting peptides were extracted from the

gel by three steps: a first incubation in 40 mM NH_4HCO_3, 10% ACN for 15 min at room temperature and two incubations in 47.5 % ACN, 5% formic acid for 15 min at room temperature. The three collected extractions were pooled with the initial digestion supernatant, dried in a SpeedVac, and resuspended with 25 µL of 0.1% formic acid before nanoLC-MS/MS analysis.

NanoLC-MS/MS analysis - Online nanoLC-MS/MS analyses were performed using an Ultimate 3000 system (Dionex, Amsterdam, The Netherlands) coupled to a nanospray LTQ Orbitrap XL mass spectrometer (Thermo Fisher Scientific, Bremen, Germany). Ten microliters of each peptide extract were loaded on a 300 µm ID x 5 mm PepMap C_{18} precolumn (LC Packings, Dionex, USA) at a flow rate of 20 µL/min. After 5 min desalting, peptides were online separated on a 75 µm ID x 15 cm C_{18}PepMap™ column (LC packings, Dionex, USA) with a 2-40% linear gradient of solvent B (0.1% formic acid in 80% ACN) during 108 min. The separation flow rate was set at 200 nL/min. The mass spectrometer operated in positive ion mode at a 1.8 kV needle voltage and a 42 V capillary voltage. Data were acquired in a data-dependent mode alternating an FTMS scan survey over the range m/z 300-1700 with the resolution set to a value of 60 000 at m/z 400 and six ion trap MS/MS scans with Collision Induced Dissociation (CID) as activation mode. MS/MS spectra were acquired using a 3 m/z unit ion isolation window and normalized collision energy of 35. Mono-charged ions and unassigned charge-state ions were rejected from fragmentation. Dynamic exclusion duration was set to 30 sec.

Database search and results processing - Mascot and Sequest algorithms through Proteome Discoverer 1.4 Software (Thermo Fisher Scientific Inc.) were used for protein identification in batch mode by searching the Trypanosoma brucei TREU927 database (TritrypDB release 6.0, 90307 entries) at http://tritrypdb.org/. Two missed enzyme cleavages were allowed. Mass tolerances in MS and MS/MS were set to 10 ppm and 0.6 Da. Oxidation of methionine, acetylation of lysine and deamidation of asparagine and glutamine were searched as variable modifications. Carbamidomethylation on cysteine was searched as fixed modification. Peptide validation was performed using Percolator algorithm [31] and only "high confidence" peptides were retained corresponding to a 1% false positive rate at peptide level.

Label-Free Quantitative Data Analysis - Raw LC-MS/MS data were imported in Progenesis LC-MS 4.1 (Nonlinear Dynamics Ltd, Newcastle, U.K) for feature detection, alignment, and quantification. All sample features were aligned according to retention times by manually inserting up to two hundred landmarks followed by automatic alignment to maximally overlay all the two-dimensional (m/z and retention time) feature maps. Singly charged ions and ions with higher charge states than six were excluded from analysis. All remaining features were used to calculate a normalization factor for each sample that corrects for experimental variation. Peptide identifications (with $p < 0.01$, see above) were imported into Progenesis. For quantification, all unique peptides of an identified protein were included and the total cumulative abundance was calculated by summing the abundances of all peptides allocated to the respective protein. No minimal thresholds were set for the method of peak picking or selection of data to use for quantification. For each biological replicate, the mean normalized intensities and standard deviation were calculated and ratio was deducted. Noticeably, only non-conflicting features and unique peptides were considered for calculation at protein level. Quantitative data were considered for proteins quantified by a minimum of 2 peptides. As an indication of the confidence of that protein's presence, the sum of the peptide scores (confidence score) is calculated for each protein from the search algorithm. This score includes unique peptides as well as switched off peptides, the later decreasing the confidence score.

Results:

We started with the hypothesis that carbon storage in the form of lipid droplets (LD) is a physiological adaptation to nutrient supply in *T. brucei* and quantified LDs under excess lipid feeding conditions. Oleate was chosen as fatty acid species likely to be taken up and metabolized by trypanosomes. The lipid or phospholipid content of bloodstream and procyclic *T. brucei* cells has determined [32,33], but no detailed analyses of the TAG species has been reported. We investigated procyclic trypanosomes, as lipid storage may be advantageous to face the nutritional bottlenecks during their subsequent development in the tsetse.

Oleate uptake and storage in lipid droplets

After oleate/BSA feeding of procyclic trypanosomes for 2-3 days the number of nile red stained LDs increased (Fig.1A), as previously shown upon drug treatment with myriocin [34] and included here for reference (Fig.1A). Whereas myriocin treatment led to a cytokinesis phenotype [34], feeding with oleate/BSA did not change the growth rate (see Fig.5B). The effect of oleate feeding was quantified by counting the number of nile red stained LDs per cell in stacks of confocal laser scanning images. The average number of LDs per cell increased almost 5-fold compared to unfed cells (Fig.2A). The histogram in Fig.2B shows the bell-shaped, apparently normal, distribution of the LD numbers per cell in the populations. The maximum number of LDs that a single cell can build up, nine LDs in oleate fed cells in our experiments with strain AnTat1.1, may depend on cell clone-specific properties like uptake capacity and growth rate. A similar argument applies to the average number of lipid droplets in unfed cells that is also likely to depend on the batch of FCS and the amount of fatty acids (FAs) contained within.

As a routine assay to quantify LDs in *T. brucei*, we optimized flow cytometry after BODIPY 493/503 staining. The microscopic picture upon BODIPY 493/503 staining is not different from nile red staining (Fig.1B). Yet, nile red has wide and overlapping emission spectra when bound to polar and nonpolar lipids, whereas BODIPY 493/503 accumulates more specifically in the nonpolar lipophilic environment in LDs [20]. Flow cytometry integrates the fluorescence signal of the whole cell, and therefore low background from membrane lipid staining is essential for LD quantification by flow cytometry. The validity of the flow cytometric assay was demonstrated by an increase of the fluorescence signal between the unfed and oleate fed cells (Fig.2C), that was very close (4.6-fold) to the increase determined by microscopic LD counting (4.7-fold, Fig.2A). The TAG content of cells incubated with or without oleate was also directly quantified by thin layer chromatography (TLC) (Fig.2D), again resulting in the very same increase (4.6-fold). The perfect quantitative correlation of LD numbers, flow cytometry and TAG analysis upon oleate feeding, strongly suggests that oleate uptake results in TAG storage in LDs.

The TAG species in oleate fed and unfed cells were then analyzed by mass spectrometry. A high number of 96 TAG species were resolved and identified (Fig.S1). Such a high number of TAG species has already been observed in serum and butter [35,36]. In both conditions the 54:2,3,4 TAG species were by far the predominant species and were significantly increased upon oleate feeding (Fig.3A). As oleate is a C18 fatty acid with one unsaturated double bond, the predominant 54:3 TAG species provides evidence that at least part of the oleate taken up is esterified with glycerol for storage in lipid droplets. To directly follow incorporation of oleate into TAGs, we performed a labeling experiment with [^{14}C]-oleate (Fig.3B). Procyclic trypanosomes were cultured in the presence of radiolabeled oleate up to 8 hours. Samples were collected during this uptake time course and labeled lipid species were separated by TLC and quantified using a phosphor imager. Oleate was incorporated into TAG as well as into phospholipids (PPL) in a time-dependent manner.

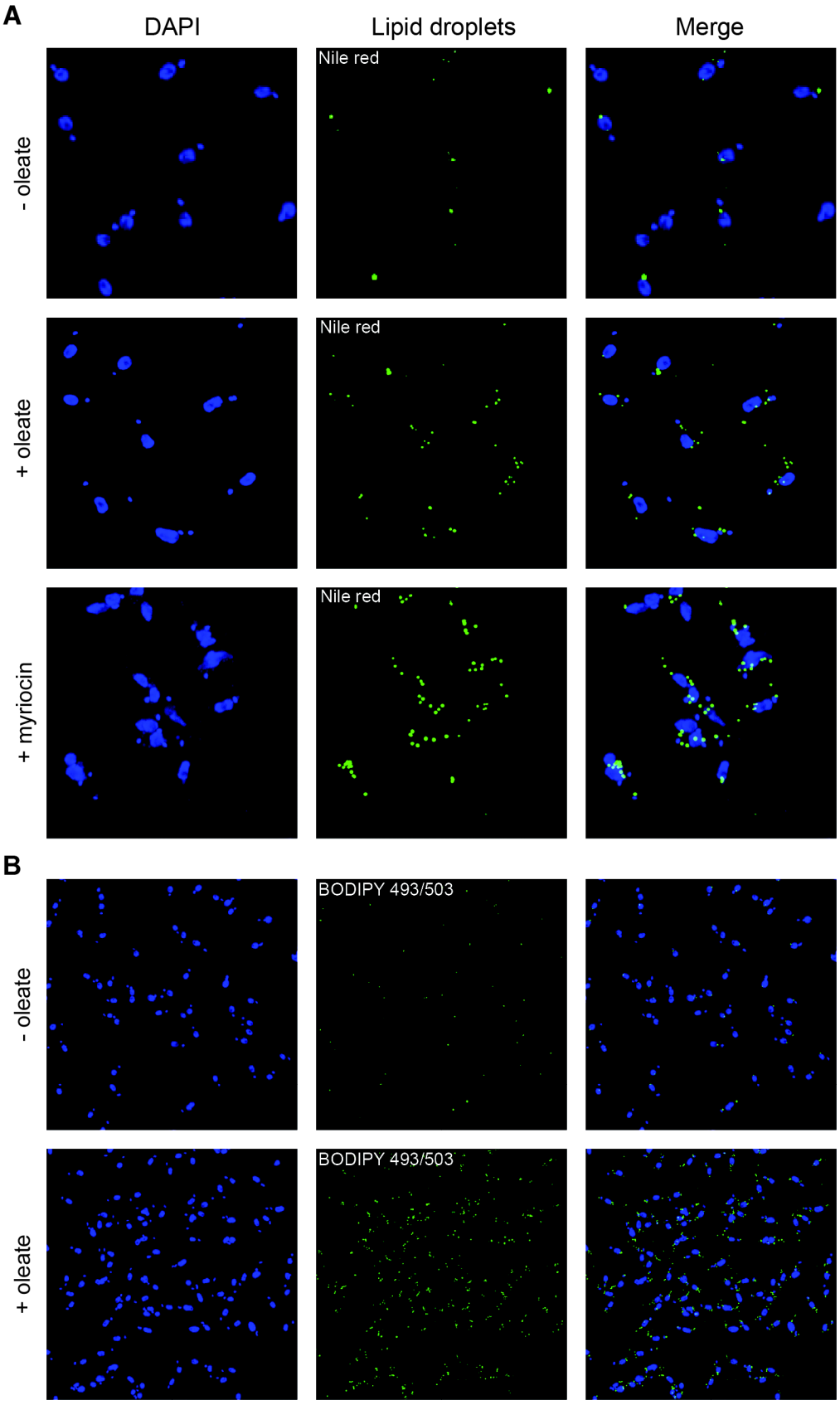

Fig.1: Oleate feeding stimulates lipid droplet formation in procyclic *T. brucei* cells. Staining of lipid droplets with nile red (A) or BODIPY 493/503 (B) was performed as detailed in experimental procedures. Myriocin treatment (0.5 µM for 24h) was included for comparison to a previous report [9]. An example of several experiments is shown.

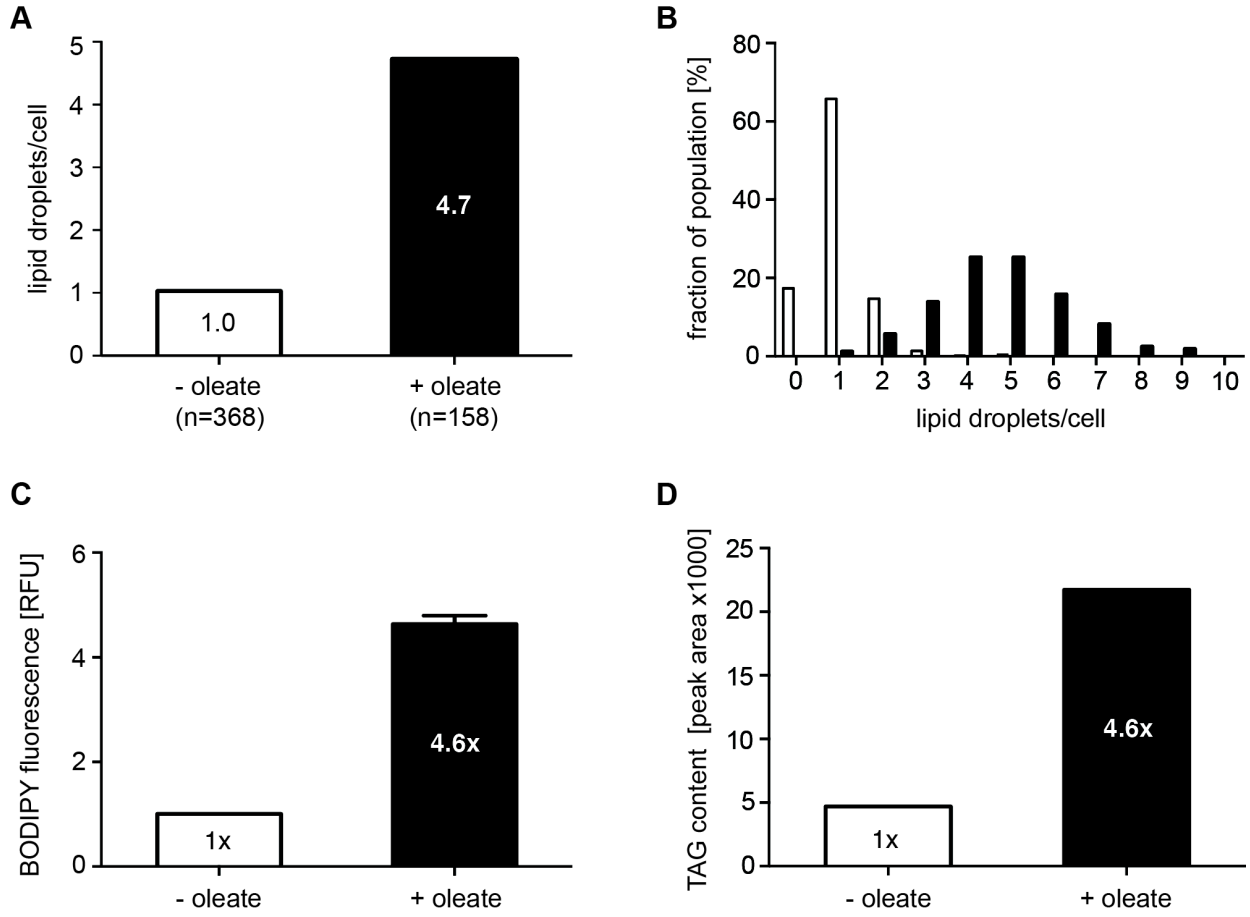

Fig.2: Quantification of the oleate-induced lipid droplet formation. (A) BODIPY 493/503 stained LDs were counted in stacks of confocal laser scanning microscopy (CLSM) images; the average number of LDs per cell is given after oleate feeding (black column) or in the control (white column). (B) Distribution of LD numbers per cells in the population after oleate feeding (black columns) or in the control (white columns). (C) Quantification of BODIPY-stained LDs by flow cytometry after oleate feeding (black column) or in the control (white column). BODIPY 493/503 preferentially stains nonpolar lipids. Error bars give the SEM (n=3) of values normalized to the control. (D) Quantification of TAG content by HPTLC and densitometry after oleate feeding (black columns) or in the control (white columns). Values are normalized to the control.

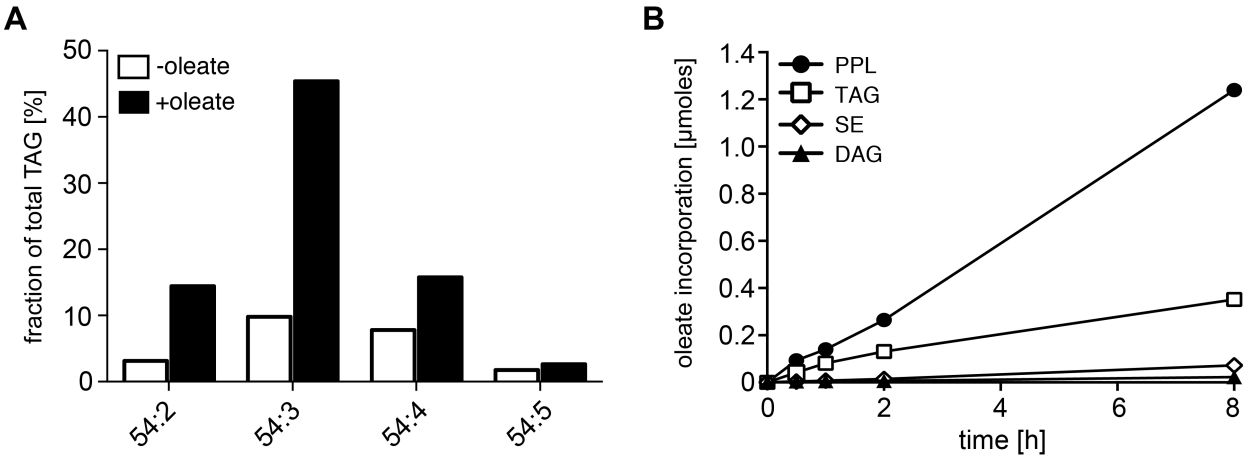

Fig.3: TAG species analysis and uptake of labeled oleate. (A) Dominant TAG species in procyclic *T. brucei* cells identified by ESI/MS/MS after oleate feeding days (black columns) or in the control (white columns). For a complete list of TAG species detected see Fig. S1. The nomenclature 54:X indicates the total carbon number of all three acyl chains and the sum of all unsaturated double bonds within the acyl chains. (B) Uptake kinetics upon growth in the presence of radiolabeled oleate for up to 8h. The incorporation of ^{14}C oleate into lipid species was quantified by HPTLC and a Storm 860 phosphorimager. PPL, phospholipids; TAG, triacylglycerol; SE, Steryl-esters; DAG, diacylglycerol.

Characterisation of a β-oxidation pathway candidate gene

A likely rationale for uptake and storage of lipids in a specific cellular compartment is later use for energy production by β-oxidation. In cell lysates of procyclic *T. brucei* the enzymatic activities of 2-enoyl-CoA hydratase and 3-hydroxyacyl-CoA dehydrogenase, two essential enzymatic steps in β-oxidation have previously been detected [9]. In order to explore the genomic capacity for β-oxidation in *T. brucei*, a bioinformatic search for candidate genes for these two activities was undertaken. The β-oxidation pathway consists of four steps, being an acyl-CoA dehydrogenation, an enoyl-CoA hydratation, a 3-hydroxyacyl-CoA dehydrogenation and a thiolytic cleavage reaction. In most organisms, the first reaction of this pathway is catalyzed by a monofunctional enzyme, while the three other reactions are catalyzed by a trifunctional enzyme (TFE) complex, composed of a bifunctional TFEα subunit (enoyl-CoA hydratase and 3-hydroxyacyl-CoA dehydrogenase activities) and a monofunctional TFEβ subunit (thiolase activity). Most eukaryotes contain two phylogenetically distinct TFEα, one located in the mitochondrion (named TFEα2) and the other in peroxisomes (named TFEα1). The *Leishmania spp.* and *T. cruzi* genomes contain one mitochondrial and one glycosomal type gene with a mitochondrial targeting motif or a peroxisomal targeting sequence 2 (PTS2) present, respectively. However, only one gene encoding the putative glycosomal TFEα1 isoform, is detected in the African trypanosome genomes (Fig.4).

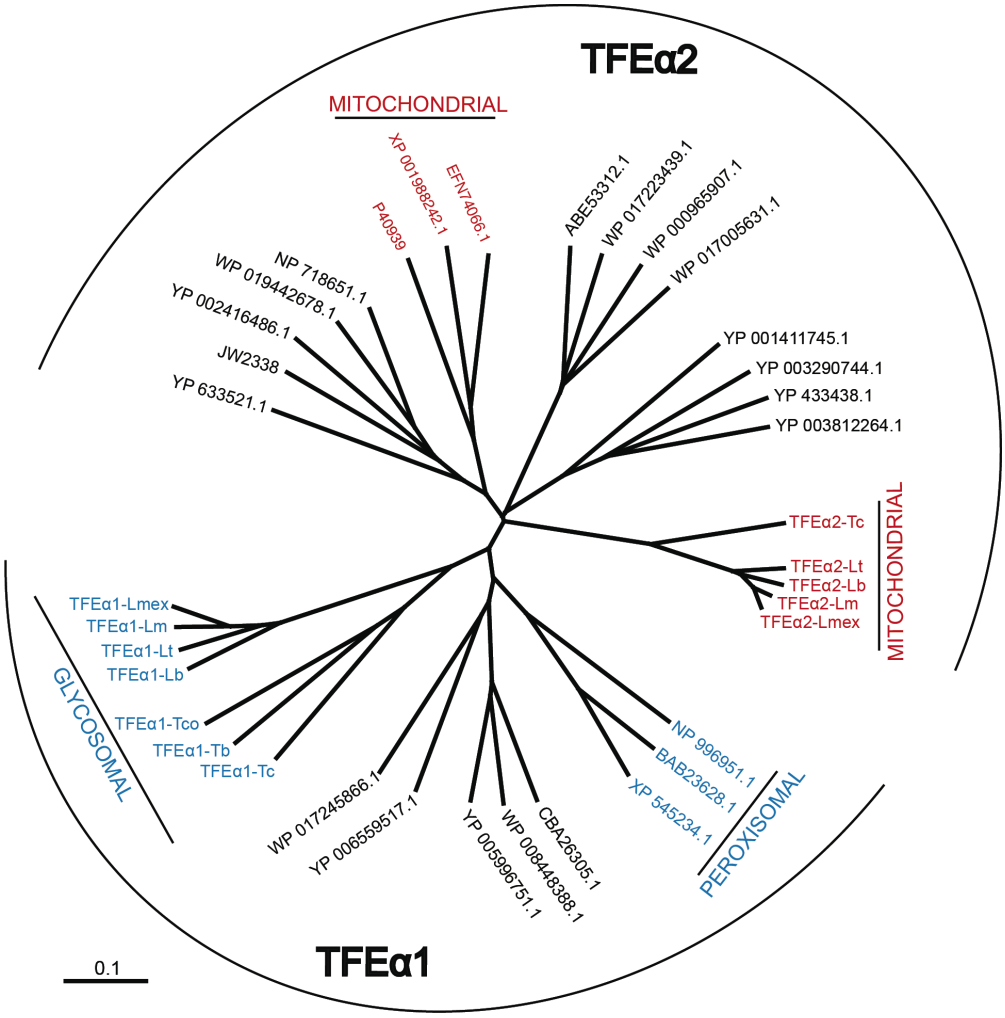

Fig.4: Dendrogram of trifunctional enzyme (TFE) isoforms. Prokaryotic (black characters) and eukaryotic (colored characters) TFEα sequences are represented by their GenBank accession codes. Glycosomal/peroxisomal (TFEα1) or mitochondrial (TFEα2) proteins are highlighted in blue and red. Experimental evidence for glycosomal localization of trypanosomatid TFEα1 isoforms, which all contain a PTS2 motif, is limited to *T. brucei* TFEα1 (see [38] and Table S1). Mitochondrial localization of the trypanosomatid TFEα2 isoforms is assumed due to an N-terminal mitochondrial targeting motif and the absence of a PTS motif. Abbreviations: Lb, *Leishmania braziliensis*; Lm, *L. major*; Lmex, *L. mexicana*; Lt, *L. tarentolae*; Tb, *T. brucei*; Tc, *T. cruzi*; Tco, *T. congolense*.

This leaves *T. brucei* with a single candidate gene for the measured enoyl-CoA hydratase and 3-hydroxyacyl-CoA dehydrogenase activities. Therefore, the *TFEα1* candidate gene was deleted by a homologous recombination-mediated homozygous gene replacement with two antibiotic resistance markers. The identity of the resulting *Δtfeα1/Δtfeα1* null mutant was verified by locus PCR and by Southern blot analysis (Fig.S3).

As glucose starvation may induce the putative β-oxidation pathway to restore the energy balance, the growth rate of WT and *Δtfeα1/Δtfeα1* null mutant cells was determined in our new glucose-free medium (SDM79GluFree, see Methods) supplemented or not with 10 mM glucose. Growth of the null mutant is only moderately affected compared to WT regardless of the amount of glucose (Fig.5A). TFEα1 contains a peroxisomal targeting signal 2 motif (PTS2, RLETISSHV) [37] and has recently been found enriched in glycosomal fractions [38]. This is consistent with the enrichment of the 2-enoyl-CoA hydratase and 3-hydroxyacyl-CoA dehydrogenase enzymatic activities in glycosomal fractions [9]. In addition, TFEα1 contains a putative 24 amino acid N-terminal mitochondrial target motif predicted by MitoProt (http://ihg.gsf.de/ihg/mitoprot.html) with a moderate probability (0.41). In absence of antibody reagents, we used proteomic analysis of partially purified glycosome fractions from WT and *Δtfeα1/Δtfeα1* null mutant cells to probe expression and subcellular localization. We compared the ratio of peptide counts of WT over *Δtfeα1/Δtfeα1* for all glycosomal proteins detected with confidence by Güther et al. [38] in the proteome of affinity purified glycosomes (Fig.5B, Table S1). A ratio around 1 for all proteins detected, showed that the protein composition of glycosomes is not altered in the *Δtfeα1/Δtfeα1.* Only for TFEα1, a 140-fold ratio of peptide counts of WT over *Δtfeα1/Δtfeα1* verified the knock out and demonstrated that the candidate gene product is expressed in procyclic *T. brucei.* Furthermore, the presence in a partially purified glycosome fraction is compatible with its glycosomal localization.

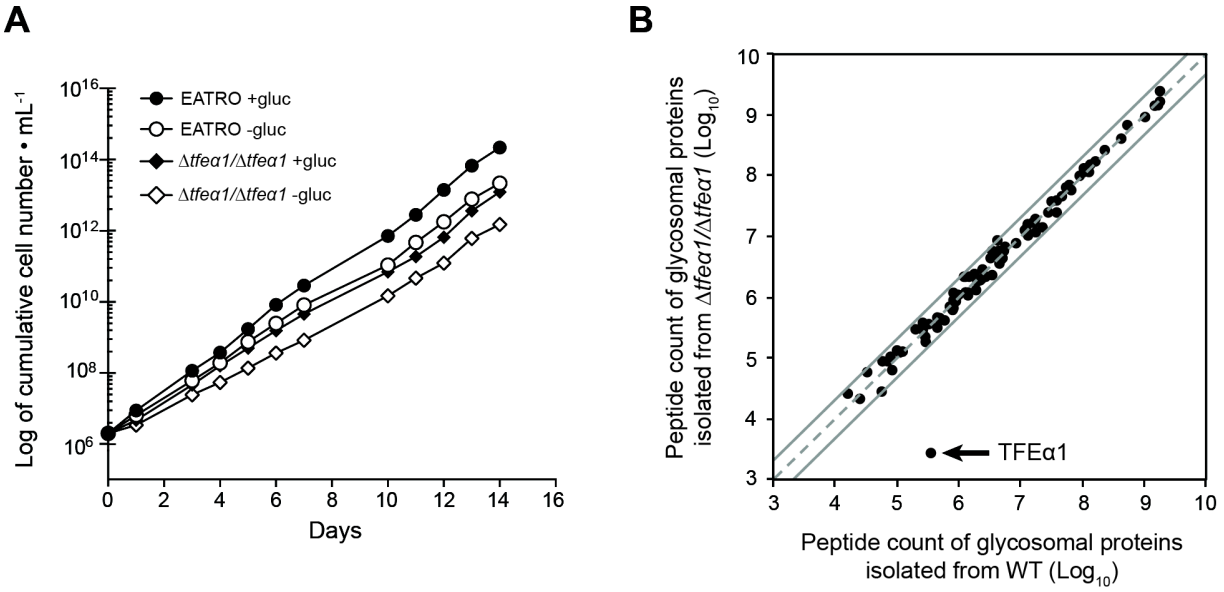

Fig.5: Phenotypic analysis of Δ*tfeα1*/Δ*tfeα1* cell. (A) growth curve of WT and Δ*tfeα1*/Δ*tfeα1* cell knock cells in glucose-rich (SDM79 with 10 mM glucose) or glucose-free (SDM79GluFree) conditions. (B) Global protein abundance in the partially purified glycosome fraction of WT (x-axis) and Δ*tfeα1*/Δ*tfeα1* cell knock cells (y-axis). Each protein identification is presented by a point at $\log_{10}$ of normalized peptide count values taken from the proteome data in Table S1. Proteins on the dashed grey line have identical normalized peptide counts in both samples; the grey lines represent a 2-fold abundance in one condition.

Enzymatic activity was then measured in WT and *Δtfeα1/Δtfeα1* knockout cells using whole cell extracts and partially purified glycosome fractions (Table 4.1). Surprisingly, the 3-hydroxyacyl-CoA dehydrogenase activity was identical in WT and *Δtfeα1/Δtfeα1* whole cell lysates and in the

respective glycosome preparations. We concluded that the *TFEα1* candidate gene is not encoding the measured and previously reported [9] 3-hydroxyacyl-CoA dehydrogenase activity. Furthermore, the assignment of this activity to glycosomes cannot be confirmed. Whereas a glycosomal marker, glycerol-3-phosphate dehydrogenase (GPDH) activity, is 7-fold higher in our partially purified glycosome preparations, the measured 3-hydroxyacyl-CoA dehydrogenase activity was less than 2-fold enriched in those preparations (Table1).

Table1: 3-hydroxyacyl-CoA dehydrogenase activity in WT and Δ*tfeα1*/Δ*tfeα1* cells

	3 hydroxyacyl-CoA dehydrogenase[3]	GPDH[3]
WT WCE[1] +gluc[4]	6.62 ± 0.63 (n=5)	32.20 ± 3.48 (n=3)
WT WCE[1] -gluc[5]	5.22 ± 0.40 (n=5)	34.92 ± 2.71 (n=3)
Δ*tfeα1*/Δ*tfeα1* WCE[1] +gluc[4]	6.04 ± 0.71 (n=5)	22.80 ± 2.45 (n=3)
Δ*tfeα1*/Δ*tfeα1* WCE[1] -gluc[5]	5.00 ± 0.47 (n=5)	35.40 ± 1.89 (n=3)
WT glyco[2] +gluc[4]	11.76 ± 0.52 (n=6)	213.18 ± 4.12 (n=3)
Δ*tfeα1*/Δ*tfeα1* glyco[2] +gluc[4]	9.12 ± 0.77 (n=6)	208.22 ± 12.19 (n=3)

[1] WCE, whole cell exctract

[2] glyco, partially purified glycosome fraction

[3] Mean ±SEM of n experiments (mU/mg of protein)

[4] +gluc: cells cultured in SDM79 containing 10 mM glucose

[5] -gluc: cells cultured in glucose-depleted SDM79GluFree

We cannot formally exclude that the *TFEα1* candidate gene encodes a 3-hydroxyacyl-CoA dehydrogenase enzyme that is inactive in procyclic trypanosomes or for which our enzyme assay is inappropriate. As the putative β-oxidation pathway may be induced by glucose starvation, we measured the 3-hydroxyacyl-CoA dehydrogenase activity in both WT and *Δtfeα1*/*Δtfeα1* cells grown in SDM79GluFree for one week, but no differences were observed compared to glucose-rich conditions. In summary, it seems very unlikely that the *TFEα1* candidate gene is encoding a protein with 3-hydroxyacyl-CoA dehydrogenase activity. Therefore, previous arguments in favor of a β-oxidation pathway in *T. brucei*, that combined genomic evidence for a *TFEα1* candidate gene [37] with reported enzymatic activities and affirmed glycosomal localization [9] cannot be held up, even in glucose-free conditions.

Lipid droplet and TAG turnover

In absence of evidence for β-oxidation as the canonical lipid degradation pathway, the question of the fate of the accumulated LDs in oleate fed cells was raised. We quantified the kinetics of LD reduction upon oleate withdrawal and culture in normal SDM79 medium. The LD decay kinetic was first analyzed by flow cytometry with BODIPY 493/503 staining. After maximal feeding for 3 days, samples were collected over a period of 32 hours. We assumed that in a growing cell population the preformed lipid droplets are equally distributed to daughter cells and therefore calculated the expected fluorescent signal decrease using the population doubling time in the actual experiment as derived from the growth curve in Fig.6A. The thereby calculated minimal decay kinetics is represented by filled squares in Fig.6A. The measured fluorescence decrease from flow cytometry data (open circles) was identical with the calculated kinetic. Thus, dilution during cell divisions can fully account for the kinetics of LD decay to basal level.

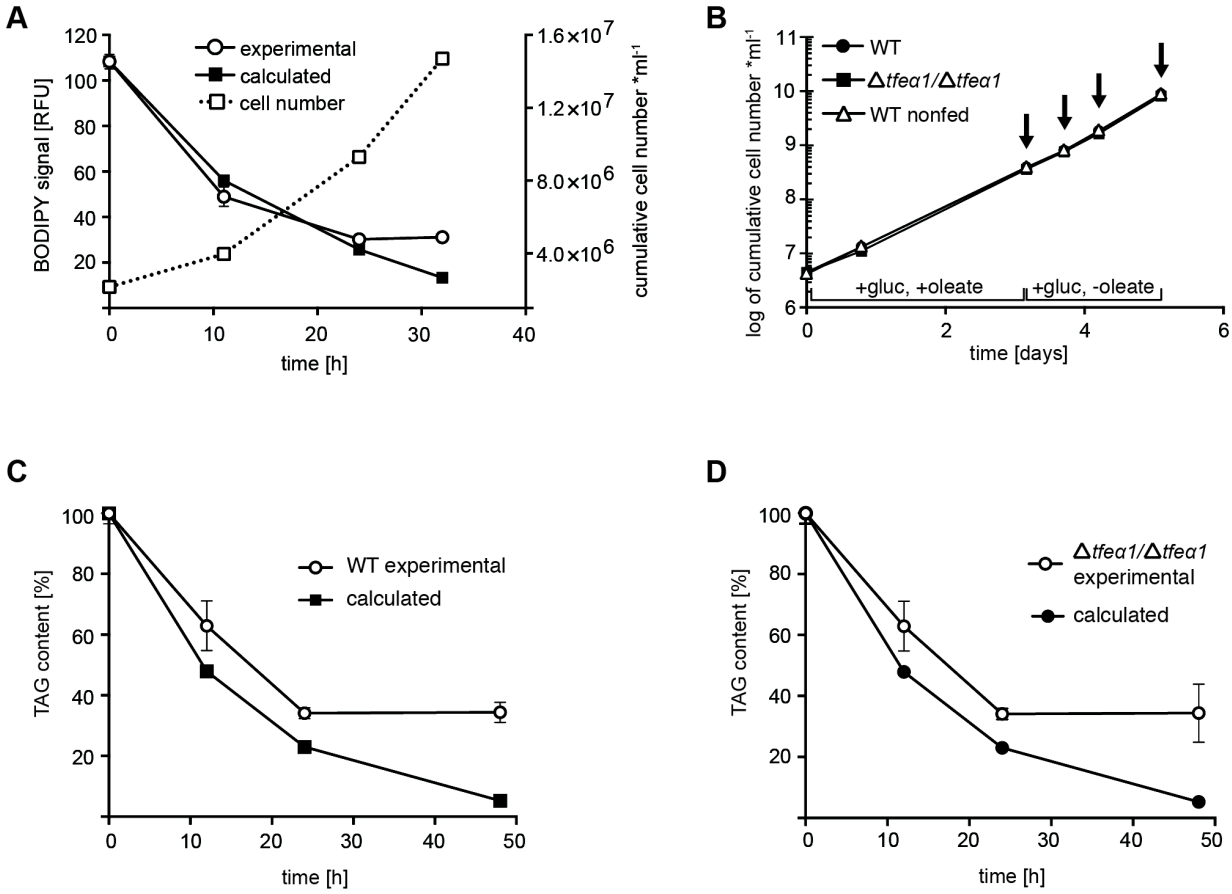

Fig.6: LD and TAG turnover in WT and *Δtfeα1/Δtfeα1* cells. Cells were fed with oleate in glucose-rich SDM79 medium for three days and after oleate withdrawal samples were taken at the time points indicated. (A) WT cells stained with BODIPY and analyzed by flow cytometry (left y-axis). Error bars represent the SEM of independent replicates (n=3). The growth curve is given as dashed line (right y-axis). (B) Growth curve and sampling time points (arrows) for the experiments in panels (C) and (D). Total TAG content was determined by HPTLC and densitometry (technical triplicates) in WT (C) and *Δtfeα1/Δtfeα1* (D) cells. The calculated values (filled symbols) account for dilution of LDs or TAG content by cell division, based on the matched growth data.

The same kinetic experiment was performed with quantification of the total TAG content by TLC. The growth curve and sampling time points are shown in Fig.6B and the TAG content kinetics in Fig.6C,D. Again, a very similar decrease of calculated and experimentally determined TAG content is seen upon oleate withdrawal. Whereas the calculated dilution curve predicts very low TAG levels after several cell cycles, the experimental values return to the basal level maintained by the lipid uptake in normal medium and lipid synthesis. Importantly, the experimental values were never found below the calculated prediction, negating any argument in favor of net catabolism of the accumulated TAGs. The *Δtfeα1/Δtfeα1* null mutant was also analyzed in this experiment (Fig.6D). The results were identical, and the kinetics for WT and *Δtfeα1/Δtfeα1* were perfectly superimposed. This is expected if TFEα1 is not involved in lipid catabolism in procyclic trypanosomes.

Discussion

Carbon storage is widespread in organisms to maintain energy homeostasis during transient nutrient shortage and periods of starvation of individual cells or of metazoan organisms. The predominant forms of storage carbon are fat in the form of triacylglycerol and carbohydrate polymers like glycogen in animals and yeast or starch in plants [39-41]. In the kinetoplastid protozoan *Leishmania major* the carbohydrate polymer mannan has apparently replaced glycogen [42]. In *Trypanosoma* mannan has not been detected, but lipid droplets (LDs) have been described

as a regulated compartment [8], compatible with a role in lipid storage. LD biogenesis is dependent on a protein kinase, termed LDK (lipid droplet kinase) as shown by RNAi-mediated repression [8]. An electron microscopic study reports that number and size of LDs vary during insect stage differentiation from the midgut to the salivary glands [14]. These observations are correlative, but point to a physiological function in the parasite´s adaptation, probably to nutritional bottlenecks during development and migration in the tsetse alimentary tract. Here we report for the first time that an induced physiological change in environmental conditions, namely the supplementation of cell culture medium with fatty acids (oleate), can stimulate the buildup of LDs in procyclic *T. brucei* without any impact on the cell´s growth rate. The inhibitor myriocin also increased LD numbers in procyclic *T. brucei* in a previous report, but caused a severe cytokinesis phenotype [8]. We provide evidence that oleate is taken up and esterified to triacylglycerol (TAG) for storage in LDs: (1) upon feeding, the LD number, the quantity of stained lipids and the cellular TAG content increase by the very same factor of 4-5; (2) radiolabelled oleate is incorporated into TAGs (and phospholipids); (3) out of 96 TAG species detected by mass spectrometry, the 54:3 TAG species (e.g. oleate) was by far the most abundant in cells fed and unfed with oleate. The fact that in unfed cells the most abundant TAG species was of the 54:3 type, suggests that oleate is normally selected from serum lipids for storage in trypanosomes.

The question remains how these lipid stores are used by the cell. One possibility is their use for rapid synthesis or remodeling of membrane lipids upon proliferation or differentiation under limiting nutrient supply. In *T. cruzi* for example, the fatty acid composition of phospholipids (PPL) changes in response to the environmental temperature. Increasing temperature causes a higher ratio of saturated to unsaturated fatty acids in PPL, this being balanced by an inverse change in cellular TAG pools, that may represent LDs. Exchange of fatty acids between the TAG pool and the membrane PPL pool maybe part of an environmental adaptation [43]. The alternative fate of lipid stores is catabolism for energy production upon starvation. We first considered the most widespread pathway of fatty acid catabolism present in most organisms, fatty acid β-oxidation. This was motivated by the previous report of enzymatic activities compatible with a β-oxidation pathway in *T. brucei* [9] and the prediction of a candidate gene in the genome [37]. In contrast to expectation, the only recognizable candidate gene, *TFEa1,* did not encode the reported activity, in spite of evidence for TFEa1 expression. The presence of a peroxisomal targeting sequence 2 (PTS2) and detection in an enriched glycosomal fraction suggested glycosomal localization of TFEa1, but the 3-hydroxyacyl-CoA dehydrogenase activity was not enriched in that glycosomal fraction in contrast to a previous report [9]. Thus, two key arguments cited in favor of the existence of glycosomal β-oxidation in *T. brucei* vanished. The reported 3-hydroxyacyl-CoA dehydrogenase activity was very low and independent of the presence or absence of glucose (Table I). It seems possible therefore that the enzyme assay is not completely specific in crude cellular extracts, explaining the apparent 3-hydroxyacyl-CoA dehydrogenase-specific activity.

Another previous argument for catabolism by β-oxidation was the identification of a glycosomal ABC transporter (GAT1) with a specificity for oleoyl-CoA [44]. GAT1 becomes essential in the absence of glucose [44]. However, this transporter might also be important to supply etherlipid biosynthesis in glycosomes [45,46]. The kinetics of LD decay and decrease of cellular TAG content upon oleate withdrawal (Fig.6) can be fully accounted for by the dilution effect of cellular proliferation. Thus, there is nothing left to support an active catabolism of lipids stored in LDs in procyclic trypanosomes. This contrasts with *Leishmania spp.* that can take up fatty acids in culture, with evidence for esterification and catabolism by β-oxidation [47-49]. β-oxidation was also reported for *T. cruzi* [50] and *T. gondii* [51,52], and in *C. fasciculata* α-oxidation has been shown [53], suggesting subsequent β-oxidation. Interestingly, the lack of evidence for β-oxidation in *T. brucei* correlates with the presence in the African trypanosome genomes of only one gene encoding a putative TFEα1 subunit of the trifunctional enzyme complex. The *Leishmania spp.* and *T.*

cruzi genomes contain two *TFEα1* candidates, one mitochondrial and one glycosomal type gene with a mitochondrial targeting motif or a peroxisomal targeting sequence 2 (PTS2), respectively. It is convincible that a functional pathway has been lost during evolution of *Trypanosomatidae.* Alternatively, TFEα1 in *T. brucei* may be an enzyme activated only in a developmental stage in the tsetse, that is not available for biochemical analysis. The low expression, the absence of a growth phenotype in *Δtfeα1/Δtfeα1* knockout cells and the unchanged glycosomal proteome in these mutant cells are compatible with a developmental stage-specific function. Also, in cultured *L. major,* significant β-oxidation flux or a physiological role of that pathway have not been detected, and the contribution of fatty acids to TCA cycle intermediates was rather minor compared to the contribution of amino acids [54]. This opens the possibility, that also in *Leishmania* the pathway may be activated only in developmental stages not investigated in that study [54].

Our study leaves no doubt that available fatty acids can be stored as TAG in lipid droplets, but the time of usage of those stores and the pathways involved remain to be investigated.

References:

1. Waltermann M, Steinbuchel A (2005) Neutral lipid bodies in prokaryotes: recent insights into structure, formation, and relationship to eukaryotic lipid depots. J Bacteriol 187: 3607-3619.
2. Martin S, Parton RG (2006) Lipid droplets: a unified view of a dynamic organelle. Nat Rev Mol Cell Biol 7: 373-378.
3. Igal RA, Coleman RA (1996) Acylglycerol recycling from triacylglycerol to phospholipid, not lipase activity, is defective in neutral lipid storage disease fibroblasts. J Biol Chem 271: 16644-16651.
4. Igal RA, Coleman RA (1998) Neutral lipid storage disease: a genetic disorder with abnormalities in the regulation of phospholipid metabolism. J Lipid Res 39: 31-43.
5. Leber R, Zinser E, Hrastnik C, Paltauf F, Daum G (1995) Export of steryl esters from lipid particles and release of free sterols in the yeast, Saccharomyces cerevisiae. Biochim Biophys Acta 1234: 119-126.
6. Zinser E, Paltauf F, Daum G (1993) Sterol composition of yeast organelle membranes and subcellular distribution of enzymes involved in sterol metabolism. J Bacteriol 175: 2853-2858.
7. Gross SP, Guo Y, Martinez JE, Welte MA (2003) A determinant for directionality of organelle transport in Drosophila embryos. Curr Biol 13: 1660-1668.
8. Flaspohler JA, Jensen BC, Saveria T, Kifer CT, Parsons M (2010) A novel protein kinase localized to lipid droplets is required for droplet biogenesis in trypanosomes. Eukaryot Cell 9: 1702-1710.
9. Wiemer EA, L IJ, van Roy J, Wanders RJ, Opperdoes FR (1996) Identification of 2-enoyl coenzyme A hydratase and NADP(+)-dependent 3-hydroxyacyl-CoA dehydrogenase activity in glycosomes of procyclic Trypanosoma brucei. Mol Biochem Parasitol 82: 107-111.
10. Rotureau B, Van Den Abbeele J (2013) Through the dark continent: African trypanosome development in the tsetse fly. Front Cell Infect Microbiol 3: 53.
11. Hao Z, Kasumba I, Aksoy S (2003) Proventriculus (cardia) plays a crucial role in immunity in tsetse fly (Diptera: Glossinidiae). Insect Biochem Mol Biol 33: 1155-1164.
12. Liniger M, Acosta-Serrano A, Van Den Abbeele J, Kunz Renggli C, Brun R, et al. (2003) Cleavage of trypanosome surface glycoproteins by alkaline trypsin-like enzyme(s) in the midgut of Glossina morsitans. Int J Parasitol 33: 1319-1328.
13. Rotureau B, Ooi CP, Huet D, Perrot S, Bastin P (2013) Forward motility is essential for trypanosome infection in the tsetse fly. Cell Microbiol.
14. Steiger RF (1973) On the ultrastructure of Trypanosoma (Trypanozoon) brucei in the course of its life cycle and some related aspects. Acta Trop 30: 64-168.
15. Voorheis HP (1980) Fatty acid uptake by bloodstream forms of Trypanosoma brucei and other species of the kinetoplastida. Mol Biochem Parasitol 1: 177-186.
16. Brun R, Schonenberger (1979) Cultivation and in vitro cloning or procyclic culture forms of Trypanosoma brucei in a semi-defined medium. Short communication. Acta Trop 36: 289-292.
17. Allmann S, Morand P, Ebikeme C, Gales L, Biran M, et al. (2013) Cytosolic NADPH homeostasis in glucose-starved procyclic Trypanosoma brucei relies on malic enzyme and the pentose phosphate pathway fed by gluconeogenic flux. J Biol Chem.
18. Azema L, Claustre S, Alric I, Blonski C, Willson M, et al. (2004) Interaction of substituted hexose analogues with the Trypanosoma brucei hexose transporter. Biochem Pharmacol 67: 459-467.
19. Ebikeme CE, Peacock L, Coustou V, Riviere L, Bringaud F, et al. (2008) N-acetyl D-glucosamine stimulates growth in procyclic forms of Trypanosoma brucei by inducing a metabolic shift. Parasitology 135: 585-594.

20. Listenberger LL, Brown DA (2007) Fluorescent Detection of Lipid Droplets and Associated Proteins. Current Protocols in Cell Biology 35: 24.22.21-24.22.11.
21. Bringaud F, Robinson DR, Barradeau S, Biteau N, Baltz D, et al. (2000) Characterization and disruption of a new Trypanosoma brucei repetitive flagellum protein, using double-stranded RNA inhibition. Mol Biochem Parasitol 111: 283-297.
22. Riviere L, van Weelden SW, Glass P, Vegh P, Coustou V, et al. (2004) Acetyl:succinate CoA-transferase in procyclic Trypanosoma brucei. Gene identification and role in carbohydrate metabolism. J Biol Chem 279: 45337-45346.
23. Gassen A, Brechtefeld D, Schandry N, Arteaga-Salas JM, Israel L, et al. (2012) DOT1A-dependent H3K76 methylation is required for replication regulation in Trypanosoma brucei. Nucleic Acids Res 40: 10302-10311.
24. Lander N, Bernal C, Diez N, Anez N, Docampo R, et al. (2010) Localization and developmental regulation of a dispersed gene family 1 protein in Trypanosoma cruzi. Infect Immun 78: 231-240.
25. Laloi M, Perret AM, Chatre L, Melser S, Cantrel C, et al. (2007) Insights into the role of specific lipids in the formation and delivery of lipid microdomains to the plasma membrane of plant cells. Plant Physiol 143: 461-472.
26. Misset O, Bos OJ, Opperdoes FR (1986) Glycolytic enzymes of Trypanosoma brucei. Simultaneous purification, intraglycosomal concentrations and physical properties. Eur J Biochem 157: 441-453.
27. Wanders RJ, L IJ, van Gennip AH, Jakobs C, de Jager JP, et al. (1990) Long-chain 3-hydroxyacyl-CoA dehydrogenase deficiency: identification of a new inborn error of mitochondrial fatty acid beta-oxidation. J Inherit Metab Dis 13: 311-314.
28. Venkatesan R, Wierenga RK (2013) Structure of mycobacterial beta-oxidation trifunctional enzyme reveals its altered assembly and putative substrate channeling pathway. ACS Chem Biol 8: 1063-1073.
29. Bringaud F, Baltz D, Baltz T (1998) Functional and molecular characterization of a glycosomal PPi-dependent enzyme in trypanosomatids: pyruvate, phosphate dikinase. Proc Natl Acad Sci U S A 95: 7963-7968.
30. Medina-Acosta E, Cross GA (1993) Rapid isolation of DNA from trypanosomatid protozoa using a simple 'mini-prep' procedure. Mol Biochem Parasitol 59: 327-329.
31. Kall L, Canterbury JD, Weston J, Noble WS, MacCoss MJ (2007) Semi-supervised learning for peptide identification from shotgun proteomics datasets. Nat Methods 4: 923-925.
32. Patnaik PK, Field MC, Menon AK, Cross GA, Yee MC, et al. (1993) Molecular species analysis of phospholipids from Trypanosoma brucei bloodstream and procyclic forms. Mol Biochem Parasitol 58: 97-105.
33. Dixon H, Williamson J (1970) The lipid composition of blood and culture forms of Trypanosoma lewisi and Trypanosoma rhodesiense compared with that of their environment. Comp Biochem Physiol 33: 111-128.
34. Fridberg A, Olson CL, Nakayasu ES, Tyler KM, Almeida IC, et al. (2008) Sphingolipid synthesis is necessary for kinetoplast segregation and cytokinesis in Trypanosoma brucei. J Cell Sci 121: 522-535.
35. Bird SS, Marur VR, Sniatynski MJ, Greenberg HK, Kristal BS (2011) Serum lipidomics profiling using LC-MS and high-energy collisional dissociation fragmentation: focus on triglyceride detection and characterization. Anal Chem 83: 6648-6657.
36. Kalo P, Kemppinen A, Ollilainen V (2009) Determination of triacylglycerols in butterfat by normal-phase HPLC and electrospray-tandem mass spectrometry. Lipids 44: 169-195.
37. Opperdoes FR, Szikora JP (2006) In silico prediction of the glycosomal enzymes of Leishmania major and trypanosomes. Mol Biochem Parasitol 147: 193-206.
38. Guther ML, Urbaniak MD, Tavendale A, Prescott A, Ferguson MA (2014) High-Confidence Glycosome Proteome for Procyclic Form Trypanosoma brucei by Epitope-Tag Organelle Enrichment and SILAC Proteomics. J Proteome Res 13: 2796-2806.
39. Cabib E, Rothman-Denes LB, Huang K (1973) The regulation of glycogen synthesis in yeast. Ann N Y Acad Sci 210: 192-206.
40. Geiger DR, Servaites JC (1994) Diurnal Regulation of Photosynthetic Carbon Metabolism in C3 Plants. Annual Review of Plant Physiology and Plant Molecular Biology 45: 235-256.
41. Murphy DJ (2001) The biogenesis and functions of lipid bodies in animals, plants and microorganisms. Prog Lipid Res 40: 325-438.
42. Ralton JE, Naderer T, Piraino HL, Bashtannyk TA, Callaghan JM, et al. (2003) Evidence that intracellular beta1-2 mannan is a virulence factor in Leishmania parasites. J Biol Chem 278: 40757-40763.
43. Florin-Christensen M, Florin-Christensen J, de Isola ED, Lammel E, Meinardi E, et al. (1997) Temperature acclimation of Trypanosoma cruzi epimastigote and metacyclic trypomastigote lipids. Mol Biochem Parasitol 88: 25-33.
44. Igoillo-Esteve M, Mazet M, Deumer G, Wallemacq P, Michels PA (2011) Glycosomal ABC transporters of Trypanosoma brucei: characterisation of their expression, topology and substrate specificity. Int J Parasitol 41: 429-438.
45. Opperdoes FR (1984) Localization of the initial steps in alkoxyphospholipid biosynthesis in glycosomes (microbodies) of Trypanosoma brucei. FEBS Lett 169: 35-39.
46. Zomer AW, Opperdoes FR, van den Bosch H (1995) Alkyl dihydroxyacetone phosphate synthase in glycosomes of Trypanosoma brucei. Biochim Biophys Acta 1257: 167-173.
47. Berman JD, Gallalee JV, Best JM, Hill T (1987) Uptake, distribution, and oxidation of fatty acids by Leishmania mexicana amastigotes. J Parasitol 73: 555-560.

48. Blum JJ (1990) Effects of culture age and hexoses on fatty acid oxidation by Leishmania major. J Protozool 37: 505-510.
49. Hart DT, Coombs GH (1982) Leishmania mexicana: energy metabolism of amastigotes and promastigotes. Exp Parasitol 54: 397-409.
50. Acosta H, Dubourdieu M, Quinones W, Caceres A, Bringaud F, et al. (2004) Pyruvate phosphate dikinase and pyrophosphate metabolism in the glycosome of Trypanosoma cruzi epimastigotes. Comp Biochem Physiol B Biochem Mol Biol 138: 347-356.
51. Charron AJ, Sibley LD (2002) Host cells: mobilizable lipid resources for the intracellular parasite Toxoplasma gondii. J Cell Sci 115: 3049-3059.
52. Quittnat F, Nishikawa Y, Stedman TT, Voelker DR, Choi JY, et al. (2004) On the biogenesis of lipid bodies in ancient eukaryotes: synthesis of triacylglycerols by a Toxoplasma DGAT1-related enzyme. Mol Biochem Parasitol 138: 107-122.
53. Vakirtzi-Lemonias C, Karahalios CC, Levis GM (1972) Fatty acid oxidation in Crithidia fasciculata. Can J Biochem 50: 501-506.
54. Naderer T, Ellis MA, Sernee MF, De Souza DP, Curtis J, et al. (2006) Virulence of Leishmania major in macrophages and mice requires the gluconeogenic enzyme fructose-1,6-bisphosphatase. Proc Natl Acad Sci U S A 103: 5502-5507.

Acknowledgements

We are grateful to Larissa Ivanova (Munich) for competent technical support. We thank Dr. Matthias Ellerbeck (Munich) for his expert introduction to the CLSM.

Work in Munich was supported by the University of Munich and grants DFG 1100/6-2 and BELSPO PAI 6/15 to MB. Work in Bordeaux was supported by the Agence Nationale de la Recherche (ANR) through grants ACETOTRYP of the ANR-BLANC-2010 call to FB and PM; FB is also supported by the Centre National de la Recherche Scientifique (CNRS), the Université of Bordeaux, the Laboratoire d'Excellence (LabEx) ParaFrap ANR-11-LABX-0024 and the ParaMet PhD programme of Marie Curie Initial Training Network (FP7). MB and FB have been supported by a research cooperation grant of the Franco-Bavarian university cooperation center (BFHZ/CCUFB).

5. Acetate Metabolism

The observation of a partially active TCA cycle in *T. brucei* insect stages, the lack of glucose oxidation via this pathway, together with a low CS activity in the presence of glucose raised the interest into how the parasite feeds its *de novo* lipid biosynthesis. In chapter 6.1 we show that it takes advantage of a massive production of acetate within the mitochondrion. The acetate diffuses or is shuttled out of the mitochondrion and part of it is excreted. The other part of it is used by a newly discovered cytosolic acetyl-CoA-synthetase (ACS), which is essential for *de novo* lipid biosynthesis. Therefore a citrate lyase (CL) is nonessential.

In chapter 5.2 we investigated the citrate lyase candidate gene in more detail, as it displayed a not so common mitochondrial localization. This lead to the hypothesis of a putative glyoxylate cycle, which was investigated by yeast complementation experiments and enzymatic activity assays further on.

5.1 Acetate produced in the mitochondrion is the essential precursor for lipid biosynthesis in procyclic trypanosomes

Proceedings of the National Academy of Sciences (2009), Riviere, L., Moreau, P., Allmann, S., Hahn, M., Biran, M., Plazolles, N., Franconi, J. M., Boshart, M. & Bringaud, F. (2009) Acetate produced in the mitochondrion is the essential precursor for lipid biosynthesis in procyclic trypanosomes,

doi: 10.1073/pnas.0903355106.

5.2 Functional analysis of a CL candidate gene

The citrate lyase (CL) candidate (Tb927.8.6820) shows a low identity with other CL genes, the best hit is the *Roseobacter litoralis* CL (27% identity, GenBank). The prediction of a mitochondrial targeting sequence (MITOP, p=0.7) at the N-terminus of the CL candidate gene and the fact that the CL candidate is part of the Pfam superfamily (PF03328; HpcH/HpaI aldolase/citrate lyase family) raised the hypothesis of a putative glyoxylate cycle. The Pfam family is characterized by carbon-carbon lyase activity and includes isocitrate lyase (ICL) and malate synthase (MLS). This could explain the partially active TCA cycle in *T. brucei*. There might be a switch between glyoxylate and TCA cycle activity depending on nutrient availability. Indeed in *E. coli* the switch between TCA cycle and the glyoxylate cycle is regulated by a phosphorylation of the IDH, which inhibits its catalytic function and thus isocitrate is shuttled into the glyoxylate cycle. This is triggered by the growth on acetate, a C2 carbon source (Garnak and Reeves, 1979; LaPorte et al., 1985). The two key enzymes necessary for a glyoxylate cycle in addition to TCA cycle enzymes are the ICL and MLS.

First bioinformatic analyses (M. Kador, this lab) didn't reveal any homologues to ICL or MLS genes of other organisms. Neither was a homologue to the bifunctional ICL/MLS protein found, which is present in *C. elegans* or *E. gracilis* (Kondrashov et al., 2006). It has to be mentioned that there are also alternative glyoxylate cycles, which run with a MLS and without any ICL activity (Albers and Gottschalk, 1976; Han and Reynolds, 1997; Kornberg and Lascelles, 1960). We looked for putative ICL or MLS activities by a yeast complementation strategy. This was carried out in collaboration with Andreas Brachmann (LMU). A prerequisite for the complementation analysis is a growth phenotype of the MLS1 and ICL1 null mutants on C2-carbon sources, which is the case, as they do not grow on acetate or ethanol as sole carbon sources (McCammon, 1996).

Results

For the yeast complementation experiments, the 10 N-terminal amino acids of the CL ORF have been deleted and replaced with a methionine, as the glyoxylate cycle is located in the peroxisomes of *S. cerevisiae,* and the putative mitochondrial targeting sequence could have caused unintended mitochondrial localization. Due to the dual localization of the MLS1 protein in *S. cerevisiae* in the cytoplasm but also in the peroxisomes, two Δ10CL constructs have been created. One received the C-terminal PTS1 signal (SKL) of the yeast MLS1 gene. The yeast null mutants *Δmls1* and *Δicl1* have been transformed with both constructs and growth on HC-U medium with glucose, acetate or ethanol as only carbon source was observed. As positive controls plasmids containing the MLS1 or the ICL1 gene were used, as well as an empty vector (pBL100) control has been done (Fig.10). Same results were obtained for both complementations. Only the respective yeast genes could restore growth on medium with acetate or ethanol. These negative results led us step back from the glyoxylate cycle hypothesis, and towards the intention to gain more basic knowledge about the CL candidate first, e.g. its expression in the different life cycle stages and its subcellular localization.

To accomplish this we raised a polyclonal antibody in rabbits against the *Tb*CL candidate gene. Recombinant HIS-tagged CL has been expressed in *E. coli* and immunization was performed by Pineda Antikörper-Service (Berlin) according to the methods section. In Fig.11 it can be seen that the antibody recognizes the *Tb*CL protein in PCF and BSF and that the corresponding band is missing in the PCF ΔCL null mutant. The differential expression is well explained by the higher mitochondrial activity of PCF parasites. The predicted mitochondrial localization was verified by a digitonin titration (Fig.12). The CL candidate protein is released at higher concentrations of digitonin, which is typical for mitochondrial proteins like HSP60 or the ASCT, which were used as mitochondrial markers in this experiment.

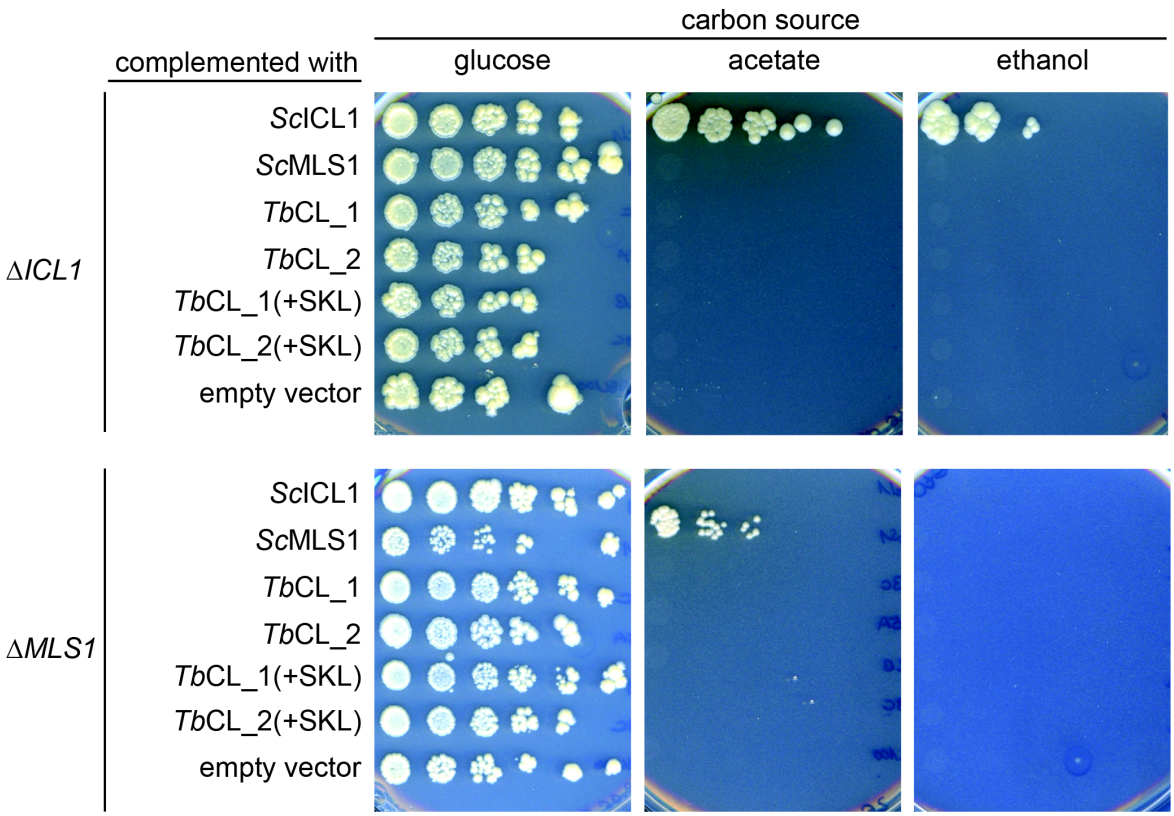

Fig.10: Yeast complementation assay of the *Δicl1* and *Δ*mls1 null mutants on minimal medium. The *Δicl1* and *Δ*mls1 mutants have been transformed with pBL100 vector containing different inserts and growth on different carbon sources has been observed. *Sc*ICL1 and ScMLS1 served as positive controls and empty vector as negative control. Neither of the two *Tb*ACL alleles independent of the presence of the PTS1 signal could restore growth on C2-carbon sources. Only the positive controls could rescue the deletion mutants. Both alleles of *Tb*CL have been used, as an allelic polymorphism was detected during cloning.

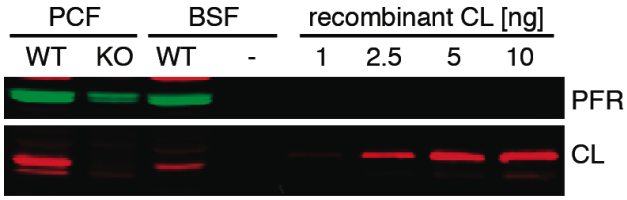

Fig.11: Western Blot using the αACL antibody. The antibody recognizes the CL in wildtype cell extracts (WT), whereas there is no band in the cell extract of the null mutant (KO). Protein abundance is higher in PCFs than in BSFs.

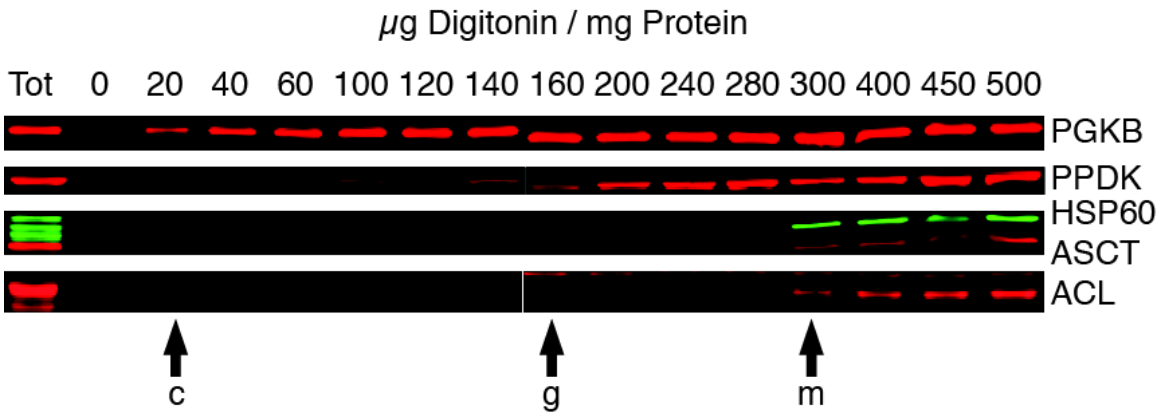

Fig.12: Subcellular localization of the ACL candidate protein by digitonin titration. The same number of cells has been exposed to increasing amounts of digitonin with a subsequent separation of soluble and insoluble fraction. The soluble fractions have been probed with antibodies against proteins with specific localizations. Marker proteins: cytosolic (PGKB), glycosomal (PPDK) and mitochondrial (HSP60, ASCT). c, indicates release of cytosolic proteins; g, release of glycosomal proteins; m, release of mitochondrial proteins.

So far no citrate lyase activity has been detected in *T.* brucei cell lysates (personal communication F. Bringaud) and the previous yeast complementations revealed no activity as ICL or MLS. Considering the verified mitochondrial localisation we decided to reanalyse putative enzymatic activities of this protein: citrate synthase (CS), citrate lyase (CL), MLS and ICL. The latter ones have already been tested by yeast complementation, but we didn't exclude the possibility of posttranslational modifications taking place in *T.* brucei that could have an influence on the activity. Transgenic trypanosome lines were created with an inducible overexpression plasmid containing the Ty1-tagged CL gene. The following enzymatic analyses have been performed in the course of a bachelor's thesis (Ferdinand Huber) and thus are just summarized briefly. All assays have been performed with both alleles of the CL candidate, due to the observed allelic polymorphism. Cell extracts as well as immunopurified protein has been used and additionally cell extracts from cells grown in glucose-depleted medium in order to see a putative carbon source dependent switch. Neither of the four enzymatic activities could be observed under any of the named conditions.

6. Concluding Discussion

6.1 Gluconeogenic flux – costs and benefits for metabolic homeostasis

In the bloodstream form of *T. brucei* the oxidative pentose phosphate pathway (PPP) is essential and inhibition by a specific inhibitor is not tolerated (Cordeiro et al., 2009). We have shown that this is not the case for the procyclic form of the parasite. We demonstrated the cytosolic malic enzyme (MEc) as an alternative NADPH source compensating a loss of PPP activity. This is in agreement with the general consensus of a more versatile and flexible metabolism of the insect stages, here to maintain the cellular redox balance. Surprisingly the PPP produces NADPH in the absence of glucose. We identified proline and gluconeogenic flux as the responsible glucose-6-phosphate (G6P) source.

Although we applied oxidative stress over periods of 24/48 hours, outmatching a one-time H_2O_2 application, the total capacity of gluconeogenic flux has to be questioned in its physiological importance due to potential flux limitations. These limitations could be ATP availability or NAD^+/NADH imbalance. The production of proline-derived malate contributes to the mitochondrial ATP production and redox balance (reviewed in (Bringaud et al., 2006)), however, the further gluconeogenic flux will imbalance the cytosolic and glycosomal ATP/ADP ratio. Thus, gluconeogenesis is limited to ATP availability or requires compensating mechanisms. ATP depletion might be the lesser of two evils when facing extreme ROS concentrations in the cytosol, jeopardizing the survival of the cell but a lack of glycosomal ATP results in the incapability of performing gluconeogenesis.

Each molecule of G6P produced via proline-derived gluconeogenic flux consumes four molecules of ATP, two in the cytosol (Fig.13, step 4) and two in glycosomes (Fig.13, steps 1, 3). The net ATP production within the cell during gluconeogenic flux from proline is ensured by the mitochondrial processing to malate (Fig.; steps 36, 37, 40, 29, 30, 32) and the subsequent oxidative phosphorylation. But the cytosolic and glycosomal ATP would be depleted over time. One possibility to cope with the cytosolic and glycosomal ATP depletion are ADP/ATP translocases, transferring mitochondrial ATP into the other two subcellular compartments. A putative mitochondrial translocase (Tb927.10.14820) has been identified in a proteomic approach (Colasante et al., 2009) and characterized later (Pena-Diaz et al., 2012). Here the ADP/ATP transport function and its essentiality for proline metabolism in the absence of glucose has been shown. So indeed, this translocase could replenish the cytosolic ATP pool during gluconeogenic flux.

Yet the glycosomal ATP supply during gluconeogenic flux stays unclear. So far no glycosomal ADP/ATP translocase has been identified in *T. brucei*, yet being discussed in the context of glycosomal phosphate leakage (Kerkhoven et al., 2013), leaving this open for future investigation. At the moment it is not clear how the glycosomal ADP/ATP balance is maintained and whether this is only possible in culture. Putative candidates can be combined with the ΔMEc mutant to a double mutant and screened for their oxidative stress susceptibility in the absence of glucose. Loss of a functional glycosomal translocase in this situation could result in increased susceptibility to ROS, in absence of alternative ATP supplying mechanisms.

As already mentioned, a glycosomal ADP/ATP translocase could prevent ATP depletion. Computational analyses modeling glycosomal phosphate metabolism implemented such an antiporter as solution to glycosomal phosphate leakage (Kerkhoven et al., 2013), resulting in a situation comparable to BSF parasites lacking glycosomes. For these parasites glucose metabolism is toxic (Furuya et al., 2002). This effect is owed to the “turbo design” of glycolysis, which is usually

prevented by feedback inhibition and in *T. brucei* by the partial compartmentalization of glycolysis, which ensures a glycolytic net ATP balance of zero within the glycosomes (Bakker et al., 1999; Haanstra et al., 2008). This balance would be disturbed by such an antiporter and accumulate sugar-phosphates as well as deplete ATP throughout the cell. The glycolytic flux would use as much glycosomal ATP as available and the ADP/ATP antiporter would supply ATP to the glycosomes, creating a lack of cytosolic ATP.

An alternative glycosomal ATP generating source could be an adenylate kinase (ADK), prolonging ATP supply for an extended period by transferring phosphate groups between ADP molecules, producing ATP and AMP. This solution would only help for short periods of time, as it is limited by the glycosomal ADP pool. In *T. brucei* an ADK has been localized to the glycosomes (Hart and Opperdoes, 1984; Opperdoes et al., 1981).

Another open question concerning gluconeogenic flux from proline is the respective contribution of alternative routes to PEP and if there is a preferential one. From cytosolic malate there are two alternatives generating PEP, either via MDH and PEPCK (Fig.13, grey arrows) or via MEc and PPDK (Fig.13, white arrows). Both options consume one glycosomal molecule of ATP per PEP molecule generated (Fig.13, steps 1, 3). The difference is the reduction of one NAD^+ per utilized molecule of malate by MDH (Fig.13, step 2). NADH is required later during the GAPDH reaction (Fig.13, step 5). This implies that the gluconeogenic flux through MDH and PEPCK should be more prominent for biosynthetic purposes like ribose-5-phosphate (R5P) production, as it maintains the glycosomal redox balance. On the other hand flux through the MEc already generates cytosolic NADPH, suggesting that in the presence of a functional MEc this path will likely be chosen preferentially if cytosolic ROS detoxification is required. Thereby cytosolic NADPH will be generated and pyruvate can be channeled into the mitochondrion to fuel acetyl-CoA/acetate production.

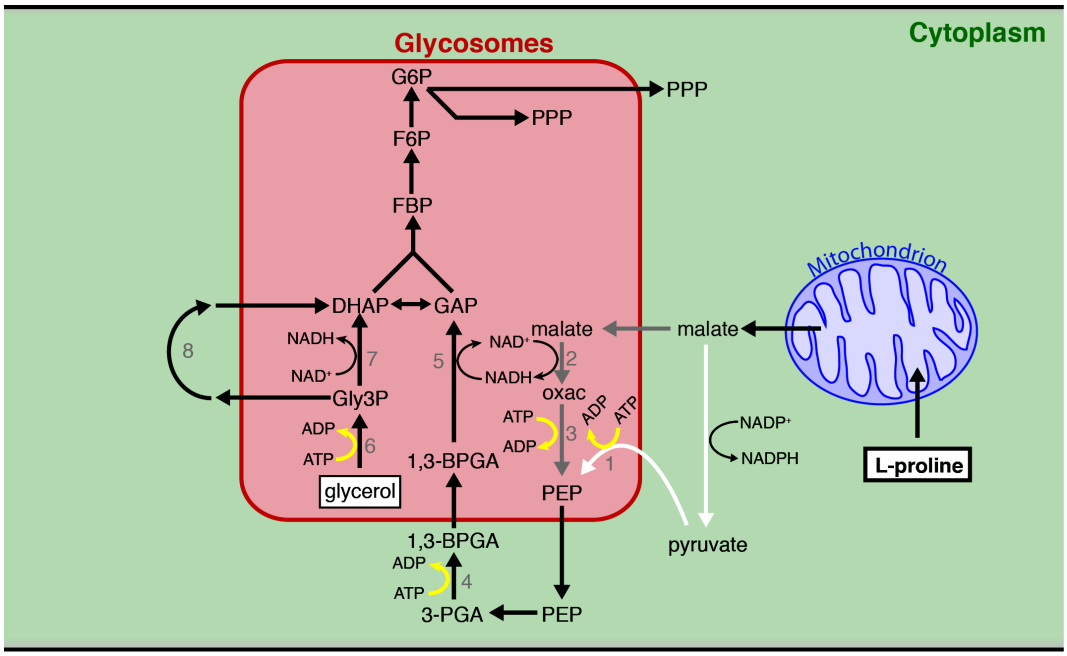

Fig.13: Schematic representation of proline-derived gluconeogenic flux. Grey and white arrows represent the alternative routes available for PEPm production from malate. enzymatic steps: 1, pyruvate phosphate dikinase; 2, mitochondrial malate dehydrogenase; 3, phosphoenolpyruvate carboxykinase; 4, cytosolic phosphoglycerate kinase; 5, glyceraldehyde-3-phosphate dehydrogenase; 6 glycerol kinase; 7, glycerol-3-phosphate dehydrogenase; 8, mitochondrial FAD-dependent glycerol-3-phosphate dehydrogenase.

The presence of glycerol may change the flux distribution. It has been shown that glycerol can be utilized as carbon source in the absence of glucose (Dodson et al., 2011). This could on the one hand also produce G6P or R5P, but in addition reduce NAD+ (Fig.13, step 7), which would have to be

reoxidized. This could be achieved by increasing flux through the PPDK (Fig.13, step 1) and GAPDH (Fig.13, step 5) or by reversing the afore mentioned PEPCK and MDH reactions (Fig.13, steps 3, 2). But without a suitable mechanism supplying glycosomal ATP, either the redox imbalance or the lack of ATP will prevent sustained high gluconeogenic flux necessary for oxidative stress defense. But as gluconeogenic flux is only profitable in the absence of glucose, an active glycosomal ADP/ATP antiporter could supply ATP without damaging side effects in this situation. This could be regulated by carbon source dependent protein expression as observed for several metabolic enzymes in the scope of this thesis. Thus putting a glycosomal proteome into focus, which should be analyzed for parasites grown in absence of glucose. Here putative transporters, which have not been found in proteomes performed in presence of glucose, can be analyzed as candidates to elucidate the potential presence of such an antiporter.

The observation of gluconeogenic flux supplying the trypanothione system with NADPH for oxidative stress defense raised the question, if there is some kind of metabolic channeling assuring that G6P is supplied into the cytosol and not used in the glycosomal PPP. For the PPP a dual localization in the cytosol as well as the glycosomes has been reported (Colasante et al., 2006; Duffieux et al., 2000; Heise and Opperdoes, 1999; Vertommen et al., 2008). More recent data suggest a predominantly cytosolic localization (Guther et al., 2014; Kerkhoven et al., 2013; Stoffel et al., 2011). Low or no glycosomal PPP activity would reduce the problem of glycosomal phosphate leakage in the presence of glucose and in the absence of an ADP/ATP antiporter (predicted by (Kerkhoven et al., 2013)). Furthermore it would solve the problem of required channeling towards the cytosolic PPP in case of ROS detoxification. Consequently only the question of G6P transport through the glycosomal membrane into the cytosol remains to be elucidated. Usually G6P transporters are found in the ER membrane in organisms capable of glycogen storage. *T. brucei* is not known for glycogen storage and there are no putative G6P transporters identified so far. An alternative could be the dephosphorylation of G6P to glucose, which can diffuse through the glycosomal membrane and subsequently being phosphorylated by cytosolic hexokinase. An additional advantage of this would be the retained phosphate within the glycosome.

6.2 Lipid storage and its role in *T. brucei*

A previous publication had shown enzymatic activities possibly involved in β-oxidation to be localized within the glycosomes of *T. brucei* (Wiemer et al., 1996). We have identified a candidate gene that could have been responsible for these activities, but deletion of this gene had no effect on the measured enzymatic activities. Furthermore we could not confirm the glycosomal localization of the activity. The lack of other candidate genes, the low activity measured and the non-glycosomal localization make glycosomal β-oxidation in *T. brucei* very unlikely.

However, data from previous publications as well as from our work suggest a role for carbon storage in this parasite. It has been observed that number and size of lipid droplets (LDs) change during stage development in the insect host. Short stumpy BSFs show no LDs, but during establishment of a midgut infection PCFs form LDs. Followed by a decrease in number and size during maturation into metacyclic cells, suggesting utilization of LDs during development (Steiger, 1973). Furthermore a lipid droplet kinase (LDK) has been identified and shown to be essential for LD formation (Flaspohler et al., 2010), indicating dynamic regulation of this storage. We could show that oleic acid is taken up, esterified and stored in LDs by *T. brucei* PCF in culture. The esterification of FAs by Acyl-CoA synthase requires ATP, suggesting a benefit from LDs, otherwise it would be an energy sink without use.

Considering these findings, LDs may have other benefits than β-oxidation of FAs, justifying their existence. The two other main components of LDs are glycerol as part of triacylglycerols and cholesteryl esters. As mentioned above (chapter 6.1), glycerol can serve as carbon source and as

side effect produce NADH (Fig.13, step 7) during its metabolization. NADH can be used during gluconeogenic flux for the GAPDH activity (Fig.13, step 5).

This would emphasize the role of LDs in the absence of glucose as carbon source. A possibility to test the role of glycerol from LDs would require a more restrictive medium, containing no glucose and no glycerol and the use of a recombinant cell line incapable of performing gluconeogenic flux from proline. The latter requirement is met by the ΔPPDK/ΔPEPCK (Fig.13, steps 1, 3) double knockout. Inducing LD formation in this cell line by oleate feeding and subsequent transfer to the restrictive medium could reveal promoted growth of fed cells compared to non-fed cells. A putative difference could be quantified by measuring intracellular glycerol-3-phosphate levels as done before (Dodson et al., 2011) or by stable isotope labeling with ^{13}C-glycerol to track the distribution within the cell. Critical points here are the difficulties restrictive media bring along, as they very often already affect growth of wildtype cells. Experiments replacing the standard fetal calf serum (FCS) completely or partially by dialyzed, delipidated or synthetic serum resulted in fluctuating and non-satisfying cell growth. This makes it difficult to create a lipid-depleted medium for improved analyses of the lipid metabolism.

Furthermore it has been shown that *T. brucei* parasites contain significant amounts of sterols, with a high abundance of cholesterol (Zhou et al., 2007). Here the authors show that the availability of cholesterol in the culture medium affects its intracellular abundance. LDs could serve as storage organelles of cholesterol to buffer availability fluctuations. The extracellular cholesterol abundance can explain the LD degradation kinetics we observed, as in the complex culture medium, the intracellular cholesterol storage is not necessary.

Another putative function of LDs can be the role as FA storage for membrane remodeling upon environmental changes. In fact in *T. cruzi* it has been observed that upon temperature change from 28°C to 37°C the ratio of saturated to unsaturated FAs in phospholipids (PPL) increased, while this ratio simultaneously changed the opposite way in TAGs (Florin-Christensen et al., 1997). This suggests an exchange of FA moieties between membrane PPL and TAG species triggered by environmental changes. To elucidate this, thin layer chromatography (TLC) and mass spectrometry (MS) analyses of *T. brucei*'s membrane in response to different putative environmental triggers have to be performed. In case a change is noticed, fluorescent fatty acid analogues could be used to induce LD formation, followed by microscopic analysis and subcellular localization of these upon trigger exposure.

The catabolic utilization of LDs might depend on the developmental stage, thus playing only a minor role in PCFs. This has to be considered for further in culture investigations by taking advantage of the RBP6-induced differentiation system.

6.3 Acetate metabolism and the enigma of the CL candidate gene

We identified a new mechanism, the 'acetate shuttle', being essential for *de novo* lipid synthesis in *T. brucei*. This shuttle takes advantage of the high amounts of acetate produced in the parasite's energy metabolism. The acetate shuttle was thought to play a crucial role in the insect stage but not the bloodstream form, due to the BSF's generally low mitochondrial activity. But a recent publication demonstrated that it is also essential in BSF parasites (Mazet et al., 2013). An alternative cytosolic acetyl-CoA supply can formally not be excluded, as it may be relevant in other developmental stages or depending on nutrient availability. This could be via the common citrate/malate shuttle and a cytosolic citrate lyase. A candidate for the latter has not yet been identified in *T. brucei*'s genome. There is a putative mitochondrial carboxylate transporter MCP12 (Colasante et al., 2009). It shows similarity (BLASTP, 48%; (Colasante et al., 2009)) to a previously discovered novel di-tricarboxylate carrier protein in *A. thaliana*, which is capable of transporting di- and tricarboxylates (Picault et al., 2004). In agreement with a putative citrate transporter we

found that ectopic expression of a cytosolic aconitase (ACO) was able to rescue a lethal phenotype resulting from mitochondrial citrate accumulation (N. Ziebart, this lab, unpublished). We therefore assume that citrate transport out of the mitochondrion takes place, yet the corresponding transporter has to be identified. As a potential function of cytosolic citrate that is not essential for *de novo* synthesis of lipids, we suggest a role in glycosomal NADPH production. The NADPH pathway will be discussed in more detail in chapter 6.4.

The contribution of threonine and glucose to acetate production and their respective coupling to either ASCT or ACH have been elucidated (Millerioux et al., 2013; Millerioux et al., 2012), yet the mechanism of this metabolic channeling is unclear. Metabolic channeling provides the advantage of a faster flux and perhaps even more important in this case, it protects the substrate from competing reactions. A competing activity for mitochondrial acetyl-CoA could be the CS or free acetyl-CoA could lead to acetylation of certain proteins and influence the metabolic activity within the mitochondrion. To avoid this it might be necessary to channel acetyl-CoA, keeping the concentration of free acetyl-CoA within the mitochondrion as low as possible. In plants it has been shown that a number of mitochondrial proteins are acetylated (Konig et al., 2014). Potential protein-protein interactions will be addressed in the future by using a recently established biotinylation method called BioID (Morriswood et al., 2013). This will give insights into the protein interactions in this pathway and putative regulation upon carbon source availability.

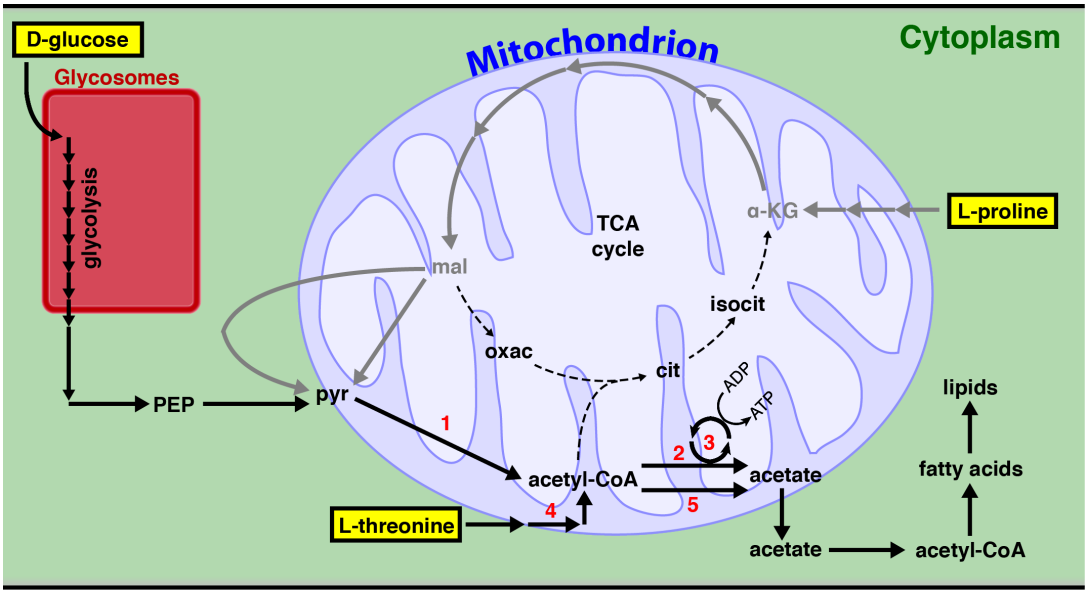

Fig.14 : Acetate production pathways in *T. brucei*. Dashed arrows: no experimental evidence for fluxes. Grey arrows: experimental evidence for fluxes, but no evidence for role in acetate production. Enzymes: 1, pyruvate dehydrogenase complex; 2, acetate:succinate CoA- transferase; 3, succinyl-CoA synthetase; 4, threonine dehydrogenase; 5, acetyl-CoA hydrolase. Abbreviations: α-KG, alpha-ketoglutarate; cit, citrate; isocit, isocitrate; mal, malate; oxac, oxaloacetate; PEP, phosphoenolpyruvate; pyr, pyruvate; TCA, tricarboxylic acid;

It has been shown that glucose derived acetate involves the pyruvate dehydrogenase (PDH) complex and ASCT (Fig.14, steps, 1, 2), whereas threonine involves threonine dehydrogenase (TDH) and ACH (Fig.14, steps, 4, 5). An important difference between those pathways is the fact that the ASCT reaction is coupled to ATP production (Fig.14, step, 3). As proline catabolism can also lead to pyruvate production (Fig.14, grey arrows) it can possibly contribute to the acetate pool. So there are three carbon sources available for acetyl-CoA production and two subsequent acetate converters. Combining the above mentioned BioID approach with varying carbon sources might reveal regulation or changes in the channeling of acetate production and thus the involved protein interactions.

We characterized a mitochondrial ATP-dependent citrate lyase (CL)-like candidate gene without identifying its catalytic activity so far. We demonstrated its mitochondrial localization,

which excludes a function in *de novo* lipid synthesis, compared to a cytosolic CL-like candidate. Recent analyses (Daniel Inaoka, University of Tokyo) revealed a structural similarity to a prokaryotic ATP-independent citrate lyase. This consists of three subunits (α, β, γ), with the CL candidate being similar to the β-subunit. This is the subunit conducting the conversion of citryl-ACP (acyl carrier protein) to acetyl-ACP and oxaloacetate. There are no homologues for the other subunits in the *T. brucei* genome. This situation is equivalent to the one found in *M. tuberculosis* (Goulding et al., 2007). Both, the *T. brucei* and the *M. tuberculosis* protein show a similar structure prediction. The authors (Goulding et al., 2007) suggest a novel role for this stand-alone subunit of the citrate lyase complex due to an operon organization analysis of the β-subunit across several species. Focusing on *M. tuberculosis*, they find an acyl-CoA dehydratase/hydratase and an acyl-CoA dehydrogenase downstream, two enzymes involved in acetyl-CoA carboxylation. In addition they refer to a distant sequence similarity to the L-malyl-CoA/β-methylmalyl-CoA lyase (MclA; EC 4.1.3.24; BLAST e-score of $6.0e^{-14}$ and 28% sequence identity) from *Methylobacterium extorquens*. *M. extorquens* MclA reversibly catalyzes the hydrolysis of L-malyl-CoA into acetyl-CoA and glyoxylate. They hypothesize that the *M. tuberculosis* β-subunit performs an analogous cleavage, during the conversion of citryl-CoA into acetyl-CoA and oxaloacetate.

These findings shed new light on the CL candidate gene of *T. brucei*, as a citrate lyase activity could not be determined (see chapter 5.2), but the required activation of citrate by a CoA or an ACP prior to cleavage could explain this. So indeed investigation of this specific enzymatic activity should be performed. Such a citrate lyase activity within the mitochondrion would fill the missing gap for a reductive branch of the TCA cycle. There are examples where a branched TCA metabolism instead of a classical TCA cycle has been observed. It was suggested for *P. falciparum* (Olszewski et al., 2010) without any identified mitochondrial CL, but this assumption had to be retracted due to some metabolite contaminants from the feeder cells. Nevertheless it has been shown that glutamine-derived reductive carboxylation has an emphasized role in tumor cells (Mullen et al., 2012). Here glutamine/glutamate enters the TCA cycle via α-ketoglutarate and is carboxylated by $NADP^+$-dependent isocitrate dehydrogenases followed by conversion to citrate by an aconitase. This citrate served as C4 source (OAA) and as precursor for lipid synthesis (acetyl-CoA) in those tumor cells. The identification of a mitochondrial CL and further MS stable isotope analyses of CS, ACO, IDHm and CL single and double knockouts in changing nutritional environments could reveal a branched TCA metabolism with flux redistribution between oxidative and reductive branch depending on nutrient availability.

6.4 Insect stage differentiation and its multitude of regulators

We took advantage of the recent publication of a novel differentiation system enabling the insect stage differentiation in culture (Kolev et al., 2012). We discovered the inhibitory effect on differentiation of glucose and glycerol. The role of glycerol on some early differentiation markers has been shown before (Vassella et al., 2000; Vassella et al., 2004). Here the switch of the surface protein from GPEET to EP procyclin is inhibited in procyclic forms. During our RBP6-induced culture experiments glucose and glycerol cause a block or delay in differentiation between epimastigote and metacyclic forms.

Previous findings showed, that the activities of mitochondrial enzymes regulated the surface protein expression (Vassella et al., 2004). One additional similarity shared by them is their link to glycolysis. Hypoxia and SHAM affect the alternative oxidase (AOX), which is involved in the before mentioned Gly3P/DHAP-shuttle, reoxidizing glycosomal NADH, reduced during glycolysis. Although this pathway plays a minor role in procyclic parasites (Ebikeme et al., 2010), interfering with it may induce metabolic cross-talk and cause a differentiation block/delay. PDH and SCoAS are involved in subsequent conversion of glucose-derived pyruvate into acetyl-CoA, acetate and ATP.

Decreasing their activity results in a lower acetate excretion indicating a lower glycolytic flux (Millerioux et al., 2013; Millerioux et al., 2012). All this suggests that feedback regulation exists between the cellular metabolic pathways, "sensing" the nutritional environment resulting in a metabolic cross-talk. A first observation in this direction was the discovery of glucose-induced repression of proline metabolism (Lamour et al., 2005).

The ways of feedback regulation can be diverse. We reported glucose-regulated protein expression, although this was just the case for a small number of proteins. This can occur by the stabilization or destabilization of mRNAs, which is very common in *T. brucei*, lacking almost any regulation by transcription initiation. Another mechanism, especially for proteins expressed with constant protein levels are post translational modifications (PTM), which we also suggest for the IDHg, where the increase in activity is higher than the increase in protein levels upon glucose withdrawal.

How can metabolic flux influence these regulations? It has been reported that metabolites like succinate can serve as PTM (Park et al., 2013; Zhang et al., 2011) and succinate and fumarate have been reported to be involved in epigenetic and transcriptional regulation (Cai and Tu, 2012; Ito et al., 2010; Mills and O'Neill, 2014; Moran-Crusio et al., 2011; Quivoron et al., 2011). High abundance of a certain carbon source can lead to accumulation of intermediate metabolites due to differential catalytic properties of consecutive enzymes. The accumulation of this metabolite can increase the probability to be used as PTM, which can exhibit regulatory functions. Furthermore the importance of lysine acetylation has been shown to play a role in plant mitochondria (Konig et al., 2014) and the fact that acetylations or succinylations can occur non-enzymatically due to the basic pH of the mitochondrial matrix (Wagner and Payne, 2013). In this study the deacetylation of mitochondrial proteins was achieved by the SIRT3 deacetylase, a Sir2 homolog (Lombard et al., 2007). The *T. brucei* genome contains three Sir2-related proteins (SIR2rp1-3), with two of them showing a mitochondrial localization (Alsford et al., 2007). These proteins could be responsible for the deacetylation of mitochondrial proteins.

Metabolite levels can also indirectly exhibit such regulatory functions. Depending on substrate availability the respective enzyme has an occupied or unoccupied binding site and it has been demonstrated that metabolic enzymes can fulfill alternative functions. The most prominent examples are dehydrogenases and their NAD^+/$NADP^+$ -binding Rossmann fold (Nagy et al., 2000), which is capable of binding RNA. There are other examples, which go beyond simple RNA binding and exhibit ribonuclease activity on the bound RNA (Barbas et al., 2013). In *T. brucei* the α-ketoglutarate dehydrogenase (α-KD) E2 subunit has been shown to bind mitochondrial DNA and play a role in the segregation during cell division (Sykes and Hajduk, 2013). There are more examples of metabolic enzymes with additional functions strengthening the idea that they serve as metabolic sensors and directly participate in regulation (Ciesla, 2006; Kim and Dang, 2005).

We demonstrated the impact of an isocitrate dehydrogenase null mutant (ΔIDHg) on differentiation in culture, as well as in the fly and postulated a pathway for glycosomal NADPH production involving citrate synthase (CS), aconitase (ACO) and IDHg (Fig.15). In culture the lack of IDHg caused a differentiation block in epimastigote stage, whereas the ΔACO null mutant is blocked in the procyclic form. We suggest that both are acting in the same pathway, but the accumulation of intracellular citrate exhibits a stronger phenotype than the lack of glycosomal NADPH and thus masking the less severe phenotype. We know that the overexpression of CS in the genetic background of a ΔACO mutant is lethal, but can be rescued by ectopic expression of a cytosolic ACO (N. Ziebart, this lab, unpublished).

The fact that neither ΔCS nor ΔIDHm null mutants display a block in differentiation supports our hypothesis of the IDHm acting in the reverse direction, enabling both enzymes to produce isocitrate. Due to this redundancy the glycosomal NADPH production is not impaired in the single mutants. Creating a ΔCS/ΔIDHm double mutant for further analysis has been tried but

was not successful, strengthening the postulated redundancy, as both single knockouts are viable. These phenotypes bring up the question of the biological use of glycosomal NADPH produced by IDHg. As already mentioned in chapter 6.1 the oxidative branch of the PPP is partially localized within the glycosomes, including two enzymatic reactions producing NADPH (G6PDH, 6PGDH). The main disadvantage of the PPP pathway compared to IDHg mediated NADPH production is glycosomal phosphate leakage when ribose-5-phosphate is transferred out of the glycosomes. Additionally a new glycosomal proteome raises uncertainty, whether there is a full PPP with glycosomal localization (Guther et al., 2014). They confirmed glycosomal localization for G6PDH, 6PGL and SBP, but not for ribulose 5-phosphate isomerase, transketolase, transaldolase, 6PGDH and more. Concluding, the NADPH production via IDHg has metabolic advantages and may become essential during specific stages of development.

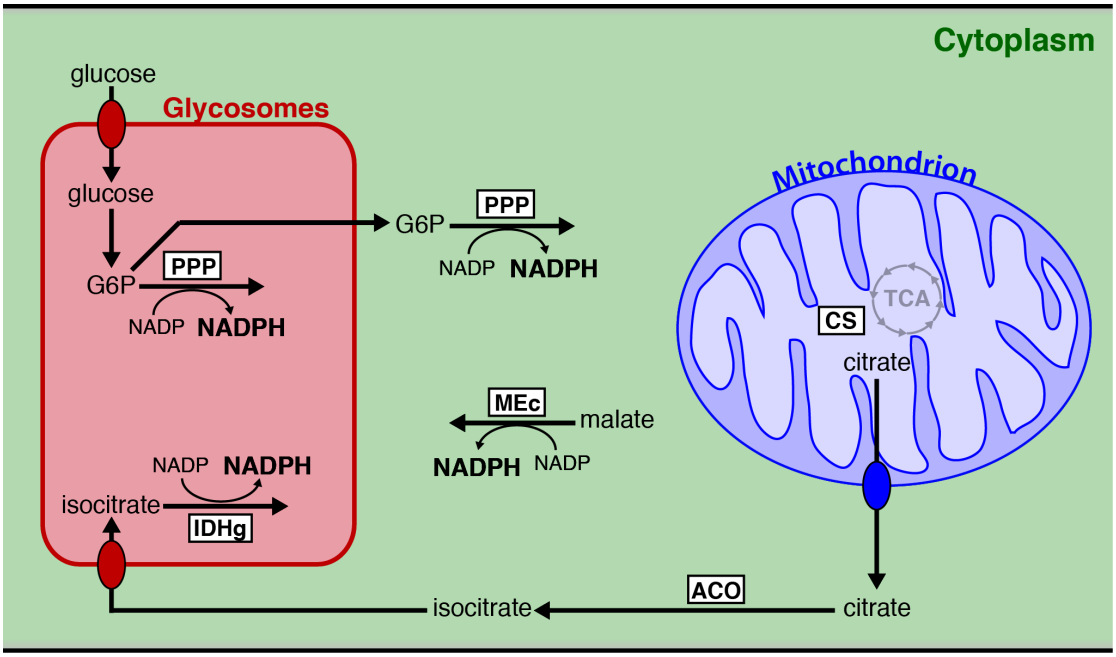

Fig.15: Glycosomal and cytosolic NADPH producing pathways. ACO: aconitase, CS: citrate synthase, G6P: glucose-6-phosphate, IDHg: glycosomal isocitrate dehydrogenase, MEc: cytosolic malic enzyme, PPP: oxidative branch of the pentose phosphate pathway, TCA: tricarboxylic acid cycle.

There are several metabolic pathways utilizing NADPH and therefore candidates for an essential role during differentiation. The most prominent candidate is the trypanothione system responsible for ROS detoxification in *T. brucei* (see introduction 1.4). Until recently, the NADPH consuming step, the trypanothione reductase (TR) was proposed to be located in the cytosol and the reduced trypanothione molecules were shuttled into the glycosomes (Krauth-Siegel and Comini, 2008; Smith et al., 1991). These proteomic screens did not identify the TR within the glycosomes, but in (Guther et al., 2014), the authors see a glycosomal localization of TR. A cytosolic contamination cannot be excluded. The so far overlooked glycosomal presence of TR might also be an indication for low protein abundance and thus a minor role.

An alternative pathway requiring NADPH is the β-oxidation of unsaturated fatty acids, which is depending on a peroxisomal IDH in yeast (Henke et al., 1998). Although some glycosomal β-oxidation activities have been reported (Wiemer et al., 1996), we could not confirm this and exclude this as possible NADPH sink. Even an active β-oxidation pathway would only require NADPH for unsaturated, but not saturated fatty acids. This situation cannot be applied in culture due to the requirements of a complex culture medium and is unlikely to happen *in vivo*.

T. brucei contains a significant amount of sterols with a major part of cholesterol. The levels of intracellular sterols decreased upon growth in lipid-depleted medium (Zhou et al., 2007),

demonstrating uptake of external sterols. The presence of sterols, especially cholesterol within membranes affects the physical properties and thus could be part of the developmental adaptations during stage development. In order to assure constant supply of sterols and to bypass starvation periods *de novo* synthesis is an option. Some steps of the mevalonate/squalene biosynthetic pathway have been proposed to be located in the glycosomes (Michels et al., 2006), of which the 3-hydroxy-3-methyl-glutaryl Coenzyme A reductase (HMGR) usually requires NADPH. In contradiction to this a more recent publication showed mitochondrial localization of this enzyme (Carrero-Lerida et al., 2009), whereas the experimental data cannot rule out a partial localization to the glycosomes. But even with dual localization of this biosynthetic pathway and a probably minor contribution of the glycosomal compartment the essentiality of glycosomal NADPH for cholesterol synthesis is doubtful.

The last putative NADPH consuming pathway within glycosomes is the synthesis of ether-linked lipids. The enzymatic reduction of the DHAP to a Gly3P backbone by the 1-alkyl-DHAP-oxidorecuctase is NADPH-dependent (see chapter 1.4). Their presence in *T. brucei* has been established (Patnaik et al., 1993), as well as some enzymatic reactions of the pathway have been identified and localized to the glycosomes (Opperdoes, 1984; Zomer et al., 1995). Furthermore, deletion and downregulation of two glycosomal transporters caused decreased levels of ether-linked lipids. The two PEX11-related proteins GIM5A and GIM5B cannot be deleted together in BSF parasites, but low levels of GIM5B in a ΔGIM5A background are tolerated by the PCF parasite. This leads to a decreased number of glycosomes and osmotically fragile cells (Voncken et al., 2003). These data suggest an important role of the ether-lipid content for the cellular integrity, which maybe crucial during insect stage differentiation, when facing extreme pH or mechanical stress. Therefore this hypothesis is being tested by creating an 1-alkyl-DHAP synthase (ADS)(Fig.7) null mutant and observing its behavior in the RBP6 culture differentiating system.

Recent data support the potential link of ether-lipid synthesis and glycosomal NADPH supply. A collaboration partner (F. Bringaud, Bordeaux) observed the two GIM5A and GIM5B proteins to be significantly downregulated in our ΔIDHg or ΔIDHm null mutants. GIM5A expression was 6.8-fold and 4.4-fold decreased in ΔIDHg and ΔIDHm, respectively. GIM5B expression was 3.6-fold and 2.5-fold decreased in ΔIDHg and ΔIDHm, respectively. The ether-lipid biosynthesis is a good candidate for an essential, glycosomal NADPH consuming pathway and will be investigated further. Next steps will be the analyses of WT and mutant cell lines by mass spectrometry and HPTLC for their ether-lipid content. Candidates are the null mutants of the 1-Alkyl-DHAP synthase (Fig.7, step 2) or the ΔIDHg null mutant in combination with dihydroepiandrosterone (DHEA) (G6PDH inhibitor).

References

Akoda, K., Van den Bossche, P., Lyaruu, E.A., De Deken, R., Marcotty, T., Coosemans, M., and Van den Abbeele, J. (2009a). Maturation of a Trypanosoma brucei infection to the infectious metacyclic stage is enhanced in nutritionally stressed tsetse flies. Journal of medical entomology *46*, 1446-1449.

Akoda, K., Van den Bossche, P., Marcotty, T., Kubi, C., Coosemans, M., De Deken, R., and Van den Abbeele, J. (2009b). Nutritional stress affects the tsetse fly's immune gene expression. Medical and veterinary entomology *23*, 195-201.

Albers, H., and Gottschalk, G. (1976). Acetate metabolism in Rhodopseudomonas gelatinosa and several other Rhodospirillaceae. Arch Microbiol *111*, 45-49.

Alibu, V.P., Storm, L., Haile, S., Clayton, C., and Horn, D. (2005). A doubly inducible system for RNA interference and rapid RNAi plasmid construction in Trypanosoma brucei. Molecular and biochemical parasitology *139*, 75-82.

Allmann, S., Morand, P., Ebikeme, C., Gales, L., Biran, M., Hubert, J., Brennand, A., Mazet, M., Franconi, J.M., Michels, P.A.*, et al.* (2013). Cytosolic NADPH homeostasis in glucose-starved procyclic Trypanosoma brucei relies on malic enzyme and the pentose phosphate pathway fed by gluconeogenic flux. The Journal of biological chemistry *288*, 18494-18505.

Alsford, S., Kawahara, T., Isamah, C., and Horn, D. (2007). A sirtuin in the African trypanosome is involved in both DNA repair and telomeric gene silencing but is not required for antigenic variation. Molecular microbiology *63*, 724-736.

Amberg, D.C., Burke, D.J., and Strathern, J.N. (2005). Methods in yeast genetics: A Cold Spring Harbor Laboratory course manual (Cold Spring Harbor Laboratory Press, Cold Spring Harbor, NY).

Arrick, B.A., Griffith, O.W., and Cerami, A. (1981). Inhibition of glutathione synthesis as a chemotherapeutic strategy for trypanosomiasis. J Exp Med *153*, 720-725.

Aussenac, F., Lavigne, B., and Dufourc, E.J. (2005). Toward bicelle stability with ether-linked phospholipids: temperature, composition, and hydration diagrams by 2H and 31P solid-state NMR. Langmuir *21*, 7129-7135.

Bakker, B.M., Michels, P.A., Opperdoes, F.R., and Westerhoff, H.V. (1997). Glycolysis in bloodstream form Trypanosoma brucei can be understood in terms of the kinetics of the glycolytic enzymes. The Journal of biological chemistry *272*, 3207-3215.

Bakker, B.M., Michels, P.A., Opperdoes, F.R., and Westerhoff, H.V. (1999). What controls glycolysis in bloodstream form Trypanosoma brucei? The Journal of biological chemistry *274*, 14551-14559.

Barbas, A., Popescu, A., Frazao, C., Arraiano, C.M., and Fialho, A.M. (2013). Rossmann-fold motifs can confer multiple functions to metabolic enzymes: RNA binding and ribonuclease activity of a UDP-glucose dehydrogenase. Biochemical and biophysical research communications *430*, 218-224.

Bastin, P., Bagherzadeh, Z., Matthews, K.R., and Gull, K. (1996). A novel epitope tag system to study protein targeting and organelle biogenesis in Trypanosoma brucei. Molecular and biochemical parasitology *77*, 235-239.

Berriman, M., Ghedin, E., Hertz-Fowler, C., Blandin, G., Renauld, H., Bartholomeu, D.C., Lennard, N.J., Caler, E., Hamlin, N.E., Haas, B.*, et al.* (2005). The genome of the African trypanosome Trypanosoma brucei. Science *309*, 416-422.

Besteiro, S., Biran, M., Biteau, N., Coustou, V., Baltz, T., Canioni, P., and Bringaud, F. (2002). Succinate secreted by Trypanosoma brucei is produced by a novel and unique glycosomal enzyme, NADH-dependent fumarate reductase. The Journal of biological chemistry *277*, 38001-38012.

Biebinger, S., Wirtz, L.E., Lorenz, P., and Clayton, C. (1997). Vectors for inducible expression of toxic gene products in bloodstream and procyclic Trypanosoma brucei. Molecular and biochemical parasitology *85*, 99-112.

Brasaemle, D.L., Rubin, B., Harten, I.A., Gruia-Gray, J., Kimmel, A.R., and Londos, C. (2000). Perilipin A increases triacylglycerol storage by decreasing the rate of triacylglycerol hydrolysis. The Journal of biological chemistry *275*, 38486-38493.

Brasaemle, D.L., Subramanian, V., Garcia, A., Marcinkiewicz, A., and Rothenberg, A. (2009). Perilipin A and the control of triacylglycerol metabolism. Mol Cell Biochem *326*, 15-21.

Bringaud, F., Baltz, D., and Baltz, T. (1998). Functional and molecular characterization of a glycosomal PPi-dependent enzyme in trypanosomatids: pyruvate, phosphate dikinase. Proceedings of the National Academy of Sciences of the United States of America *95*, 7963-7968.

Bringaud, F., Ebikeme, C., and Boshart, M. (2010). Acetate and succinate production in amoebae, helminths, diplomonads, trichomonads and trypanosomatids: common and diverse metabolic strategies used by parasitic lower eukaryotes. Parasitology *137*, 1315-1331.

Bringaud, F., Peyruchaud, S., Baltz, D., Giroud, C., Simpson, L., and Baltz, T. (1995). Molecular characterization of the mitochondrial heat shock protein 60 gene from Trypanosoma brucei. Molecular and biochemical parasitology *74*, 119-123.

Bringaud, F., Riviere, L., and Coustou, V. (2006). Energy metabolism of trypanosomatids: adaptation to available carbon sources. Molecular and biochemical parasitology *149*, 1-9.

Bringaud, F., Robinson, D.R., Barradeau, S., Biteau, N., Baltz, D., and Baltz, T. (2000). Characterization and disruption of a new Trypanosoma brucei repetitive flagellum protein, using double-stranded RNA inhibition. Molecular and biochemical parasitology *111*, 283-297.

Broach, J.R. (2012). Nutritional control of growth and development in yeast. Genetics *192*, 73-105.

Brun, R., and Schonenberger (1979). Cultivation and in vitro cloning or procyclic culture forms of Trypanosoma brucei in a semi-defined medium. Short communication. Acta Trop *36*, 289-292.

Cai, L., and Tu, B.P. (2012). Driving the cell cycle through metabolism. Annual review of cell and developmental biology *28*, 59-87.

Carrero-Lerida, J., Perez-Moreno, G., Castillo-Acosta, V.M., Ruiz-Perez, L.M., and Gonzalez-Pacanowska, D. (2009). Intracellular location of the early steps of the isoprenoid biosynthetic pathway in the trypanosomatids Leishmania major and Trypanosoma brucei. International journal for parasitology *39*, 307-314.

Carruthers, V.B., van der Ploeg, L.H., and Cross, G.A. (1993). DNA-mediated transformation of bloodstream-form Trypanosoma brucei. Nucleic acids research *21*, 2537-2538.

Cassio, F., Leao, C., and van Uden, N. (1987). Transport of lactate and other short-chain monocarboxylates in the yeast Saccharomyces cerevisiae. Appl Environ Microbiol *53*, 509-513.

Ciesla, J. (2006). Metabolic enzymes that bind RNA: yet another level of cellular regulatory network? Acta biochimica Polonica *53*, 11-32.

Colasante, C., Ellis, M., Ruppert, T., and Voncken, F. (2006). Comparative proteomics of glycosomes from bloodstream form and procyclic culture form Trypanosoma brucei brucei. Proteomics *6*, 3275-3293.

Colasante, C., Pena Diaz, P., Clayton, C., and Voncken, F. (2009). Mitochondrial carrier family inventory of Trypanosoma brucei brucei: Identification, expression and subcellular localisation. Molecular and biochemical parasitology *167*, 104-117.

Comini, M.A., Krauth-Siegel, R.L., and Flohe, L. (2007). Depletion of the thioredoxin homologue tryparedoxin impairs antioxidative defence in African trypanosomes. The Biochemical journal *402*, 43-49.

Cordeiro, A.T., Thiemann, O.H., and Michels, P.A. (2009). Inhibition of Trypanosoma brucei glucose-6-phosphate dehydrogenase by human steroids and their effects on the viability of cultured parasites. Bioorganic & medicinal chemistry *17*, 2483-2489.

Coustou, V., Besteiro, S., Biran, M., Diolez, P., Bouchaud, V., Voisin, P., Michels, P.A., Canioni, P., Baltz, T., and Bringaud, F. (2003). ATP generation in the Trypanosoma brucei procyclic form: cytosolic substrate level is essential, but not oxidative phosphorylation. The Journal of biological chemistry *278*, 49625-49635.

Coustou, V., Biran, M., Breton, M., Guegan, F., Riviere, L., Plazolles, N., Nolan, D., Barrett, M.P., Franconi, J.M., and Bringaud, F. (2008). Glucose-induced remodeling of intermediary and energy metabolism in procyclic Trypanosoma brucei. The Journal of biological chemistry *283*, 16342-16354.

Cronin, C.N., and Tipton, K.F. (1985). Purification and regulatory properties of phosphofructokinase from Trypanosoma (Trypanozoon) brucei brucei. The Biochemical journal *227*, 113-124.

Cronin, C.N., and Tipton, K.F. (1987). Kinetic studies on the reaction catalysed by phosphofructokinase from Trypanosoma brucei. The Biochemical journal *245*, 13-18.

Cross, G.A., Klein, R.A., and Linstead, D.J. (1975). Utilization of amino acids by Trypanosoma brucei in culture: L-threonine as a precursor for acetate. Parasitology *71*, 311-326.

Cullen, P.J., and Sprague, G.F., Jr. (2000). Glucose depletion causes haploid invasive growth in yeast. Proceedings of the National Academy of Sciences of the United States of America *97*, 13619-13624.

Cullen, P.J., and Sprague, G.F., Jr. (2012). The regulation of filamentous growth in yeast. Genetics *190*, 23-49.

Dang, L., White, D.W., Gross, S., Bennett, B.D., Bittinger, M.A., Driggers, E.M., Fantin, V.R., Jang, H.G., Jin, S., Keenan, M.C.*, et al.* (2009). Cancer-associated IDH1 mutations produce 2-hydroxyglutarate. Nature *462*, 739-744.

Dannenmuller, O., Arakawa, K., Eguchi, T., Kakinuma, K., Blanc, S., Albrecht, A.M., Schmutz, M., Nakatani, Y., and Ourisson, G. (2000). Membrane properties of archaeal macrocyclic diether phospholipids. Chemistry *6*, 645-654.

Dean, S., Marchetti, R., Kirk, K., and Matthews, K.R. (2009). A surface transporter family conveys the trypanosome differentiation signal. Nature *459*, 213-217.

Des Rosiers, C., Fernandez, C.A., David, F., and Brunengraber, H. (1994). Reversibility of the mitochondrial isocitrate dehydrogenase reaction in the perfused rat liver. Evidence from isotopomer analysis of citric acid cycle intermediates. The Journal of biological chemistry *269*, 27179-27182.

Dodson, H.C., Morris, M.T., and Morris, J.C. (2011). Glycerol 3-phosphate alters Trypanosoma brucei hexokinase activity in response to environmental change. The Journal of biological chemistry *286*, 33150-33157.

Dufernez, F., Yernaux, C., Gerbod, D., Noel, C., Chauvenet, M., Wintjens, R., Edgcomb, V.P., Capron, M., Opperdoes, F.R., and Viscogliosi, E. (2006). The presence of four iron-containing superoxide dismutase isozymes in trypanosomatidae: characterization, subcellular localization, and phylogenetic origin in Trypanosoma brucei. Free Radic Biol Med *40*, 210-225.

Duffieux, F., Van Roy, J., Michels, P.A., and Opperdoes, F.R. (2000). Molecular characterization of the first two enzymes of the pentose-phosphate pathway of Trypanosoma brucei. Glucose-6-phosphate dehydrogenase and 6-phosphogluconolactonase. The Journal of biological chemistry *275*, 27559-27565.

Durieux, P.O., Schutz, P., Brun, R., and Kohler, P. (1991). Alterations in Krebs cycle enzyme activities and carbohydrate catabolism in two strains of Trypanosoma brucei during in vitro differentiation of their bloodstream to procyclic stages. Molecular and biochemical parasitology *45*, 19-27.

Ebikeme, C., Hubert, J., Biran, M., Gouspillou, G., Morand, P., Plazolles, N., Guegan, F., Diolez, P., Franconi, J.M., Portais, J.C.*, et al.* (2010). Ablation of succinate production from glucose metabolism in the procyclic trypanosomes induces metabolic switches to the glycerol 3-phosphate/dihydroxyacetone phosphate shuttle and to proline metabolism. The Journal of biological chemistry *285*, 32312-32324.

Eidels, L., and Preiss, J. (1970). Citrate synthase. A regulatory enzyme from Rhodopseudomonas capsulata. The Journal of biological chemistry *245*, 2937-2945.

Engstler, M., and Boshart, M. (2004). Cold shock and regulation of surface protein trafficking convey sensitization to inducers of stage differentiation in Trypanosoma brucei. Genes & development *18*, 2798-2811.

Fairlamb, A.H., Blackburn, P., Ulrich, P., Chait, B.T., and Cerami, A. (1985). Trypanothione: a novel bis(glutathionyl)spermidine cofactor for glutathione reductase in trypanosomatids. Science *227*, 1485-1487.

Ferguson, M.A., Brimacombe, J.S., Brown, J.R., Crossman, A., Dix, A., Field, R.A., Guther, M.L., Milne, K.G., Sharma, D.K., and Smith, T.K. (1999). The GPI biosynthetic pathway as a therapeutic target for African sleeping sickness. Biochimica et biophysica acta *1455*, 327-340.

Flaspohler, J.A., Jensen, B.C., Saveria, T., Kifer, C.T., and Parsons, M. (2010). A novel protein kinase localized to lipid droplets is required for droplet biogenesis in trypanosomes. Eukaryotic cell *9*, 1702-1710.

Florin-Christensen, M., Florin-Christensen, J., de Isola, E.D., Lammel, E., Meinardi, E., Brenner, R.R., and Rasmussen, L. (1997). Temperature acclimation of Trypanosoma cruzi epimastigote and metacyclic trypomastigote lipids. Molecular and biochemical parasitology *88*, 25-33.

Fridberg, A., Olson, C.L., Nakayasu, E.S., Tyler, K.M., Almeida, I.C., and Engman, D.M. (2008). Sphingolipid synthesis is necessary for kinetoplast segregation and cytokinesis in Trypanosoma brucei. Journal of cell science *121*, 522-535.

Furuya, T., Kessler, P., Jardim, A., Schnaufer, A., Crudder, C., and Parsons, M. (2002). Glucose is toxic to glycosome-deficient trypanosomes. Proceedings of the National Academy of Sciences of the United States of America *99*, 14177-14182.

Garnak, M., and Reeves, H.C. (1979). Phosphorylation of Isocitrate dehydrogenase of Escherichia coli. Science *203*, 1111-1112.

Geigy, R., Jenni, L., Kauffmann, M., Onyango, R.J., and Weiss, N. (1975). Identification of T. brucei-subgroup strains isolated from game. Acta Trop *32*, 190-205.

Gietz, R.D., and Schiestl, R.H. (2007). Large-scale high-efficiency yeast transformation using the LiAc/SS carrier DNA/PEG method. Nature protocols *2*, 38-41.

Gimenez, R., Nunez, M.F., Badia, J., Aguilar, J., and Baldoma, L. (2003). The gene yjcG, cotranscribed with the gene acs, encodes an acetate permease in Escherichia coli. J Bacteriol *185*, 6448-6455.

Goulding, C.W., Bowers, P.M., Segelke, B., Lekin, T., Kim, C.Y., Terwilliger, T.C., and Eisenberg, D. (2007). The structure and computational analysis of Mycobacterium tuberculosis protein CitE suggest a novel enzymatic function. Journal of molecular biology *365*, 275-283.

Guther, M.L., Urbaniak, M.D., Tavendale, A., Prescott, A., and Ferguson, M.A. (2014). High-Confidence Glycosome Proteome for Procyclic Form Trypanosoma brucei by Epitope-Tag Organelle Enrichment and SILAC Proteomics. Journal of proteome research *13*, 2796-2806.

Haanstra, J.R., Kerkhoven, E.J., van Tuijl, A., Blits, M., Wurst, M., van Nuland, R., Albert, M.A., Michels, P.A., Bouwman, J., Clayton, C.*, et al.* (2011). A domino effect in drug action: from metabolic assault towards parasite differentiation. Molecular microbiology *79*, 94-108.

Haanstra, J.R., Stewart, M., Luu, V.D., van Tuijl, A., Westerhoff, H.V., Clayton, C., and Bakker, B.M. (2008). Control and regulation of gene expression: quantitative analysis of the expression of phosphoglycerate kinase in bloodstream form Trypanosoma brucei. The Journal of biological chemistry *283*, 2495-2507.

Hajra, A.K., and Bishop, J.E. (1982). Glycerolipid biosynthesis in peroxisomes via the acyl dihydroxyacetone phosphate pathway. Ann N Y Acad Sci *386*, 170-182.

Han, L., and Reynolds, K.A. (1997). A novel alternate anaplerotic pathway to the glyoxylate cycle in streptomycetes. J Bacteriol *179*, 5157-5164.

Hao, Z., Kasumba, I., and Aksoy, S. (2003). Proventriculus (cardia) plays a crucial role in immunity in tsetse fly (Diptera: Glossinidiae). Insect Biochem Mol Biol *33*, 1155-1164.

Harlow, E., and Lane, D., eds. (1988). Antibodies : a laboratory manual (Cold Spring Harbor Laboratory Press).

Hart, D.T., and Opperdoes, F.R. (1984). The occurrence of glycosomes (microbodies) in the promastigote stage of four major Leishmania species. Molecular and biochemical parasitology *13*, 159-172.

Heise, N., and Opperdoes, F.R. (1999). Purification, localisation and characterisation of glucose-6-phosphate dehydrogenase of Trypanosoma brucei. Molecular and biochemical parasitology *99*, 21-32.

Henke, B., Girzalsky, W., Berteaux-Lecellier, V., and Erdmann, R. (1998). IDP3 encodes a peroxisomal NADP-dependent isocitrate dehydrogenase required for the beta-oxidation of unsaturated fatty acids. The Journal of biological chemistry *273*, 3702-3711.

Hirumi, H., and Hirumi, K. (1989). Continuous cultivation of Trypanosoma brucei blood stream forms in a medium containing a low concentration of serum protein without feeder cell layers. The Journal of parasitology *75*, 985-989.

Horn, D., and McCulloch, R. (2010). Molecular mechanisms underlying the control of antigenic variation in African trypanosomes. Curr Opin Microbiol *13*, 700-705.

Hu, C., and Aksoy, S. (2006). Innate immune responses regulate trypanosome parasite infection of the tsetse fly Glossina morsitans morsitans. Molecular microbiology *60*, 1194-1204.

Huynh, T.T., Huynh, V.T., Harmon, M.A., and Phillips, M.A. (2003). Gene knockdown of gamma-glutamylcysteine synthetase by RNAi in the parasitic protozoa Trypanosoma brucei demonstrates that it is an essential enzyme. The Journal of biological chemistry *278*, 39794-39800.

Igoillo-Esteve, M., Mazet, M., Deumer, G., Wallemacq, P., and Michels, P.A. (2011). Glycosomal ABC transporters of Trypanosoma brucei: characterisation of their expression, topology and substrate specificity. International journal for parasitology *41*, 429-438.

Ito, S., D'Alessio, A.C., Taranova, O.V., Hong, K., Sowers, L.C., and Zhang, Y. (2010). Role of Tet proteins in 5mC to 5hmC conversion, ES-cell self-renewal and inner cell mass specification. Nature *466*, 1129-1133.

Kerkhoven, E.J., Achcar, F., Alibu, V.P., Burchmore, R.J., Gilbert, I.H., Trybilo, M., Driessen, N.N., Gilbert, D., Breitling, R., Bakker, B.M.*, et al.* (2013). Handling uncertainty in dynamic models: the pentose phosphate pathway in Trypanosoma brucei. PLoS computational biology *9*, e1003371.

Kihara, M., and Macnab, R.M. (1981). Cytoplasmic pH mediates pH taxis and weak-acid repellent taxis of bacteria. J Bacteriol *145*, 1209-1221.

Kim, J.W., and Dang, C.V. (2005). Multifaceted roles of glycolytic enzymes. Trends in biochemical sciences *30*, 142-150.

Kohl, L., Sherwin, T., and Gull, K. (1999). Assembly of the paraflagellar rod and the flagellum attachment zone complex during the Trypanosoma brucei cell cycle. J Eukaryot Microbiol *46*, 105-109.

Kolev, N.G., Ramey-Butler, K., Cross, G.A., Ullu, E., and Tschudi, C. (2012). Developmental progression to infectivity in Trypanosoma brucei triggered by an RNA-binding protein. Science *338*, 1352-1353.

Kondrashov, F.A., Koonin, E.V., Morgunov, I.G., Finogenova, T.V., and Kondrashova, M.N. (2006). Evolution of glyoxylate cycle enzymes in Metazoa: evidence of multiple horizontal transfer events and pseudogene formation. Biol Direct *1*, 31.

Konig, A.C., Hartl, M., Boersema, P.J., Mann, M., and Finkemeier, I. (2014). The mitochondrial lysine acetylome of Arabidopsis. Mitochondrion.

Kornberg, H.L., and Lascelles, J. (1960). The formation of isocitratase by the Athiorhodaceae. J Gen Microbiol *23*, 511-517.

Krauth-Siegel, R.L., and Comini, M.A. (2008). Redox control in trypanosomatids, parasitic protozoa with trypanothione-based thiol metabolism. Biochimica et biophysica acta *1780*, 1236-1248.

Krieger, S., Schwarz, W., Ariyanayagam, M.R., Fairlamb, A.H., Krauth-Siegel, R.L., and Clayton, C. (2000). Trypanosomes lacking trypanothione reductase are avirulent and show increased sensitivity to oxidative stress. Molecular microbiology *35*, 542-552.

Lamour, N., Riviere, L., Coustou, V., Coombs, G.H., Barrett, M.P., and Bringaud, F. (2005). Proline metabolism in procyclic Trypanosoma brucei is down-regulated in the presence of glucose. The Journal of biological chemistry *280*, 11902-11910.

LaPorte, D.C., Thorsness, P.E., and Koshland, D.E., Jr. (1985). Compensatory phosphorylation of isocitrate dehydrogenase. A mechanism for adaptation to the intracellular environment. The Journal of biological chemistry *260*, 10563-10568.

Leroux, A.E., Maugeri, D.A., Cazzulo, J.J., and Nowicki, C. (2011). Functional characterization of NADP-dependent isocitrate dehydrogenase isozymes from Trypanosoma cruzi. Molecular and biochemical parasitology *177*, 61-64.

Li, F., and Gottesdiener, K.M. (1996). An efficient method for stable transfection of bloodstream-form Trypanosoma brucei. Nucleic acids research *24*, 534-535.

Liniger, M., Acosta-Serrano, A., Van Den Abbeele, J., Kunz Renggli, C., Brun, R., Englund, P.T., and Roditi, I. (2003). Cleavage of trypanosome surface glycoproteins by alkaline trypsin-like enzyme(s) in the midgut of Glossina morsitans. International journal for parasitology *33*, 1319-1328.

Linstead, D.J., Klein, R.A., and Cross, G.A. (1977). Threonine catabolism in Trypanosoma brucei. J Gen Microbiol *101*, 243-251.

Lombard, D.B., Alt, F.W., Cheng, H.L., Bunkenborg, J., Streeper, R.S., Mostoslavsky, R., Kim, J., Yancopoulos, G., Valenzuela, D., Murphy, A.*, et al.* (2007). Mammalian Sir2 homolog SIRT3 regulates global mitochondrial lysine acetylation. Molecular and cellular biology *27*, 8807-8814.

Mannaerts, G.P., and Van Veldhoven, P.P. (1993). Metabolic pathways in mammalian peroxisomes. Biochimie *75*, 147-158.

Marche, S., Michels, P.A., and Opperdoes, F.R. (2000). Comparative study of Leishmania mexicana and Trypanosoma brucei NAD-dependent glycerol-3-phosphate dehydrogenase. Molecular and biochemical parasitology *106*, 83-91.

Martin, S., and Parton, R.G. (2006). Lipid droplets: a unified view of a dynamic organelle. Nat Rev Mol Cell Biol *7*, 373-378.

Martinez-Calvillo, S., Vizuet-de-Rueda, J.C., Florencio-Martinez, L.E., Manning-Cela, R.G., and Figueroa-Angulo, E.E. (2010). Gene expression in trypanosomatid parasites. J Biomed Biotechnol *2010*, 525241.

Mazet, M., Morand, P., Biran, M., Bouyssou, G., Courtois, P., Daulouede, S., Millerioux, Y., Franconi, J.M., Vincendeau, P., Moreau, P.*, et al.* (2013). Revisiting the central metabolism of the bloodstream forms of Trypanosoma brucei: production of acetate in the mitochondrion is essential for parasite viability. PLoS neglected tropical diseases *7*, e2587.

McCammon, M.T. (1996). Mutants of Saccharomyces cerevisiae with defects in acetate metabolism: isolation and characterization of Acn- mutants. Genetics *144*, 57-69.

McCulloch, R., Vassella, E., Burton, P., Boshart, M., and Barry, J.D. (2004). Transformation of monomorphic and pleomorphic Trypanosoma brucei. Methods Mol Biol *262*, 53-86.

Michels, P.A., Bringaud, F., Herman, M., and Hannaert, V. (2006). Metabolic functions of glycosomes in trypanosomatids. Biochimica et biophysica acta *1763*, 1463-1477.

Michels, P.A.M., Michels, J.P.J., Boonstra, J., and Konings, W.N. (1979). Generation of an electrochemical proton gradient in bacteria by the excretion of metabolic end products. FEMS Microbiology Letters *5*, 357-364.

Millerioux, Y., Ebikeme, C., Biran, M., Morand, P., Bouyssou, G., Vincent, I.M., Mazet, M., Riviere, L., Franconi, J.M., Burchmore, R.J.*, et al.* (2013). The threonine degradation pathway of the Trypanosoma brucei procyclic form: the main carbon source for lipid biosynthesis is under metabolic control. Molecular microbiology *90*, 114-129.

Millerioux, Y., Morand, P., Biran, M., Mazet, M., Moreau, P., Wargnies, M., Ebikeme, C., Deramchia, K., Gales, L., Portais, J.C.*, et al.* (2012). ATP synthesis-coupled and -uncoupled acetate production from acetyl-CoA by mitochondrial acetate:succinate CoA-transferase and acetyl-CoA thioesterase in Trypanosoma. The Journal of biological chemistry *287*, 17186-17197.

Mills, E., and O'Neill, L.A. (2014). Succinate: a metabolic signal in inflammation. Trends in cell biology *24*, 313-320.

Moran-Crusio, K., Reavie, L., Shih, A., Abdel-Wahab, O., Ndiaye-Lobry, D., Lobry, C., Figueroa, M.E., Vasanthakumar, A., Patel, J., Zhao, X.*, et al.* (2011). Tet2 loss leads to increased hematopoietic stem cell self-renewal and myeloid transformation. Cancer cell *20*, 11-24.

Morand, S., Renggli, C.K., Roditi, I., and Vassella, E. (2012). MAP kinase kinase 1 (MKK1) is essential for transmission of Trypanosoma brucei by Glossina morsitans. Molecular and biochemical parasitology *186*, 73-76.

Morriswood, B., Havlicek, K., Demmel, L., Yavuz, S., Sealey-Cardona, M., Vidilaseris, K., Anrather, D., Kostan, J., Djinovic-Carugo, K., Roux, K.J.*, et al.* (2013). Novel bilobe components in Trypanosoma brucei identified using proximity-dependent biotinylation. Eukaryotic cell *12*, 356-367.

Mullen, A.R., Wheaton, W.W., Jin, E.S., Chen, P.-H., Sullivan, L.B., Cheng, T., Yang, Y., Linehan, W.M., Chandel, N.S., and DeBerardinis, R.J. (2012). Reductive carboxylation supports growth in tumour cells with defective mitochondria. Nature *481*, 385-388.

Murphy, D.J. (2012). The dynamic roles of intracellular lipid droplets: from archaea to mammals. Protoplasma *249*, 541-585.

Nagy, E., Henics, T., Eckert, M., Miseta, A., Lightowlers, R.N., and Kellermayer, M. (2000). Identification of the NAD(+)-binding fold of glyceraldehyde-3-phosphate dehydrogenase as a novel RNA-binding domain. Biochemical and biophysical research communications *275*, 253-260.

Ngo, H., Tschudi, C., Gull, K., and Ullu, E. (1998). Double-stranded RNA induces mRNA degradation in Trypanosoma brucei. Proceedings of the National Academy of Sciences of the United States of America *95*, 14687-14692.

Nwagwu, M., and Opperdoes, F.R. (1982). Regulation of glycolysis in Trypanosoma brucei: hexokinase and phosphofructokinase activity. Acta Trop *39*, 61-72.

Olszewski, K.L., Mather, M.W., Morrisey, J.M., Garcia, B.A., Vaidya, A.B., Rabinowitz, J.D., and Llinas, M. (2010). Branched tricarboxylic acid metabolism in Plasmodium falciparum. Nature *466*, 774-778.

Opperdoes, F.R. (1984). Localization of the initial steps in alkoxyphospholipid biosynthesis in glycosomes (microbodies) of Trypanosoma brucei. FEBS letters *169*, 35-39.

Opperdoes, F.R., and Borst, P. (1977). Localization of nine glycolytic enzymes in a microbody-like organelle in Trypanosoma brucei: the glycosome. FEBS letters *80*, 360-364.

Opperdoes, F.R., Markos, A., and Steiger, R.F. (1981). Localization of malate dehydrogenase, adenylate kinase and glycolytic enzymes in glycosomes and the threonine pathway in the mitochondrion of cultured procyclic trypomastigotes of Trypanosoma brucei. Molecular and biochemical parasitology *4*, 291-309.

Overath, P., Czichos, J., and Haas, C. (1986). The effect of citrate/cis-aconitate on oxidative metabolism during transformation of Trypanosoma brucei. European journal of biochemistry / FEBS *160*, 175-182.

Park, J., Chen, Y., Tishkoff, D.X., Peng, C., Tan, M., Dai, L., Xie, Z., Zhang, Y., Zwaans, B.M., Skinner, M.E.*, et al.* (2013). SIRT5-mediated lysine desuccinylation impacts diverse metabolic pathways. Molecular cell *50*, 919-930.

Patnaik, P.K., Field, M.C., Menon, A.K., Cross, G.A., Yee, M.C., and Butikofer, P. (1993). Molecular species analysis of phospholipids from Trypanosoma brucei bloodstream and procyclic forms. Molecular and biochemical parasitology *58*, 97-105.

Pays, E., Van Meirvenne, N., Le Ray, D., and Steinert, M. (1981). Gene duplication and transposition linked to antigenic variation in Trypanosoma brucei. Proceedings of the National Academy of Sciences of the United States of America *78*, 2673-2677.

Pena-Diaz, P., Pelosi, L., Ebikeme, C., Colasante, C., Gao, F., Bringaud, F., and Voncken, F. (2012). Functional characterization of TbMCP5, a conserved and essential ADP/ATP carrier present in the mitochondrion of the human pathogen Trypanosoma brucei. The Journal of biological chemistry *287*, 41861-41874.

Picault, N., Hodges, M., Palmieri, L., and Palmieri, F. (2004). The growing family of mitochondrial carriers in Arabidopsis. Trends in plant science *9*, 138-146.

Quivoron, C., Couronne, L., Della Valle, V., Lopez, C.K., Plo, I., Wagner-Ballon, O., Do Cruzeiro, M., Delhommeau, F., Arnulf, B., Stern, M.H.*, et al.* (2011). TET2 inactivation results in pleiotropic hematopoietic abnormalities in mouse and is a recurrent event during human lymphomagenesis. Cancer cell *20*, 25-38.

Reuner, B., Vassella, E., Yutzy, B., and Boshart, M. (1997). Cell density triggers slender to stumpy differentiation of Trypanosoma brucei bloodstream forms in culture. Molecular and biochemical parasitology *90*, 269-280.

Riviere, L., Moreau, P., Allmann, S., Hahn, M., Biran, M., Plazolles, N., Franconi, J.M., Boshart, M., and Bringaud, F. (2009). Acetate produced in the mitochondrion is the essential precursor for lipid biosynthesis in procyclic trypanosomes. Proceedings of the National Academy of Sciences of the United States of America *106*, 12694-12699.

Riviere, L., van Weelden, S.W., Glass, P., Vegh, P., Coustou, V., Biran, M., van Hellemond, J.J., Bringaud, F., Tielens, A.G., and Boshart, M. (2004). Acetyl:succinate CoA-transferase in procyclic Trypanosoma brucei. Gene identification and role in carbohydrate metabolism. The Journal of biological chemistry *279*, 45337-45346.

Robinson, D.R., and Gull, K. (1991). Basal body movements as a mechanism for mitochondrial genome segregation in the trypanosome cell cycle. Nature *352*, 731-733.

Rohle, D., Popovici-Muller, J., Palaskas, N., Turcan, S., Grommes, C., Campos, C., Tsoi, J., Clark, O., Oldrini, B., Komisopoulou, E.*, et al.* (2013). An inhibitor of mutant IDH1 delays growth and promotes differentiation of glioma cells. Science *340*, 626-630.

Rotureau, B., Ooi, C.P., Huet, D., Perrot, S., and Bastin, P. (2013). Forward Motility is Essential for Trypanosome Infection In the Tsetse Fly. Cell Microbiol.

Ryley, J.F. (1962). Studies on the metabolism of the protozoa. 9. Comparative metabolism of blood-stream and culture forms of Trypanosoma rhodesiense. The Biochemical journal *85*, 211-223.

Saas, J., Ziegelbauer, K., von Haeseler, A., Fast, B., and Boshart, M. (2000). A developmentally regulated aconitase related to iron-regulatory protein-1 is localized in the cytoplasm and in the mitochondrion of Trypanosoma brucei. The Journal of biological chemistry *275*, 2745-2755.

Sambrook, J., Fritsch, E.F., and Maniatis, T., eds. (1989). Molecular cloning : a laboratory manual., 2 edn (New York: Cold Spring Harbor Laboratory Press).

Sasaki, M., Knobbe, C.B., Munger, J.C., Lind, E.F., Brenner, D., Brustle, A., Harris, I.S., Holmes, R., Wakeham, A., Haight, J.*, et al.* (2012). IDH1(R132H) mutation increases murine haematopoietic progenitors and alters epigenetics. Nature *488*, 656-659.

Schussler, A., Martin, H., Cohen, D., Fitz, M., and Wipf, D. (2006). Characterization of a carbohydrate transporter from symbiotic glomeromycotan fungi. Nature *444*, 933-936.

Shinoda, K., Shinoda, W., Baba, T., and Mikami, M. (2004). Comparative molecular dynamics study of ether- and ester-linked phospholipid bilayers. J Chem Phys *121*, 9648-9654.

Skodova, I., Verner, Z., Bringaud, F., Fabian, P., Lukes, J., and Horvath, A. (2013). Characterization of two mitochondrial FAD-dependent glycerol-3-phosphate dehydrogenases in Trypanosoma brucei. Eukaryotic cell.

Smith, K., Opperdoes, F.R., and Fairlamb, A.H. (1991). Subcellular distribution of trypanothione reductase in bloodstream and procyclic forms of Trypanosoma brucei. Molecular and biochemical parasitology *48*, 109-112.

Steiger, R.F. (1973). On the ultrastructure of Trypanosoma (Trypanozoon) brucei in the course of its life cycle and some related aspects. Acta Trop *30*, 64-168.

Stoffel, S.A., Alibu, V.P., Hubert, J., Ebikeme, C., Portais, J.C., Bringaud, F., Schweingruber, M.E., and Barrett, M.P. (2011). Transketolase in Trypanosoma brucei. Molecular and biochemical parasitology *179*, 1-7.

Sykes, S.E., and Hajduk, S.L. (2013). Dual functions of alpha-ketoglutarate dehydrogenase E2 in the Krebs cycle and mitochondrial DNA inheritance in Trypanosoma brucei. Eukaryotic cell *12*, 78-90.

Szoor, B., Dyer, N.A., Ruberto, I., Acosta-Serrano, A., and Matthews, K.R. (2013). Independent Pathways Can Transduce the Life-Cycle Differentiation Signal in Trypanosoma brucei. PLoS pathogens *9*, e1003689.

Szoor, B., Ruberto, I., Burchmore, R., and Matthews, K.R. (2010). A novel phosphatase cascade regulates differentiation in Trypanosoma brucei via a glycosomal signaling pathway. Genes & development *24*, 1306-1316.

Szoor, B., Wilson, J., McElhinney, H., Tabernero, L., and Matthews, K.R. (2006). Protein tyrosine phosphatase TbPTP1: A molecular switch controlling life cycle differentiation in trypanosomes. J Cell Biol *175*, 293-303.

ten Asbroek, A.L., Ouellette, M., and Borst, P. (1990). Targeted insertion of the neomycin phosphotransferase gene into the tubulin gene cluster of Trypanosoma brucei. Nature *348*, 174-175.

ten Brink, B., and Konings, W.N. (1986). Generation of a protonmotive force in anaerobic bacteria by end-product efflux. Methods in enzymology *125*, 492-510.

Teusink, B., Walsh, M.C., van Dam, K., and Westerhoff, H.V. (1998). The danger of metabolic pathways with turbo design. Trends in biochemical sciences *23*, 162-169.

Van Den Abbeele, J., Claes, Y., van Bockstaele, D., Le Ray, D., and Coosemans, M. (1999). Trypanosoma brucei spp. development in the tsetse fly: characterization of the post-mesocyclic stages in the foregut and proboscis. Parasitology *118 (Pt 5)*, 469-478.

van den Bosch, H., Schutgens, R.B., Wanders, R.J., and Tager, J.M. (1992). Biochemistry of peroxisomes. Annu Rev Biochem *61*, 157-197.

Van Hellemond, J.J., Opperdoes, F.R., and Tielens, A.G. (1998). Trypanosomatidae produce acetate via a mitochondrial acetate:succinate CoA transferase. Proceedings of the National Academy of Sciences of the United States of America *95*, 3036-3041.

van Weelden, S.W., Fast, B., Vogt, A., van der Meer, P., Saas, J., van Hellemond, J.J., Tielens, A.G., and Boshart, M. (2003). Procyclic Trypanosoma brucei do not use Krebs cycle activity for energy generation. The Journal of biological chemistry *278*, 12854-12863.

van Weelden, S.W., van Hellemond, J.J., Opperdoes, F.R., and Tielens, A.G. (2005). New functions for parts of the Krebs cycle in procyclic Trypanosoma brucei, a cycle not operating as a cycle. The Journal of biological chemistry *280*, 12451-12460.

Vanhamme, L., Paturiaux-Hanocq, F., Poelvoorde, P., Nolan, D.P., Lins, L., Van Den Abbeele, J., Pays, A., Tebabi, P., Van Xong, H., Jacquet, A*., et al.* (2003). Apolipoprotein L-I is the trypanosome lytic factor of human serum. Nature *422*, 83-87.

Vassella, E., Den Abbeele, J.V., Butikofer, P., Renggli, C.K., Furger, A., Brun, R., and Roditi, I. (2000). A major surface glycoprotein of trypanosoma brucei is expressed transiently during development and can be regulated post-transcriptionally by glycerol or hypoxia. Genes & development *14*, 615-626.

Vassella, E., Probst, M., Schneider, A., Studer, E., Renggli, C.K., and Roditi, I. (2004). Expression of a major surface protein of Trypanosoma brucei insect forms is controlled by the activity of mitochondrial enzymes. Molecular biology of the cell *15*, 3986-3993.

Vassella, E., Reuner, B., Yutzy, B., and Boshart, M. (1997). Differentiation of African trypanosomes is controlled by a density sensing mechanism which signals cell cycle arrest via the cAMP pathway. Journal of cell science *110 (Pt 21)*, 2661-2671.

Vertommen, D., Van Roy, J., Szikora, J.P., Rider, M.H., Michels, P.A., and Opperdoes, F.R. (2008). Differential expression of glycosomal and mitochondrial proteins in the two major life-cycle stages of Trypanosoma brucei. Molecular and biochemical parasitology *158*, 189-201.

Vickerman, K. (1985). Developmental cycles and biology of pathogenic trypanosomes. Br Med Bull *41*, 105-114.

Voncken, F., van Hellemond, J.J., Pfisterer, I., Maier, A., Hillmer, S., and Clayton, C. (2003). Depletion of GIM5 causes cellular fragility, a decreased glycosome number, and reduced levels of ether-linked phospholipids in trypanosomes. The Journal of biological chemistry *278*, 35299-35310.

Wagner, G.R., and Payne, R.M. (2013). Widespread and enzyme-independent Nepsilon-acetylation and Nepsilon-succinylation of proteins in the chemical conditions of the mitochondrial matrix. The Journal of biological chemistry *288*, 29036-29045.

Weiss, B.L., Wang, J., Maltz, M.A., Wu, Y., and Aksoy, S. (2013). Trypanosome infection establishment in the tsetse fly gut is influenced by microbiome-regulated host immune barriers. PLoS pathogens *9*, e1003318.

Wiemer, E.A., L, I.J., van Roy, J., Wanders, R.J., and Opperdoes, F.R. (1996). Identification of 2-enoyl coenzyme A hydratase and NADP(+)-dependent 3-hydroxyacyl-CoA dehydrogenase activity in glycosomes of procyclic Trypanosoma brucei. Molecular and biochemical parasitology *82*, 107-111.

Wilkinson, S.R., Prathalingam, S.R., Taylor, M.C., Ahmed, A., Horn, D., and Kelly, J.M. (2006). Functional characterisation of the iron superoxide dismutase gene repertoire in Trypanosoma brucei. Free Radic Biol Med *40*, 198-209.

Xong, H.V., Vanhamme, L., Chamekh, M., Chimfwembe, C.E., Van Den Abbeele, J., Pays, A., Van Meirvenne, N., Hamers, R., De Baetselier, P., and Pays, E. (1998). A VSG expression site-associated gene confers resistance to human serum in Trypanosoma rhodesiense. Cell *95*, 839-846.

Zhang, Z., Tan, M., Xie, Z., Dai, L., Chen, Y., and Zhao, Y. (2011). Identification of lysine succinylation as a new post-translational modification. Nature chemical biology *7*, 58-63.

Zhou, W., Cross, G.A., and Nes, W.D. (2007). Cholesterol import fails to prevent catalyst-based inhibition of ergosterol synthesis and cell proliferation of Trypanosoma brucei. Journal of lipid research *48*, 665-673.

Zomer, A.W., Michels, P.A., and Opperdoes, F.R. (1999). Molecular characterisation of Trypanosoma brucei alkyl dihydroxyacetone-phosphate synthase. Molecular and biochemical parasitology *104*, 55-66.

Zomer, A.W., Opperdoes, F.R., and van den Bosch, H. (1995). Alkyl dihydroxyacetone phosphate synthase in glycosomes of Trypanosoma brucei. Biochimica et biophysica acta *1257*, 167-173.

Supplemental Material – Chapter 2

http://www.jbc.org/content/288/25/18494/suppl/DC1

Supplemental Material – Chapter 3.1

Figure S1

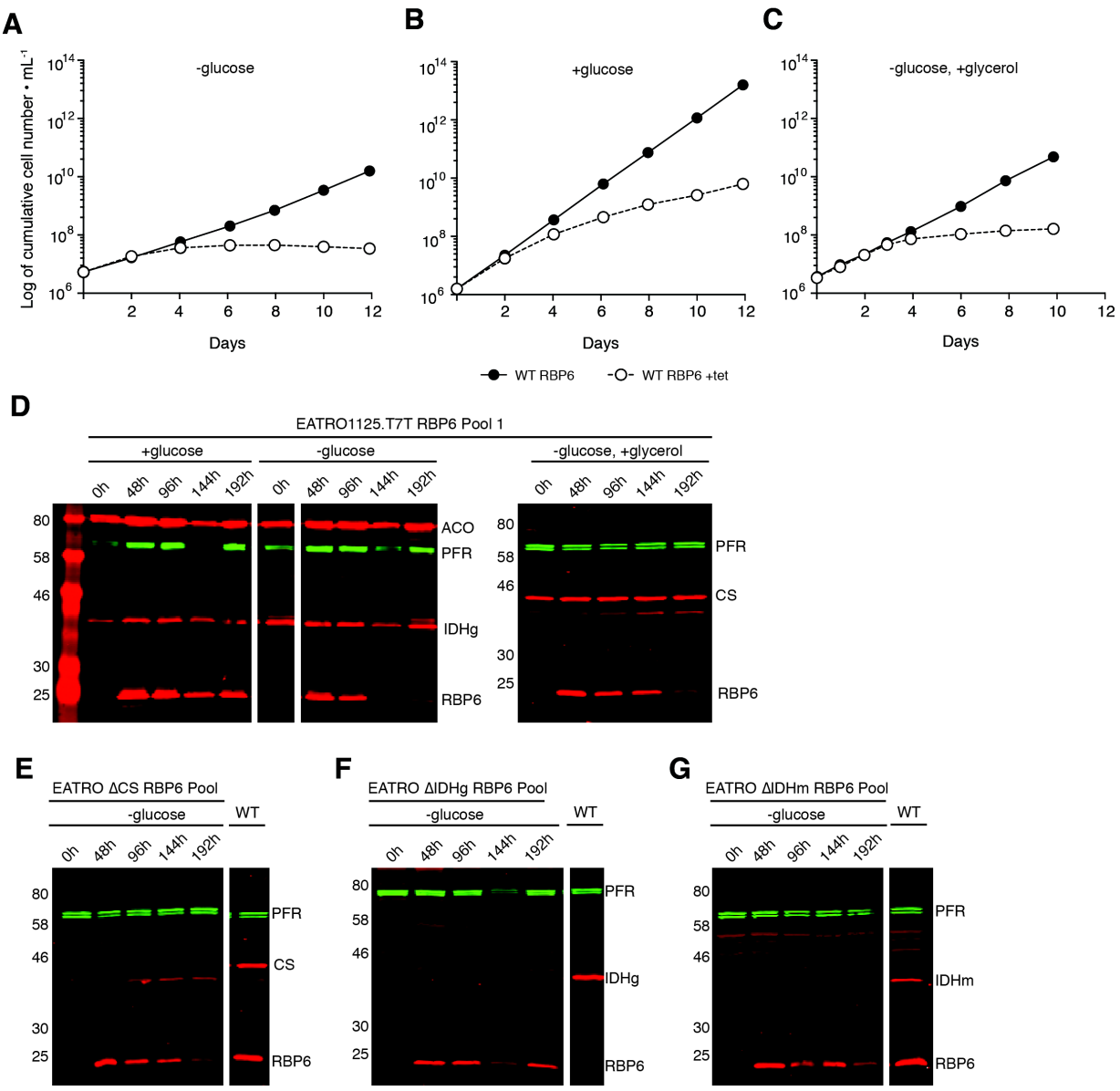

Figure S1. **Control of growth and RBP6 expression levels upon induction.** RBP6 expression was induced in EATRO1125 and growth observed in SDM79 without glucose (A), with glucose (B) and without glucose with 20 mM glycerol added (C). (D) The RBP6 expression levels during the respective growth curves were controlled by western blotting. The RBP6 expression levels upon induction were controlled by western blotting for ΔCS (E), ΔIDHg (F) and ΔIDHm (G).

Figure S2

ID	PROTEIN NAME	PATHWAY	NUMBER OF PEPTIDES DETECTED	NUMBER OF PEPTIDES ANALYSED	CONFIDENCE SCORE	WT glucose-rich MEAN	WT glucose-rich ±SD	WT glucose-rich ±SD (%)	WT glucose-depleted MEAN	WT glucose-depleted ±SD	WT glucose-depleted ±SD (%)	RATIO depleted/ rich
Tb927.10.8440	glucose transporter 1 (THT1)	Glycolysis	NOT DETECTED									
Tb927.10.8530	glucose transporter 2 (THT2)	Glycolysis	NOT DETECTED									
Tb927.10.2010	hexokinase (HK1)	Glycolysis	NOT DETECTED									
Tb927.10.2020	hexokinase (HK2)	Glycolysis	22	18	78	1293637	363353	28	1084741	83401	8	**0.84**
Tb927.1.3830	glucose-6-phosphate isomerase (PGI)	Glycolysis	24	24	73	368590	92823	25	681649	64497	9	**1.85**
Tb927.3.3270	ATP-dependent phosphofructokinase (PFK)	Glycolysis	36	29	130	3664352	125414	3	3267210	528233	16	**0.89**
Tb927.10.5620	fructose-bisphosphate aldolasel (ALD)	Glycolysis	38	38	165	12171932	3159716	26	13154322	1419147	11	**1.08**
Tb11.02.3210	triosephosphate isomerase (TIM)	Glycolysis	14	14	68	18240602	6057350	33	15495388	3247953	21	**0.85**
Tb927.6.4280	glyceraldehyde 3-phosphate dehydrogenase, glycosomal (gGAPDH)	Glycolysis	29	26	140	40196308	11156408	28	42084489	2019551	5	**1.05**
Tb927.8.3530	NAD-dependent glycerol-3-phosphate dehydrogenase (GPDH)	Glycolysis	23	22	124	13902176	1804483	13	14470425	5040227	35	**1.04**
Tb927.10.6880	glyceraldehyde 3-phosphate dehydrogenase, cytosolic (cGAPDH)	Glycolysis	17	13	66	2148780	592530	28	2165992	352365	16	**1.01**
Tb09.211.3550	glycerol kinase (GK)	Glycolysis	64	63	373	49712573	7501531	15	69034096	13696711	20	**1.39**
Tb927.1.710	phosphoglycerate kinase (PGKB)	Glycolysis	37	7	166	2683726	210242	8	2764795	336169	12	**1.03**
Tb927.1.720	phosphoglycerate kinase (PGKA)	Glycolysis	25	8	87	53668	12503	23	64108	24912	39	**1.19**
Tb927.10.7930	2,3-bisphosphoglycerate-independent phosphoglycerate mutase (PGAM)	Glycolysis	29	27	120	4122148	532730	13	3412190	410056	12	**0.83**
Tb927.10.2890	enolase (ENO)	Glycolysis	42	41	226	29044276	1588562	5	25773287	5423024	21	**0.89**
Tb927.10.14140	pyruvate kinase (PYK)	Glycolysis	18	17	76	1107102	56708	5	880766	27429	3	**0.80**
Tb11.02.4150	pyruvate phosphate dikinase (PPDK)	Glycolysis	85	80	411	24143798	2128045	9	28173866	3625275	13	**1.17**
Tb927.10.15410	malate dehydrogenase, glycosomal (gMDH)	Succinate branch	19	18	85	20371495	7526901	37	20885690	992043	5	**1.03**
Tb927.2.4210	phosphoenolpyruvate carboxykinase (PEPCK)	Succinate branch	57	56	289	39063029	4042413	10	34296519	1900099	6	**0.88**
Tb11.01.3040	malate dehydrogenase, cytosolic (cMDH)	Succinate branch	15	13	48	1536212	49066	3	1853263	139815	8	**1.21**
Tb927.3.4500	fumarate hydratase, cytosolic (FHc)	Succinate branch	53	49	226	13335431	3540723	27	5727492	1111591	19	**0.43**
Tb927.5.930	NADH-dependent fumarate reductase, glycosomal (FRDg)	Succinate branch	69	35	272	6814236	2017622	30	6119976	1056498	17	**0.90**
Tb927.3.1790	pyruvate dehydrogenase E1 beta subunit (PDH-E1)	Acetate branch	23	21	106	9169587	3166242	35	9373060	1594377	17	**1.02**
Tb927.10.12700	pyruvate dehydrogenase E1 alpha subunit (PDH-E1)	Acetate branch	40	38	140	4047268	383866	9	4017106	52724	1	**0.99**
Tb927.10.7570	dihydrolipoamide acetyltransferase E2 subunit (PDH-E2)	Acetate branch	20	18	84	3055585	700074	23	3990621	775528	19	**1.31**
Tb927.10.2350	pyruvate dehydrogenase complex E3 (PDH-E3)	Acetate branch	11	10	45	1294174	431603	33	1042461	365202	35	**0.81**
Tb11.02.0290	acetate:succinate coenzyme A- transferase (ASCT)	Acetate branch	22	22	86	6713229	507091	8	7980581	1518537	19	**1.19**
Tb927.3.4260	acetyl-CoA thioesterase (ACH)	Acetate branch	6	6	16	138160	10195	7	180536	63715	35	**1.31**
Tb927.10.13430	citrate synthase (CS)	TCA cycle	19	18	67	53024	6444	12	549190	81213	15	**10.36**
Tb927.10.14000	aconitase (ACO)	TCA cycle	56	52	230	3535156	537869	15	10865484	321820	3	**3.07**
Tb927.8.3690	**NADPH-dependent isocitrate dehydrogenase, mitochondrial (IDHm)**	TCA cycle	30	27	110	816101	106106	13	1321909	376629	28	**1.62**
Tb11.01.1740	2-oxoglutarate dehydrogenase E1 component, (KDH-E1)	TCA cycle	59	58	234	6790824	129529	2	7725252	228052	3	**1.14**
Tb11.47.0004	2-oxoglutarate dehydrogenase E1 component, (KDH-E1)	TCA cycle	54	52	239	4982382	861761	17	5887617	601185	10	**1.18**
Tb11.01.3550	2-oxoglutarate dehydrogenase E2 component, (KDH-E2)	TCA cycle	23	22	95	4718927	279067	6	5798317	472419	8	**1.23**
Tb927.10.7410	succinyl-CoA ligase [GDP-forming] beta-chain, (SCoAS)	TCA cycle	30	28	138	8518157	2079875	24	8994020	1249670	14	**1.06**
Tb927.3.2230	succinyl-CoA synthetase alpha subunit, (SCoAS)	TCA cycle	23	21	116	12875829	3460856	27	14353602	1573093	11	**1.11**
Tb927.8.6580	succinate dehydrogenase flavoprotein	TCA cycle	37	34	152	2832389	765792	27	4150690	662416	16	**1.47**
Tb09.160.4380	succinate dehydrogenase (SDH)	TCA cycle	10	9	27	663050	362399	55	1164535	332278	29	**1.76**
Tb11.02.2700	fumarate hydratase, class I (FHm)	TCA cycle	32	26	97	1254460	282732	23	1218623	117086	10	**0.97**
Tb927.10.2560	mitochondrial malate dehydrogenase (mMDH)	TCA cycle	19	19	120	17059035	5448863	32	22705275	5389761	24	**1.33**
Tb927.10.2490	**glucose-6-phosphate 1-dehydrogenase (G6PDH)**	Pentose phosphate pathway	10	8	29	77305	24036	31	85204	34728	41	**1.10**
Tb11.02.4200	6-phosphogluconolactonase (6PGL)	Pentose phosphate pathway	7	6	20	149788	58893	39	302976	99596	33	**2.02**
Tb09.211.3180	**6-phosphogluconate dehydrogenase (6PGDH)**	Pentose phosphate pathway	19	19	58	556044	19366	3	602398	44896	7	**1.08**
Tb927.10.12210	ribulose-5-phosphate 3-epimerase	Pentose phosphate pathway	2	2	5	112820	56018	50	115294	38679	34	**1.02**
Tb11.01.0700	ribose 5-phosphate isomerase	Pentose phosphate pathway	10	9	53	2086451	989855	47	2714928	899682	33	**1.30**
Tb927.8.6170	transketolase (TK)	Pentose phosphate pathway	32	32	137	5094773	587400	12	4946858	446366	9	**0.97**
Tb927.8.5600	transaldolase	Pentose phosphate pathway	19	15	62	821374	298274	36	965548	78856	8	**1.18**
Tb11.03.0230	**NADPH-dependent isocitrate dehydrogenase, glycosomal (IDHg)**	NADPH production	35	32	148	1558846	78693	5	5697812	1084299	19	**3.66**
Tb11.02.3130	**malic enzyme, mitochondrial (MEm)**	NADPH production	29	24	109	1456805	108996	7	1680212	50664	3	**1.15**
Tb11.02.3120	**malic enzyme, cytosolic (MEc)**	NADPH production	27	26	120	6788358	176420	3	5658436	910932	16	**0.83**
Tb927.6.4030	superoxide dismutase (SOD)	Response to oxidative stress	1	1	3	46539	22220	48	44809	18715	42	**0.96**
Tb11.01.7480	superoxide dismutase (SOD)	Response to oxidative stress	2	2	8	69203	25071	36	120536	60196	50	**1.74**
Tb11.01.7550	iron superoxide dismutase	Response to oxidative stress	4	1	14	497797	12138	2	480182	18212	4	**0.96**
Tb927.10.10390	trypanothione reductase (TR)	Response to oxidative stress	28	26	87	3719711	1116860	30	3404356	476254	14	**0.92**
Tb927.2.4370	trypanothione synthetase (TRYS)	Response to oxidative stress	32	30	92	930037	106646	11	821591	55676	7	**0.88**
Tb09.160.4250	tryparedoxin peroxidase (TRYP1)	Response to oxidative stress	NOT DETECTED									
Tb927.7.1120	trypanothione/tryparedoxin dependent peroxidase 1 (TDPX1)	Response to oxidative stress	9	0								
Tb927.7.1130	trypanothione/tryparedoxin dependent peroxidase 2 (TDPX2)	Response to oxidative stress	10	1	28	53314	24561	46	85220	49957	59	**1.60**
Tb927.7.1140	trypanothione/tryparedoxin dependent peroxidase 3 (TDPX3)	Response to oxidative stress	NOT DETECTED									
Tb11.01.7560	glutathione peroxidase	Response to oxidative stress	NOT DETECTED									
Tb927.10.12370	gamma-glutamylcysteine synthetase (GCS)	Response to oxidative stress	2	2	5	9023	3165	35	5945	2000	34	**0.66**
Tb927.5.2650	L-galactonolactone oxidase (ascorbate synthesis) (GAL/ALO)	Response to oxidative stress	4	4	10	55478	9770	18	39740	17295	44	**0.72**
Tb927.2.6230	iron/ascorbate oxidoreductase family protein	Response to oxidative stress	NOT DETECTED									
Tb927.2.6310	iron/ascorbate oxidoreductase family protein	Response to oxidative stress	NOT DETECTED									
Tb11.02.5720	ribonucleoside-diphosphate reductase large chain (RNR1)	Response to oxidative stress	15	13	43	184651	45896	25	216564	13657	6	**1.17**
Tb927.7.4000	glutathione synthetase	Trypanothione synthesis	14	13	34	215333	52889	25	302970	47826	16	**1.41**
Tb11.01.5300	ornithine decarboxylase (ODC)	Trypanothione synthesis	4	3	11	13808	5351	39	35813	10323	29	**2.59**
Tb09.v1.0380	spermidine synthase (SpSyn)	Trypanothione synthesis	16	12	65	5907121	1869982	32	6044519	1343291	22	**1.02**
Tb927.7.3500	glutathione-S-transferase/glutaredoxin	Trypanothione synthesis	17	15	51	888946	400254	45	1602776	234255	15	**1.80**
Tb927.10.11590	nicotinate phosphoribosyltransferase, (NaPRT)	NADP synthesis	2	2	5	3436	1190	35	3386	1643	49	**0.99**
Tb927.5.2640	Nicotinamide mononucleotide adenylyltransferase, (NMNAT)	NADP synthesis	3	3	9	24497	10481	43	45807	16321	36	**1.87**
Tb11.01.6500	NAD synthase	NADP synthesis	4	3	11	18952	5370	28	15981	7861	49	**0.84**
Tb927.7.5080	ATP-NAD kinase-like protein	NADP synthesis	NOT DETECTED									

Figure S2. **Label-free proteomics screen for glucose-dependent regulated proteins.** The TriTrypDB ID and name of each protein is indicated in the 1st and 2nd columns. The 3rd column displays the respective pathway The data represent the average of 3 analyses of the same samples (technical replicate). The last column indicates the ratio between glucose-depleted and glucose-rich.

Figure S3

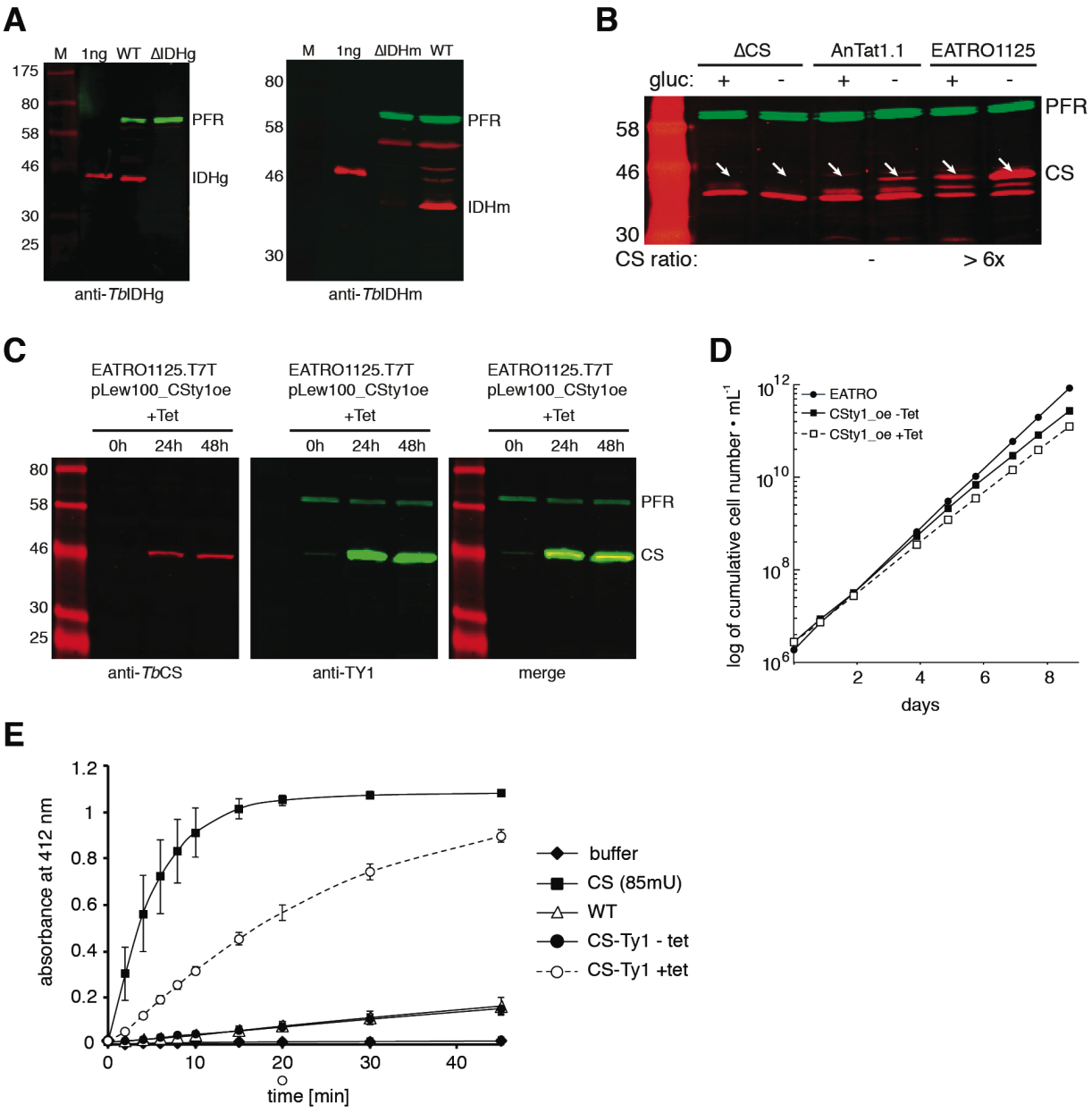

Figure S3. **Verification of IDH antisera and the CS overexpressing cell line.** (A) The specificity of the two IDH antisera was evaluated by western blotting and probing recombinant protein of each IDH isoform as well as WT and KO cell extracts of IDHg (left panel) and IDHm (right panel) respectively. (B) The upregulation of the CS protein (Fig3.3A) was validated by including the CS null mutant.The expression levels of the CS overexpression cell line were controlled by western blotting (C) and the growth observed upon CS induction (D). (E) The CS candidate gene (Tb927.10.13430) was overexpressed and analyzed for CS activity. Here whole cell lysates of the different cell lines were analyzed and compared to a commercial CS.

Figure S4

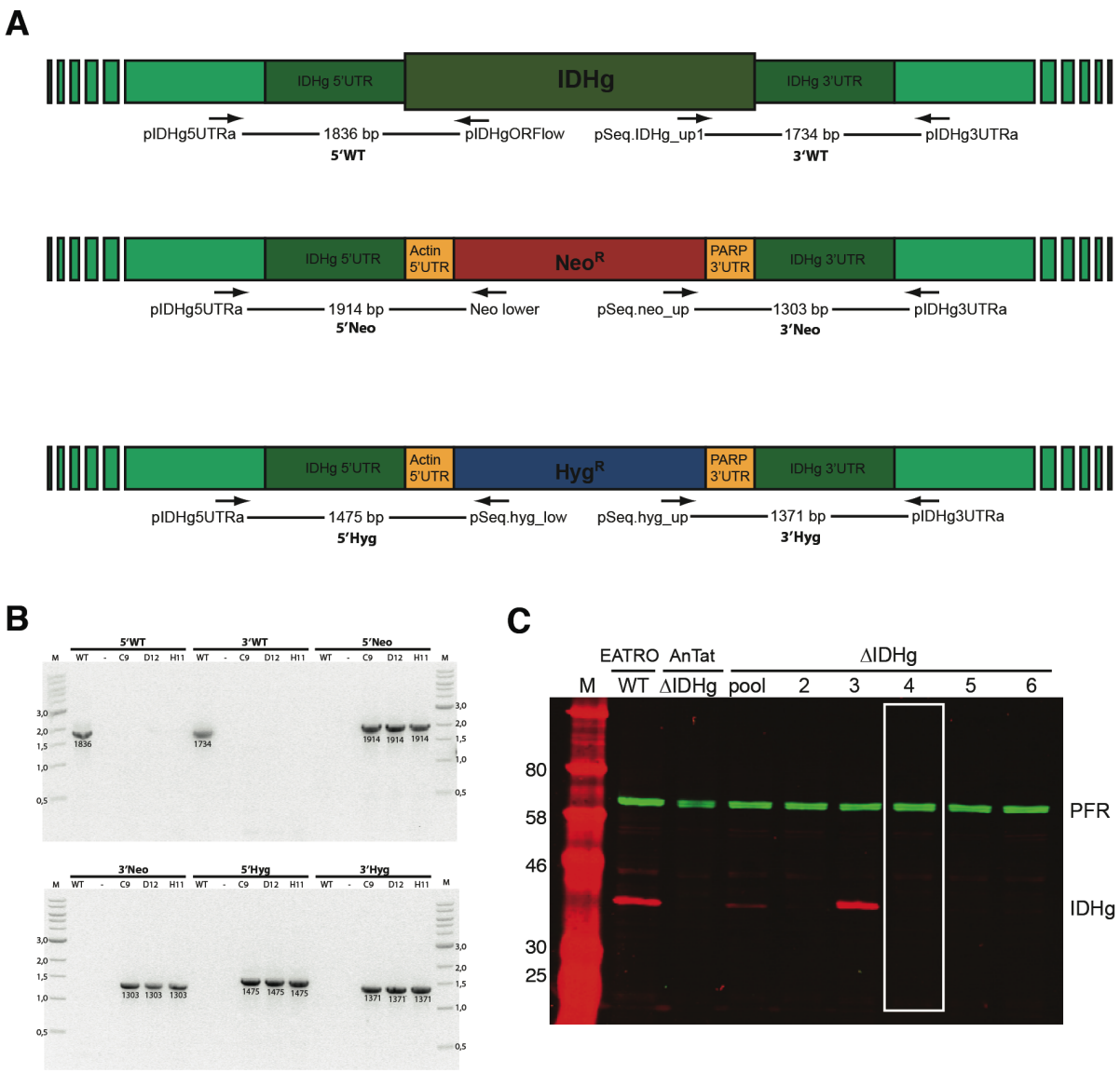

Figure S4. **Verification of the ΔIDHg null mutants.** The null mutant in the Antat 1.1 strain was created and controlled as depicted. (A) Schematic representation of the selection markers replacing the endogenous alleles and the primers used for integration control PCR. (B) Agarose gel of the integration PCR products for three independent clones. The null mutant in the EATRO1125 strain was controlled by western blotting (C) and clone 4 (white frame) was chosen for all further experiments.

Figure S5

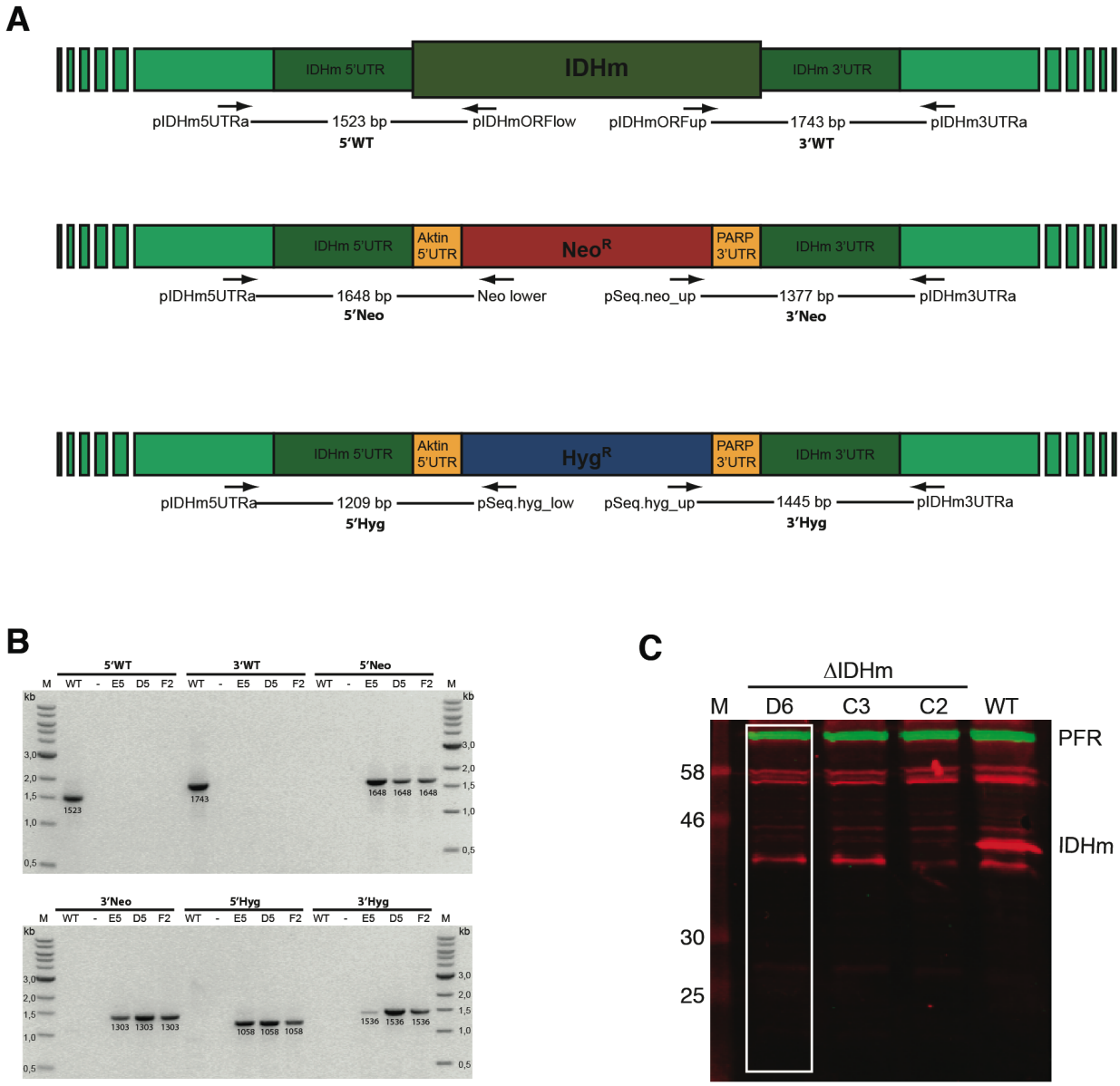

Figure S5. **Verification of the ΔIDHm null mutants.** (A) Schematic representation of the selection markers replacing the endogenous alleles and the primers used for integration control PCR. (B) Agarose gel of the integration PCR products for three independent clones. The null mutant in the EATRO1125 strain was controlled by western blotting (C) and clone D6 (white frame) was chosen for all further experiments

Figure S6

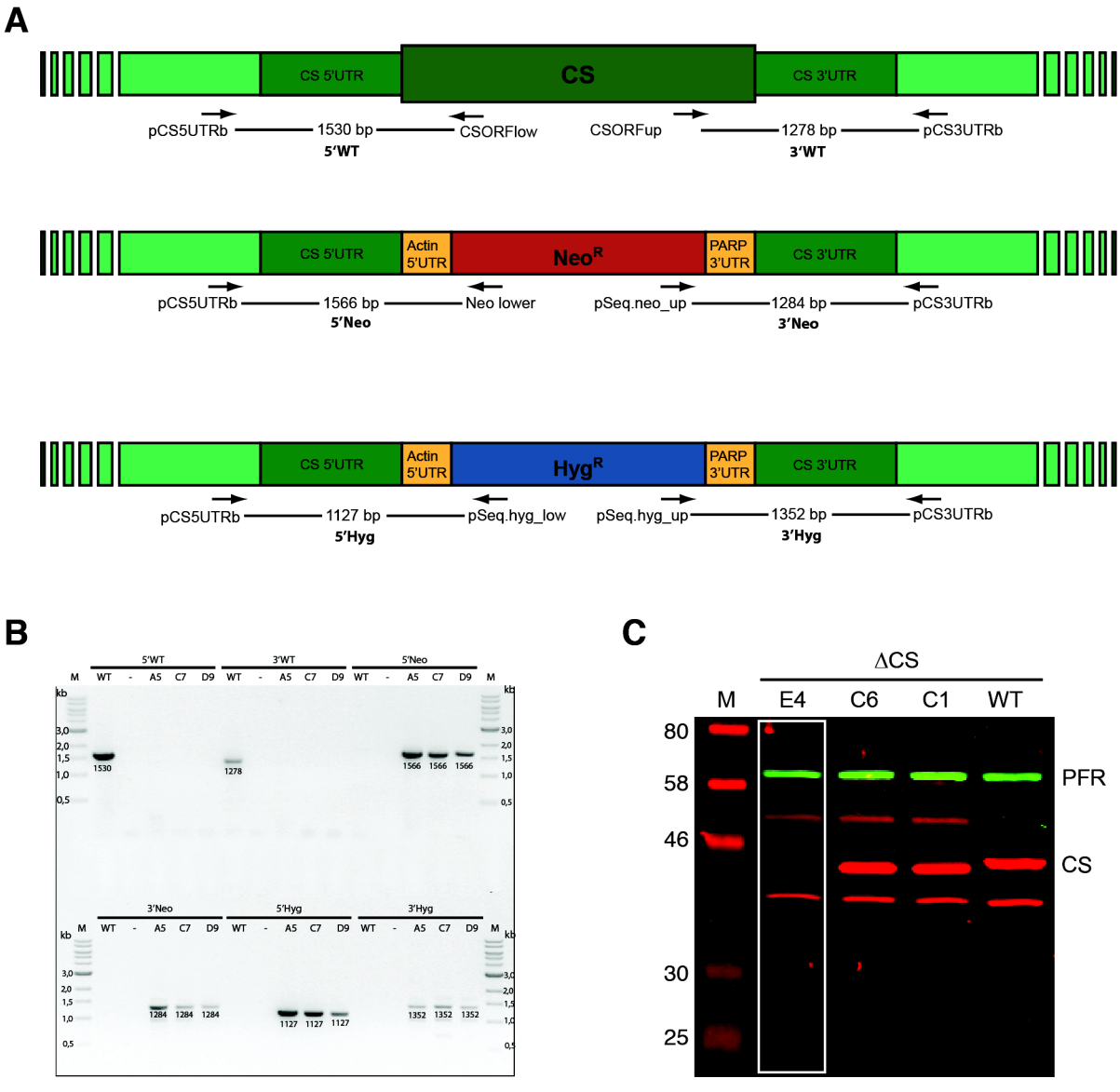

Figure S6. **Verification of the ΔCS null mutants.** (A) Schematic representation of the selection markers replacing the endogenous alleles and the primers used for integration control PCR. (B) Agarose gel of the integration PCR products for three independent clones. The null mutant in the EATRO1125 strain was controlled by western blotting (C) and clone E4 (white frame) was chosen for all further experiments

Figure S7

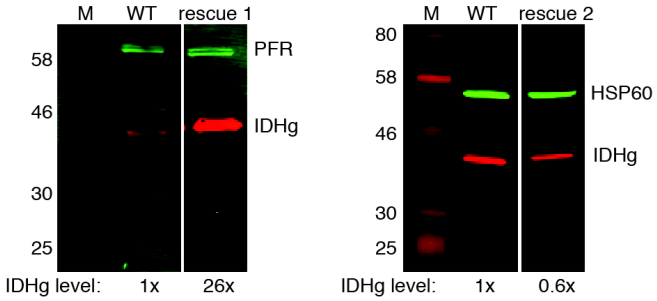

Figure S7. **IDHg Expression levels in the IDHg rescue cell lines.** The ΔIDHg expression level in the two independent rescue cell lines was determined by western blotting and put in relation to the endogenous expression level of the WT.

Supplemental Material – Chapter 4

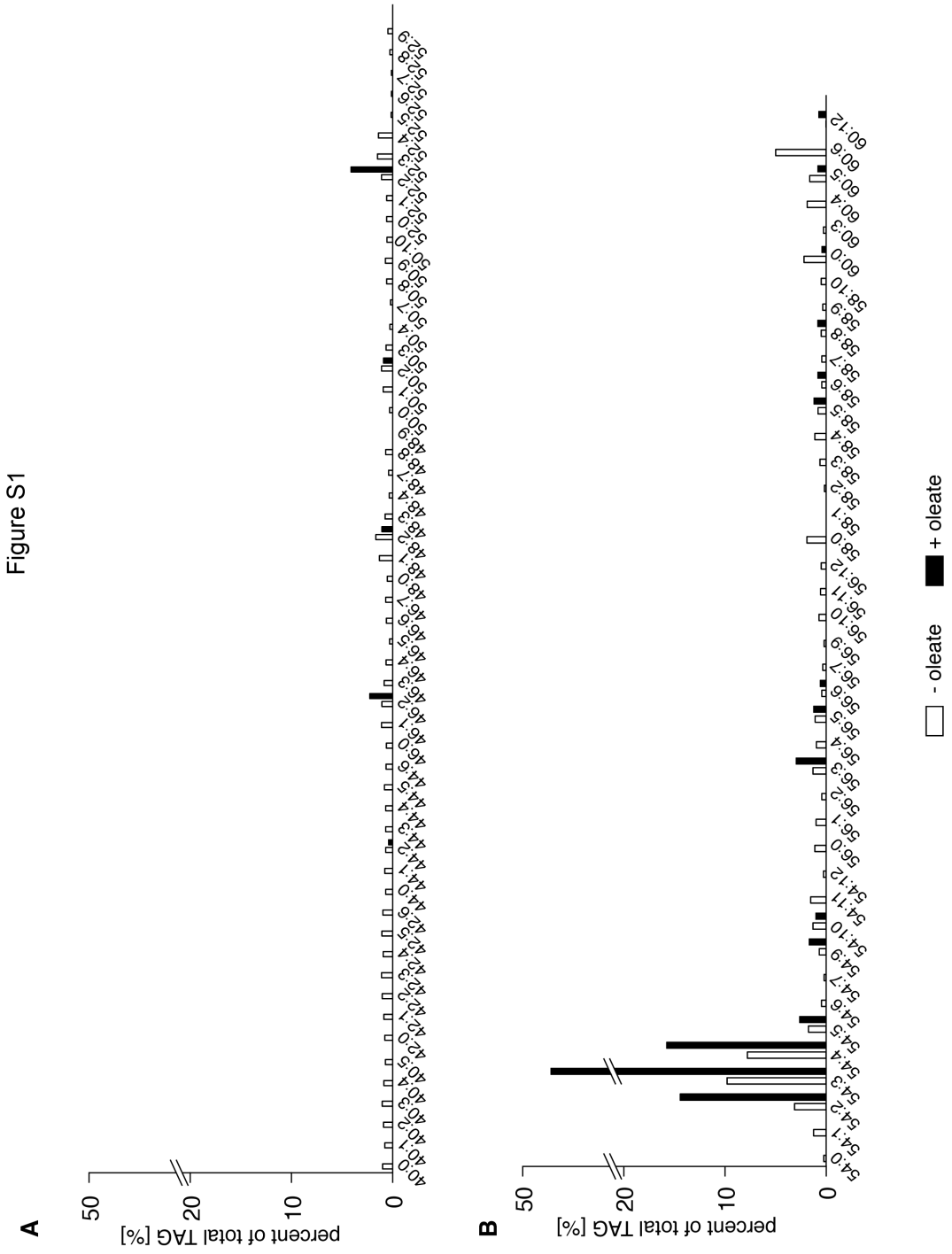

Figure S1. **TAG species identified in procyclic *T. brucei* cells.** Relative abundances of TAG species were determined by ESI/MS/MS after oleate feeding days (black columns) or in the control (white columns). The nomenclature 54:X indicates the total carbon number of all three acyl chains and the sum of all unsaturated double bonds within the acyl chains. Most TAG species are minor contributions to the total TAG content.

Figure S2

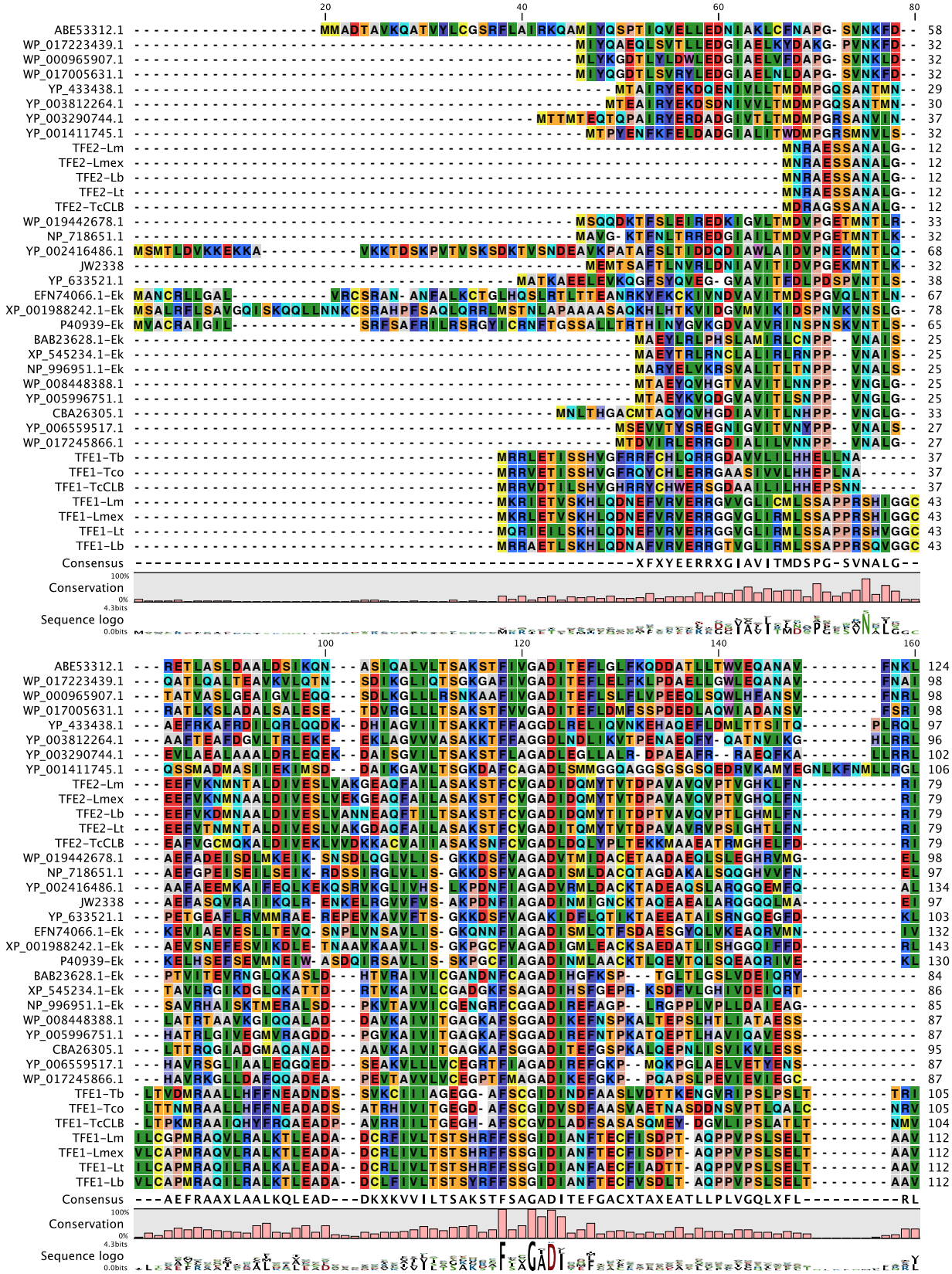
ABE53312.1
WP_017223439.1
WP_000965907.1
WP_017005631.1
YP_433438.1
YP_003812264.1
YP_003290744.1
YP_001411745.1
TFE2-Lm
TFE2-Lmex
TFE2-Lb
TFE2-Lt
TFE2-TcCLB
WP_019442678.1
NP_718651.1
YP_002416486.1
JW2338
YP_633521.1
EFN74066.1-Ek
XP_001988242.1-Ek
P40939-Ek
BAB23628.1-Ek
XP_545234.1-Ek
NP_996951.1-Ek
WP_008448388.1
YP_005996751.1
CBA26305.1
YP_006559517.1
WP_017245866.1
TFE1-Tb
TFE1-Tco
TFE1-TcCLB
TFE1-Lm
TFE1-Lmex
TFE1-Lt
TFE1-Lb
Consensus
Conservation
Sequence logo

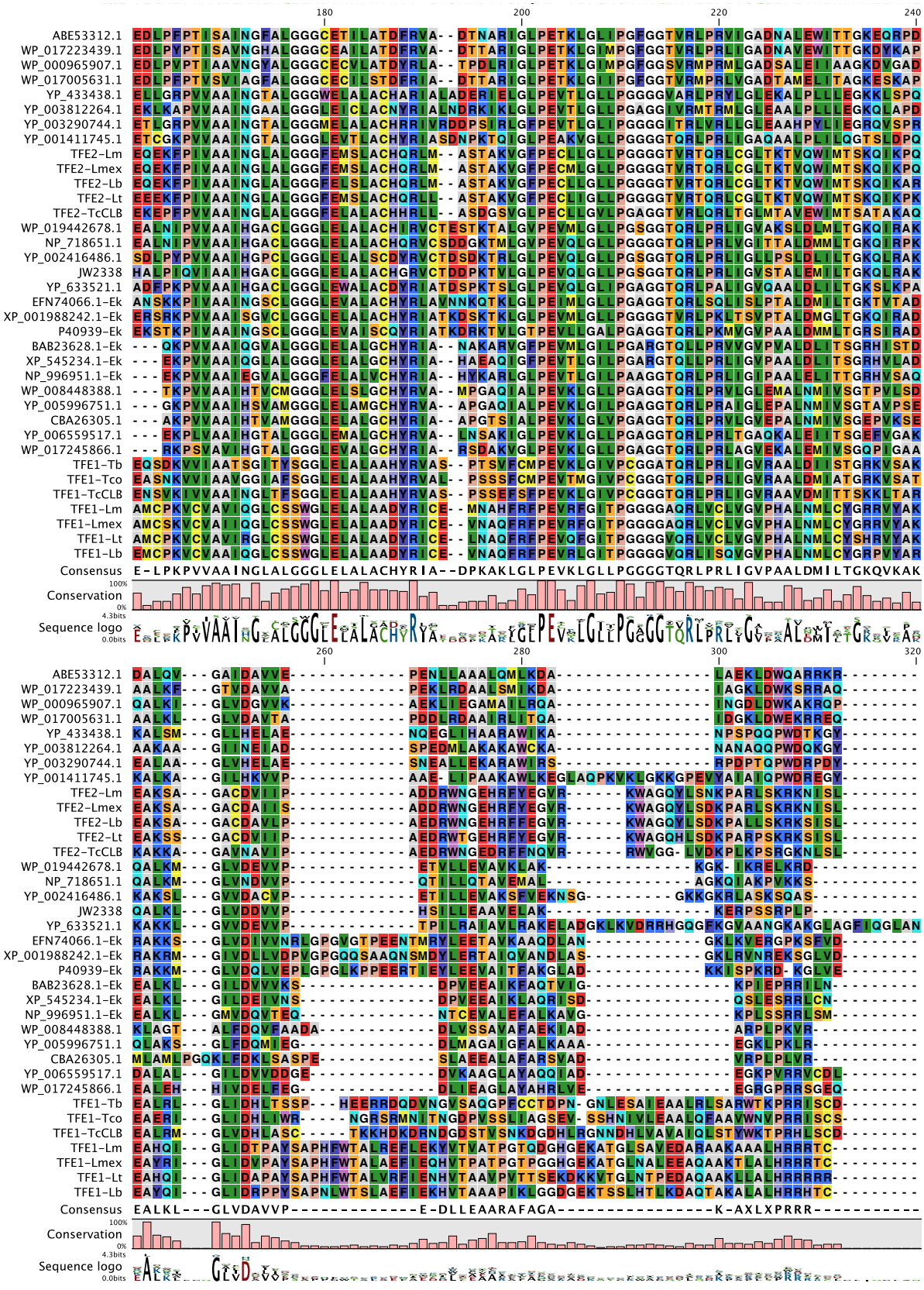
180
200
220
240
ABE53312.1
WP_017223439.1
WP_000965907.1
WP_017005631.1
YP_433438.1
YP_003812264.1
YP_003290744.1
YP_001411745.1
TFE2-Lm
TFE2-Lmex
TFE2-Lb
TFE2-Lt
TFE2-TcCLB
WP_019442678.1
NP_718651.1
YP_002416486.1
JW2338
YP_633521.1
EFN74066.1-Ek
XP_001988242.1-Ek
P40939-Ek
BAB23628.1-Ek
XP_545234.1-Ek
NP_996951.1-Ek
WP_008448388.1
YP_005996751.1
CBA26305.1
YP_006559517.1
WP_017245866.1
TFE1-Tb
TFE1-Tco
TFE1-TcCLB
TFE1-Lm
TFE1-Lmex
TFE1-Lt
TFE1-Lb
Consensus
100%
Conservation
0%
4.3bits
Sequence logo
0.0bits
260
280
300
320
ABE53312.1
WP_017223439.1
WP_000965907.1
WP_017005631.1
YP_433438.1
YP_003812264.1
YP_003290744.1
YP_001411745.1
TFE2-Lm
TFE2-Lmex
TFE2-Lb
TFE2-Lt
TFE2-TcCLB
WP_019442678.1
NP_718651.1
YP_002416486.1
JW2338
YP_633521.1
EFN74066.1-Ek
XP_001988242.1-Ek
P40939-Ek
BAB23628.1-Ek
XP_545234.1-Ek
NP_996951.1-Ek
WP_008448388.1
YP_005996751.1
CBA26305.1
YP_006559517.1
WP_017245866.1
TFE1-Tb
TFE1-Tco
TFE1-TcCLB
TFE1-Lm
TFE1-Lmex
TFE1-Lt
TFE1-Lb
Consensus
100%
Conservation
0%
4.3bits
Sequence logo
0.0bits

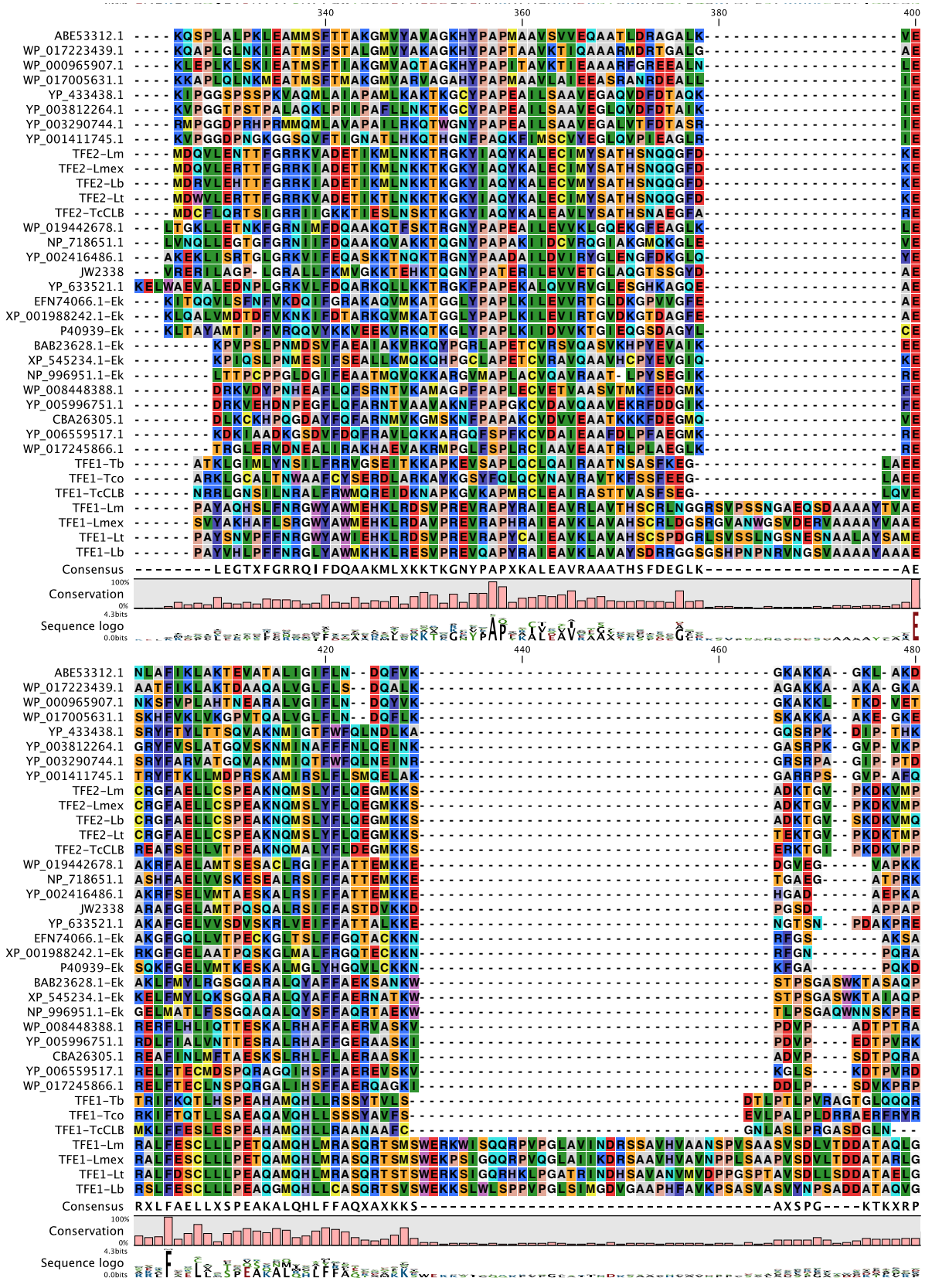
340
360
380
400
ABE53312.1
WP_017223439.1
WP_000965907.1
WP_017005631.1
YP_433438.1
YP_003812264.1
YP_003290744.1
YP_001411745.1
TFE2-Lm
TFE2-Lmex
TFE2-Lb
TFE2-Lt
TFE2-TcCLB
WP_019442678.1
NP_718651.1
YP_002416486.1
JW2338
YP_633521.1
EFN74066.1-Ek
XP_001988242.1-Ek
P40939-Ek
BAB23628.1-Ek
XP_545234.1-Ek
NP_996951.1-Ek
WP_008448388.1
YP_005996751.1
CBA26305.1
YP_006559517.1
WP_017245866.1
TFE1-Tb
TFE1-Tco
TFE1-TcCLB
TFE1-Lm
TFE1-Lmex
TFE1-Lt
TFE1-Lb
Consensus
Conservation
Sequence logo
420
440
460
480
ABE53312.1
WP_017223439.1
WP_000965907.1
WP_017005631.1
YP_433438.1
YP_003812264.1
YP_003290744.1
YP_001411745.1
TFE2-Lm
TFE2-Lmex
TFE2-Lb
TFE2-Lt
TFE2-TcCLB
WP_019442678.1
NP_718651.1
YP_002416486.1
JW2338
YP_633521.1
EFN74066.1-Ek
XP_001988242.1-Ek
P40939-Ek
BAB23628.1-Ek
XP_545234.1-Ek
NP_996951.1-Ek
WP_008448388.1
YP_005996751.1
CBA26305.1
YP_006559517.1
WP_017245866.1
TFE1-Tb
TFE1-Tco
TFE1-TcCLB
TFE1-Lm
TFE1-Lmex
TFE1-Lt
TFE1-Lb
Consensus
Conservation
Sequence logo

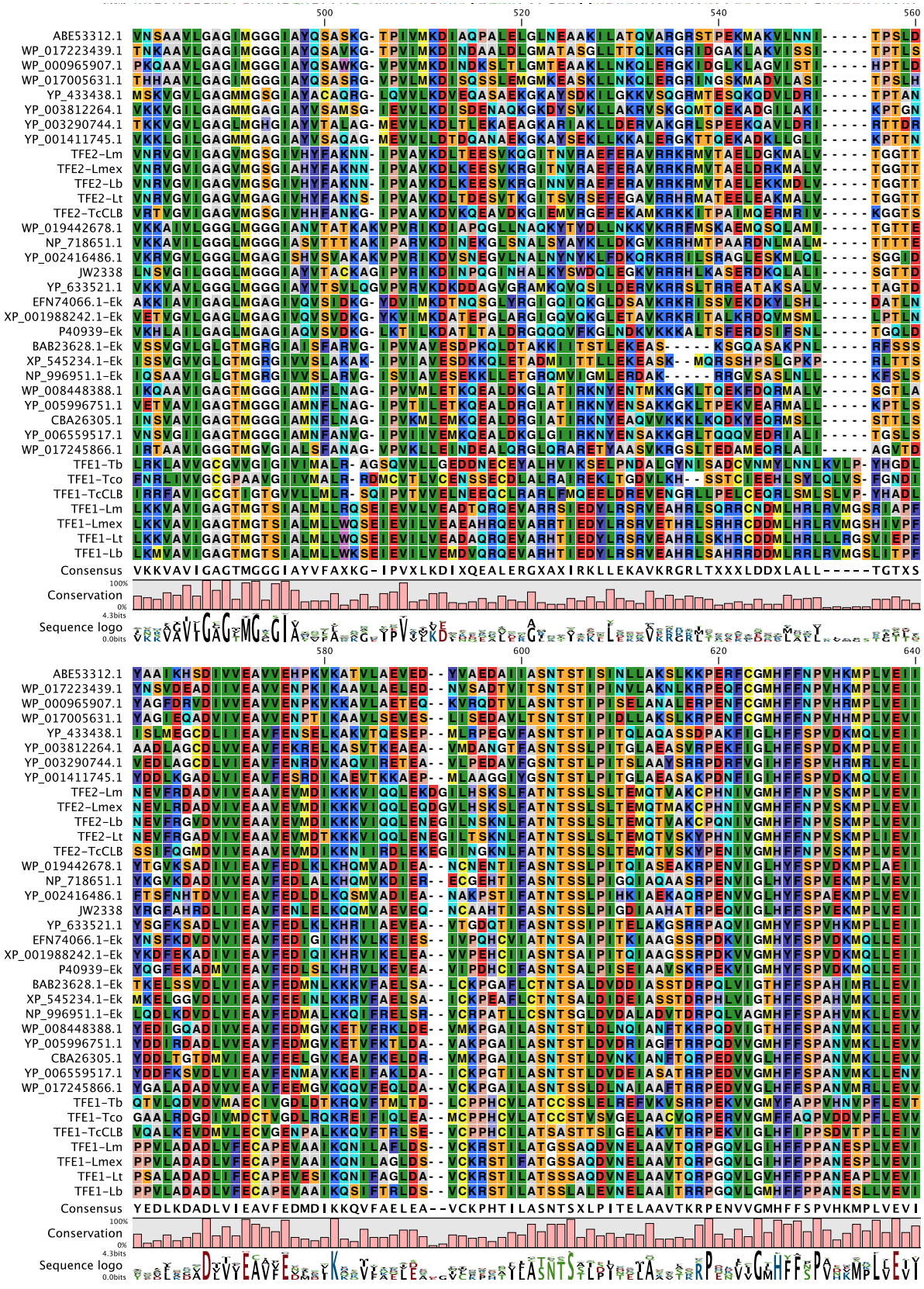
500
520
540
560
ABE53312.1 VNSAAVLGAGIMGGGIAYQSASKG-TPIVMKDIAQPALELGLNEAAKILATQVARGRSTPEKMAKVLNNI-----TPSLD 412
WP_017223439.1 TNKAAVLGAGIMGGGIAYQSAVKG-TPVIMKDINDAALDLGMATASGLLTTQLKRGRIDGAKLAKVISSI-----TPTLS 386
WP_000965907.1 PKQAAVLGAGIMGGGIAYQSAWKG-VPVVMKDINDKSLTLGMTEAAKLLNKQLERGKIDGLKLAGVISTI-----HPTLD 386
WP_017005631.1 THHAAVLGAGIMGGGIAYQSASRG-VPVLMKDISQSSSLEMGMKEASKLLNKQLERGRINGSKMADVLASI-----TPSLH 386
YP_433438.1 MSKVGVLGAGMMGSGIAYACAQRG-LQVVLKDVEQASAEKGKAYSDKILGKKVSQGRMTESQKQDVLDRI-----TPTAN 389
YP_003812264.1 VKKVGILGAGMMGAGIAYVSAMSG-IEVVLKDISDENAQKGKDYSVKLLAKRVSKGQMTQEKADGILAKI-----KPTGN 388
YP_003290744.1 TKKVGVLGAGLMGHGIAYVTALAG-MEVVLKDLTLEKAEAGKARIAKLLDERVAKGRLSPEEKQAVLDRI-----RTTDR 394
YP_001411745.1 VKKLGILGAGMMGAGIAYVSAQAG-MEVVLLDTDQANAEKGKAYSEKLLKKALERGKTTQEKADKLLGLI-----KPTTN 413
TFE2-Lm VNRVGVIGAGVMGSGIVHYFAKNN-IPVAVKDLTEESVKQGITNVRAEFERAVRRKRMVTAELDGKMALV-----TGGTT 380
TFE2-Lmex VNRVGVIGAGVMGSGIAHYFAKNN-IPVAVKDLKEESVKRGITNVRAEFERAVRRKRMVTAELDRKMALV-----TGGTT 380
TFE2-Lb VNRVGVIGAGVMGSGIVHYFAKNN-IPVAVKDLKEESVKRGINNVRAEFERAVRRKRMVTAELEKKMDLV-----TGGTT 380
TFE2-Lt VNRVGVIGAGVMGAGIVHYFAKNS-IPVAVKDLTDESVTKGITSVRSEFEGAVRRHRMATEELEAKMALV-----TGGTT 380
TFE2-TcCLB VRTVGVIGAGVMGSGIVHHFANKG-IPVAVKDVKQEAVDKGIEMVRGEFEKAMKRKKITPAIMQERMRIV-----KGGTS 379
WP_019442678.1 VKKAIVLGGGLMGGGIANVTATKAKVPVRIKDIAPQGLLNAQKYTYDLLNKKVKRRFMSKAEMQSQLAMI-----TGTTE 386
NP_718651.1 VKKAVILGGGLMGGGIASVTTTKAKIPARVKDINEKGLSNALSYAYKLLDKGVKRRHMTPAARDNLMALM-----TTTTE 386
YP_002416486.1 VKRVGVLGGGLMGAGISHVSVAKAKVPVRIKDVSNEGVLNALNYNYKLLFDKQRKRRILSRAGLESKMLQL-----SGGID 428
JW2338 LNSVGILGGGLMGGGIAYVTACKAGIPVRIKDINPQGINHALKYSWDQLEGKVRRRHLKASERDKQLALI-----SGTTD 382
YP_633521.1 VKKVAVLGGGLMGGGIAYVTSVLQGVPVRVKDKDDAGVGRAMKQVQSILDERVKRRSLTRREATAKSALV-----TAGTD 423
EFN74066.1-Ek AKKIAVIGAGLMGAGIVQVSVDKG-YDVIMKDTNQSGLYRGIGQIQKGLDSAVKRKRISSVEKDKYLSHL-----DATLN 437
XP_001988242.1-Ek VETVGVLGAGLMGAGIVQVSVDKG-YKVIMKDATEPGLARGIGQVQKGLETAVKRKRITALKRDQVMSML-----LPTLN 448
P40939-Ek VKHLAILGAGLMGAGIAQVSVDKG-LKTILKDATLTALDRGQQQVFKGLNDKVKKKALTSFERDSIFSNL-----TGQLD 434
BAB23628.1-Ek VSSVGVLGLGTMGRGIAISFARVG-IPVVAVESDPKQLDTAKKIITSTLEKEAS-----KSGQASAKPNL-----RFSSS 363
XP_545234.1-Ek ISSVGVVGLGTMGRGIVVSLAKAK-IPVIAVESDKKQLETADMIITTLLEKEASK--MQRSSHPSLGPKP-----RLTTS 368
NP_996951.1-Ek IQSAAVIGLGTMGRGIVVSLARVG-ISVIAVESEKKLLETGRQMVIGMLERDAK-----RRGVSASLNLL-----KFSLS 363
WP_008448388.1 IKQAAVIGAGTMGGGIAMNFLNAG-IPVVMLETKQEALDKGLATIRKNYENTMKKGKLTQEKFDQRMALV-----SGTLA 367
YP_005996751.1 VETVAVIGAGTMGGGIAMNFLNAG-IPVTILETKQEALDRGIATIRKNYENSAKKGKLTPEKVEARMALL-----KPTLS 365
CBA26305.1 INSVAVIGAGTMGGGIAMNFLNAG-IPVKMLEMKQEALDRGIATIRKNYEAQVVKKKLKQDKYEQRMSLL-----STTLS 378
YP_006559517.1 VNSVGIIGAGTMGGGIAMNFANVG-IPVIIVEMKQEALDKGLGIIRKNYENSAKKGRLTQQQVEDRIALI-----TGSLS 369
WP_017245866.1 IRTAAVIGGGTMGVGIALSFANAG-VPVKLLEINDEALQRGLQRARETYAASVKRGSLTEDAMEQRLALI-----AGVTD 368
TFE1-Tb LRKLAVVGCGVVGIGIVTMALR-AGSQVVLLGEDDNECEEYALHVIKSELPNDALGYNISADCVNMYLNNLKVLP-YHGDL 427
TFE1-Tco FNRLIVVGCGPAAVGIIVMALR-RDMCVTLVCENSSECDLALRAIREKLTGDVLKH--SSTCIEEHLSYLQLVS-FGNDI 423
TFE1-TcCLB IRRFAVIGCGTIGTGVVLLMLR-SQIPVTVVELNEEQCLRARLFMQEELDREVENGRLLPELCEQRLSMLSLVP-YHADL 422
TFE1-Lm LKKVAVIGAGTMGTSIALMLLRQSEIEVVLVEADTQRQEVARRSIEDYLRSRVEAHRLSQRRCNDMLHRLRVMGSRIAPF 492
TFE1-Lmex LKKVAVIGAGTMGTSIALMLLWQSEIEVILVEAEAHRQEVARRTIEDYLRSRVETHRLSRHRCDDMLHRLRVMGSHIVPF 492
TFE1-Lt LKKVAVIGAGTMGTSIALMLLWQSEIEVILVEADAQRQEVARHTIEDYLRSRVEAHRLSKHRCDDMLHRLLLRGSVIEPF 492
TFE1-Lb LKMVAVIGAGTMGTSIALMLLWKSEIEVILVEMDVQRQEVARHTIEDYLRSRVEAHRLSAHRRDDMLRRLRVMGSLITPF 492
Consensus VKKVAVIGAGTMGGGIAYVFAXKG-IPVXLKDIXQEALERGXAXIRKLLEKAVKRGRLTXXXLDDXLALL-----TGTXS
100%
Conservation
0%
4.3bits
Sequence logo
0.0bits
580
600
620
640
ABE53312.1 YAAIKHSDIVVEAVVEHPKVKATVLAEVED--YVAEDAIIASNTSTISINLLAKSLKKPERFCGMHFFNPVHKMPLVEII 490
WP_017223439.1 YNSVDEADIIVEAVVENPKIKAAVLAELED--NVSADTVITSNTSTIPINVLAKNLKRPEQFCGMHFFNPVHKMPLVEII 464
WP_000965907.1 YAGFDRVDIVVEAVVENPKVKKAVLAETEQ--KVRQDTVLASNTSTIPISELANALERPENFCGMHFFNPVHRMPLVEII 464
WP_017005631.1 YAGIEQADVIVEAVVENPTIKAAVLSEVES--LISEDAVLTSNTSTIPIDLLAKSLKRPENFCGMHFFNPVHHMPLVEVI 464
YP_433438.1 ISLMEGCDLIIEAVFENSELKAKVTQESEP--MLRPEGVFASNTSTIPITQLAQASSDPAKFIGLHFFSPVDKMQLVEII 467
YP_003812264.1 AADLAGCDLVVEAVFEKRELKASVTKEAEA--VMDANGTFASNTSSLPITGLAEASVRPEKFIGLHFFSPVDKMPLVEII 466
YP_003290744.1 VEDLAGCDLVIEAVFENRDVKAQVIRETEA--VLPEDAVFGSNTSTLPITSLAAYSRRPDRFVGIHFFSPVHRMRLVELI 472
YP_001411745.1 YDDLKGADLVIEAVFESRDIKAEVTKKAEP--MLAAGGIYGSNTSTLPITGLAEASAKPDNFIGIHFFSPVDKMQLVEII 491
TFE2-Lm NEVFRDADVIVEAAVEVMDIKKKVIQQLEKDG-ILHSKSLFATNTSSLSLTEMQTVAKCPHNIVGMHFFNPVSKMPLVEVI 460
TFE2-Lmex NEVLRDADVIVEAAVEVMDIKKKVIQQLEQDG-VLHSKSLFATNTSSLSLTEMQTMAKCPHNIVGMHFFNPVSKMPLVEVI 460
TFE2-Lb NEVFRGVDVVVEAAVEVMDIKKKVIQQLENEG-ILNSKNLFATNTSSLSLTEMQTVAKCPQNIVGMHFFNPVSKMPLVEVI 460
TFE2-Lt NEVFRGADVIVEAAVEVMDTKKKVIQQLENEG-ILTSKNLFATNTSSLSLTEMQTVSKYPHNIVGMHFFNPVSKMPLIEVI 460
TFE2-TcCLB SSIFQGMDVIVEAAVEVMDIKKNIIRDLEKEG-IINGKNLFATNTSSLSLTEMQTVSKYPENIVGMHFFNPVSKMPLVEVI 459
WP_019442678.1 YTGVKSADIVIEAVFEDLKLKHQMVADIEA--NCNENTIFASNTSSLPITQIASEAKRPENVIGLHYFSPVDKMPLAEII 464
NP_718651.1 YKGVKDADIVVEAVFEDLALKHQMVKDIER--ECGEHTIFASNTSSLPIGQIAQAASRPENVIGLHYFSPVEKMPLVEVI 464
YP_002416486.1 FTSFNHTDVVIEAVFEDLDLKQSMVADIEA--NAKPSTIFATNTSSLPIHKIAEKAQRPENVVGLHYFSPAEKMPLVEVI 506
JW2338 YRGFAHRDLIIEAVFENLELKQQMVAEVEQ--NCAAHTIFASNTSSLPIGDIAAHATRPEQVIGLHFFSPVEKMPLVEII 460
YP_633521.1 YSGFKSADLVIEAVFEDLKLKHRIIAEVEA--VTGDQTIFASNTSSIPITELAKGSRRPAQVIGMHYFSPVHKMPLLEII 501
EFN74066.1-Ek YNSFKDVDVVIEAVFEDIGIKHKVLKEIES--IVPQHCVIATNTSAIPITKIAAGSSRPDKVIGMHYFSPVDKMQLLEII 515
XP_001988242.1-Ek YKDFEKADIVIEAVFEDIQIKHRVIKELEA--VVPEHCIIASNTSAIPITQIAAGSSRPDKVVGMHYFSPVDKMQLLEII 526
P40939-Ek YQGFEKADMVIEAVFEDLSLKHRVLKEVEA--VIPDHCIFASNTSALPISEIAAVSKRPEKVIGMHYFSPVDKMQLLEII 512
BAB23628.1-Ek TKELSSVDLVIEAVFEDMNLKKKVFAELSA--LCKPGAFLCTNTSALDVDDIAASSTDRPQLVIGTHFFSPAHIMRLLEVI 441
XP_545234.1-Ek MKELGGVDLVIEAVFEEINLKKRVFAELSA--ICKPEAFLCTNTSALDIDEIAASSTDRPHLVIGTHFFSPAHVMKLLEII 446
NP_996951.1-Ek LQDLKDVDLVIEAVFEDMALKKQIFRELSR--VCRPATLLCSNTSGLDVDALADVTDRPQLVAGMHFFSPAHVMKLLEVV 441
WP_008448388.1 YEDIGQADIVVEAVFEDMGVKETVFRKLDE--VMKPGAILASNTSTLDLNQIANFTKRPQDVIGLHFFSPANVMKLLEIV 445
YP_005996751.1 YDDIRDADLVVEAVFEDMGVKETVFKTLDA--VAKPGAILASNTSTLDVDRIAGFTRRPQDVVGMHFFSPANVMKLLEVV 443
CBA26305.1 YDDLTGTDMVIEAVFEELGVKEAVFKELDR--VMKPGAILASNTSTLDVNKIANFTQRPEDVVGLHFFSPANVMKLLEVV 456
YP_006559517.1 YDDFKSVDLVIEAVFENMAVKKEIFAKLDA--ICKPGTILASNTSTLDVDEIASATRRPEDVVGMHFFSPANVMKLLENV 447
WP_017245866.1 YGALADADVVVEAVFEEMGVKQQVFEQLDA--VCKPGAILASNTSSLDLNAIAAFTRRPEDVVGLHFFSPANVMRLLEVV 446
TFE1-Tb QTVLQDVDVMAECIVGDLDTKRQVFTMLTD--LCPPHCVLATCCSSLELREFVKVSRRPEKVVGMYFAPPVHNVPFLEVT 505
TFE1-Tco GAALRDGDIVMDCTVGDLRQKREIFIQLEA--MCPPHCVLATCCSTVSVGELAACVQRPERVVGMFFAQPVDDVPFLEVV 501
TFE1-TcCLB VQALKEVDMVLECVGENPALKKQVFTRLSE--VCPPHCILATSASTTSIGELAKVTRRPEKVIGLHFIPPSDVTPLLEIV 500
TFE1-Lm PPVLADADLVFECAPEVAAIKQNILAFLDS--VCKRSTILATGSSAQDVNELAAVTQRPGQVLGIHFFPPANESPLVEVI 570
TFE1-Lmex PPVLADADLVFECAPEVAAIKQNILAGLDS--VCKRSTIFATGSSAQDVNELAAVTQRPGQVLGIHFFPPANESPLVEVI 570
TFE1-Lt PSALADADLIFECAPEVESIKQNIFAGLDA--VCKRSTILATSSSAQDVNELAAVTQRPGQVLGVHFFPPANEAPLVEVI 570
TFE1-Lb PPVLADADLVFECAPEVAAIKQSIFTRLDS--VCKRSTILATSSLALEVNELAAITRRPGQVLGMHFFPPANESLLVEVI 570
Consensus YEDLKDADLVIEAVFEDMDIKKQVFAELEA--VCKPHTILASNTSXLPITELAAVTKRPENVVGMHFFSPVHKMPLVEVI
100%
Conservation
0%
4.3bits
Sequence logo
0.0bits

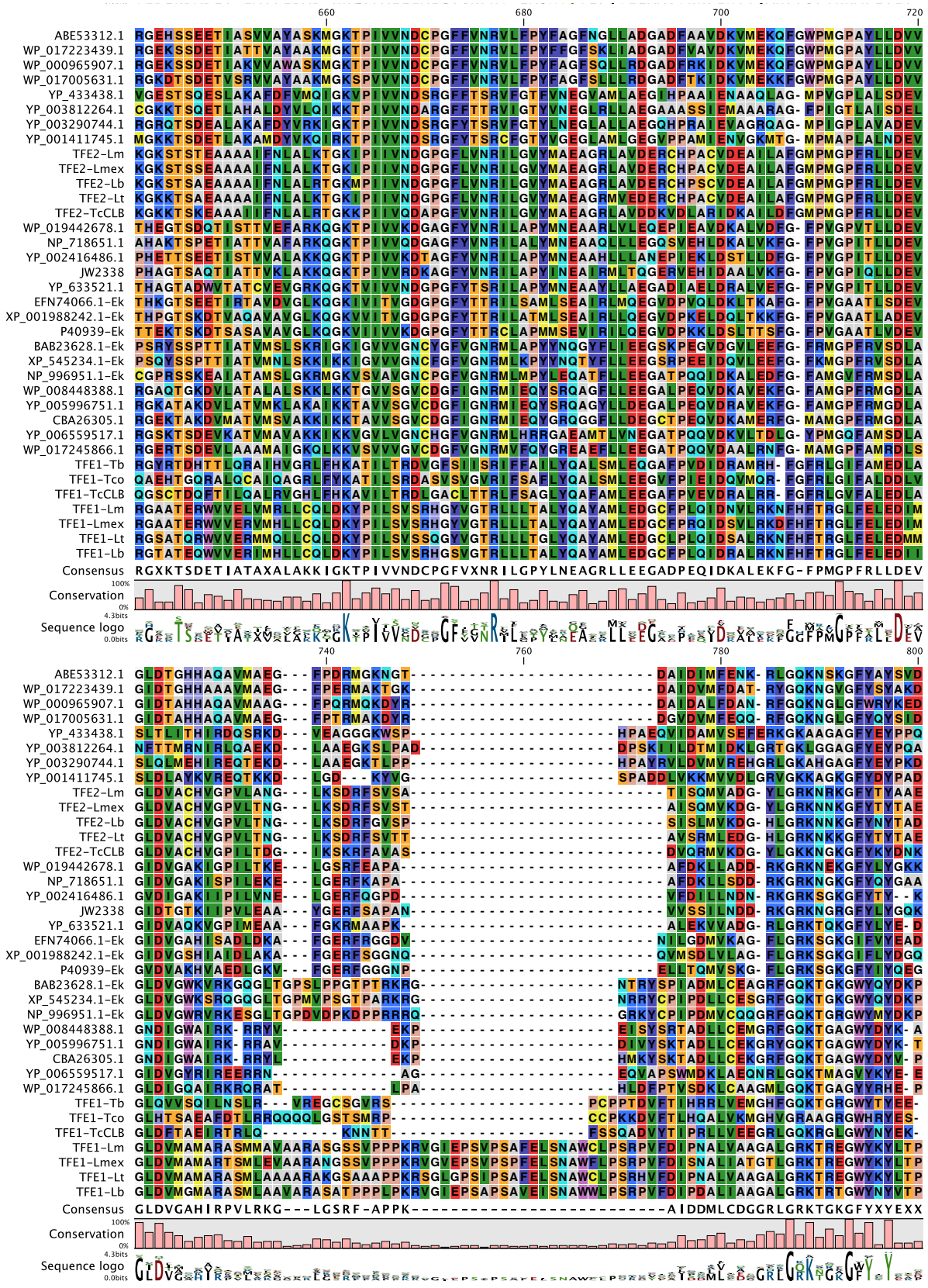
660
680
700
720
ABE53312.1 570
WP_017223439.1 544
WP_000965907.1 544
WP_017005631.1 544
YP_433438.1 546
YP_003812264.1 545
YP_003290744.1 551
YP_001411745.1 570
TFE2-Lm 540
TFE2-Lmex 540
TFE2-Lb 540
TFE2-Lt 540
TFE2-TcCLB 539
WP_019442678.1 543
NP_718651.1 543
YP_002416486.1 585
JW2338 539
YP_633521.1 580
EFN74066.1-Ek 594
XP_001988242.1-Ek 605
P40939-Ek 591
BAB23628.1-Ek 520
XP_545234.1-Ek 525
NP_996951.1-Ek 520
WP_008448388.1 524
YP_005996751.1 522
CBA26305.1 535
YP_006559517.1 526
WP_017245866.1 525
TFE1-Tb 584
TFE1-Tco 580
TFE1-TcCLB 579
TFE1-Lm 650
TFE1-Lmex 650
TFE1-Lt 650
TFE1-Lb 650
Consensus
Conservation
Sequence logo
740
760
780
800
ABE53312.1 621
WP_017223439.1 595
WP_000965907.1 595
WP_017005631.1 595
YP_433438.1 602
YP_003812264.1 602
YP_003290744.1 607
YP_001411745.1 623
TFE2-Lm 590
TFE2-Lmex 590
TFE2-Lb 590
TFE2-Lt 590
TFE2-TcCLB 589
WP_019442678.1 592
NP_718651.1 592
YP_002416486.1 632
JW2338 589
YP_633521.1 628
EFN74066.1-Ek 645
XP_001988242.1-Ek 656
P40939-Ek 642
BAB23628.1-Ek 580
XP_545234.1-Ek 585
NP_996951.1-Ek 580
WP_008448388.1 571
YP_005996751.1 569
CBA26305.1 582
YP_006559517.1 572
WP_017245866.1 573
TFE1-Tb 640
TFE1-Tco 639
TFE1-TcCLB 630
TFE1-Lm 730
TFE1-Lmex 730
TFE1-Lt 730
TFE1-Lb 730
Consensus
Conservation
Sequence logo

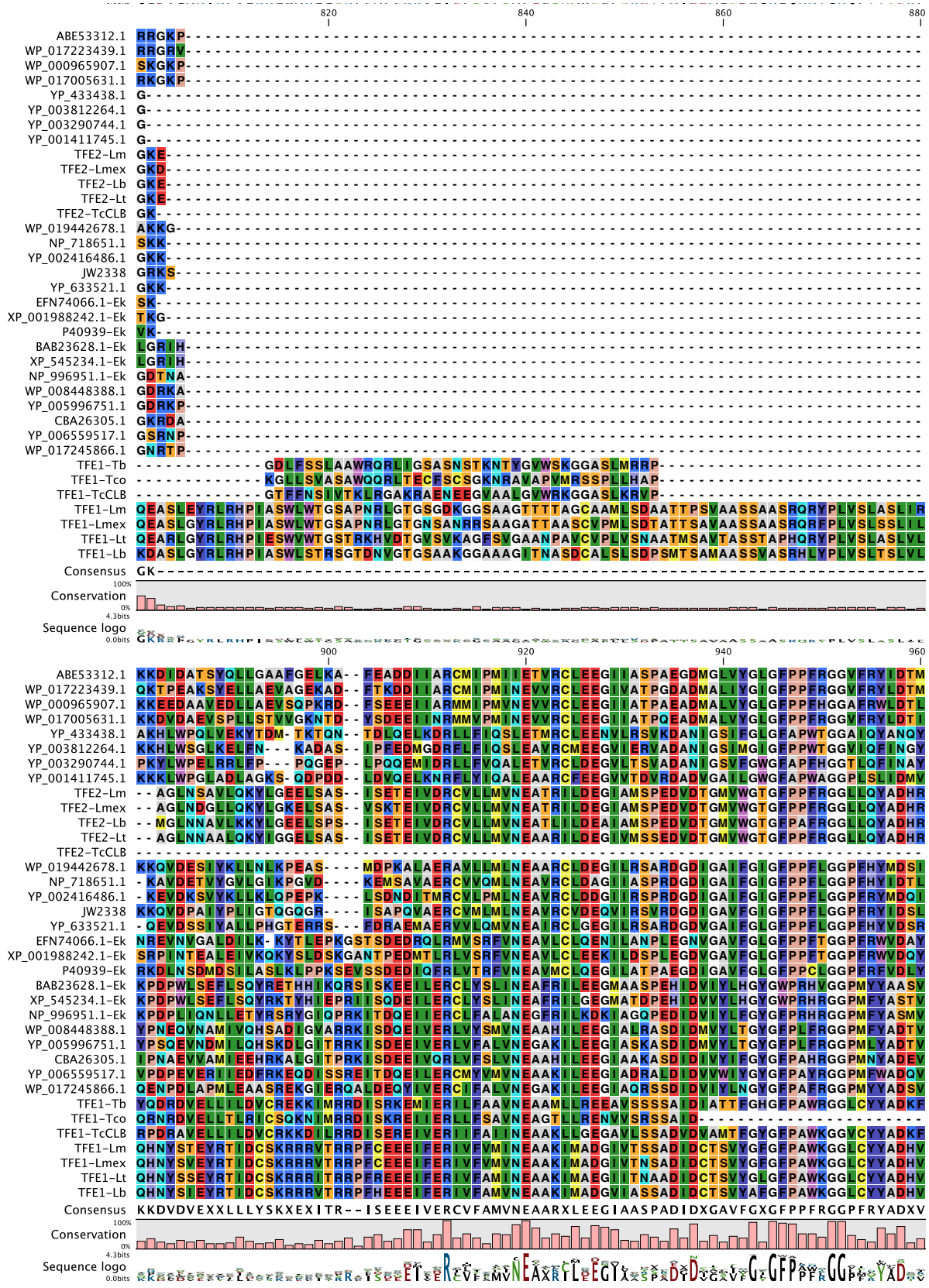
820
840
860
880
ABE53312.1 626
WP_017223439.1 600
WP_000965907.1 600
WP_017005631.1 600
YP_433438.1 603
YP_003812264.1 603
YP_003290744.1 608
YP_001411745.1 624
TFE2-Lm 593
TFE2-Lmex 593
TFE2-Lb 593
TFE2-Lt 593
TFE2-TcCLB 591
WP_019442678.1 596
NP_718651.1 595
YP_002416486.1 635
JW2338 593
YP_633521.1 631
EFN74066.1-Ek 647
XP_001988242.1-Ek 659
P40939-Ek 644
BAB23628.1-Ek 585
XP_545234.1-Ek 590
NP_996951.1-Ek 585
WP_008448388.1 576
YP_005996751.1 574
CBA26305.1 587
YP_006559517.1 577
WP_017245866.1 578
TFE1-Tb 680
TFE1-Tco 679
TFE1-TcCLB 670
TFE1-Lm 810
TFE1-Lmex 810
TFE1-Lt 810
TFE1-Lb 810
Consensus
100%
Conservation
0%
4.3bits
Sequence logo
0.0bits
900
920
940
960
ABE53312.1 704
WP_017223439.1 678
WP_000965907.1 678
WP_017005631.1 678
YP_433438.1 680
YP_003812264.1 678
YP_003290744.1 683
YP_001411745.1 701
TFE2-Lm 669
TFE2-Lmex 669
TFE2-Lb 669
TFE2-Lt 669
TFE2-TcCLB 591
WP_019442678.1 672
NP_718651.1 670
YP_002416486.1 710
JW2338 669
YP_633521.1 707
EFN74066.1-Ek 726
XP_001988242.1-Ek 739
P40939-Ek 724
BAB23628.1-Ek 665
XP_545234.1-Ek 670
NP_996951.1-Ek 665
WP_008448388.1 656
YP_005996751.1 654
CBA26305.1 667
YP_006559517.1 657
WP_017245866.1 658
TFE1-Tb 760
TFE1-Tco 736
TFE1-TcCLB 750
TFE1-Lm 890
TFE1-Lmex 890
TFE1-Lt 890
TFE1-Lb 890
Consensus
100%
Conservation
0%
4.3bits
Sequence logo
0.0bits

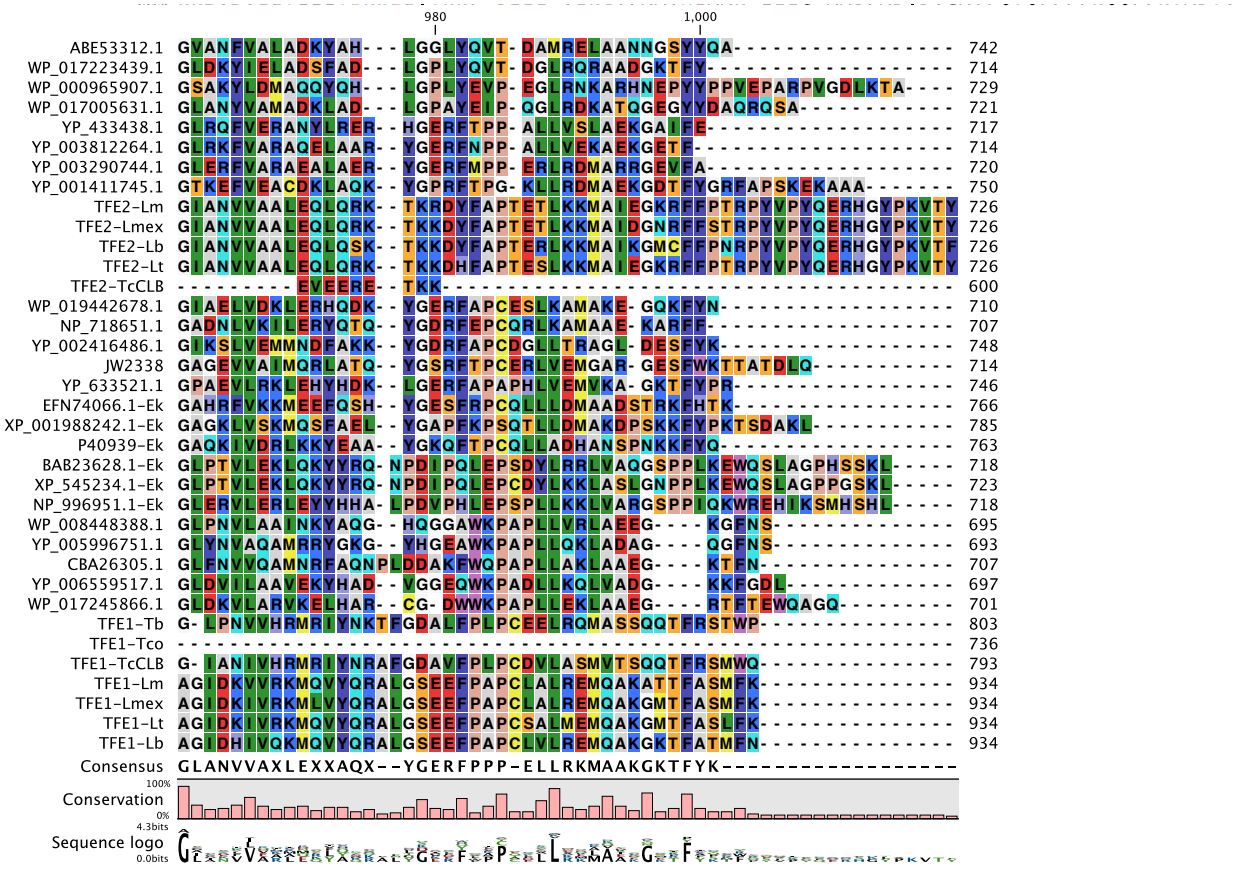

Figure S2. **Alignment of TFEα1 and TFEα2 protein sequences.** The TriTrypDB IDs (http://tritrypdb.org/tritrypdb/) of trypanosomatid sequences are LmjF.33.2600 (TFE1-Lm), LmxM.32.2600 (TFE1-Lmex), LbrM.33.2880 (TFE1-Lb), LtaP33.2830 (TFE1-Lt), Tb927.2.4130 (TFE1-Tb), TcIL3000_2_640 (TFE1-Tco), TcCLB.507547.40 (TFE1-TcCLB), LmjF.26.1550 (TFE2-Lm), LmxM.26.1550 (TFE2-Lmex), LbrM.26.1570 (TFE2-Lb), LtaP26.1590 (TFE2-Lt), TcCLB.508981.39 (TFE2-TcCLB). The names of TFEs from other species correspond to their GenBank accession numbers. Gaps (-) were introduced to maximize the alignments. The graphical output of the Clustal alignment was performed with CLC Main Workbench 6.

Figure S3

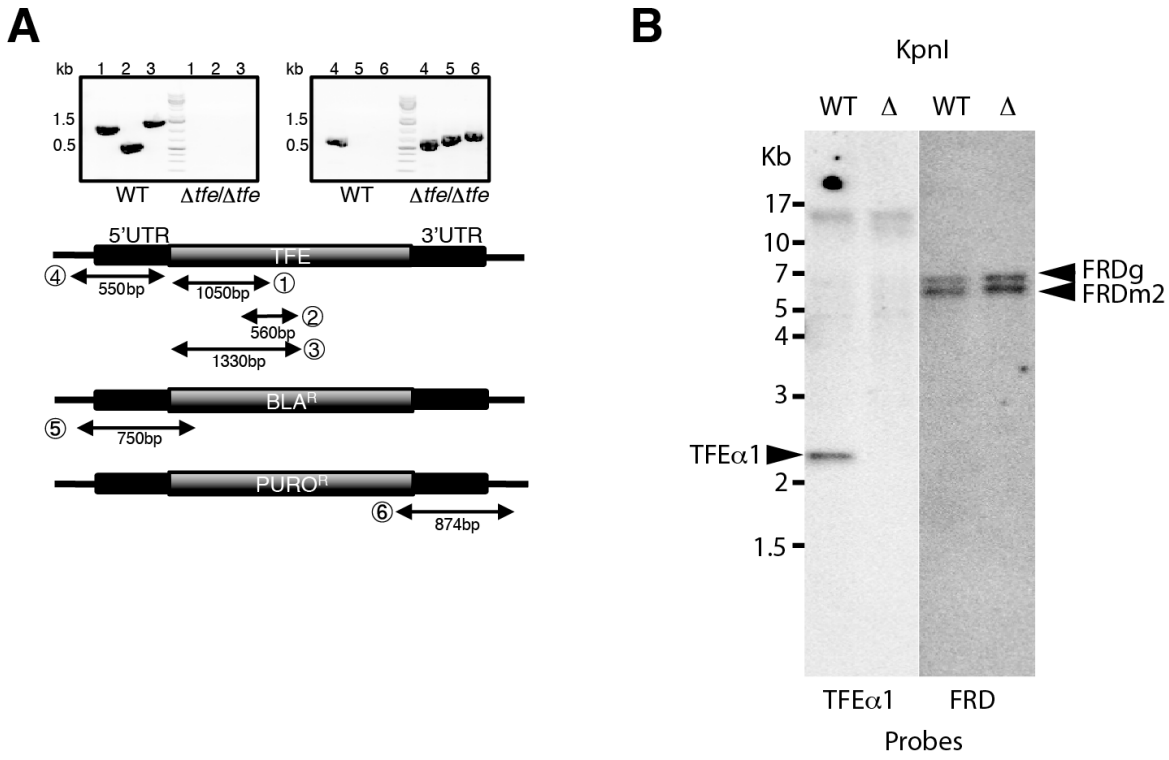

Figure S3. **Verification of the Δ*tfeα1*/Δ*tfeα1* null mutant.** (A) Verification of the Δ*tfeα1*/Δ*tfeα1* null mutant by integration control PCRs. The lanes of the gel are numbered according to the primer combinations used. (B) Southern blot analysis of the Δ*tfeα1*/Δ*tfeα1* null mutant. Hybridization of KpnI-digested wild-type genomic DNA with the TFE*α*1 probe revealed the expected 2.2 kb band, whereas loss of this band in the Δ*tfeα1*/Δ*tfeα1* genomic DNA is diagnostic for loss of the *TFEα1* gene. As a control, hybridization of the same blot with the fumarate reductase (FRD) probe showed the identical band pattern in both wild-type and Δ*tfeα1*/Δ*tfeα1* cell lines, corresponding to the FRDg and FRDm2 genes. DNA fragment sizes are indicated in kilobases (kb).

Figure S4

ID	PROTEIN NAME	NUMBER OF PEPTIDES DETECTED	NUMBER OF PEPTIDES ANALYSED	CONFIDENCE SCORE	WT			Δ*tfeα1*/Δtfeα1			RATIO WT/ Δ*tfeα1*
					MEAN	±SD	±SD (%)	MEAN	±SD	±SD (%)	
Tb927.11.5520	triosephosphate isomerase (TIM)	55	55	2526	1863305369	152977466	8.21	1778386406	214720264	12.07	1.0
Tb927.2.4210	glycosomal phosphoenolpyruvate carboxykinase (PEPCK)	121	118	5730	1808920564	34186729	1.89	2508732366	228826089	9.12	0.7
Tb927.6.4300	glyceraldehyde 3-phosphate dehydrogenase, glycosomal (GAPDH)	59	56	2649	1753325180	145878012	8.32	1459707495	156566626	10.73	1.2
Tb927.9.12590	glycerol kinase, glycosomal (glk1)	101	98	4742	1537228959	26045698	1.69	1449461192	135760076	9.37	1.1
Tb927.10.15410	glycosomal malate dehydrogenase (gMDH)	33	31	1751	1071814817	109387983	10.21	949222288	63298906	6.67	1.1
Tb927.8.3530	glycerol-3-phosphate dehydrogenase [NAD], glycosomal (GPDH)	53	52	2386	538828571	5514549	1.02	672535180	40480089	6.02	0.8
Tb927.11.6280	pyruvate phosphate dikinase (PPDK)	125	122	5494	437877250	22451846	5.13	432517560	40211120	9.30	1.0
Tb927.10.5620	fructose-bisphosphate aldolase, glycosomal (ALD)	44	43	2054	238278743	13262542	5.57	272654402	27725719	10.17	0.9
Tb927.10.16120	inosine-5'-monophosphate dehydrogenase,IMP dehydrogenase	52	51	2670	164703990	2559654	1.55	181794386	29723862	16.35	0.9
Tb927.7.7500	thymine-7-hydroxylase, putative (TLP7)	34	31	1323	139112664	4346531	3.12	158402808	26916407	16.99	0.9
Tb927.11.1020	ribokinase (RK)	22	22	1059	128914700	7052847	5.47	115505531	10418675	9.02	1.1
Tb927.8.6170	transketolase, putative (TK)	38	37	1670	109371465	4538020	4.15	132666743	11716329	8.83	0.8
Tb927.10.1390	hypoxanthine-guanine phosphoribosyltransferase (HGPRT)	27	27	1327	105904891	4985524	4.71	117274733	19183641	16.36	0.9
Tb927.8.7410	calreticulin, putative	37	37	1281	91402195	4320824	4.73	99898864	11827717	11.84	0.9
Tb927.5.930	NADH-dependent fumarate reductase (FRDg)	73	35	3114	66071553	3115804	4.72	60737040	4228258	6.96	1.1
Tb927.11.14780	phosphomannose isomerase, putative	30	30	1207	61539669	1552166	2.52	69783735	9441603	13.53	0.9
Tb927.3.3270	ATP-dependent phosphofructokinase (TbPFK)	44	42	1842	55115780	927590	1.68	66315147	5305232	8.00	0.8
Tb927.11.900	isocitrate dehydrogenase, putative (IDH)	39	36	1542	47900447	1203527	2.51	46461710	6993439	15.05	1.0
Tb927.11.11520	glycosomal membrane protein (PEX11)	13	13	573	38391550	524180	1.37	25525829	628633	2.46	1.5
Tb927.4.4070	mevalonate kinase (MK)	16	16	658	38339032	2377834	6.20	42018225	9281968	22.09	0.9
Tb927.1.3830	glucose-6-phosphate isomerase, glycosomal (PGI)	34	34	1399	32067471	782098	2.44	39186532	4810148	12.28	0.8
Tb927.10.2020	hexokinase (HK2)	28	28	1375	28225301	1049800	3.72	25883251	2840089	10.97	1.1
Tb927.3.3780	tryparedoxin	8	7	285	22930543	1240192	5.41	14336722	1293732	9.02	0.6
Tb927.10.10390	trypanothione reductase	21	19	833	18349989	1567671	8.54	11809985	429244	3.63	1.6
Tb927.5.2080	guanosine monophosphate reductase, putative	23	23	993	17687160	800817	4.53	19107962	2087274	10.92	0.9
Tb927.4.1360	hypothetical protein, conserved	15	14	578	16524626	533159	3.23	17471200	2444768	13.99	0.9
Tb927.7.1790	Adenine phosphoribosyltransferase, putative	17	17	743	16154994	543777	3.37	17129462	2928231	17.09	0.9
Tb927.6.1500	alkyl-dihydroxyacetone phosphate synthase (DHAP)	23	23	765	13305687	247620	1.86	10548755	1759853	16.68	1.3
Tb927.8.6390	lysophospholipase, putative,alpha/beta hydrolase, putative (TbLysoPLA)	20	18	761	13252278	829452	6.26	16591212	3482486	20.99	0.8
Tb927.8.7170	inositol polyphosphate 1-phosphatase, putative	15	15	617	12122208	67772	0.56	13356266	1443717	10.81	0.9
Tb927.5.3810	orotidine-5-phosphate decarboxylase/orotate phosphoribosyltransferase (OMPDCase-OPRTase)	24	23	852	11731648	254286	2.17	12890988	1712997	13.29	0.9
Tb927.11.15910	iron superoxide dismutase	5	2	264	8927350	660367	7.40	7833161	297045	3.79	1.1
Tb927.10.5760	adenylate kinase (AK)	11	11	325	5638958	207864	3.69	7086651	436722	6.16	0.8
Tb927.10.1470	hypoxanthine-guanine phosphoribosyltransferase (HGPRT)	11	11	459	5287280	306659	5.80	5687830	1222340	21.49	0.9
Tb927.6.3050	aldehyde dehydrogenase family, putative	17	17	678	5182254	100802	1.95	4347363	622180	14.31	1.2
Tb927.10.2490	glucose-6-phosphate 1-dehydrogenase (G6PD)	12	12	387	5100445	128736	2.52	4416772	331562	7.51	1.2
Tb927.7.5680	deoxyribose-phosphate aldolase, putative	12	12	494	4857246	397342	8.18	5142377	201134	3.91	0.9
Tb927.10.9890	hypothetical protein, conserved	17	17	567	4787697	1408358	29.42	3838079	651186	16.97	1.2
Tb927.10.13130	UTP-glucose-1-phosphate uridylyltransferase	19	19	682	4686187	333175	7.11	5405290	249391	4.61	1.2
Tb927.11.5180	hypothetical protein, conserved	13	13	455	4394023	297079	6.76	5700300	342701	6.01	1.3
Tb927.8.6640	hypothetical protein, conserved	14	14	575	4184483	812651	19.42	8932692	425582	4.76	0.5
Tb927.11.9920	polyubiquitin, putative	5	5	125	3570441	83765	2.35	2261798	141703	6.27	0.6
Tb927.9.6090	PTP1-interacting protein, 39 kDa	41	4	1393	3511684	378483	10.78	6071001	680299	11.21	0.6
Tb927.5.4350	NUDIX hydrolase, putative	6	6	121	3366959	332456	9.87	4445169	151084	3.40	0.8
Tb927.6.2200	hypothetical protein, conserved	7	7	204	2820818	99925	3.54	2327202	148505	6.38	1.2
Tb927.9.6100	TFIIF-stimulated CTD phosphatase, putative	38	1	1321	2471989	70677	2.86	2908251	439787	15.12	0.8
Tb927.8.1910	acetylornithine deacetylase, putative,metallo-peptidase, Clan MH, Family M18 (ArgE)	5	5	235	2328873	169831	7.29	2012215	87421	4.34	1.2
Tb927.9.11600	unspecified product (gim5B)	32	3	1681	2246567	229566	10.22	1868050	320764	17.17	1.2
Tb927.10.240	peroxin 14, putative (PEX14)	6	6	259	1998356	147260	7.37	1941263	50446	2.60	1.0
Tb927.7.1130	trypanothione/tryparedoxin dependent peroxidase 2,glutathione peroxidase-like 2 (TDPX2)	8	2	283	1912896	48255	2.52	1354486	68866	5.08	1.4
Tb927.9.9000	isopentenyl-diphosphate delta-isomerase (type II), putative	9	9	222	1782820	122912	6.89	2492125	689665	27.67	0.7
Tb927.9.10310	mitochondrial carrier protein (MCP11)	8	8	253	1517492	91382	6.02	2284359	119954	5.25	1.5
Tb927.9.8720	fructose-1,6-bisphosphatase (FBPase)	7	7	231	1443459	38432	2.66	1133218	14298	1.26	1.3
Tb927.9.11580	Gim5A protein,glycosomal membrane protein (gim5A)	35	6	1732	1379199	114013	8.27	1232880	118656	9.62	1.1
Tb927.3.1840	3-oxo-5-alpha-steroid 4-dehydrogenase, putative	3	3	69	1362291	46822	3.44	2288390	170911	7.47	1.7
Tb927.2.5800	sedoheptulose-1,7-bisphosphatase (SBPase)	7	7	193	1301735	36028	2.77	1149159	106183	9.24	1.1
Tb927.9.4210	fatty acyl CoA synthetase 3 (ACS3)	5	5	160	1281037	101193	7.90	1254254	80664	6.43	1.0
Tb927.3.4420	hypothetical protein, conserved	9	9	297	1258442	206469	16.41	2123326	75721	3.57	0.6
Tb927.3.2340	peroxin-2,glycosome import protein (gim1) (PEX2)	3	3	155	1072835	74080	6.91	1206666	79195	6.56	0.9
Tb927.10.10610	protein tyrosine phosphatase, putative	2	2	90	978287	60166	6.15	1071285	107056	9.99	1.1
Tb927.11.15020	iron superoxide dismutase (TbSODB)	5	2	204	943375	39786	4.22	885297	155980	17.62	1.1
Tb927.1.720	phosphoglycerate kinase (PGKA)	12	4	344	842113	47781	5.67	674257	88743	13.16	1.2
Tb927.11.2620	hypothetical protein, conserved	7	7	203	837654	34739	4.15	909963	27107	2.98	0.9
Tb927.5.2590	hypothetical protein, conserved	3	3	128	815653	80322	9.85	1190074	325566	27.36	0.7
Tb927.10.6810	guanylate kinase, putative	5	4	236	785251	92549	11.79	637326	37858	5.94	1.2
Tb927.9.4190	fatty acyl CoA syntetase 1 (ACS1)	8	7	220	748497	8829	1.18	732806	51578	7.04	1.0
Tb927.11.2380	phosphoglycerate kinase, putative	1	1	2	623199	118451	19.01	416533	7597	1.82	0.7
Tb927.11.1070	glycosomal transporter (GAT3), putative	4	4	224	482545	37749	7.82	438514	58596	13.36	1.1
Tb927.10.8410	hypothetical protein, conserved	3	3	59	459739	23103	5.03	465506	25401	5.46	1.0
Tb927.11.6330	splicing factor Prp31 (6PGL)	4	4	114	447412	26323	5.88	331616	10099	3.05	0.7
Tb927.11.2520	UDP-N-acetylglucosamine pyrophosphorylase, putative	4	4	175	447112	32978	7.38	471168	57707	12.25	0.9
Tb927.2.4130	enoyl-CoA hydratase/Enoyl-CoA isomerase/3-hydroxyacyl-CoA dehydrogenase	2	2	48	368458	53900	14.63	2643	4578	173.21	139.4
Tb927.9.6450	hypothetical protein, conserved	2	2	56	348164	30704	8.82	371519	23500	6.33	0.9
Tb927.7.1140	trypanothione/tryparedoxin dependent peroxidase 3 (TDPX3)	7	1	211	306761	48177	15.71	184177	32983	17.91	1.7
Tb927.5.2370	hydrolase, alpha/beta fold family, putative	4	4	114	289316	17479	6.04	225927	135331	59.90	1.3
Tb927.1.5000	hypothetical protein, conserved	3	3	78	270417	12631	4.67	286964	48879	17.03	0.9
Tb927.11.10260	hypothetical protein, conserved	3	3	166	259302	17778	6.86	396337	90007	22.71	0.7
Tb927.5.1210	short-chain dehydrogenase, putative	3	2	109	197306	2898	1.47	298241	13485	4.52	1.5
Tb927.3.2410	peroxisome assembly protein, putative	1	1	3	128200	23820	18.58	132743	25756	19.40	1.0
Tb927.4.1600	hypothetical protein, conserved	1	1	63	116928	9704	8.30	130205	11774	9.04	0.9
Tb927.10.8630	hypothetical protein, conserved	1	1	46	102280	3377	3.30	137867	25632	18.59	1.3
Tb927.9.1720	peroxisomal membrane protein 4	1	1	48	85280	13869	16.26	64199	6755	10.52	1.3
Tb927.8.6080	hypothetical protein, conserved	2	2	4	82135	4740	5.77	106387	12421	11.68	1.3
Tb927.10.3080	methionine biosynthetic protein, putative	1	1	21	71102	15139	21.29	88823	18402	20.72	1.2
Tb927.11.2730	UDP-galactose 4-epimerase (galE)	2	2	14	57947	8172	14.10	89116	5288	5.93	0.7
Tb927.4.2010	acyl-CoA binding protein, putative (ACBP)	1	1	23	55641	4010	7.21	27283	868	3.18	2.0
Tb927.5.2650	L-galactonolactone oxidase (GAL/ALO)	1	1	72	32131	384	1.19	59699	18496	30.98	0.5
Tb927.3.5090	tryparedoxin, putative	3	2	49	24859	1206	4.85	21215	5115	24.11	0.9
Tb927.4.3160	dihydroxyacetone phosphate acyltransferase, putative (DAT)	1	1	74	15679	2346	14.96	25498	4995	19.59	0.6

Table S4. Proteomic analysis of a glycosomal preparation. From proteome analysis of the post-large granule fraction from WT and Δ*tfeα1*/Δ*tfeα1* cell lines, only the glycosomal enzymes, identified with high confidence (group III) in Güther et al. [38] are shown in this table. The TriTrypDB ID and name of each protein is indicated in the 1st and 2nd columns. The data represent the SEM of 3 analyses of the same samples (technical replicate). Log_{10} of the "mean" values are used in Figure 4.5B. The last column indicates the ratio between the WT and Δ*tfeα1*/Δ*tfeα1* data.

Supplemental Material – Chapter 5.2

6.2.1 Oligonucleotides and plasmids

name	sequence(5'-3')	function
ACL_up	GGCCATTACGGCCAACATGGCA GCCACCGGCGTCTTC	amplification of putative *Tb*CL without N-terminal 10 aa; *SfiI* site
ACL_low	GGCCGAGGCGGCCCTAAACGAC CGATCCTTGTGG	amplification of putative *Tb*CL without N-terminal 10 aa; *SfiI* site
ACL_SKL_low	GGCCGAGGCGGCCCTACAATTT GCTAACGACCGATCCTTGTGG	amplification of putative *Tb*CL without N-terminal 10 aa; *SfiI* site With *Sc*MLS1 PTS signal
ICL1_up	GGCCATTACGGCCAACATGCCT ATCCCCGTTGGAAAT	amplification of *Sc*ICL1 gene *SfiI* site
ICL1_low	GGCCGAGGCGGCCCTATTTCTT TACGCCATTTTC	amplification of *Sc*ICL1 gene *SfiI* site
MLS1_up	GGCCATTACGGCCAACATGGTTA AGGTCAGTTTGGAT	amplification of *Sc*MLS1 gene *SfiI* site
MLS1_low	GGCCGAGGCGGCCTCACAATTTGC TCAAATCAGT	amplification of *Sc*MLS1 gene *SfiI* site

The obtained PCR products have been sequenced and then cloned into the PCR4-TOPO vector (Invitrogen), digested with *SfiI* and subsequently cloned into the yeast expression vector pBL100 ((Schussler et al., 2006); pDR196sfi). The PCR products have been sequenced and due to an observed allelic polymorphism of the CL candidate gene, two (allelic variants) clones have been analyzed for each construct.

name	sequence(5'-3')	function
5'ACL-TY_2	CGAATTCCCCAAGCTTTATGTGG AAATGTTACCCTCTTCGCT	amplification of putative *Tb*CL; C-terminal *Ty1* tag
3'ACL-TY_2	CGAATTCCTAGGATCCTCA *GTCAAGTGGGTCCTGGTTAGTATGGACCTC* AACGACCGATCCTTGTGGCA	amplification of putative *Tb*CL; C-terminal *Ty1* tag

The obtained PCR product has been cloned into pLew100v5 (George Cross, New York) via HindIII/BamHI. Due to the allelic polymorphism, both alleles have been cloned and tested in enzymatic activity assays after overexpression in EATRO 1125 T7T cells.

6.2.2 Yeast complementation

yeast strains:

BY 4741 Δicl1 null mutant of the ICL1 gene

BY 4741 Δmls1 null mutant of the MLS1 gene

Media:

Hartwell's complete medium: HC-U (Amberg et al., 2005) without uracil; instead of 2% glucose also 2% EtOH or 2% acetate have been added respectively. The transformation has been performed according to (Gietz and Schiestl, 2007).

6.2.3 Antibodies

αPFR A/C (L13D6)	monoclonal antibody (mouse) against *Tb*PFR-A/C, by K. Gull, Manchester (Kohl et al., 1999)
αHSP60	monoclonal antibody (mouse) against heat shock protein60 F. Bringaud, Bordeaux (Bringaud et al., 1995)
αPGKB	polyclonal antibody (rabbit) against recombinant *Tb*PGKB by P. Michels, Brussels; 1:5000
αASCT	polyclonal antibody (rabbit) against recombinant *Tb*ASCT by F. Bringaud, Bordeaux (Riviere et al., 2004)
αPPDK	polyclonal antibody (rabbit) against recombinant *Tb*PPDK by F. Bringaud, Bordeaux (Bringaud et al., 1998)
αACL	polyclonal antibody (rabbit) against recombinant *Tb*CL S. Allmann, Munich. animal 2, bleed: 180th day, 1:2000

The antibodies from Pineda Antikörperservice (αACL, αCS, αIDHg, αIDHm) have been raised according to the standard protocol, but with differences in the immunization period.

Protocol:

day 1:	primary immunization,	i.d.,	FCA	
day 20:	1st boost	s.c.,	FIA	
day 30:	2nd boost	s.c.,	FIA	
day 40:	3rd boost	s.c.,	FIA	blood withdrawal
day 61:	4th boost	s.c.,	FIA	
day 75:	5th boost	s.c.,	FIA	blood withdrawal
day 90:	6th boost	s.c.,	FIA	blood withdrawal
following months:				
every 14 days:	boost	s.c.,	FIA	
every 30 days:				blood withdrawal

Abbreviations: i.d., intradermal; s.c., subcutan; FCA, Freund's complete adjuvant; FIA, Freund's incomplete adjuvant.

6.2.4 *Trypanosoma brucei* cell lines

Wildtype strains:

T. brucei AnTat 1.1	(Antwerp Trypanozoon antigen type 1.1) Clone of EATRO1125 from E. Pays (Brussels, Belgium) and P. Overath (Tübingen) (Geigy et al., 1975)
T. brucei EATRO 1125	from F. Bringaud (Bordeaux, France) (Bringaud et al., 2000)

Transgenic strains:

AnTat 1.1 1313	Tetracyclin-repressor cell line based on AnTat 1.1, Tet-Repressor-Vector: pHD1313 (Alibu et al., 2005)
EATRO 1125 T7T	Tetracyclin-repressor cell line based on EATRO 1125 (Bringaud et al., 2000), Tet-Repressor-Vector pHD114, T7-Vector pHD328
AnTat 1.1 1313 ΔACL C9	deletion mutant of the CL candidate gene, (Riviere et al., 2009)
EATRO 1125 T7T ACL-Ty1 1	inducible overexpression cell line for Ty1-tagged CL protein. Vector: pLew100v5, G. Cross, NYC. allele 1

EATRO 1125 T7T ACL-Ty1 5	inducible overexpression cell line for Ty1-tagged CL protein. Vector: pLew100v5, G. Cross, NYC. allele 2

6.2.5 Immunoblotting

SDS-PAGE and immunoblotting has been performed as described in the material and methods section of (Allmann et al., 2013) (chapter 3).

6.2.6 Digitonin fractionation

Subcellular fractionation of *T. brucei* cells has been performed as described in (Allmann et al., 2013) (chapter 3).

Acknowledgements

First of all I would like to express my sincere gratitude to Prof. Dr. Michael Boshart for the opportunity to work on this project, the fruitful scientific discussions and the chance to evolve my scientific skills by visiting international conferences and the freedom to pursue also my own ideas.

Special thanks goes to Prof. Dr. Geigenberger for being the second examiner of this thesis and writing the corresponding report.

I offer my sincere gratitude to our collaboration partners:
Dr. Frédéric Bringaud and his lab members for the free and uncomplicated exchange of data, material and ideas.
Dr. Patrick Moreau for the valuable input and expertise in the field of lipidomics.
Dr. Jean-Charles Portais for the input and discussion of the metabolomics experiments.
Dr. Jan Van Den Abbeele for input, discussion and execution of the fly infection experiments.

A big thank you goes to all the former and present members of the AG Boshart and AG Janzen for the nice atmosphere in the lab, the discussions and input in seminars, the help with different methods and our shared free time activities.

A special thanks goes to Larissa for supplying me with chocolate and vitamins but especially for preparing all the countless customized media variations.

Namely, I want to thank Sabine Bachmaier, Matthias Ellerbeck and George Githure for helpful discussions and input concerning experiments and methods.

I want to thank all of my friends for their support and sympathy that they showed during these last years, which kept me going.

Last but not least I would like to express my gratitude to my family, who always supported me and tolerated all the cancelled weekend appointments, especially my mother for her support and the opportunity to study.

Curriculum Vitae

Personal Data

Name	Stefan Allmann
Date of birth	January 8, 1982
Place of birth	Munich

Experience

06/2009 – 10/2014 **Research associate** (PhD), Ludwig-Maximilians-Universität (LMU) Munich

Education

06/2009 – 10/2014 **PhD thesis**, LMU Munich, Section of Genetics, Group of Prof. Dr. Michael Boshart

- Thesis Title: "Developmental adaptations of energy and lipid metabolism in *Trypanosoma brucei* insect forms"
- Member of the international **graduate school** "Life Science Munich" (LSM)

09/2004 - 03/2009 **Study of biology** (diploma) LMU Munich

- Degree: *Dipl.-Biol.* (grade: 1.0)
- Thesis Title: " Genetic analysis to investigate the synthesis of NADPH and Acetyl-CoA in trypanosomes"
- Advanced study period with genetics as major; cell biology and neurobiology as minor subjects

09/2001 – 07/2003 **Study of chemistry** (diploma), Technische Universität (TU) Munich

09/1993 – 07/2001 **Grammar school**, Carl-Orff Gymnasium, Unterschleißheim, Germany

- Degree: Abitur (grade: 2.0)

Publications

Riviere, L., Moreau, P., Allmann, S., Hahn, M., Biran, M., Plazolles, N., Franconi, J. M., Boshart, M. & Bringaud, F. (2009) Acetate produced in the mitochondrion is the essential precursor for lipid biosynthesis in procyclic trypanosomes. ***PNAS***. 106(31); 12694-9.

Allmann, S., Morand, P., Ebikeme, C., Gales, L., Biran, M., Hubert, J., Brennand, A., Mazet, M., Franconi, J. M., Michels, P. A., Portais, J. C., Boshart, M. & Bringaud, F. (2013) Cytosolic NADPH homeostasis in glucose-starved procyclic *Trypanosoma brucei* relies on malic enzyme and the pentose phosphate pathway fed by gluconeogenic flux. ***J. Biological Chemistry***. 288(25); 18494-505.

S. Allmann, M. Mazet, N. Ziebart, G. Bouyssou, L. Fouillen, J.-W. Dupuy, M. Bonneu, P. Moreau, F. Bringaud and M. Boshart. (2014). Fatty Acid Feeding-Mediated Buildup and Turnover of Lipid Droplets in Procyclic *Trypanosoma brucei.* **Manuscript** submitted to *PLOS ONE*.

S. Allmann, N. Ziebart, J.-W. Dupuy, M. Bonneu, F. Bringaud, J. Van Den Abbeele and M. Boshart. (2014) Carbon Source Regulated Glycosomal NADPH Production is Essential for the Developmental Cycle of *Trypanosoma brucei* in the insect. **Manuscript.**

Conferences – Posters and Talks

Allmann, S., Morand, P., Ebikeme, C., Gales, L., Michels, P., Portais, J.-C., Boshart, M., Bringaud, F. Cytosolic NADPH homeostasis in glucose-starved procyclic *Trypanosoma brucei* relies on malic enzyme and gluconeogenic flux. (**Talk**) *5th Kinetoplastid Molecular Cell Biology Meeting*. Woods Hole, MA, USA (2013)

Allmann, S., Morand, P., Ebikeme, C., Gales, L., Portais, J. C., Bringaud, F. & Boshart, M. Carbon source adapted oxidative stress management due to metabolic flux redistribution in procyclic *T. brucei*. (**Talk**). 43rd microsymposium - 'Glycosomes/Trypanosomatid Metabolism/Drug Design'. Brussels, Belgium (2011).

Allmann S., Morand P., Van den Abbeele J., Bringaud F., Portais J.-C. and Boshart M. *Trypanosoma brucei* – Metabolic adaptations to changing hosts. (**Poster**). *Life Science Munich* (LSM) *conference*, Schliersee, Germany (2011)

Allmann, S., Morand, P., Bringaud, F. & Boshart, M. (2010) *Trypanosoma brucei* – NADPH sources and oxidative stress management. (**Talk**). *Life Science Munich* (LSM) *conference,.* Wildbad Kreuth, Germany (2010)

Allmann, S., Van Den Abbeele, J., Morand, F., Bringaud F. &Boshart M. *Trypanosoma brucei* – Metabolic adaptations to changing hosts. (**Poster**). *Molecular dialogue in host-parasite interaction*. Brussels, Belgium (2010)

Press:

- LMU homepage: http://www.uni-muenchen.de/forschung/news/2013/boshart.html
- Deutschlandfunk: http://www.dradio.de/dlf/sendungen/forschak/2302134/

Teaching

2012-14:	Lecturer in the course “Biologie für Mediziner” (“Biology for physicians”)
2013	Assistance in the course “Molecular methods in parasitology” funded by “Science Without Borders”
2010-13:	Involvement in the supervision and organization of the course “Genetik 2”
2012:	Supervision of a lab rotation, J. Schwarz Supervision of a “Summer School” (Amgen) Student, T. Kardash
2011:	Supervision of two “Summer School” (LSM, Amgen) Students, N. Palanisamy, M. Franzén. Malmros
2010:	Supervision of a bachelor thesis, F. Huber